

A076216

FINAL REPORT

JUNE 1, 1979

LEVEL

2
DO19052
VOL IV

**OPTICAL SUBMARINE COMMUNICATIONS
BY AEROSPACE RELAY
(OSCAR) (U)**

VOLUME III: MODEL DEVELOPMENT

CONTRACT NO. N00039-77-C-0100

DDC
REF ID: A66116
NOV 5 1979
E

Prepared for
NAVAL ELECTRONICS SYSTEM COMMAND

Prepared by
P. Titterton, H. Sweeney, W. Scott,
G. Elston and T. Flom

DDC FILE COPY

This document has been approved
for public release and its
distribution is unlimited.

GTE SYLVANIA
INCORPORATED
ELECTRONIC SYSTEMS GROUP/WESTERN DIVISION

79 09 26 064

DISCLAIMER NOTICE

THIS DOCUMENT IS BEST QUALITY PRACTICABLE. THE COPY FURNISHED TO DTIC CONTAINED A SIGNIFICANT NUMBER OF PAGES WHICH DO NOT REPRODUCE LEGIBLY.

UNCLASSIFIED

SECURITY CLASSIFICATION OF THIS PAGE (When Data Entered)

REPORT DOCUMENTATION PAGE		READ INSTRUCTIONS BEFORE COMPLETING FORM
1. REPORT NUMBER	2. GOVT ACCESSION NO.	3. RECIPIENT'S CATALOG NUMBER
4. TITLE (and Subtitle) OPTICAL SUBMARINE COMMUNICATIONS BY AEROSPACE RELAY (OSCAR). VOLUME III. MODEL DEVELOPMENT. FINAL REPORT		5. TYPE OF REPORT & PERIOD COVERED FINAL REPORT
6. AUTHOR(s) P. TITTERTON, H. SWEENEY, W. SCOTT, G. ELSTON T. FLOM		7. CONTRACT OR GRANT NUMBER(s) N/A
8. PERFORMING ORGANIZATION NAME AND ADDRESS GTE SYLVANIA INCORPORATED P.O. BOX 186 MT. VIEW CA 94042		9. PROGRAM ELEMENT PROJECT TASK AREA & WORK UNIT NUMBERS 12/324
11. CONTROLLING OFFICE NAME AND ADDRESS NAVAL ELECTRONIC SYSTEM COMMAND, ELEX 310 NATIONAL CENTER 1, CRYSTAL CITY WASHINGTON, D.C. 20360		12. REPORT DATE 1 JUNE 1979
14. MONITORING AGENCY NAME & ADDRESS (if different from Controlling Office)		13. NUMBER OF PAGES 395
		15. SECURITY CLASS (of this report) UNCLASSIFIED
		16a. DECLASSIFICATION/DOWNGRADING SCHEDULE
16. DISTRIBUTION STATEMENT (of this Report) DOCUMENT DISTRIBUTION CONTROLLED BY CLASSIFICATION This document is classified for public release distribution is unlimited		
17. DISTRIBUTION STATEMENT (of the abstract entered in Block 20, if different from Report) ABSTRACT APPROVED FOR PUBLIC RELEASE & DISTRIBUTION UNLIMITED		
18. SUPPLEMENTARY NOTES		
19. KEY WORDS (Continue on reverse side if necessary and identify by block number) STRATEGIC COMMUNICATIONS, LASERS, PROPAGATION, SUBMARINES		
20. ABSTRACT (Continue on reverse side if necessary and identify by block number) THIS STUDY EXPLORED THE CAPABILITY OF BLUE-GREEN OPTICAL COMMUNICATIONS TO PERFORM WIDE AREA BROADCAST TO SUBMERGED SUBMARINES. EMERGENCY ACTION MESSAGES, SELECTIVE CALL MESSAGES, AND GENERAL BROADCAST TRAFFIC WERE SPECIFICALLY ADDRESSED. AS A RESULT OF OPERATING CONCEPT SELECTION, MODEL DEVELOPMENT AND PRELIMINARY PER- FORMANCE EVALUATION, IT HAS BEEN CONCLUDED THAT THE SYSTEM IS FEASIBLE AND OPTICAL COMMUNICATIONS CAN BE MAINTAINED FROM ORBITING SATELLITES TO SUBMERGED SUBMARINES.		

DD FORM 1473

JAN 73

EDITION OF 1 NOV 65 IS OBSOLETE

UNCLASSIFIED

SECURITY CLASSIFICATION OF THIS PAGE (When Data Entered)

4106 571

JEB

2

FINAL REPORT

June 1, 1979

**Optical Submarine Communications by Aerospace Relay
(OSCAR)**

VOLUME III: Model Development

Prepared for
Naval Electronic Systems Command

Contract N00039-77-C-0100

D D C
RECEIVED
NOV 5 1979
E

Prepared by
P. Titterton, H. Sweeney, W. Scott, G. Elston and T. Flom

GTE SYLVANIA INCORPORATED
ELECTRONIC SYSTEMS GROUP-WESTERN DIVISION
Post Office Box 188
Mountain View, California 94042

This document has been approved
for public distribution
distribution

Approved for
 NPI
 by *on file* *h* *th*
 A

TABLE OF CONTENTS

<u>Section</u>	<u>Title</u>	<u>Page</u>
1	INTRODUCTION AND SUMMARY	1-1
2	GLOSSARY	2-1
	2.1 English Symbols	2-2
	2.2 Greek Symbols	2-12
3	SINGLE PULSE DOWNLINK PROPAGATION MODEL - SIGNAL	3-1
	3.1 Model Philosophy and Flow Chart	3-2
	3.1.1 Philosophy of Approach	3-2
	3.1.2 Model Flow Chart	3-3
	3.2 Input for Signal Calculation	3-6
	3.2.1 Source	3-6
	3.2.2 Clear Atmosphere	3-6
	3.2.3 Cloud	3-7
	3.2.4 Cloud to Water	3-7
	3.2.5 Air/Water Interface	3-8
	3.2.6 Water	3-8
	3.2.7 Receiver	3-8
	3.3 Sub-Models	3-9
	3.3.1 Clear Atmospheric Transmission - Signal	3-10
	3.3.2 Cloud Energy Transmission - Signal	3-12
	3.3.3 Cloud to Water Energy Transmission	3-18
	3.3.4 Air-Water Interface Transmission - Signal	3-21
	3.3.5 Air-Water Angular Effects - Signal	3-24
	3.3.6 Relative Surface Foam Coverage	3-26
	3.3.7 Water Energy Transmission -Signal	3-28
	3.3.8 Water Distribution of Radiance - Signal	3-31
	3.3.9 Received Pulse Width/Shape	3-38
	3.3.10 Overall Signal Equations	3-46
	3.4 Model Uncertainties	3-50
	3.4.1 Energy Transmission	3-50

TABLE OF CONTENTS (Continued)

<u>Section</u>	<u>Title</u>	<u>Page</u>
3.4.2	Angular Effects	3-50
3.4.3	Temporal Effects	3-51
3.5	"Parameter Value" Uncertainties	3-53
3.5.1	Cloud	3-53
3.5.2	Air Water Interface	3-54
3.5.3	Water	3-54
4	SINGLE PULSE DOWNLINK PROPAGATION MODEL - NOISE	4-1
4.1	Model Philosophy and Flow Chart-Noise	4-3
4.1.1	Philosophy of Approach - Noise	4-3
4.1.2	Model Flow Chart-Noise	4-5
4.2	Input Information for Noise Calculation	4-9
4.2.1	Source	4-9
4.2.2	Clear Atmosphere	4-11
4.2.3	Cloud	4-12
4.2.4	Cloud to Water	4-12
4.2.5	Water	4-12
4.2.6	Air/Water Interface	4-13
4.2.7	Receiver	4-13
4.2.8	Signal Characteristics	4-14
4.3	Sub-Models	4-15
4.3.1	Clear Atmospheric Transmission-Noise	4-16
4.3.2	Cloud Energy Transmission - Noise	4-19
4.3.3	Cloud to Water Energy Transmission - Noise	4-27
4.3.4	Air-Water Transmission - Noise	4-28
4.3.5	Air-Water Interface Angular Effects - Noise	4-31
4.3.6	Relative Surface Foam Coverage	4-33
4.3.7	Water Energy Transmission - Noise	4-35
4.3.8	Water Distribution of Radiance - Noise	4-37
4.3.9	Detection Bandwidth	4-41
4.3.10	Average Background Power Due to Sunlight	4-43
4.3.11	Average Background Power Due to Moonlight	4-46
4.3.12	Average Background Power Due to Blue Skylight	4-49

TABLE OF CONTENTS (Continued)

<u>Section</u>	<u>Title</u>	<u>Page</u>
4.3.13	Average Background Power Due to Stellar/Zodiacal Light	4-52
4.3.14	Average Background Power Due to Bioluminescence	4-55
4.3.15	Noise Equivalent Optical Power Dependence on Noise Sources	4-56
4.4	Computer Program for Complete SPDPM	4-59
4.4.1	Introduction	4-59
4.4.2	Names of Variables	4-59
4.4.3	Listing	4-71
4.5	Model Uncertainties	4-93
4.5.1	Average Power Transmission	4-93
4.5.2	Angular Effects	4-93
4.5.3	Temporal Effects	4-93
4.6	Parameter Value Uncertainties	4-95
5	DOWNLINK COMMUNICATION MODEL	5-1
5.1	Downlink Communications Model-Philosophy and Flow Chart	5-3
5.1.1	Philosophy of Approach-Downlink Communications Model	5-3
5.1.2	Model Flow Chart-Downlink Communication Model	5-5
5.2	Input Information	5-9
5.2.1	Environment	5-9
5.2.2	Requirements	5-9
5.2.3	System Design	5-10
5.3	Sub-Models	5-13
5.3.1	Area Relationships	5-14
5.3.2	Temporal Relationships	5-25
5.3.3	Message	5-26
5.3.4	Modulation/Demodulation	5-27
5.3.5	Scanning Relationships	5-42
5.3.6	Receiver and Source	5-50
5.3.7	Availability/System Effectiveness and Adaptive Scanning	5-58

TABLE OF CONTENTS (Continued)

<u>Section</u>	<u>Title</u>	<u>Page</u>
5.4	Computer Program for the DCM	5-69
5.4.1	Introduction	5-69
5.4.2	Names of Variables	5-71
5.4.3	DMC Listing	5-77
5.5	Model Uncertainties	5-127
5.5.1	Area Relationships	5-127
5.5.2	Temporal Relationships	5-127
5.5.3	Message	5-127
5.5.4	Modulation/Demodulation	5-127
5.5.5	Scanning Relationships	5-127
5.5.6	Receiver and Source	5-127
5.5.7	Availability/System Effectiveness and Adaptive Scanning	5-128
5.5.8	Included SPDPM Sub-Models	5-128
5.6	"Parameter Value" Uncertainties	5-131
5.6.1	Environment	5-131
5.6.2	Requirements	5-132
5.6.3	System Design	5-132
6	FULL OSCAR SYSTEM MODEL	6-1
6.1	Full OSCAR System Model -- Philosophy and Flow Charts	6-3
6.1.1	Philosophy of Approach -- Full OSCAR System Model (FOSM)	6-3
6.1.2	Model Flow Chart -- Full OSCAR System Model	6-4
6.2	Input Information	6-7
6.2.1	Environment	6-7
6.2.2	Requirements	6-9
6.2.3	System Design Inputs	6-9
6.3	Environment, Requirements and System Design Considerations	6-13

TABLE OF CONTENTS (Continued)

<u>Section</u>	<u>Title</u>	<u>Page</u>
6.3.1	Environment	6-14
6.3.2	System Effectiveness and Life Cycle Cost Models	6-19
6.3.3	System Design Analyses	6-24
6.4	Model Implementation	6-67
6.5	Discussion of Analyses	6-71
6.5.1	Environmental Models	6-71
6.6	Parameter "Value" Uncertainties	6-73
6.6.1	Environmental Parameters	6-73

LIST OF ILLUSTRATIONS

<u>Figure</u>	<u>Title</u>	<u>Page</u>
1-1	Development Procedure for a Full OSCAR Model	1-2
1-2	Representation of OSCAR Model Development	1-3
1-3	Parameters for the Single-Pulse Signal Downlink Model	1-5
1-4a	Schematic of "Signal" Single-Pulse Downlink Propagation Model	1-6
1-4b	Schematic of Typical Single-Pulse "Noise Equivalent Power" Downlink Propagation Model	1-6
1-5	Schematic of Downlink Communication Model	1-8
1-6	Schematic of Full OSCAR System Model	1-9
3-1	Schematic of Signal Single-Pulse Downlink Propagation Model	3-4
3-2	Flow Diagram of Single Pulse Downlink Propagation Model (Signal)	3-5
3-3	Typical Clear Atmospheric Transmission ($b = 0.357$)	3-11
3-4	Thin and Thick Cloud Energy Transmission Versus Zenith Angles, for $\langle \cos \theta \rangle = 0.83$, $\mu_0 = 1$.	3-14
3-5	Thin and Thick Cloud Zenith Angle Dependence of Cloud Transmission Normalized to Zenith	3-17
3-6	Thick Cloud to Water Surface Energy Transmission	3-19
3-7	Thin Cloud Air-Sea Interface Transmission as a Function of Signal Zenith Angle (θ_s) and Surface Wind Speed, V	3-23
3-8	Half-Angle RMS Air-Water Interface Effects as a Function of Wind Speed V	3-25
3-9	Foam/Streak Surface Coverage Transmission versus Surface Wind Speed	3-27
3-10	Relation Between In-Air and In-Water Signal Zenith Angles (Assuming Sea-Water Index of Refraction, $n = 1.33$)	3-29
3-11a	$f(\theta_R, \theta_0, \delta)$ for $\theta_0 = 30^\circ$	3-36
3-11b	$f(\theta_R, \theta_0, \delta)$ for $\theta_0 = 70^\circ$	3-36
3-12	Comparison of $f(t)$ and Bucher's Monte Carlo Pulse Shape	3-40
3-13	In-Water Pulse Width Calculation Geometry	3-41

LIST OF ILLUSTRATIONS (Continued)

<u>Figure</u>	<u>Title</u>	<u>Page</u>
3-14	Signal Zenith Angle Induced Additional Pulse Stretching	3-42
3-15	Cloud Induced Pulse Stretching as a Function of Optical Thickness ($s_c=0.04 \text{ m}^{-1}$, $w_0=1$)	3-43
3-16	Representative Normalized Pulse Shapes as a Function of Cloud Optical Thickness	3-44
4-1	Schematic of Typical Single-Pulse Noise Equivalent Power Downlink Propagation Model	4-6
4-2	Flow Diagram of Single-Pulse Downlink Propagation Model (Noise)	4-7
4-3	Flow Diagram of Single-Pulse Downlink Propagation Model Noise due to Bioluminescence	4-8
4-4	Typical Clear Atmospheric Transmission ($b = 0.357$)	4-17
4-5	Thick and Thin Cloud Energy Transmission Versus Optical Thickness, for $\langle \cos \theta \rangle = 0.83$, $w_0 = 1$.	4-22
4-6	Thin and Thick Cloud Zenith Angle Dependence of Cloud Transmission Normalized to Zenith	4-23
4-7	Typical Cloud Energy Transmission for Blue Skylight and Stellar Light ($\langle \cos \theta \rangle = 0.83$, $w_0=1$.)	4-26
4-8	Air-Sea Interface Transmittance as a Function of Sun or Moon Zenith Angle and Surface Wind Speed V	4-30
4-9	RMS Air-Water Interface Effect as a Function of Wind Speed V	4-32
4-10	Foam/Streak Surface Coverage Transmission Versus Surface Wind Speed	4-34
4-11	Detection Bandwidth for Pulse-Widths of Table 3-11	4-42
4-12	Complete SPDPM Computer Program Block Diagram	4-60
5-1	Schematic of Downlink Communication Model	5-5
5-2	Flow Diagram of Downlink Communication Model	5-7
5-3	Latitude and Range Satellite to Earth Geometry	5-15
5-4	Signal Zenith Entrance Angle Geometry	5-17
5-5	Illustration of Four Area Relations	5-18
5-6	$k=3$, $M_L=9$ PPM Example	5-28
5-7	Threshold Demodulation for PPM Format	5-29
5-8	Time-of-Peak Demodulation for PPM Format	5-36
5-9	Square-in-Circle Overlap Scan Pattern	5-43

LIST OF ILLUSTRATIONS (Continued)

<u>Figure</u>	<u>Title</u>	<u>Page</u>
5-9d	Escape Geometry	5-44
5-9e	Escape Geometry	5-46
5-10	OSCAR Coordinate Transformation	5-51
5-11	Layout of the DCM Program	5-70
6-1	Complete Model-Flow Chart	6-5
6-2	Definition of Lunar Phase Angle, α_{pm}	6-16
6-3	System Effectiveness Communication Tree	6-19
6-4	Inertially Oriented Orbits	6-26
6-5	Geocentric Equatorial Coordinates and Orbital Elements	6-26
6-6	Orbital Parameters	6-27
6-7	Ground Station and Submarine Coordinate System	6-33
6-8	Satellite Coordinate System	6-33
6-9	Rectangular and Spherical Coordinate Systems Centered on Earth's Surface	6-35
6-10	Line of Sight Geometry	6-41
6-11a	Uplink/Backlink Configuration	6-45
6-11b	Crosslink Configuration	6-46
6-12	Variation in Bit Error Probability with E_b/N_0	6-47
6-13	Attenuation Distributions for Calendar Year 1970 at Roseman, North Carolina	6-50
6-14	Rainfall Intensity Occurrences for Different Geographic Locations	6-51
6-15	Attenuation Factor	6-53
6-16	Summary of Sea-Level Atmospheric Attenuation	6-55
6-17	Noise Caused by Heavy Cloud, Fog, and Rain	6-56

LIST OF TABLES

Table	Title	Page
3-1	Typical Clear Atmospheric Transmission ($b=0.357$)	3-11
3-2	Typical "Thick" Cloud Zenith Signal Energy Transmission ($\langle \cos \theta \rangle = 0.83$), $\tau_0=1$.	3-13
3-3	"Thin" Cloud Zenith Signal Energy Transmission (Matched to the Thick Cloud Expression at τ_{opt} for $\langle \cos \theta \rangle = 0.83$)	3-14
3-4	Zenith Angle vs Signal Energy Transmission (Normalized to $\tau_s = 0$).	3-17
3-5	Thick Cloud-to-Water Surface Signal Energy Transmission	3-19
3-6	τ_{aw} Time-Averaged Downlink Air-Sea Interface Transmittance (For Thin Clouds, $\tau_{opt} \leq 10$)	3-22
3-7	Half-Angle RMS Air-Water Interface Effects	3-25
3-8	Air-Water Energy Transmission Due to Surface Foam and Streaks (Assuming a foam/streak albedo = 1)	3-27
3-9	Relation Between In-Air and In-Water Signal Zenith Angles (Assuming Sea-Water Index of Refraction, $n = 1.33$)	3-29
3-10	Relation of Radiance Zero Point, τ_0 , and Received Radiance Half-Power Point, $\tau_{1/2}$, for $1 - (\sin \tau_w / \sin \tau_0)^2$ Radiance	3-33
3-11	Typical "Thick" Cloud Pulse Broadening for $\tau_0 = 1$, $\theta = 37^\circ$ and $\tau_c = 0.04 \text{ m}^{-1}$	3-43
3-12	Status of Signal Portion Models of SPDPM	3-52
3-13	Status of "Input Parameters" to the Signal Portion of the SPDPM	3-55
4-1	Typical Clear Atmospheric Transmission ($b=0.357$)	4-17
4-2	Typical Energy Transmission for Sunlight and Moonlight at Zenith ($\langle \cos \theta \rangle = 0.83$, $\tau_0 = 1$).	4-22
4-3	Zenith Angle Dependence of Sun and Moon Cloud Energy Transmission (Normalized to $\tau_{su} = 0$ and $\tau_{mu} = 0$)	4-23
4-4	Typical Cloud Energy Transmission for Blue Skylight and Stellar/Zodiacal Light ($\langle \cos \theta \rangle = 0.83$, $\tau_0=1$)	4-26
4-5	τ_{awls}/τ_{awlms} Time Averaged Downlink Air Sea Interface Transmittance (for Thin Clouds, $\tau_{opt} \leq 10$)	4-29
4-6	RMS Air-Water Interface Induced Half-Angle Effects ($\tau_{opt} \leq 10$) Sun and/or Moon	4-32
4-7	Air Water Energy Transmission Due to Surface Foam and Streaks (Assuming a Foam/Streak Albedo = 1)	4-34

LIST OF TABLES (Continued)

<u>Table</u>	<u>Title</u>	<u>Page</u>
4-8	Relation of radiance zero point, θ_0 , and received radiance half-power point, $\theta_{1/2}$, for $1 - (\sin \theta_w / \sin \theta_0)^2$ radiance	4-38
4-9	Typical Detection Bandwidths for Pulse Width Conditions of Table 3-11	4-41
4-10	Status of Noise Portion Models of SPDPM	4-94
4-11	Status of "Input Parameters" to the Noise Portion of the SPDPM	4-96
5-1	Resolution Element Angular Coordinates	5-21
5-2	Number of Illuminated Spots Per Resolution Elements for Square in Circle Overlap	5-24
5-3	Status of Sub-Models of the DCM	5-129
5-4	Status of "Input Parameters" to the DCM	5-135
6-1	Solar Latitude Model	6-15
6-2	Lunar Brightness as a Function of Phase Angles	6-17
6-3	Inputs for Sample System Effectiveness Calculations	6-23
6-4	Sun/Moon Locations for Sample FOSM Runs	6-69
6-5	Uncertain Parameters for the FOSM	6-73

Section I

INTRODUCTION AND SUMMARY

This is Volume III, OSCAR System Model Development, of the final report on Phase IA of the Optical Submarine Communications by Aerospace Relay (OSCAR) program, performed by GTE Sylvania under Contract Number N00039-77-C-0100. The model has been developed as a design tool, and is used to evaluate performance of alternate designs, and assess critical technology.

The ability to provide a communication link between aerospace relays and submarines at operating depths would significantly enhance the NAVY's command, control and communications (C³) capability. The most promising technology for accomplishing this objective is optical communications that exploit the blue-green transmission characteristics of seawater.

The Naval Electronics System Command has defined a program for using optical communications for certain specific NAVY C³ requirements. The program, "Optical Submarine Communications by Aerospace Relay" (OSCAR), explores the capability of optical communications to perform wide area broadcast to submerged submarines. General broadcast traffic, Emergency Action Messages, and Selective Call messages are specifically addressed by the OSCAR program.

The three major parts of the OSCAR phase IA program are:

1. Operating Concept Selection, reported in Volume II.
2. Model Development, reported in this volume;
3. System Definition, reported in Volume IV.*

Volume II, Operating Concept Definition, analyzed all the logical concepts for meeting the system requirements, and selected one concept for further study. The selected concept uses a radio frequency uplink to satellites at or near synchronous altitudes, and a blue-green laser downlink from the satellites to the operational area. This selection was based on a top level and approximate model relating all requirements (except system effectiveness) to the system concept(s).

* Volume I contains an Executive Summary of the entire program.

1. (Continued)

This volume presents the OSCAR system modeling (developed subsequent to the Operating Concept Selection) for describing all aspects of the OSCAR performance i.e., an analytic model relating system requirements, the operating environment, and system design to system performance. The earlier model has been revised and expanded to include all the practical aspects of actual system behavior, so that a more precise estimate of the system performance for a given system design is available.

The logical development of a complete OSCAR system model is shown in Figure 1-1, while Figure 1-2 shows another view of the three levels of detail involved. The first step is a detailed model for the signal and noise characteristics of the optical downlink on a pulse by pulse basis. The second step is to incorporate these pulses in a communication message, and treat the downlink communications and scanning aspects of OSCAR during a single time interval. Only one portion of the total required coverage area is treated at a time since the model applies to a single satellite during a single time interval. The full system effectiveness is not included since only the communication "downlink" availability is analyzed.

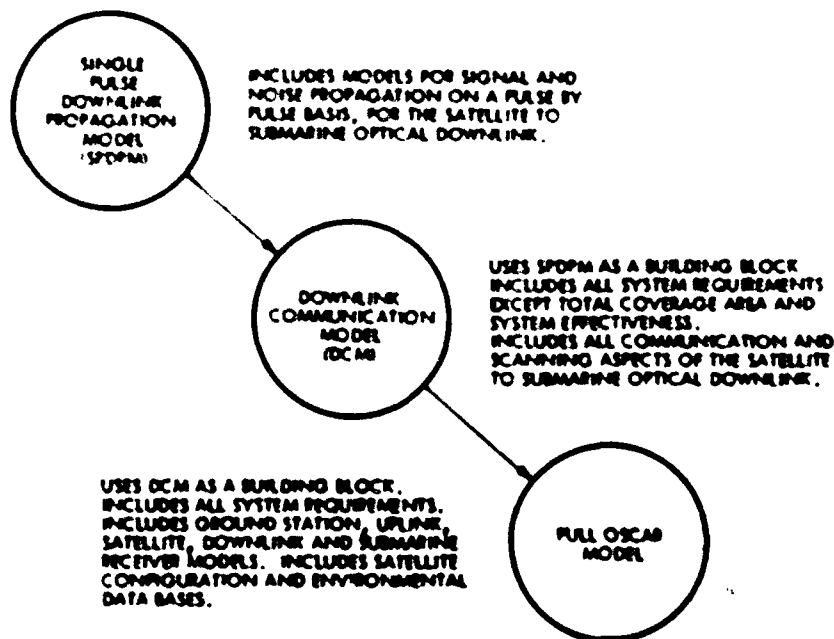


Figure 1-1. Development Procedure for a Full OSCAR Model

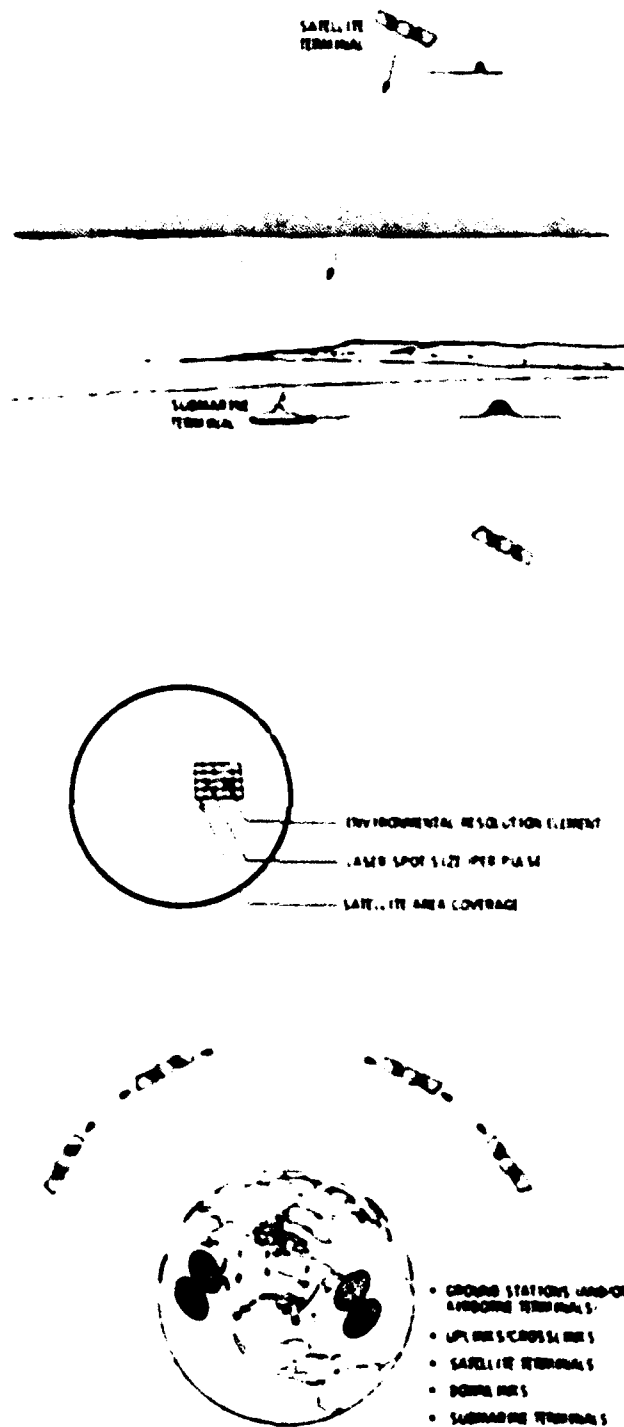


Figure 1-2. Representation of OSCAR Model Development

1. (Continued)

The third step, the Full OSCAR Model, treats all aspects of system behavior including the uplink, evolving data bases, time varying locations of background sources, and the complete satellite constellation. The full system effectiveness is included.

This report presents all three steps in the complete OSCAR model: the Single Pulse Downlink Propagation Model (SPDPM), the Downlink Communication Model (DCM), and the Full OSCAR System Model (FOSM), as well as a Glossary of all symbols used in these models. (The Glossary is described in Section 2.0.)

A draft of the SPDPM was submitted on July 1, 1978. Extensive review, by both NAVY and Government Contractor personnel over the succeeding eleven months, has led to some minor revisions. The approved version is presented in this report.

Section 3 discusses all aspects of the signal portion of the single pulse downlink propagation model. The parameters used are shown in Figure 1-3. The laser pulse originates on the satellite, propagates through the atmosphere (including whatever clouds are present), the air-water interface and the water, and is detected by the submarine receiver.

Section 4 discusses all aspects of the noise portion of the single pulse downlink propagation model. Some portions of the background light (sunlight, moonlight) traverse a path like that of the signal (although usually at a different zenith angle), while other portions of it (blue sky-light and star-light/zodiacal light) do not arise from single point-like sources, and must be treated differently. The bioluminescent light originates from sources in the water itself, and so the atmospheric conditions have no direct effects on its properties.

Sections 3 and 4 are organized in the same manner. First the method of approach used in the models is discussed, and then a detailed flow chart showing the interactions between all the equations is illustrated. (A top level schematic of these flow charts is shown in Figure 1-4). The second subsection defines and discusses all the input information needed to perform the calculations. The third subsection (3.3 and 4.3 respectively) contains the derivations and justifications of all the equations used. These equations and derivations are organized in a discrete modular fashion, so that future revision (e.g., cloud and water models) may be made in an efficient and inexpensive manner.

ENERGY PER PULSE
OPTICS TRANSMISSION
BEAM DIVERGENCE
DIVERGENCE CORRECTION FOR
ZENITH ANGLE SPREAD
RANGE TO SUBMARINE

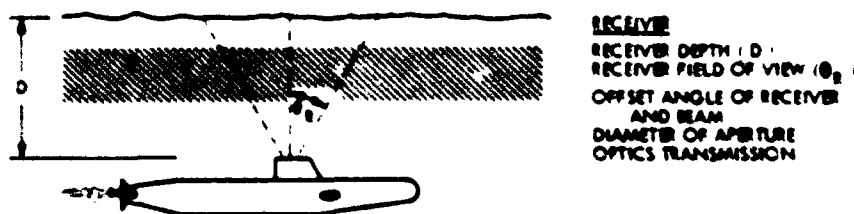
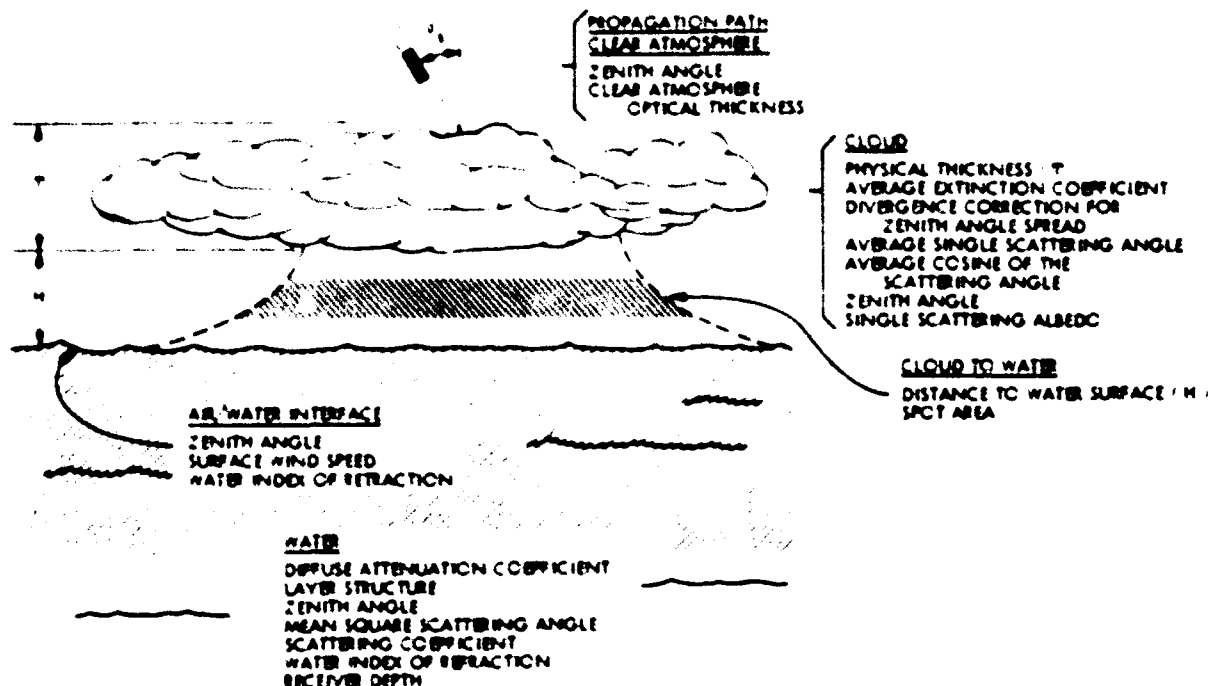
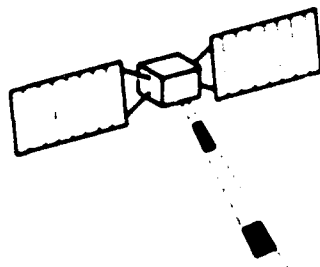


Figure 1-3. Parameters for the Single-Pulse signal Downlink Model

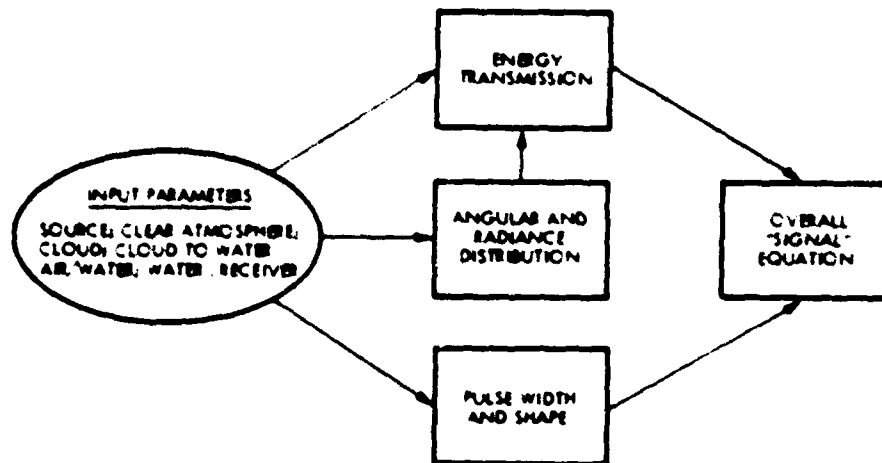


Figure 1-4a. Schematic of "Signal" Single-Pulse Downlink Propagation Model

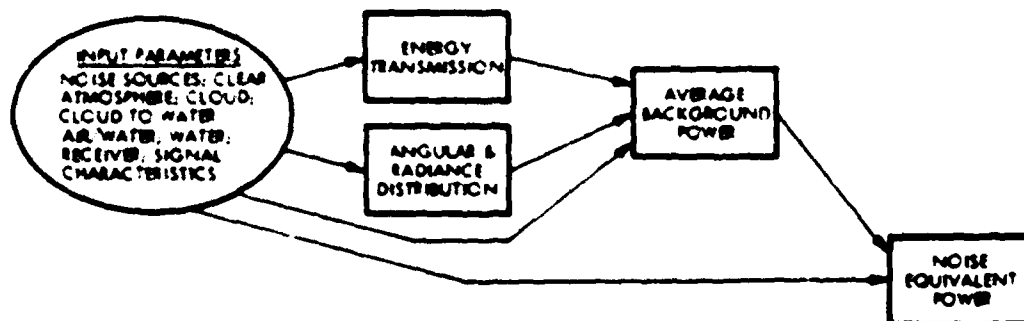


Figure 1-4b. Schematic of Typical Single-Pulse "Noise Equivalent Power" Downlink Propagation Model

1. (Continued)

Section 4.4 presents the computer program for the complete Single Pulse Downlink Propagation Model.

Both Sections 3 and 4 conclude with a discussion of the uncertainties in the present sub-models, and the values of the parameters entering into these sub-models. Key uncertainties include the cloud and water propagation models, and the strength and temporal characteristics of the bioluminescent background.

The Downlink Communication Model (DCM) is derived in Section 5. It considers the problem of communicating one message to a given area during a single time interval while the satellite, sun and moon are each at a single known location, and the environment is specified for all the necessary propagation paths. It includes the effects of laser warm-up time, interframe dead time, time to scan to a new spot, and spot overlap during the scan. It allows for system design choices of modulation format (the number of bits per pulse), demodulation format (threshold or time-of-peak), post detection processing format for anti-jam protection (if time of peak demodulation is chosen), and scanning approach (non-adaptive, adaptive for assumed thick cloud zenith angle effects, and fully adaptive).

The model outputs include the downlink availability,* and the number of pulses used to achieve this availability, both during a single time interval. In addition, the satellite prime power and the number of jamming and spoofing events per year are derived.

Section 5 is organized in the same manner as Section 3 and 4. The method of approach used is first described, and then a detailed flow chart showing the interactions between the equations and design decisions is shown. Figure 1-5 is a top-level schematic of this flow chart. (The SPDPM is utilized within the availability block.) The second sub-section defines and discusses all the input information needed to perform the calculations and the third subsection presents detailed derivations of all the DCM sub-models.

Section 5.4 presents the computer program for the complete Downlink Communication Model.

* In this context, downlink availability is defined as that fraction of the allocated area to which the message can be successfully transmitted within the required time interval.

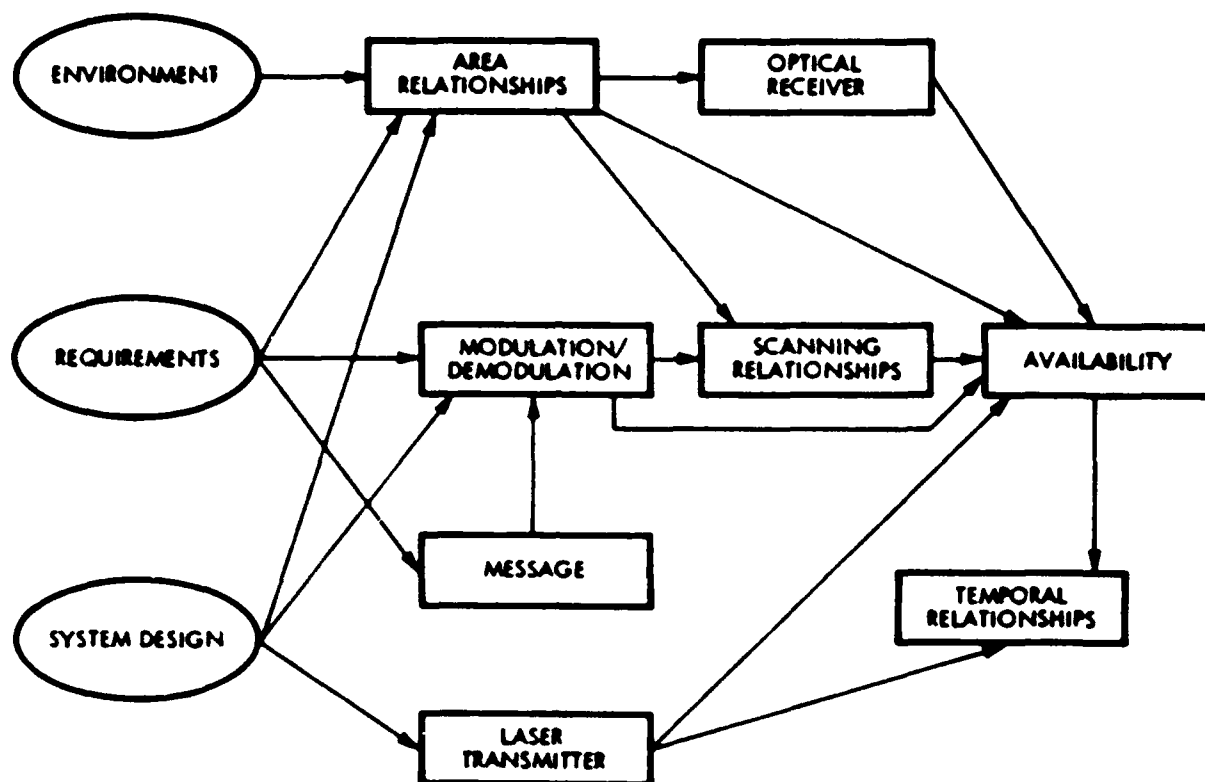


Figure 1-5. Schematic of Downlink Communication Model

1. (Continued)

Section 5 concludes with a discussion of the uncertainties in the sub-models used, and the values of the parameters entering into these sub-models. There are negligible uncertainties in the models, and the key area of uncertainty involves the values of the cloud parameters which apply during a single time interval.

The architecture for the Full OSCAR System Model (FOSM) is derived in Section 6. It considers the problem of communicating three types of messages to the complete required coverage area over a long time (normally, one year). Therefore, the time evolution of the environmental inputs is included, all requirements are treated (including system effectiveness), and the complete system design is used including the ground stations, the uplink, and the full satellite constellation.

The model outputs the system effectiveness for a given system design, with enough intermediate steps to indicate those aspects of system design which are driving the system performance.

1. (Continued)

Section 6 is organized in the same manner as Sections 3, 4, and 5. The method of approach is first described, and then a flow chart showing the interactions between the models and design decisions is shown. Figure 1-6 is a top-level schematic of this flow chart. (The DCM is utilized within the "Downlink Performance, Single Time Interval" block.) The second sub-section defines and discusses all the input information needed to perform the calculations and the third sub-section presents detailed derivations of all the FOSM submodels.

Section 6.4 presents our approach toward implementations of the FOSM. The architecture is completed (as called for in the Statement of Work) and this section discusses the exemplary results to be derived with this architecture.

The section concludes with a discussion of the uncertainties in the analysis, and the values of the parameters entering into the FOSM. The analysis is uncertain, and may be revised in the future, in the areas of system effectiveness formulation, and remote sensor performance. The parameters for the cloud and water data bases are uncertain in both their magnitude, their spectral correlation and their temporal evolution, and should undergo future revision.

Volume IV uses these models to define an OSCAR system able to meet the full requirements, for the environment as presently characterized.

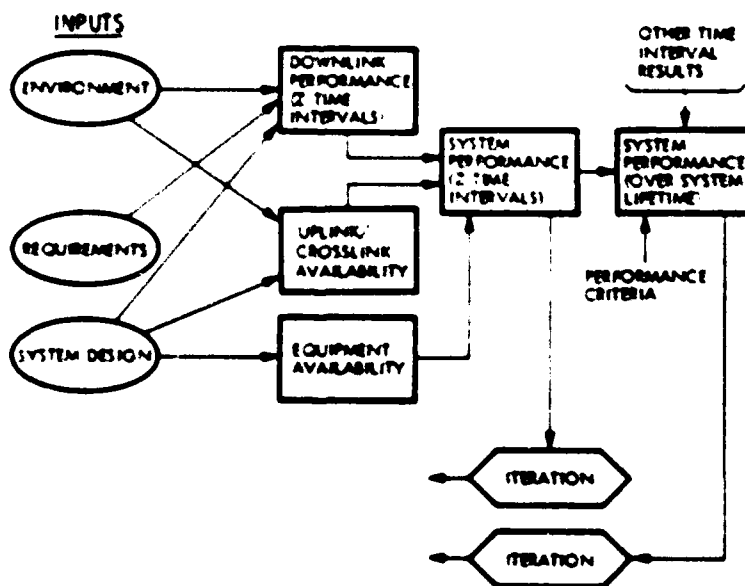


Figure 1-6. Schematic of Full OSCAR System Model

Section 2

GLOSSARY

This section defines all the English and Greek symbols used in the models developed in Sections 3, 4, 5 and 6. The English symbols are listed alphabetically in Subsection 2.1 and the Greek symbols are listed alphabetically in Subsection 2.2.

2.1 ENGLISH SYMBOLS

a = semi-major axis

A_{CL} = crosslink availability

A_{DL} = downlink availability

A_E = energy to instantaneous power normalization parameter

A_{GS} = ground station availability

A_i = single satellite/single time interval coverage area responsibility

A_{RCT} = area of rectangle within the ellipse

$A_{RCTijMIN}$ = minimum useful spot area in ij resolution element for elliptical spots.

A_{RE} = area of an environmental resolution element

A_{REij} = area of ij resolution element

A_{SAT} = satellite availability

A_{SB} = submarine receiver availability

A_{SC} = area of useful coverage within the spot, for square in circle pattern

A_{SCij} = useful spot area in ij resolution element

A_{SCMIN} = minimum useful spot area

A_{Sp} = area of illuminated spot, to $\exp(-2)$ irradiance points

A_{UL} = uplink availability

A_{UNVL} = system unavailability based on area for which FOM $ij < 1$

A_{VL} = area-based system availability

b = effective clear atmosphere optical thickness

B = electrical detection bandwidth

B_B = # of bits to be transferred on the backlink

B_C = # of bits to be transferred on the crosslink

B_{OPT} = receiver optical filter bandpass

2.1 (Continued)

B_U = # of bits to be transferred on the uplink

c = speed of light

C_f = fraction of sea-surface covered by foam and streaks

d = diameter of receiver aperture

D = receiver depth

DCM = downlink communication model

D_G = ground station RF antenna diameter

D_i = thickness of i 'th water layer

D_{OCij} = mean ocean depth of ij 'th ERE

D_S = satellite RF antenna diameter

D_{SP} = diameter of illuminated spot atop water, to exp-2 irradiance points

D_{SPMIN} = minimum spot diameter

D_{SQ} = edge length of square inscribed within the illuminated circular spot

e = charge on the electron

E = eccentric anomaly

E_2 = exponential integral

E_{ff} (SYST) = system effectiveness

E_p = transmitter energy per pulse per terminal

E_{TOT} = total transmitter energy per pulse

E_R = total received energy per pulse

ERE = environmental resolution element

E_{RF} = RF energy per message bit

exp = exponential

2.1 (Continued)

F = amplifier noise figure

$f' (:0, \theta_R)$ = fraction of incident radiance within receiver field of view

$f' (:0, \theta_R, \theta_{su})$ = fraction of incident radiance within receiver field of view

f_a = atmospheric contribution to received beam radiance

f_{cw} = air-water interface contribution to received beam half-angle

f_L = "wall-plug" source efficiency

FOM_{ij} = figure of merit for the ij resolution element, which is the ratio of the achieved signal to noise ratio to the required signal to noise ratio

FOM_{ss} = smallest FOM_{ij} for $\theta_{opt}=50$, throughout the coverage area

$f(t)$ = received pulse shape

f_w = water contribution to received beam half-angle

f_{w1} = contribution of i 'th water layer to received beam half angle

g = "cost" of jam/spoof system, relative to OSCAR

G = detection gain

G_{AZ} = receiver azimuth pointing angle, relative to local longitude

G_{AZij} = receiver azimuth pointing angle in the ij resolution element

G_{EL} = receiver zenith pointing angle

G_{ELij} = receiver zenith pointing angle in the ij resolution element

G_R = RF antenna gain

H = distance from cloud base to water surface

h = energy per signal photon

i = inclination angle

I = peak signal current

2.1 (Continued)

$i_{C_{ij}}$ = fraction of i 'th ERE which is covered by ice

I_d = dark current at the photo-cathode

I_n = RMS noise current

I_t = threshold current

$I(\lambda^w)$ = water radiance distribution

J = number of water layers present from surface to submarine receiver

J = jammer noise power

k = diffuse attenuation coefficient of the water

k_i = diffuse attenuation coefficient of i 'th water layer

(kt) = thermal noise energy = (Boltzmann's constant) \times (absolute temperature)

r = number of bits per pulse

L_B = clear sky exo-atmospheric effective radiance due to blue skylight

L_{BL} = spectral irradiance at receiver aperture due to bioluminescence

L_{BS} = spectral radiance at receiver aperture due to blue skylight

L_m = exo-atmospheric effective lunar radiance

L_{MU} = spectral radiance at receiver aperture due to the moon

L_S = exo-atmospheric effective solar radiance

L_{SU} = spectral radiance at receiver aperture due to the sun

L_Z = clear sky exo-atmospheric effective radiance due to stellar and zodiacal light

L_{ZS} = spectral radiance at receiver aperture due to stellar and zodiacal light

m = number of sources or terminals per satellite

$MARG$ = System margin used to compensate for unmodelled noise sources.

M_B = RF margin on the backlink

2.1 (Continued)

M_C = RF margin on the crosslink

M_D = Message length to be delivered, system requirement

M_L = Total message length.

M_{LD} = Message length to be delivered, system requirement

M_{OV} = Overhead bits added to each message

$MTBF_C$ = Mean time between environmental conditions which are sufficient to cause an outage

$MTBF_{SUB}$ = Mean time between failure

$MTTR_C$ = Mean time for outage-causing condition to clear

$MTTR_{SUB}$ = Mean time to repair

M_U = RF margin on the uplink

n = water index of refraction

N_{CC} = Number of crosslinks used in the entire system

NEP_B = Noise equivalent optical power due to shot-noise generated by the background

NEP_{DC} = Noise equivalent optical power due to photo-detector dark current

NEP_{TH} = Noise equivalent optical power due to thermal or amplifier noise

NEP_{SS} = Noise equivalent optical power due to shot-noise generated by the signal

NEP_{TOT} = Total noise equivalent optical power due to all sources

NEP_{TOTij} = Total noise equivalent optical power in the ij resolution element

N_J = Number of jammed messages per year per boat, single pulse processing

N_{J2} = Number of jammed messages per year per boat, two pulse processing

N_{J1} = Allowed number of jamming messages per year per boat, system requirement

N_M = Number of missed messages per year per boat, system requirement

N_0 = Noise power per hertz density at the receiver

2.1 (Continued)

N_{PL} = Total number of pulses used to communicate to the area

N_{S1} = Number of signal pulses received in T_A

spN_{S1} = Number of jam/spoof pulses received in T_A

N_{Sp} = Number of spoofed messages per year per boat

N_{Sp1} = Allowed number of spoofed messages per year per boat, system requirement

N_{SRE} = Number of spots within a resolution element

N_{SRE1} = Number of spots in the 1st resolution element

N_{SREMAX} = Maximum number of spots within a resolution element

N_{TOTRE} = Number of resolution elements within the area of responsibility

N_{TOTSP} = Total number of spots within this coverage area

$N_{TOTSPMAX}$ = Maximum number of spots required to cover the area of responsibility

P_L = Probability of a jam/spoof pulse occurring in any time slot

P_{AV} = Average power of a single terminal

P_{BS} = Average optical power at receiver due to the blue sky

P_{BL} = Average optical power at receiver due to bioluminescence

P_E = Bit error probability

P_{EN} = Penalty time for a link outage

P_F = Probability that a single threat pulse occurs in an unoccupied slot

P_{2F} = Probability that two threat pulses occur in a given frame

P_{FS} = Probability of false signature, in time-of-peak demodulation

P_{FA} = Single Pulse probability of a false alarm

P_B = Ground station transmitter power

P_{A0} = Prime power on the satellite required for all non-laser functions

P_J = Jamming probability, single pulse processing

P_{J2} = Jamming probability for two pulse processing

2.1 (Continued)

- P_{MU} = Average optical power at receiver due to the moon
- P_{J1} = Probability of at least one extra pulse occurring in the M_L/L frames
- (P_{J0J}) = Effective radiated jammer power
- P_L = Total prime power (in the satellite) required to sustain the laser sources
- P_M = Probability of a missed message
- P_N = Probability of a noise spike within one of $2^L - 1$ slots
- PPM = Pulse position modulation
- P_R = Peak received signal power
- PRF = Pulse repetition frequency of the transmitter
- P_{R1J} = Peak received optical power in the $1J$ resolution element
- $P_R(t)$ = Instantaneous received signal power
- P_S = Satellite transmitter power
- P_{Sp} = Spoof probability
- P_{SU} = Average optical power at receiver due to the sun
- P_{TOT} = Total prime-power capability required on the satellite
- P_Z = Average optical power at receiver due to stellar and zodiacal light

- q = Parameter describing ability of satellite transmitter to correct for zenith angle spot spreading. $0 \leq q \leq 1$

- R = Range from satellite to submarine
- R_E = Mean earth radius
- R_{GJ} = Range from jammer to the ground station
- R_{GS} = Range from ground station to the satellite
- R_{1J} = Range from satellite to boat located at x_1, z_j
- R_{1JMAX} = Maximum range within the assigned coverage area
- R_{JS} = Distance from jammer to satellite

2.1 (Continued)

R_L = Load resistance

R_{MU} = Moon altitude

R_S = Satellite altitude

\dot{R}_S = Rate of change of satellite altitude

R_{SJ} = Distance between 2 satellites

R_{SU} = Sun altitude

$R(\lambda_s)$ = Sea-surface reflectance

s = water scattering coefficient

s_i = scattering coefficient of i 'th water layer

SPDPM = Single pulse downlink propagation model

$\left(\frac{S}{N}\right)$ = Signal to noise ratio

$\left(\frac{S}{N}\right)_{ij}$ = Signal to noise ratio achieved in the ij resolution element

$\left(\frac{S}{N}\right)_{REQ}$ = Required signal to noise ratio, throughout the coverage area

S_{RF} = RF signal power at the receiver

S_T = Parameter describing area allocated

t = time

T = geometrical thickness of the cloud

T_A = time allowed to cover the allocated area, system requirement

T_{ARV} = adjacent spot revisit time

t_f = dead time between frames

t_{ij} = time to cover the ij resolution element

t_m = time after pulse start at which peak value occurs

T_{NR} = threshold to noise ratio

2.1 (Continued)

T_{ON} = Total source on time for a single coverage time

$T_{O,t}$ = time to cover resolution element for which T_{PART} changes from $<T_A$ to $>T_A$

T_{PART} = time to cover the resolution elements with $FOM_{ij} > 1$, from largest FOM to smallest

t_s = Slot width

t_{st} = dead time between messages, or time to scan to a new spot and to develop the appropriate beam width

T_{sp} = Time devoted to each spot, including slewing time

T_{TOT} = time required to cover the allocated area

$T_{TOT MAX}$ = Maximum time required to illuminate the total allocated area

t_w = source turn-on/warm-up time

Δt_c = pulse width due to cloud portion of the path

Δt_{cw} = pulse width due to cloud to water portion of the path

Δt_w = pulse width due to water portion of the path

t = time of day at Greenwich (0° longitude) (Sect. 6.3)

T_{AV} = time over which availabilities are averaged in order to obtain E_{ff} (SYST)

t_B = time allowed to complete backlink

t_C = time allowed to complete crosslink

t_{no} = time after full moon

t_{nm} = time after sunset

T_{ORB} = Period of the orbit

t_p = time when perigee of the orbit was traversed

t_U = Time allowed to complete uplink

T_{EARTH} = Earth noise temperature

$TECH_{FOM}$ = technology figure of merit

2.1 (Continued)

T_{RAIN} = rain noise temperature

$T_{RECEIVER}$ = Receiver noise temperature

T_{SUN} = sun noise temperature

V = Surface wind speed

V_M = Maximum submarine velocity during communication time, system requirement

w = Number of additional pulses added to message to meet quality of service requirements of time-of-peak demodulation approach

W = Extent of spread spectrum

x_E = receiver coordinate in earth-centered system

x_{MU} = lunar coordinate in earth-centered system

x_S = satellite coordinate in earth-centered system

x_{SU} = solar coordinate in earth centered system

y_E = receiver coordinate in earth-centered system

y_{MU} = lunar coordinate in earth-centered system

y_S = satellite coordinate in earth-centered system

y_{SU} = solar coordinate in earth-centered system

z_E = receiver coordinate in earth-centered system

z_{MU} = lunar coordinate in earth-centered system

z_S = satellite coordinate in earth-centered system

z_{SU} = solar coordinate in earth-centered system

2.2 GREEK SYMBOLS

The Greek symbols are listed in order according to the Greek alphabet: $\alpha, \beta, \gamma, \delta, \epsilon, \zeta, \eta, \theta, \iota, \kappa, \lambda, \mu, \nu, \xi, \omicron, \pi, \rho, \sigma, \tau, \upsilon, \phi, \chi, \psi, \omega$.

- α_{A_i} = latitude of a point within the coverage area
- α_{GS} = latitude of ground station
- α_i = mean latitude value for all i resolution elements
- α_J = latitude of jammer
- α_{MU} = lunar latitude
- α_{pm} = phase of the moon
- α_S = satellite latitude
- α_{SU} = solar latitude
- α_{SUB} = latitude of submarine receiver
- $\dot{\alpha}_S$ = rate of change of satellite latitude
- λ_{A_j} = longitude of a point within the coverage area
- λ_{GS} = longitude of ground station
- λ_j = mean longitude value for all j resolution elements
- λ_J = longitude of jammer
- λ_{MU} = lunar longitude
- λ_0 = lunar longitude at sunset of a given day
- λ_S = satellite longitude
- λ_{SU} = solar longitude
- $\dot{\lambda}_S$ = rate of change of satellite longitude
- λ_{SUB} = longitude of submarine receiver
- τ_T = transmitter optics transmission
- τ_R = receiver optics transmission

2.2 (Continued)

- θ = offset angle between receiver optical axis and axis of the incoming light
- θ_{BRij} = in water angle between receiver axis and effective blue-sky direction
- θ_{MURij} = in water angle between receiver axis and lunar direction
- θ_{SRij} = in water angle between receiver axis and signal direction
- θ_{SURij} = in water angle between receiver axis and solar direction
- θ_{ZRIj} = in water angle between receiver axis and zodiacal/starlight direction
- α = spot overlap factor
- e = eccentricity of (orbital) ellipse
- η_G = ground station RF antenna efficiency
- η_S = satellite RF antenna efficiency
- θ = cloud particle mean scattering angle
- $\langle \cos \theta \rangle$ = mean cosine of the in-cloud scattering angle
- θ_T = Full angle exp (-2) transmitter beamwidth
- Δ_{AW}^2 = rms half-angle additional signal beam divergence due to wave action
- θ_{S1}^2 = Mean square single scattering angle in water
- θ_{S11}^2 = Mean square single scattering angle in water for 1st water layer
- θ_R = Half angle of the receiver field of view
- Δ_{AW}^{SU} = rms half-angle air-water interface induced spread for the sunlight
- Δ_{AW}^{MU} = rms half-angle air-water interface induced spread for the moonlight
- $\theta_{S/2}$ = Half the angle subtended by the sun
- $\theta_{M/2}$ = Half the angle subtended by the moon
- Δ_{AW}^B = rms half-angle air-water interface induced spread for the blue sky light
- Δ_{AW}^Z = rms half-angle air-water interface induced spread for the stellar/zodiacal light

2.2 (Continued)

θ_{TMIN} = Minimum transmitter beam divergence

σ_{TS} = RMS short term satellite pointing jitter

σ_{TDR} = RMS long term satellite pointing drift

θ_{T1} = Minimum transmitter beam divergence from all constraints

θ_{T2} = Transmitter beam divergence for temporal availability in non-adaptive scan

θ_{T1j} = Initial transmitter beam divergence to j resolution element for partially adaptive scan, or final beam divergence in fully adaptive scan

θ_{T21j} = Transmitter beam divergence for temporal availability in partially adaptive scan

θ_{SLEW} = Angle between 2 points on the earth's surface, viewed from a satellite

θ_S = Zenith angle from inertially oriented satellite to a point on the earth's surface

$\dot{\theta}_S$ = Rate of change of θ_S

θ_{SA} = Azimuth angle from inertially oriented satellite to a point on the earth's surface

$\dot{\theta}_{SA}$ = Rate of change of θ_{SA}

λ = Optical wavelength

$\Delta\lambda$ = Wavelength shift

$\Delta\lambda_{MIN}$ = Maximum useful bandwidth of optical filter

λ_{RF} = Wavelength of RF link

$\left(\frac{\Delta\lambda}{\lambda}\right)$ = Optical Doppler shift for satellite to earth path

$\left(\frac{\Delta\lambda}{\lambda}\right)_S$ = Doppler shift between 2 satellites

τ_c = mean extinction coefficient of the cloud

2.2 (Continued)

- τ_a = Signal clear atmospheric energy transmission
- τ_c = Signal cloud energy transmission
- τ_{OPT} = Optical thickness of the cloud
- τ_{cw} = Signal cloud to water energy transmission
- τ_{aw} = Signal total energy transmission of air-water interface
- τ_{aw1} = Signal air-water interface energy transmission due to the index of refraction discontinuity
- τ_{aw2} = Signal air-water interface energy transmission due to foam and streaks on the sea surface
- τ_w = Signal water energy transmission
- τ_a' = Background clear atmospheric energy transmission
- τ_{CS} = Cloud energy transmission of the direct sunlight
- τ_{CM} = Cloud energy transmission of the direct moonlight
- τ_{CB} = Cloud energy transmission of the blue skylight
- τ_{CZ} = Cloud energy transmission of the stellar and zodiacal light
- τ_{CW}' = Background cloud to water energy transmission
- τ_{AW}' = Total background energy transmission of the air-water interface
- τ_{AW1}' = Background air-water interface transmission due to index of refraction discontinuity
- τ_{AW2}' = Background air-water interface transmission due to foam and streaks on the sea surface
- τ_{AWIS}' = Solar air-water interface transmission due to index of refraction discontinuity
- τ_{AWIM}' = Lunar air-water interface transmission due to index of refraction discontinuity
- τ_{AWIB}' = Blue-skylight air-water interface transmission due to index of refraction discontinuity

2.2 (Continued)

- τ_{AWIZ} = Stellar and zodiacal light air-water interface transmission due to index of refraction discontinuity
- τ_{WSU} = Solar water energy transmission
- τ_{WLU} = Lunar water energy transmission
- τ_{WB} = Blue sky water energy transmission
- τ_{WZ} = Stellar and zodiacal light water energy transmission
- τ_{RAIN} = RF rain attenuation factor
- τ_{RADOME} = RF radome attenuation factor
- θ_S = Signal in-air zenith angle
- θ_S^W = Signal in-water zenith angle
- θ_0 = Off-axis angle at which in-water radiance goes to zero
- $\theta_{1/2}$ = Half-power angle of the received signal beam radiance
- θ_{SU} = Solar in-air zenith angle
- θ_{LU} = Lunar in-air zenith angle
- θ^W = Angle measured from the axis, or principal ray direction, of the in-water signal radiance
- θ_{SU}^W = Solar in-water zenith angle
- θ_{LU}^W = Lunar in-water zenith angle
- θ_{Sij} = Signal zenith angle to ij resolution element
- θ_{SUij} = Solar zenith angle to ij resolution element
- θ_{LUij} = Lunar zenith angle to ij resolution element
- θ_{SAij} = Signal azimuth angle relative to local longitude in ij resolution element
- θ_{SUAij} = Solar azimuth angle relative to local longitude in ij resolution element

2.2 (Continued)

μ_{AIj} = Lunar azimuth angle relative to local longitude in ij resolution element

θ_{SIj}^W = Signal in-water zenith angle to ij resolution element

θ_{SUIj}^W = Solar in-water zenith angle to ij resolution element

μ_{UIj}^W = Lunar in-water zenith angle to ij resolution element

$\dot{\theta}_S$ = Rate of change of zenith angle

θ_{SA} = Azimuth angle

$\dot{\theta}_{SA}$ = Rate of changes of azimuth angle

θ_{SLEW} = Angle between 2 satellites viewed from the earth

θ_{SLEW} = Angle between a satellite and a point on the earth's surface, viewed from another satellite

ω_0 = Argument of perigee

α = Right ascension of ascending node

α_0 = Cloud particle single scatter albedo

Ω_0 = Full solid angle containing the incoming in-water radiance

ω_R = Rotational rate of the earth

Ω_R = solid angle of the receiver

Section 3

SINGLE PULSE DOWNLINK PROPAGATION MODEL - SIGNAL

This section discusses the model for the optical propagation of a single signal pulse from a satellite to a submerged submarine. The section is organized as follows:

- 3.1 Model Philosophy and Flow Chart
 - 3.1.1 Philosophy of Approach
 - 3.1.2 Model Flow Chart
- 3.2 Input for Signal Calculation
 - 3.2.1 Source
 - 3.2.2 Clear Atmosphere
 - 3.2.3 Cloud
 - 3.2.4 Cloud to Water
 - 3.2.5 Air/Water Interface
 - 3.2.6 Water
 - 3.2.7 Receiver
- 3.3 Sub-Models
 - 3.3.1 Clear Atmospheric Transmission - Signal
 - 3.3.2 Cloud Energy Transmission - Signal
 - 3.3.3 Cloud to Water Energy Transmission
 - 3.3.4 Air-Water Interface Transmission - Signal
 - 3.3.5 Air-Water Angular Effects - Signal
 - 3.3.6 Relative Surface Foam Coverage
 - 3.3.7 Water Energy Transmission - Signal
 - 3.3.8 Water Distribution of Radiance - Signal
 - 3.3.9 Receiver Pulse Width/Shape
 - 3.3.10 Overall Signal Equations
- 3.4 Model Uncertainties
 - 3.4.1 Energy Transmission
 - 3.4.2 Angular Effects
- 3.5 Parameter Value Uncertainties
 - 3.5.1 Cloud
 - 3.5.2 Air-Water Interface
 - 3.5.3 Water

3.1 MODEL PHILOSOPHY AND FLOW CHART

This section describes the basic approach used to generate the detailed single pulse downlink propagation model and presents a flow chart showing the interrelationships of the sub-models and their required inputs.

3.1.1 Philosophy of Approach

The model:

- (1) Is organized in a modular fashion, so that the effect of each portion of the path is evident. In addition, as further experiments and analyses are undertaken, pieces of the model may be upgraded without requiring extensive modification of the total model;
- (2) Considers the following three properties of the signal, and separately models the effects of the propagation path on each:
 - (a) The energy transmission from the satellite transmitter to the submerged submarine receiver;
 - (b) The distribution of the signal radiance at the submarine receiver;
 - (c) The pulse shape and width at the submarine receiver.

These three properties are then combined to yield the instantaneous received optical power at the surface of the photodetector.
- (3) Does not attempt to treat all possible cloud conditions. Rather, a break point is established at a minimum optical thickness of 10. Below that value one set of sub-models is assumed to apply, while above it a different set applies. In many cases these sub-models do not correspond at $\tau_{opt} = \text{optical thickness} = 10$, and so the overall model should only be used for $\tau_{opt} < 10$ and $\tau_{opt} \gg 10$. (Future analysis and experiments on the "multiple-forward scattering" region should enable the sub-models to be upgraded, and this inconsistency removed.)
- (4) Assumes appropriate simple analytic forms for at-present unknown functions such as the radiance distribution, and pulse shape and width. This enables us to present analytic results (except for the receiver axis offset from the beam axis of the incident radiance), which are an aid to a physical understanding of the overall propagation problem.

3.1.2 Model Flow Chart

A schematic of the overall single pulse signal downlink propagation model is presented in Figure 3-1. Given the input parameters, the pulse width and shape and the angular and radiance distribution are derived. Then using the angular and radiance distribution and the input data the energy transmission of the path is calculated. Finally given the energy transmission and the received pulse shape, the signal (instantaneous received power) is calculated.

Figure 3-2 is a detailed flow diagram showing the calculations that must occur to arrive at the required output.

- (I) The input parameters are listed in the seven ellipses on the left hand side of the figure, including source, clear atmosphere, cloud, cloud to water, air/water interface, water and receiver parameters. (The symbols are defined in the glossary in Section 2, and also in the input discussion in Section 3.2).
- (II) The calculation equations are represented by the rectangular boxes. Within each box is the symbol for the parameter to be calculated and the equation number (from Section 3.3) for the equation to be used to calculate the parameter. The first quantity calculated is the cloud optical thickness, τ_{OPT} , since this determines the equations to be used to calculate many other parameters. Whenever // appears in a rectangular box, the equation number preceding it refers to $\tau_{OPT} + 10$, while the equation number following it refers to $\tau_{OPT} - 10$. Hence, given the value of τ_{OPT} the rest of the models to be used are specifically determined.
- (III) The second set of calculations performed are of three types:
 - (a) Path transmission, including τ_A , τ_C , τ_{CW} , τ_{AW} and τ_W ;
 - (b) Pulse width and shape, including Δt_C , Δt_{CW} , Δt_W and t_M ;
 - (c) Angular and radiance distribution, including f_A , f_{AW} , f_W , ϕ_0 and $f(\theta_R, \phi_0, \psi)$.

3.1.2 (Continued)

- (V) The path transmission, angular and radiance distribution, source and receiver parameters are then used to calculate the received energy, E_R .
- (V) The received energy and pulse width and shape are used to calculate the instantaneous received power $P_R(t)$.

The developed computer program is included with that for the noise sources, and presented in Section 3.2.

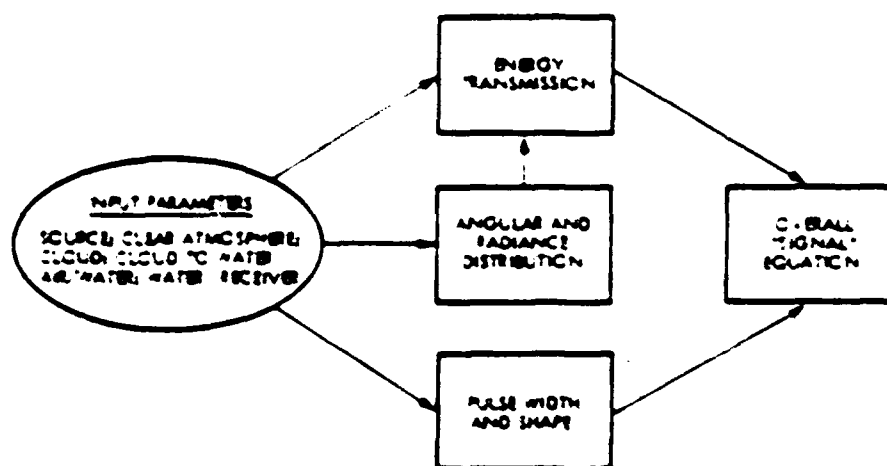


Figure 3-1. Schematic of Signal Single-Pulse Downlink Propagation Model

3.2.3 Cloud

The required parameters are:

<u>Symbol</u>	<u>Description</u>	<u>Units</u>
z	Geometric or physical thickness of the cloud	Meters
σ_c	Average extinction coefficient of the cloud	(Meters) ⁻¹
q	A parameter describing the ability of the satellite transmitter to correct for the geometric zenith angle spreading of the spot. $q = 0$ implies the spot remains the same area independent of zenith angle, while $q = 1$ means the spot grows naturally with zenith angle. Hence $0 \leq q \leq 1$.	
$\langle \cos \theta \rangle$	The average value of the cosine of the scattering angle for single scattering within the cloud	
θ_s	In-air transmitter zenith angle	Radians
ω_0	The single scattering albedo of the cloud particles, or, the ratio of the probability of scattering to the probability of extinction for a single scattering event.	
θ	The average angle for single scattering within the cloud	Radians

3.2.4 Cloud to Water

The required parameters are:

<u>Symbol</u>	<u>Description</u>	<u>Units</u>
H	Distance from Cloud Base to Water Surface	Meters
R	Range from the satellite transmitter to the submarine receiver	Meters
$\theta_{1/2}$	Full angle beam divergence to the e^{-2} irradiance points of transmitted beam	Radians

3.2.5 Air/Water Interface

The required parameters are:

<u>Symbol</u>	<u>Description</u>	<u>Units</u>
θ_S	In-air transmitter zenith angle	Radians
V	Surface wind speed	Meters/Second
n	Water index of refraction	

3.2.6 Water

The required parameters are:

<u>Symbol</u>	<u>Description</u>	<u>Units</u>
k_i	Diffuse attenuation coefficient of the i 'th water layer	(Meters) ⁻¹
D_i	Thickness of the i 'th water layer	Meters
θ_S^W	In-water transmitter zenith angle	Radians
θ_{SI}	Root-mean-square angle for a single scattering event in the water	Radians
s	Scattering coefficient for the entire water path	(Meters) ⁻¹
n	Water index of refraction	
D	Depth of the submarine receiver	Meters

3.2.7 Receiver

The required parameters are:

<u>Symbol</u>	<u>Description</u>	<u>Units</u>
θ_R	Half-angle of the receiver field of view	Radians
α	Off-set angle between the in-water signal beam axis and the receiver optical axis	Radians
D	Depth of the submarine receiver	Meters
τ_R	Transmission of the receiver optical chain	
d	Diameter of the receiver optical aperture	Meters

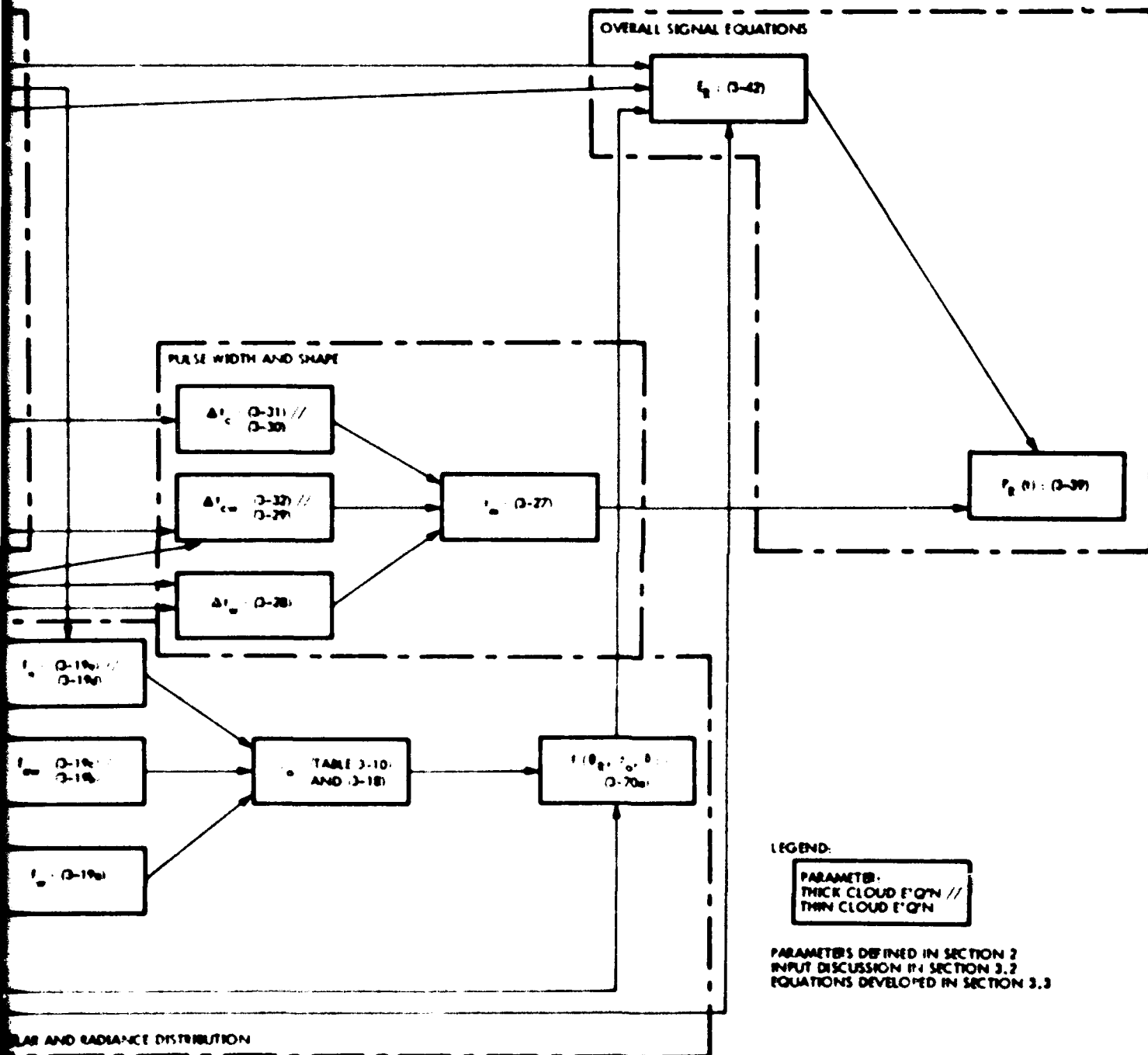


Figure 3-2. Flow Diagram of Single Pulse Downlink Propagation Model (Signal)

3.2 INPUT FOR SIGNAL CALCULATION

This section discusses the form of the required inputs to the signal single pulse downlink propagation model, in terms of the seven categories: source, clear atmosphere, cloud, cloud to water, air/water interface, water and receiver.

3.2.1 Source

The required source parameters are:

<u>Symbol</u>	<u>Description</u>	<u>Units</u>
q	A parameter describing the ability of the satellite transmitter to correct for the geometric zenith angle spreading of the spot. $q = 0$ implies the spot remains the same area, independent of zenith angle, while $q = 1$ means the spot grows naturally with zenith angle. Hence $0 \leq q \leq 1$.	
E_p	Energy per pulse of the transmitter laser.	Joules
γ_T	Transmission of the transmitter optical chain.	
R	Range from the satellite transmitter to the submarine receiver.	Meters
θ_T	Full angle beam divergence to the e^{-2} irradiance points of the transmitter beam.	Radians

3.2.2 Clear Atmosphere

The required parameters are:

<u>Symbol</u>	<u>Description</u>	<u>Units</u>
b	Effective clear atmosphere optical thickness such that for a 70%-zenith transmission, $b = 0.357$	
ϕ_s	In-air transmitter zenith angle	Radians

3.3 SUB-MODELS

This section develops all the equations used in the calculation of the instantaneous received signal power.

Sections 3.3.1, 3.3.2, 3.3.3, 3.3.4, 3.3.6 and 3.3.7 consider the path transmission of the energy.

Sections 3.3.5 and 3.3.8 consider the angular effects and the distribution of the received radiance.

Section 3.3.9 considers the received pulse shape and width.

In each of these sections, after the equations are developed they are evaluated for typical cases in both tables and figures.

Section 3.3.10 combines the previous results to obtain the received energy and the optical signal power.

3.3.1 Clear Atmospheric Transmission - Signal

In the absence of any clouds or aerosols, the clear atmospheric transmission is described by the term τ_a . Using the approximate AFCRL model¹, the signal zenith angle dependence is given by:

$$\tau_a = \exp - (b \sec \theta_s), \quad (3-1)$$

for τ_a = signal clear atmospheric transmission

b = effective clear atmospheric optical thickness

θ_s = signal zenith angle.

The typical value of b is determined from:

$$\tau_a (\theta_s = 0) = 0.7 = \exp (-b),$$

or

$$b = 0.357.$$

Table 3-1 and Figure 3-3 show the values of τ_a as a function of signal zenith angle.

References for Section 3.3.1

1. R.A. McClatchey, R.W. Fenn, J.E.A. Selby, F. E. Volz and J. S. Garing "Optical Properties of the Atmosphere (Revised)" AFRL-71-0279, 10 May 1971.

Table 3-1. Typical Clear Atmospheric Transmission ($b=0.357$)

θ_s , Signal Zenith Angle (degrees)	τ_a , Clear Atmospheric Transmission
0	0.7
10	0.7
20	0.68
30	0.66
40	0.63
50	0.57
60	0.49
70	0.35
80	0.13

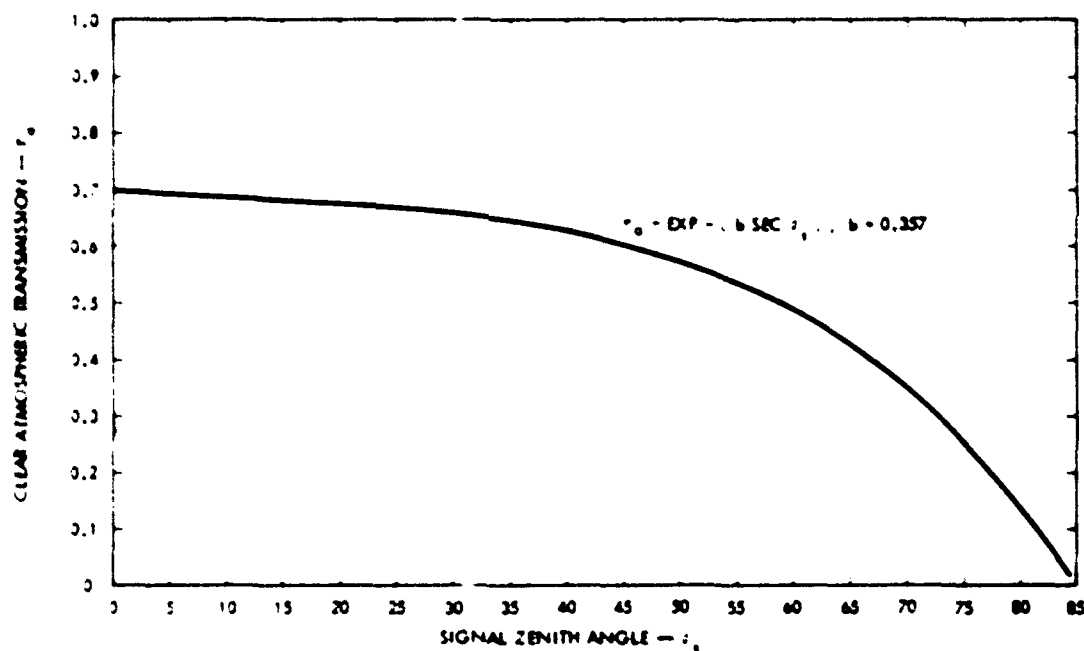


Figure 3-3. Typical Clear Atmospheric Transmission ($b = 0.357$)

3.3.2 Cloud Energy Transmission-Signal

Insofar as they affect optical propagation, clouds may be categorized as negligible to very thin, thin, and thick. There are no verified experimental results that treat any one of these three regimes. Since we are discussing an energy transmission here, and most analyses and partial experiments are in terms of the transmitted irradiance (energy per second per area), then there are few analytic expressions for the cloud energy transmission.

Our decision is to treat only two regimes - thick clouds and nearly clear weather. We do this with the understanding that evaluating the model near the transition point will yield results that are incorrect in principle, and so only for small and large optical thickness (defined below) should the overall model be expected to apply.

We propose to adopt the multiple-scattering Monte-Carlo derived diffusion-like expression of Bucher¹ and Van der Hulst² for thick clouds, so that at zenith, and neglecting in-cloud absorption:

$$\tau_c = \frac{1.69}{\tau_{opt} (1 - \langle \cos \theta \rangle) + 1.42} \quad (3-2)$$

for τ_c = Signal energy transmission through the cloud

τ_{opt} = Optical thickness of the cloud

$\langle \cos \theta \rangle$ = Mean cosine of the scattering angle.

The optical thickness of the cloud, for a homogeneous cloud, is given by:

$$\tau_{opt} = T \sigma_c$$

(3-3)

for

T = geometrical thickness of the cloud.

and σ_c = mean extinction coefficient of the cloud.

For a typical example, for a strato-cumulus cloud, we might have $T = 1200$ m and $\sigma_c = 0.04 \text{ m}^{-1}$ so $\tau_{opt} = 48$. For such a dense cloud, $\langle \cos \theta \rangle = 0.83$ ($\theta = 34^\circ$) and so

3.3.2 (Continued)

$$\tau_c = \frac{1.69}{48 (1 - 0.83) + 1.42} = 0.18$$

The zenith cloud energy transmission as a function of optical thickness is presented in Table 3-2 and Figure 3-4 for $\langle \cos \theta \rangle = 0.83$

Table 3-2. Typical "Thick" Cloud Zenith Signal Energy Transmission ($\langle \cos \theta \rangle = 0.83$), $\omega_0 = 1$.

τ_{OPT} , Optical Thickness	τ_c , Energy Transmission
10	0.54
20	0.35
30	0.26
40	0.21
50	0.17
60	0.15
70	0.13
80	0.11
90	0.10
100	0.09

From the form of Equation (3-2) it cannot apply at $\tau_{OPT} = 0$, and the lower limit of optical thicknesses at which it does apply is still to be determined. We provisionally adopt a linear fit for $\tau_{OPT} \leq 10$, so that

$$\tau_c = 1 - 0.046 \tau_{OPT}, \quad \tau_{OPT} \leq 10 \quad (3-4)$$

$\langle \cos \theta \rangle = 0.83$

Equation (3-4) is evaluated in Table 3-3, and Figure 3-4.

The zenith angle dependence for thick clouds has also been modeled by Bucher¹ and Van der Hulst². It also has no experimental verification.

Table 3-3. "Thin" Cloud Zenith Signal Energy Transmission (Matched to the Thick Cloud Expression at $\tau_{opt}=10$ for $\langle \cos \theta \rangle = 0.83$)

τ_{opt} Optical Thickness	τ_c Energy Transmission
0	1
2	0.91
4	0.82
6	0.72
8	0.63
10	0.54

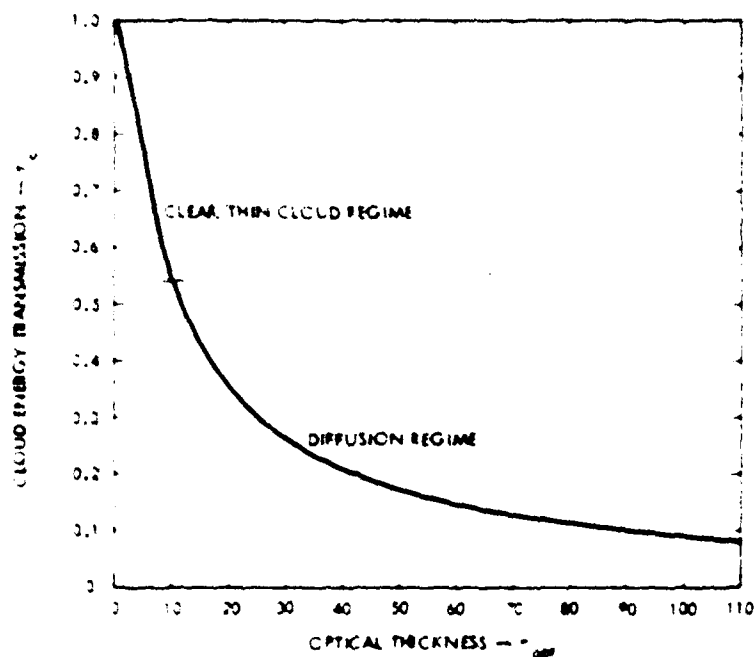


Figure 3-4. Thin and Thick Cloud Energy Transmission Versus Zenith Angles, for $\langle \cos \theta \rangle = 0.83$, $n=1$.

3.3.2 (Continued)

The resulting curve has been fit by L. Stotts of NOSC. An additional factor occurs because of the "spreading out" of the beam energy with zenith angle. Since this "spreading out" may be converted to the satellite terminal,* we shall model it as a transmission factor,

$$(\cos \theta_s)^q, \quad 0 \leq q \leq 1.$$

The complete thick cloud signal energy transmission (including the effects of the single scatter albedo³, $\omega_0 = 0.999$) is given by:

$$\begin{aligned} T_c = & \left\{ \frac{1}{\tau_{opt} (1 - \cos \theta_s) + 1.42} \right\} \left\{ \cos \theta_s \right\}^q \left\{ 1.69 - 0.5513 \theta_s + 2.7173 \theta_s^2 \right. \\ & \left. - 6.9666 \theta_s^3 + 7.1446 \theta_s^4 - 3.4249 \theta_s^5 + 0.6155 \theta_s^6 \right\} \times \\ & \left\{ 2 \sqrt{3(1 - \cos \theta_s)} (1 - \cos \theta_s) \right\} \left\{ \tau_{opt} + \frac{1.42}{1 - \cos \theta_s} \right\} \\ & \times \left\{ \exp - \left[\sqrt{3(1 - \cos \theta_s)} (1 - \cos \theta_s) \right] \left\{ \tau_{opt} + \frac{1.42}{1 - \cos \theta_s} \right\} \right] \right. \\ & \left. \left\{ 1 - \exp - \left[2 \sqrt{3(1 - \cos \theta_s)} (1 - \cos \theta_s) \right] \left\{ \tau_{opt} + \frac{1.42}{1 - \cos \theta_s} \right\} \right] \right\} \quad (3-5a) \\ & \text{for } 10 \leq \tau_{opt} \end{aligned}$$

* Except in the unusual condition of a minimum beam size constrained by satellite pointing jitter.

3.3.2 (Continued)

For thin clouds the diffusion like dependence ought not to apply. Therefore, in the $\tau_{OPT} \geq 10$ regime we assume a full cosine dependence due to the extra path length in the cloud, or

$$\tau_c = \left\{ 1 - 0.085\tau_{OPT} \left[\frac{1.69}{10(1 - \langle \cos \theta \rangle) + 1.42} \right] \right\} [\cos \theta_s]^q + 1$$

for $\tau_{OPT} \geq 10$.

For $\tau_{OPT} = 0$, we use $\tau_c = [\cos \theta_s]^q$ (3-5b)

For $\theta_s \approx 0$ these models are discontinuous at $\tau_{OPT} = 10$. The difference in value is approximately a factor of 0.58 at $\theta_s = 70^\circ$. At this stage in our knowledge of cloud propagation we do not feel that such a factor is of prime importance, and shall ignore this discrepancy until an experimentally verified model replaces it.

Table 3-4 and Figure 3-5 show the zenith angle dependence of the signal energy transmission for both τ_{OPT} regimes, with $q = 0$, i.e., satellite optics fully compensating for the zenith angle beam irradiance spread.

References for Section 3.3.2

1. E.A. Bucher, "Computer Simulation of Light Pulse Propagation for Communication Through Thick Clouds," Applied Optics, Vol. 12 (10), pp. 2391-2400, October 1973.
2. R.E. Danielson, D.R. Moore and H.C. Van de Hulst, "The Transfer of Visible Radiation Through Clouds," J. Atmos. Sci., Vol. 26 (9), pp. 1078-1087, September 1969.
3. The effect of $q \approx 1$ is taken from Appendix B, equation 14, of S. Karp, "A Test Plan for Determining the Feasibility of Optical Satellite Communications Through Clouds at Visible Frequencies," WOSC TN 279, July 1, 1978.

Table 3-4. Zenith Angle vs Signal Energy Transmission
 (Normalized to $\rho_s = 0$)

ρ_s , Signal Zenith Angle	Thick Cloud Dependence ($\tau_{OPT} \geq 10$)	Thin Cloud Dependence ($\tau_{OPT} \leq 10$)
0	1	1
10	0.97	0.98
20	0.96	0.94
30	0.92	0.87
40	0.86	0.77
50	0.78	0.64
60	0.69	0.5
70	0.58	0.34
80	0.44	0.17

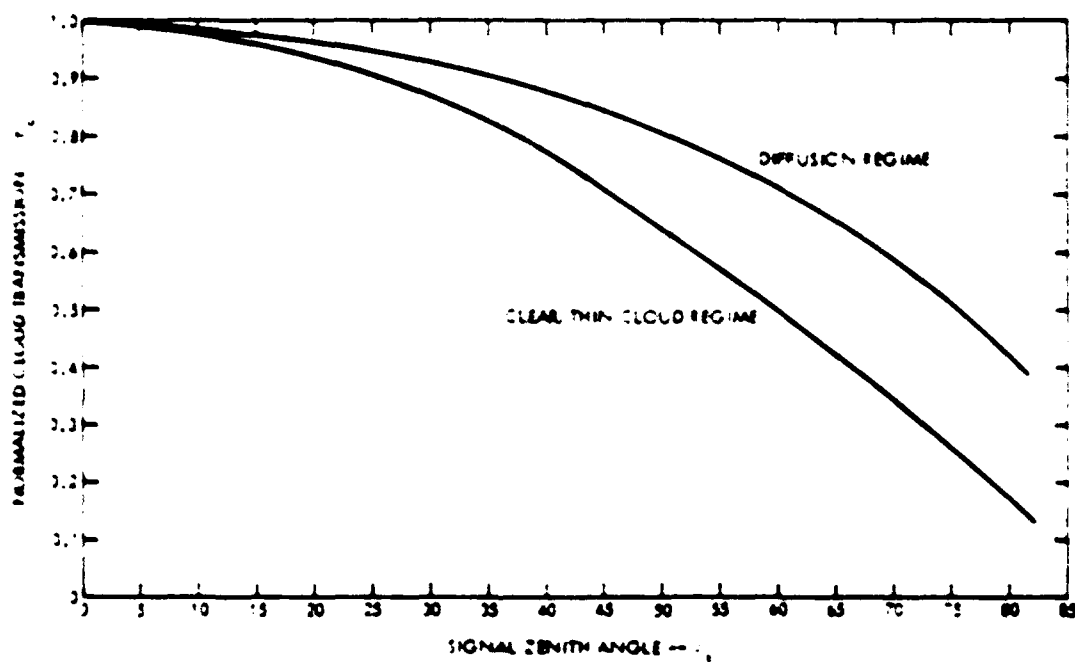


Figure 3-5. Thin and Thick Cloud Zenith Angle Dependence
 of Cloud Transmission Normalized to Zenith

The energy transmission of an assumed clear propagation path from the bottom of the cloud to the water surface is expressed as τ_{CW} . For large diameter emerging spots and representative clouds the energy transmission of this part of the propagation path is very high.

Then, assuming for a thick cloud the emerging energy has a Lambertian distribution, taking

R = range to satellite

$$I_{CW} = \frac{1}{4} \int_0^{2\pi} d\phi \int_0^{R_T/2} r dr \times (\text{"tilt" of emitting surface area})$$

$$\times (\text{Range from surface area to water surface "receiver"})^{-2}$$

$$\times (\text{"tilt" of surface "receiver"})$$

or

$$C_M = \frac{1}{2} \int_0^{2\pi} d\phi \int_0^{R_T/2} r dr \left(\frac{M}{[H^2 + r^2]^5} \right) \left(\frac{1}{[H^2 + r^2]^5} \right)^2 \left(\frac{M}{[H^2 + r^2]^5} \right).$$

$$\tau_{CW} = 1 - \frac{[H/(R a_T/2)]^2}{1 + [H/(R a_T/2)]^2} \cdot \tau_{OPT} \geq 10 \quad (3-6a)$$

3-18

Table 3-5. Thick Cloud-to-Water Surface
Signal Energy Transmission

$H / \frac{R_{0T}}{2}$	Cloud Base Height Emerging Spot Radius	τ_{CW} Energy Transmission
0		1
0.05		0.998
0.1		0.99
0.15		0.98
0.2		0.96
0.25		0.94
0.3		0.92
0.35		0.89
0.4		0.86
0.45		0.83
0.5		0.8

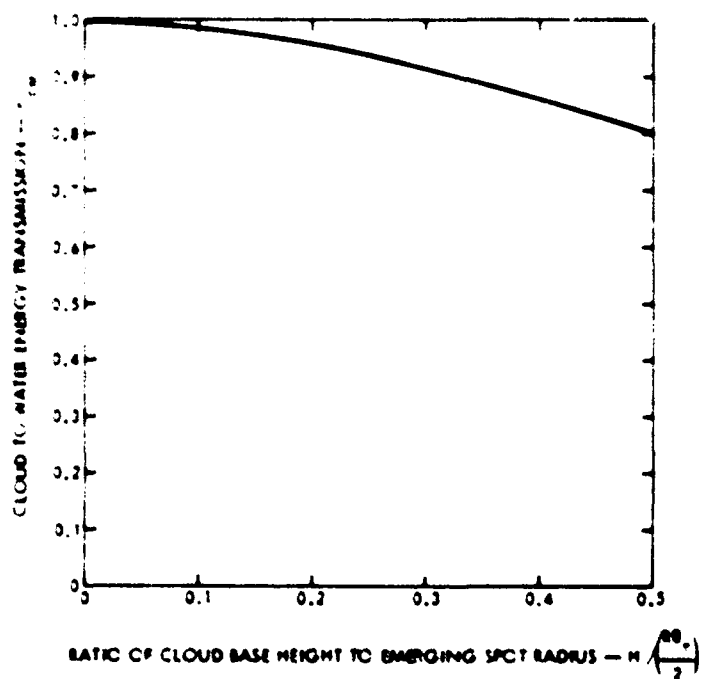


Figure 3-6. Thick Cloud to Water Surface Energy Transmission

3.3.3 (Continued)

For typical situations, $H/R\theta_T \approx 0.2$ and so this is a very small effect for thick clouds.

For thin clouds, the net transmission is even higher for large incident beams since the energy does retain its emitted angular sense. We therefore take

$$\tau_{CW} = 1, \text{ for } \tau_{OPT} \geq 10$$

(3-6b)

We further assume that there is no zenith angle dependence for τ_{CW} in either regime.

3.3.4 Air-Water Interface Transmission - Signal

The signal energy transmission of the air-water interface is composed of two factors:

$$\tau_{aw} = (\tau_{aw1}) \times (\tau_{aw2}),$$

for τ_{aw} = total energy transmission of air-water interface

τ_{aw1} = air-water interface transmission due to index of refraction discontinuity;

τ_{aw2} = air-water interface transmission due to foam and streaks on the sea surface.

This section treats τ_{aw1} while τ_{aw2} is discussed in Section 3.3.6.

For thin clouds and clear weather ($\tau_{opt} \leq 10$) we assume the signal beam retains its angular sense. Gordon¹ has estimated the value of τ_{aw1} as a function of surface wind speed and signal zenith angle, for the Cox and Munk² wave slope distribution, as shown in Table 3-6 and Figure 3-7.

For thick clouds ($\tau_{opt} > 10$), the energy is modelled as being incident on the sea surface from the entire hemisphere. Using the Fresnel refraction equation (and neglecting wave effects) we find

$$\tau_{aw1} = 1 - \int_0^{\pi/2} R(\theta_s) \sin \theta_s d\theta_s \quad (3-7)$$

for θ_s = signal zenith angle

$R(\theta_s)$ = Sea Surface reflectance as a function of zenith angle.

$$\text{and } R(\theta_s) = \frac{[f_1(\theta_s) - f_2(\theta_s)] f_3(\theta_s)}{[f_1(\theta_s) + f_2(\theta_s)] [f_3(\theta_s) + f_2(\theta_s)]} \quad (3-8)$$

$$\text{for } f_1(\theta_s) = \sin^2(\theta_s) [n^2 + \cos 2\theta_s] \quad (3-9a)$$

$$\text{for } f_2(\theta_s) = \sin \theta_s \sin 2\theta_s [n^2 - \sin^2 \theta_s]^{1/2} \quad (3-9b)$$

$$\text{and } f_3(\theta_s) = n^2 \cos 2\theta_s - \sin^2 \theta_s \cos 2\theta_s. \quad (3-9c)$$

and n = sea-water index of refraction.

Table 3-6. τ_{awl} Time-Averaged Downlink Air-Sea Interface Transmittance
(For Thin Clouds, $\tau_{opt} \leq 10$)

θ Signal Zenith Angle in Air	V Wind Speed								
	0	1.03	2.06	4.12	7.21	10.3	13.4	16.5	19.6 m/sec
	0	2	4	8	14	20	26	32	38 knots
0	0.979	0.977	0.976	0.974	0.970	0.967	0.963	0.960	0.956
5	0.975	0.974	0.972	0.970	0.966	0.963	0.959	0.956	0.952
10	0.964	0.962	0.961	0.959	0.955	0.951	0.948	0.944	0.941
15	0.945	0.944	0.943	0.940	0.936	0.933	0.929	0.926	0.922
20	0.920	0.918	0.917	0.914	0.910	0.907	0.903	0.899	0.896
25	0.887	0.885	0.884	0.881	0.877	0.873	0.870	0.866	0.863
30	0.847	0.845	0.844	0.841	0.837	0.833	0.829	0.826	0.822
35	0.800	0.798	0.797	0.794	0.790	0.786	0.782	0.779	0.775
40	0.747	0.745	0.743	0.741	0.736	0.732	0.729	0.725	0.722
45	0.687	0.685	0.684	0.681	0.677	0.673	0.669	0.666	0.663
50	0.620	0.619	0.617	0.615	0.611	0.608	0.605	0.602	0.599
55	0.548	0.546	0.545	0.543	0.540	0.538	0.536	0.534	0.532
60	0.468	0.468	0.468	0.468	0.465	0.464	0.464	0.464	0.463
65	0.385	0.385	0.385	0.386	0.387	0.389	0.391	0.393	0.396
70	0.296	0.298	0.299	0.303	0.310	0.315	0.321	0.325	0.329
75	0.203	0.208	0.214	0.224	0.236	0.247	0.255	0.262	0.268
80	0.113	0.126	0.136	0.153	0.172	0.186	0.197	0.206	0.213
85	0.0361	0.0610	0.0751	0.0908	0.119	0.135	0.148	0.157	0.165
90	0	0.0285	0.0390	0.0504	0.0608	0.0661	0.108	0.117	0.124

3.3.4 (Continued)

Using $n = 1.33$, (3-7) has been evaluated with the result

$$\tau_{awl} = 0.83, \tau_{opt} \geq 10.$$

(3-10)

Equation (3-10) is an approximation since it has neglected the wave structure of the surface and is discontinuous with the $\tau_{opt} \leq 10$ values in Table 3-6. We shall use it pending further analysis and experimentation.

There is no zenith angle dependence for thick clouds for τ_{awl} .

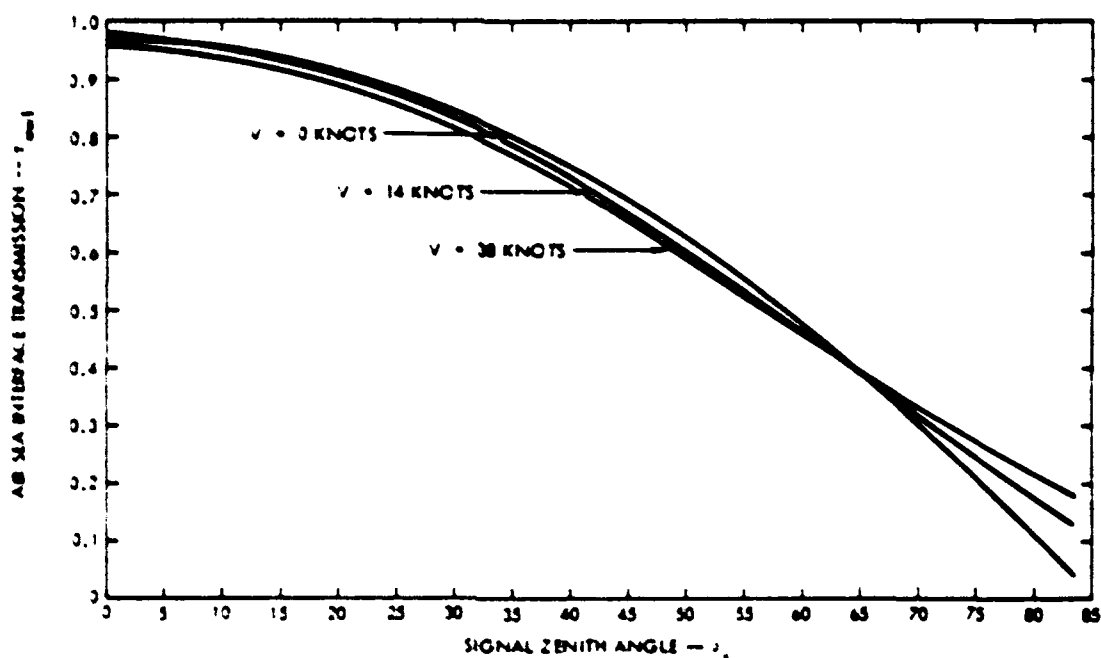


Figure 3-7. Thin Cloud Air-Sea Interface Transmission as a Function of Signal Zenith Angle (θ_s) and Surface Wind Speed, V

3.3.4 (Continued)

References for Section 3.3.4

1. J. Gordon, Directional Radiance (Luminescence) of the Sea Surface, SIO Ref. 89-20, October 1969, as cited in R.E. Howarth, M.E. Hyde and W.R. Stone, "Submarine-Aircraft and Submarine-Satellite Optical Communication Systems Model (U)," Confidential Report, NELC-TR-2021, 1977.
2. C. Cox and W. Munk, "Statistics of the Sea Surface Derived from Sun Glitter, J. Mar. Research Vol 13 2, 1954.

3.3.5 Air-Water Angular Effects - Signal

The wave slopes on the sea surface cause an overall increase in the beam divergence of an incident beam. For the propagation path considered here, only for the thin cloud and clear weather cases ($\tau_{opt} \leq 10$) will this have any effect.

We describe the statistical effects of the surface by $\Delta\theta_{AW}$ = half-angle of the rms additional beam divergence of the radiance profile. Adopting Karp's unverified model¹ we use the expression

$$\Delta\theta_{AW} = 0.0103 V^{1/2}, \quad (\tau_{opt} \leq 10) \quad (3-11a)$$

for V = surface wind speed in knots, and the index of refraction of sea water has been taken = 4/3. Equation (3-11a) is evaluated in Table 3-7 and Figure 3-8 for V in knots (and m/sec) and $\Delta\theta_{AW}$ in radians (and degrees).

The relative contribution of $\Delta\theta_{AW}$ to the distribution of radiance at the receiver will be discussed in Section 3.3.8. Except for the clearest water it is a small effect and so the impact of neglecting zenith angle effects, and dissimilar wave slopes in the downwind and crosswind direction, may be negligible. We therefore adopt this model, and

$$\Delta\theta_{AW} = 0, \quad \tau_{opt} \geq 10 \quad (3-11b)$$

until better information is available.

References for Section 3.3.5

1. As cited in R.E. Howarth, M.E. Hyde, and W.R. Stone, "Submarine-Aircraft and Submarine Satellite Optical Communications Systems Model (U)," Confidential Report, NELC-TR-2021, 1977.

Table 3-7. Half-Angle RMS Air-Water Interface Effects

V, Wind Speed		$\Delta \theta$ AW	
Knots	Meters/Sec	Milliradians	Degrees
0	0	0	0
2	1.03	14.6	0.84
4	2.06	20.7	1.18
8	4.12	29.2	1.67
14	7.21	38.6	2.21
20	10.3	46.2	2.65
26	13.4	52.6	3.0
32	16.5	58.4	3.35
38	19.6	63.6	3.64

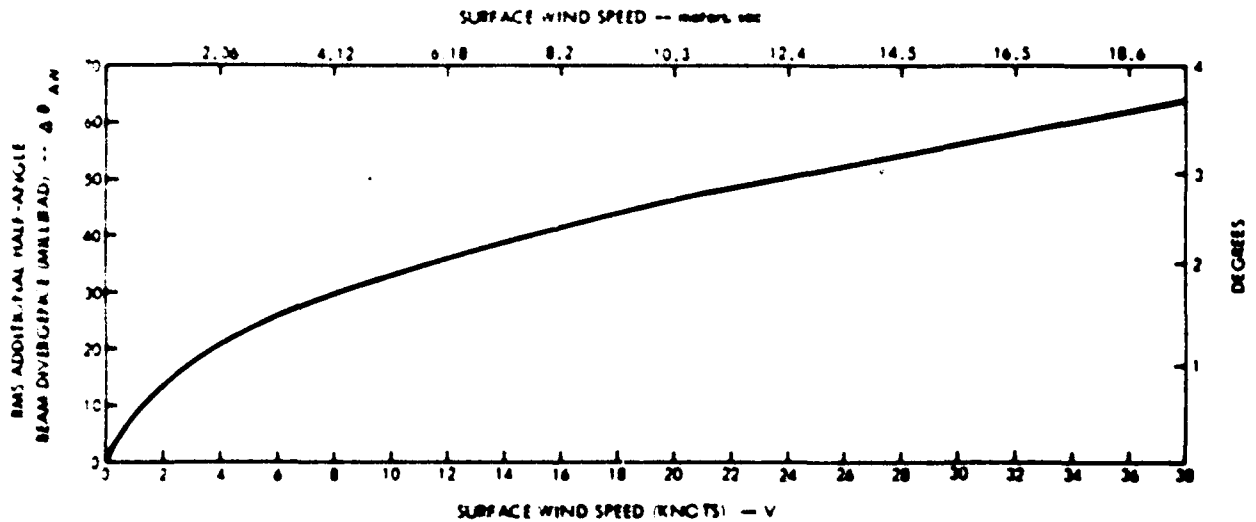


Figure 3-8. Half-Angle RMS Air-Water Interface Effects as a function of Wind Speed V

3.3.6 Relative Surface Foam Coverage

The energy transmission of the air-water interface is composed of the factors:

$$\tau_{aw} = (\tau_{aw1}) \times (\tau_{aw2}).$$

for τ_{aw} = total energy transmission of the air-water interface

τ_{aw1} = air water interface transmission due to index of refraction discontinuity

and τ_{aw2} = air water interface transmission due to foam and streaks on the water surface.

This section treats τ_{aw2} , while τ_{aw1} was discussed in Section 3.3.4. Independent of the cloud conditions, a model relating the fraction of surface covered to the surface wind speed is given by¹

$$C_f = (1.2 \times 10^{-5}) V^{3.3}, \quad V \leq 9 \text{ m/sec} \quad (3-12)$$

$$\text{and } C_f = (1.2 \times 10^{-5}) V^{3.3} (0.225 V - 0.99); \quad V \geq 9 \text{ m/sec.} \quad (3-13)$$

for C_f = fraction of surface covered

V = surface wind speed in meters/sec.

Assuming the foam and streaks have an albedo of 1, the value of τ_{aw2} is given by:

$$\tau_{aw2} = 1 - (1.2 \times 10^{-5}) V^{3.3}, \quad V \leq 9 \text{ m/sec} \quad (3-14a)$$

$$\text{and } \tau_{aw2} = 1 - (1.2 \times 10^{-5}) V^{3.3} (0.225 V - 0.99); \quad V \geq 9 \text{ m/sec} \quad (3-14b)$$

Equations (3-14a, b) are evaluated in Table 3-8 and Figure 3-9 for V in meters/sec (and knots).

Although this model neglects zenith angle effects, we shall adopt it pending further experimental work.

References for Section 3.3.6

1. As cited in H.R. Gordon and M.M. Jacobs, "Albedo of the Ocean-Atmospheric System: Influence of the Sea Foam," Appl. Opt. Vol 16 (8) pp 2257-2260, Aug 1977.

Table 3-8. Air-Water Energy Transmission Due to Surface Foam and Streaks
(Assuming a foam/streak albedo = 1)

V, Wind Speed		τ_{aw2}
Knots	Meters/Sec	
0	0	1
2	1.03	1
4	2.06	1
8	4.12	1
14	7.21	0.99
20	10.3	0.96
26	13.4	0.87
32	16.5	0.66
38	19.6	0.25

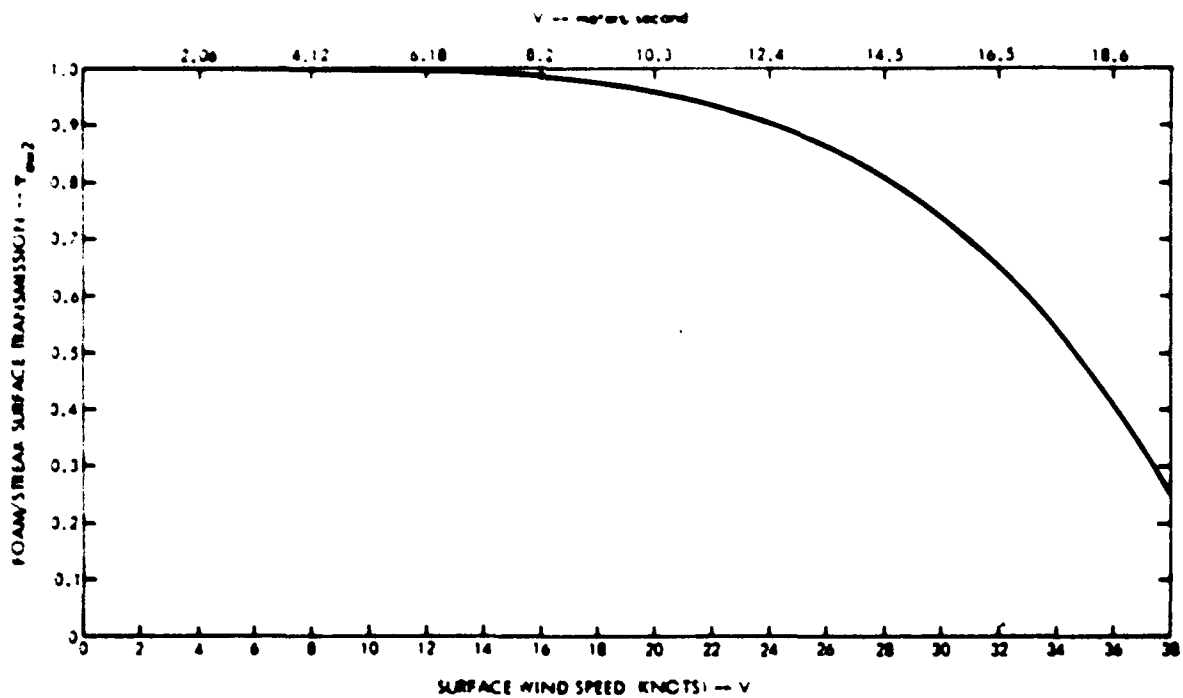


Figure 3-9. Foam/Streak Surface Coverage Transmission versus Surface Wind Speed

3.3.7 Water Energy Transmission-Signal

The energy transmission of the water portion of the propagation path is denoted by τ_w . For most water types and receiver depths the dominant cause of attenuation is the diffuse attenuation coefficient¹ of the water, k . We therefore use the model:

$$\tau_w = \exp - (k \times (\text{PATH LENGTH IN WATER})).$$

The path length in the water for $\tau_{opt} \geq 10$ is given by:

$$D / \cos (\theta_s^w).$$

for

D = receiver depth

θ_s^w = in water signal zenith angle.

From Snell's law,

$$n \sin (\theta_s^w) = \sin \theta_s. \quad (3-15)$$

for

n = water index of refraction

θ_s = in air signal zenith angle.

Table 3-9 and Figure 3-10 show the values of Equation (3-15) for $n = 1.33$.

Since many areas of the ocean have a layered structure for k , we modify our basic equation for clear weather or thin cloud conditions to yield:

$$\frac{k D}{\cos (\theta_s^w)} = \frac{1}{\cos (\theta_s^w)} \sum_{i=1}^j (k_i D_i),$$

where we have assumed there are j layers which differ in their k values, but not in their indices of refraction. Therefore, the adopted model for $\tau_{opt} \geq 10$ is

Table 3-9. Relation Between In-Air and In-Water Signal Zenith Angles
(Assuming Sea-Water Index of Refraction, $n = 1.33$)

θ_s , In-Air Signal Zenith Angle (Degrees)	θ_s^w , In-Water Signal Zenith Angle (Degrees)
0	0
5	3.75
10	7.48
15	11.19
20	14.86
25	18.48
30	22.02
35	25.48
40	28.82
45	32.03
50	35.07
55	37.91
60	40.51
65	42.82
70	44.81
75	46.42
80	47.61
85	48.34

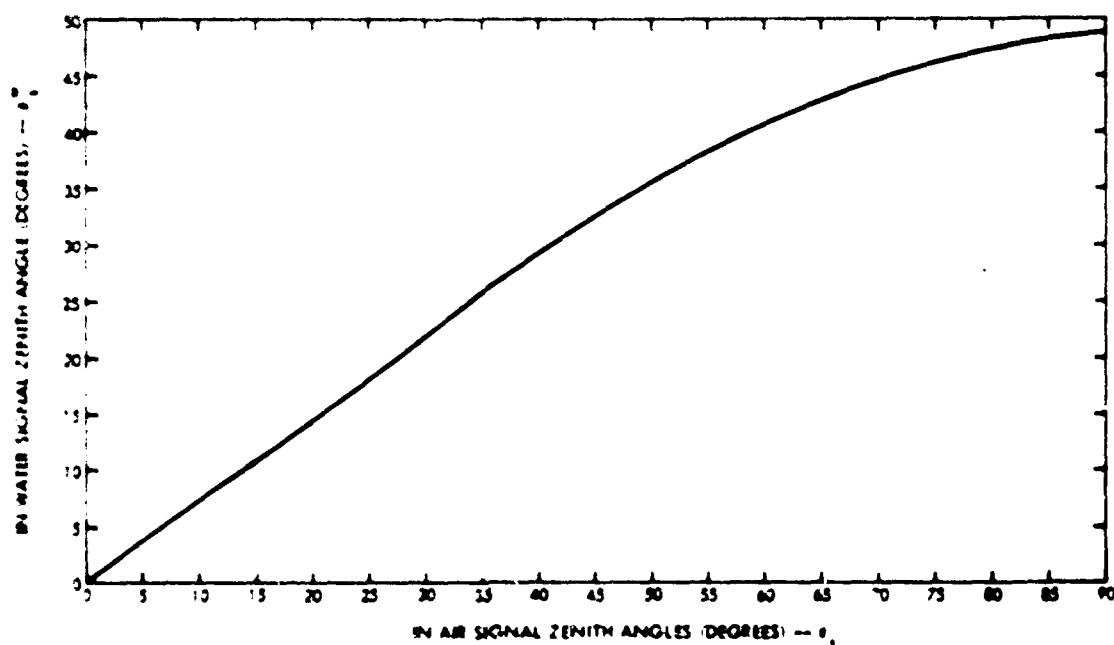


Figure 3-10. Relation Between In-Air and In-Water Signal Zenith Angles
(Assuming Sea-Water Index of Refraction, $n = 1.33$)

3.3.7 (Continued)

$$\tau_w = \exp - \left\{ \frac{\sum_{i=1}^J k_i D_i}{\cos \theta_s^w} \right\}, \text{ for } \tau_{opt} = 10$$

(3-16a)

$$\theta_s^w = \sin^{-1} \left(\frac{1}{n} \sin \theta_s \right) \text{ and } \sum_{i=1}^J D_i = 0$$

For thick cloud conditions, the energy peaks at zenith. Since k_i is an effective diffusion coefficient, the thick cloud water energy transmission is given by

$$\tau_w = \exp - \left\{ \sum_{i=1}^J k_i D_i \right\}, \text{ for } \tau_{opt} > 10$$

(3-16b)

This model is uncertain in many ways:

- (1) The value of k_i to use.
- (2) The values of D_i .
- (3) Its applicability in very clear water and/or at shallow receiver depths.

Consequently, although it is the best model available now, it may be revised when better information becomes available.

References for Section 3.3.7

1. R.E. Howarth, M.E. Hyde and W.R. Stone, "Submarine Aircraft and Submarine-Satellite Optical Communication Systems Model (U)". Confidential Report, NELC-TR-2021, 1977.
2. M. Abramowitz and I.A. Stegun, editors, Handbook of Mathematical Functions, NBS, Applied Mathematics Series 35, Government Printing Office, November 1970, p. 228, 238-243.

3.3.8 Water Distribution of Radiance - Signal

There is no experimentally verified expression for the in-water distribution of signal radiance as a function of incident beam collimation, incident beam zenith angle, water properties, and receiver depth. Any model expression must take into account the following items:

- (1) The in-air zenith angle of the signal;
- (2) The radiance distribution incident on the water;
- (3) The air-water interface effects;
- (4) The in-water zenith angle of the signal;
- (5) The in-water scattering effects;
- (6) The in-water absorption effects.

In considering these last two, we note that the energy should decrease away from zenith due to absorption, and depending on depth and the water properties. We have therefore considered the following zenith angle dependencies for the radiance at the submarine receiver:

(1) Uniform

$$(2) \quad 1 - \left(\frac{\theta^w}{\theta_0} \right)$$

$$(3) \quad \frac{\sin(\theta_0 - \theta^w)}{\sin \theta_0}$$

$$(4) \quad 1 - \left[\frac{\sin(\theta^w)}{\sin(\theta_0)} \right]^2$$

$$(5) \quad \exp - \left(\frac{\theta^w}{\theta_0} \right)$$

3.3.b (Continued)

for θ^w = angle measured from the axis, or principal ray direction, of the in-water signal radiance,

and θ_0 = angle at which the signal radiance reaches a benchmark, i.e. 0 for (2) (3) and (4), and e^{-2} for (5).

We adopt (4), $\left[\frac{1 - \sin \theta^w}{\sin \theta_0} \right]^2$, because it is easy to work with, and appears to

give a reasonable representation of the assumed radiance.

θ_0 is related to the half power point of the received radiance by the equation

$$\frac{1}{2} = \frac{1 - \cos(\theta_{1/2}) - \frac{1}{3 \sin^2 \theta_0} \left[\cos \theta_{1/2} \sin^2 \theta_{1/2} + 2 \cos \theta_{1/2} - 2 \right]}{1 - \cos \theta_0 - \frac{1}{3 \sin^2 \theta_0} \left[\cos \theta_0 \sin^2 \theta_0 + 2 \cos \theta_0 - 2 \right]} \quad (3-17)$$

Equation (3-17) is evaluated in Table 3-10. Values between those shown are obtained by linear interpolation.

Table 3-10. Relation of Radiance Zero Point, θ_0 , and Received Radiance Half-Power Point, $\theta_{1/2}$, for $1 - (\sin \theta^w / \sin \theta_0)^2$ Radiance Distribution

$\theta_{1/2}$ (degrees)	θ_0 (degrees)
3.8	5
7.6	10
11.4	15
15.2	20
19.0	25
22.7	30
26.5	35
30.2	40
33.9	45
37.5	50
41.1	55
44.6	60
48.1	65
51.6	70
54.9	75
58.2	80

3.3.8 (Continued)

We adopt the NOSC developed expression for the half-power point in terms of incident beam divergence, air-water angular effects and in-water scattering effects, and add them up as if they were three statistically* independent effects:

$$\theta_{1/2} = [f_w^2 + f_{aw}^2 + f_d^2]^{1/2} \quad (3-18)$$

for

$$f_w = \text{water contribution} \\ = \frac{\theta_{st}^2 \sin^2 \theta}{\cos^2 \theta_s} \quad \text{all } \theta_{OPT} \quad (3-19a)$$

*This is actually an empirical result, and appears to fit the NOSC experimental results. A completely consistent theory of all these effects would not use the statistical independence as the justification for this expression.

3.3.8 (Continued)

$$f_{dw} = (0.0103 v^{1/2})^2; \quad \tau_{OPT} \leq 10 \quad (3-19b)$$

$$= 0; \quad \tau_{OPT} \geq 10 \quad (3-19c)$$

and

$$f_d = \left(\frac{1}{n}\right)^2 (0.294 \theta_T)^2; \quad \tau_{OPT} \leq 10; \quad (3-19d)$$

$$= (33.8^\circ)^2; \quad \tau_{OPT} \geq 10. \quad (3-19e)$$

for σ_s^2 = mean square single scattering angle in water

s = scattering coefficient in water

D = receiver depth

θ_s^w = in-water signal zenith angle.

v = surface wind speed in knots

τ_{OPT} = cloud optical thickness

n = water index of refraction

θ_T = e^{-2} irradiance full angle of in-air incident beam.

Equation 3-19a is the MOSC¹ expression, and contains the only zenith angle dependence for the radiance distribution. We could modify it for layering effects ($\sigma_s \rightarrow \sigma_{s_i}$; $s \rightarrow s_i$; $D \rightarrow D_i$ and $f_w \rightarrow f_w(i)$) but shall not at this time, until further experimental results are obtained.

Equations 3-19b and 3-19c are based on the discussion in Section 3.3.5.

Equations 3-19d is the refraction-corrected beam divergence of the collimated incident beam, again assuming a Gaussian distribution in angle.

Equations 3-19e assumes that after penetration through thick clouds the light has a uniform angular distribution at the water surface. Then, Snell's law implies that just below the water surface, all the energy is contained within a solid angle of half-angle = 48.6° , neglecting wave action. Then, defining the half-power angle as the half-angle of the solid angle containing half of the energy, implies

3.3.8 (Continued)

$$1 - \cos \delta = \frac{1}{2} (1 - \cos 48.6^\circ)$$

or, $\delta = 33.8^\circ$.

The radiance distribution enters into the expression for the received energy by the expression

$$f(\theta_R, \theta_0, \delta) = \frac{\int_0^{\theta_R} \left[1 - \left(\frac{\sin \theta^W}{\sin \theta_0} \right)^2 \right] d\theta}{\int_0^{\theta_0} \left[1 - \left(\sin \theta^W / \sin \theta_0 \right)^2 \right] d\theta}$$

for

- θ_R = solid angle of the receiver,
- θ_0 = full solid angle which all the energy is within,
- θ_R = half-angle of the receiver field of view,
- δ = off-set angle between receiver optical axis and axis of the incoming light.

Therefore, for the general case,

$$f(\theta_R, \theta_0, \delta) = \frac{\int_0^{2\pi} d\phi \int_0^{\theta_R} d\theta \sin \theta^W \left[1 - \left(\frac{\sin \theta^W}{\sin \theta_0} \right)^2 \right]}{\int_0^{2\pi} d\phi \int_0^{\theta_0} d\theta \sin \theta^W \left[1 - \left(\frac{\sin \theta^W}{\sin \theta_0} \right)^2 \right]} \quad (3-20a)$$

for $\theta^W = \cos^{-1} \{ \cos \theta^W \cos \delta + \sin \theta^W \sin \delta \sin \phi \}$.

For perfect alignment between the received light axis and the receiver ($\delta = 0$), the integral can be analytically evaluated, with the result

$$f(\theta_R, \theta_0) = \frac{1 - \cos \theta_R - \left(\frac{1}{3 \sin^2 \theta_0} \right) \left[\cos \theta_R \sin^2 \theta_0 + 2 \cos \theta_R - 2 \right]}{1 - \cos \theta_0 - \frac{1}{3 \sin^2 \theta_0} \left[\cos \theta_0 \sin^2 \theta_0 + 2 \cos \theta_0 - 2 \right]} \quad (3-20b)$$

Equation (3-20a) has been evaluated in Figure 3-11, for $\theta_0 = 30^\circ$ (Figure 3-11a) and $\theta_0 = 70^\circ$ (Figure 3-11b) and $\theta = 0^\circ, 10^\circ, 20^\circ, 30^\circ, 40^\circ, 50^\circ, 60^\circ$.

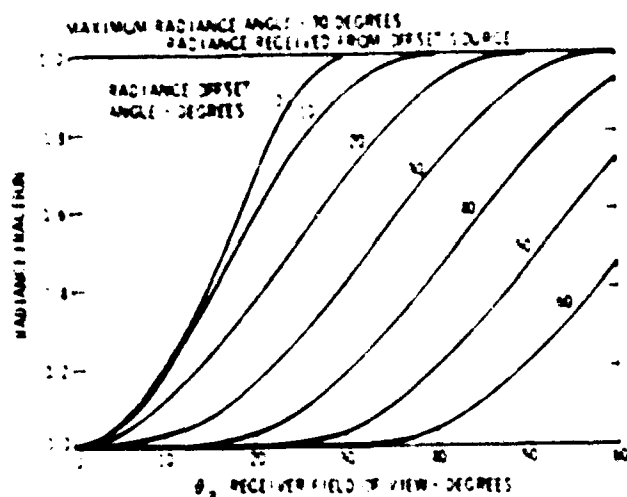


Figure 3-11a $f(\theta_R, \theta_0, \theta)$ for $\theta_0 = 30^\circ$

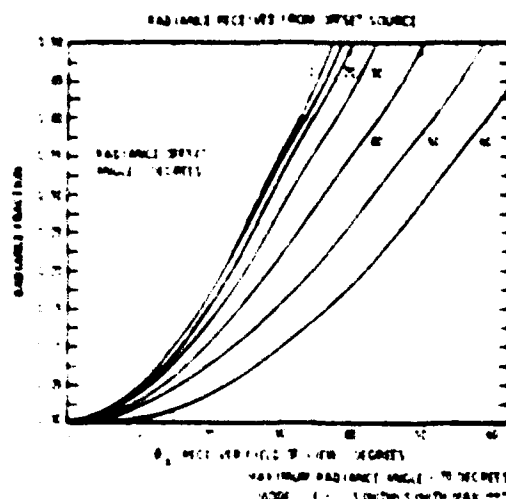


Figure 3-11b $f(\theta_R, \theta_0, \theta)$
 for $\theta_0 = 70^\circ$

These results will be used in Section 3.3.10.

3.3.8 (Continued)

References for Section 3.3.8

1. R.E. Howarth, M.E. Hyde and W.R. Stone, "Submarine-Aircraft and Submarine-Satellite Optical Communications Systems Model (U)", Confidential Report, NELC-TR2021, 1977.

3.3.9 (Continued)

The rms value of t , defined as

$$\left\{ \frac{\int_0^{\infty} t^2 f(t) dt}{\int_0^{\infty} f(t) dt} \right\}^{1/2} = \sqrt{6} t_M. \quad (3-24c)$$

Hence the variance of t is given by $\text{var } t = (\overline{t^2} - \bar{t}^2) = 2 t_M^2.$ (3-25a)

and its standard deviation by $[\overline{t^2} - \bar{t}^2]^{1/2} = \sqrt{2} t_M.$ (3-25b)

The area under the $f(t)$ curve is given by

$$\int_0^{\infty} f(t) dt = t_M^2. \quad (3-26)$$

In principle there are three significant contributions to the received pulse width, which we shall define as the time between half power points,

$2.45 t_M = (\Delta t_C + \Delta t_{CW} + \Delta t_W).$

(3-27)

where we have neglected the initial pulse width at the transmitter, assumed that the effects add serially, not statistically, and

- Δt_W = pulse width due to water portion of the path,
- Δt_{CW} = additional pulse width due to cloud-to-water path,
- Δt_C = pulse width after emerging from the cloud.

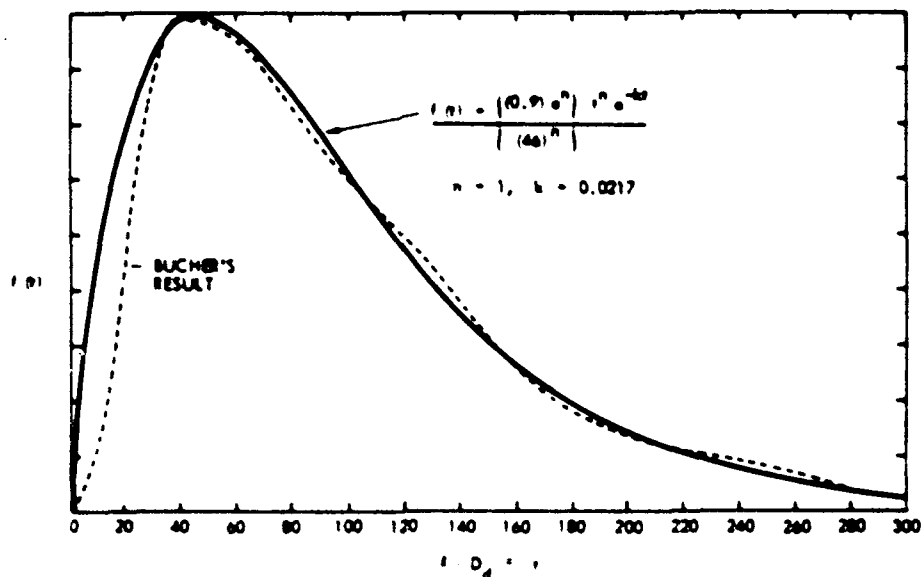


Figure 3-12. Comparison of $f(t)$ and Bucher's Monte Carlo Pulse Shape

3.3.9 (Continued)

The additional pulse width due to the water portion of the path is caused by the in-water multiple scattering, and so it occurs in the absence or presence of clouds. As seen in Figure 3-13, a signal at a zenith angle of 0° and a receiver of half angle θ_R at a depth D leads to a pulse width (for a uniform contribution throughout that field of view)

$$\Delta t_w = \frac{D}{c/n} \left(\frac{1 - \cos \theta_R}{\cos \theta_R} \right), \text{ all } \tau_{opt} \quad (3-28)$$

for c = speed of light

n = water index of refraction.

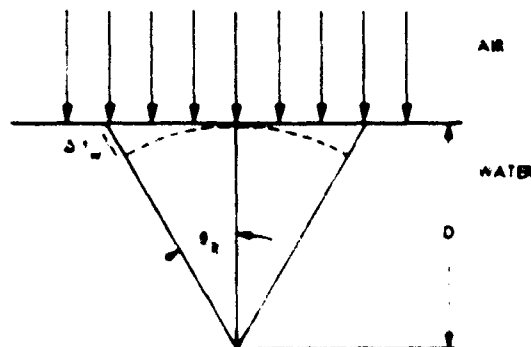


Figure 3-13. In-Water Pulse Width Calculation Geometry

3.3.9 (Continued)

When the signal zenith angle is not 0° , an additional pulse stretching occurs, as shown in Figure 3-14. The effect is given by

$$\Delta t_{cw} = \frac{2 D \tan \theta_r \sin \theta_s}{c}, \quad \tau_{opt} \leq 10 \quad (3-29)$$

for θ_s = signal zenith angle.

When thick clouds are in the path, there is no single zenith angle defined below the clouds, and so this expression will not apply.

For thin clouds ($\tau_{opt} \leq 10$) we have found no verified expression for the cloud effects or the cloud to water effects. Since Equations (3-28) and (3-29) already imply stretching to a few hundred nanoseconds, we can neglect the thin cloud effects, and take

$$\Delta t_c = 0, \quad \tau_{opt} \leq 10 \quad (3-30)$$

All zenith angles

For thick clouds we adopt the Stotts³ expression, (applicable for $\omega_0 > 0.999$) so that:

$$\Delta t_c = \frac{\tau}{c} \left\{ \frac{0.3}{\omega_0 \tau_{opt}^2} \left[(1 + 2.25 \omega_0 \tau_{opt}^2)^{1.5} - 1 \right] - 1 \right\}, \quad \tau_{opt} \leq 10 \quad (3-31)$$

All zenith angles

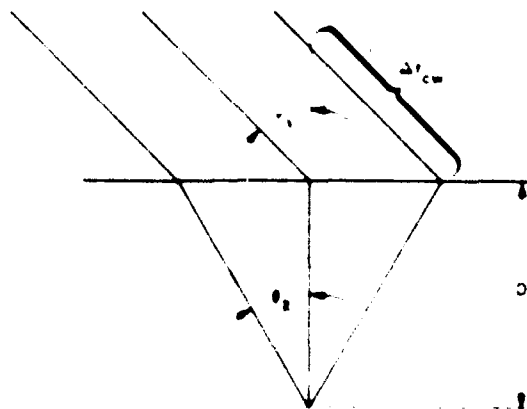


Figure 3-14. Signal Zenith Angle Induced Additional Pulse Stretching

3.3.9 (Continued)

for T = cloud geometrical thickness,

ω_0 = single scatter albedo,

θ = mean scattering angle in the cloud.

Equation (3-31) has been evaluated in Table 3-11 and Figure 3-15 for the typical values of $\omega_0 \approx 1$, $\theta = 0.66$ rad (37°), and fixing $T = \tau_{opt}/\tau_c = 25 \tau_{opt}$ suitable for a strato-cumulus cloud. (Also shown for comparison is the result estimated in Reference 2.)

These values probably overestimate the pulse widths at the lower values of τ_{opt} , but we shall adopt them until a verified model for all values of τ_{opt} is developed.

We use the values from Table 3-11 for $\tau_{opt} = 20, 40$, and 60 along with the normalized pulse shape $[F(t) = (t_M^{-2}) t \exp - (t/t_M)]$ to plot representative pulses in Figure 3-16. The drastic dependence of the pulse height and width on optical thickness for the assumed model is clearly seen.

Table 3-11. Typical "Thick" Cloud Pulse Broadening for $\omega_0=1$,
 $\theta=37^\circ$ and $\sigma_c=0.04 \text{ m}^{-1}$

τ_{opt} , Optical Thickness	T, Geometrical Thickness (km)	Δt_c , Pulse Width (μsec)
10	0.25	1.15
20	0.5	3.65
30	0.75	7.08
40	1.0	11.27
50	1.25	16.13
60	1.5	21.55
70	1.75	27.48
80	2.0	33.93
90	2.25	40.88
100	2.5	48.25

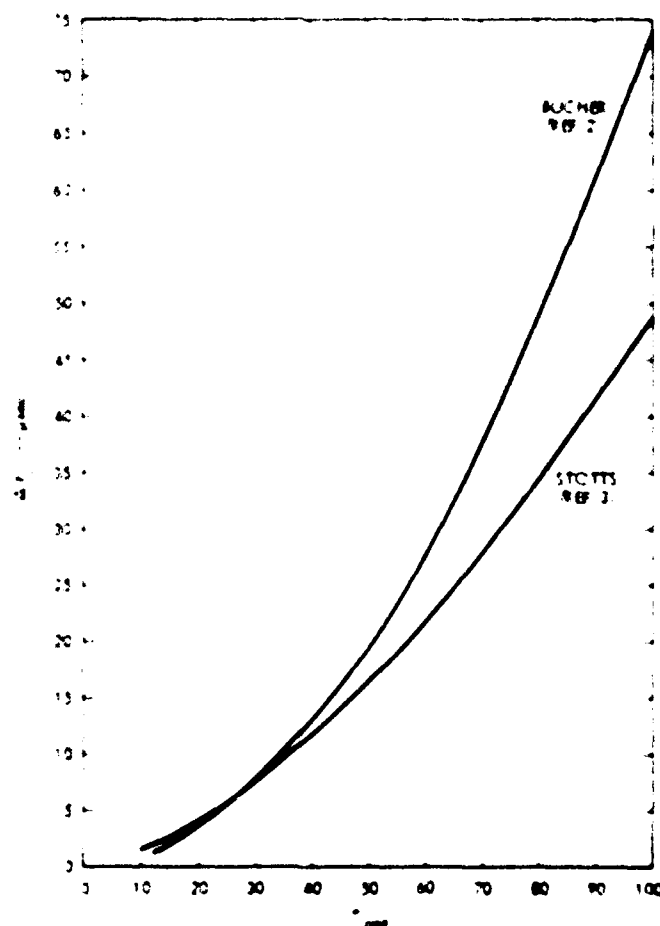
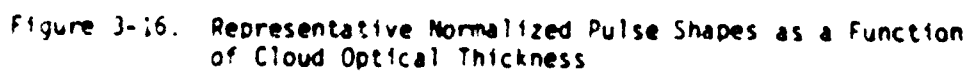


Figure 3-15. Cloud Induced Pulse Stretching as a Function
of Optical Thickness ($\sigma_c=0.04 \text{ m}^{-1}$, $\omega_0=1$)



3.3.9 (Continued)

A careful analysis of the thick cloud to water propagation region has found that it adds a negligible amount relative to Δt_c for reasonable cloud properties and cloud heights. Hence we take

$$\Delta t_{cw} = 0, \quad \tau_{opt} \geq 10.$$

(3-32)

All zenith angles

We therefore have adopted a complete model for all effects and all optical thicknesses. It shall be used further in the next section.

References for Section 3.3.9

1. All present at the NOOSC sponsored Cloud Propagation Symposium, March 1978.
2. E.A. Bucher, "Computer Simulation of Light Pulse Propagation for Communication through Thick Clouds," Applied Optics vol 12 (10) pp 2391-2400, October 1973.
3. L.B. Stotts, "Closed Form Expression for Optical Pulse Broadening in Multiple Scattering Media," Applied Optics vol 17 (4) pp 504-505, Feb 15, 1978.

3.3.10 Overall Signal Equations

The optical detection mechanism responds to the received energy as a function of time, i.e., the instantaneous optical power. The total received optical energy and the instantaneous optical power are related by:

$$E_R = \int_0^{\infty} P_R(t) dt \quad (3-33)$$

for

- E_R • total received optical energy per pulse, and
- $P_R(t)$ • instantaneous received optical power.

Writing

$$P_R(t) = A_E f(t), \quad (3-34)$$

for A_E • normalization parameter, and

$f(t)$ • received optical pulse shape,

then

$$A_E = \frac{E_R}{\int_0^{\infty} f(t) dt} \quad (3-35)$$

so that

$$P_R(t) = \frac{E_R f(t)}{\int_0^{\infty} f(t) dt} \quad (3-36)$$

3.3.10 (Continued)

Using the received pulse shape of Section 3.3.9,

$$f(t) = t \exp - \left(\frac{t}{t_m} \right). \quad (3-37)$$

$$\int_0^\infty f(t) dt = t_m^2 \quad (3-38)$$

and

$$P_R(t) = E_R t \left| \frac{\exp - (t/t_m)}{t_m^2} \right| \quad (3-39)$$

$$\text{for } t_m = (2.45)^{-1} \times (\text{time between half power points}). \quad (3-40)$$

The total received optical energy is given by the range equation:

$$E_R = (\text{Transmitted Energy per pulse}) \times (\text{Transmitter optics transmission}) \times$$

$$\left(\frac{\text{Area of the receiver}}{\text{Area of the illuminated spot at the receiver depth}} \right) \times$$

$$(\text{Clear Atmospheric Energy Transmission}) \times (\text{Cloud Energy transmission}) \times$$

$$(\text{Cloud to Water Energy Transmission}) \times$$

$$(\text{Air-Water Interface Energy Transmission}) \times (\text{Water Energy Transmission}) \times$$

$$(\text{Receiver Optics Transmission}) \times$$

$$(\text{Fraction of Incident Radiance within Receiver field-of-view}). \quad (3-41)$$

3.3.10 (Continued)

We take

- E_p = Transmitted Energy per pulse
- τ_T = Transmitter Optics Transmission
- τ_R = Receiver Optics Transmission
- d = Diameter of Receiver Aperture
- R = Range from source to receiver
- $(-d^2/4)$ = Area of the receiver
- θ = Full angle e^{-2} irradiance angle transmitted into*
- $\pi^2 \frac{-d^2}{4} \tau_T$ = Area of the illuminated spot at the receiver depth.
- τ_a = Clear atmosphere energy transmission, as discussed in Section 3.3.1
- τ_c = Cloud energy transmission, as discussed in Section 3.3.2
- τ_{cw} = Cloud to water energy transmission, as discussed in Section 3.3.3
- τ_{aw} = Air-water interface energy transmission, as discussed in Sections 3.3.4 and 3.3.6
- τ_w = Water energy transmission, as discussed in Section 3.3.7.
- $I(z^w)$ = Water radiance distribution, as discussed in Section 3.3.8.

Therefore, the received optical energy is given by

$$E_R = \left(\frac{E_p \tau_T}{(-d^2/4)} \right) \left(\frac{((-d^2/4) \tau_R)}{R^2} \right) \tau_a \tau_c \tau_{cw} \tau_{aw} \tau_w f(z_0, z_R) \quad (3-42)$$

The fraction of the incident radiance within the receiver field-of-view is given by (for perfect alignment between beam axis and receiver axis):

*This assumes such large spots that additional cloud and water spreading is negligible.

$$f(\cdot) = \frac{\int_0^{2\pi} \int_0^{\theta_R} I(\theta^W) d\Omega}{\int_0^{2\pi} \int_0^{\theta_0} I(\theta^W) d\Omega} \cdot \theta_R \leq \theta_0 \quad (3-43)$$

for

θ_R = half angle of the receiver field-of-view

θ_0 = off-axis angle at which incoming radiance equals zero.

Using the model adopted in Section 3.3.8,

$$f(\cdot) = f(\theta_0, \theta_R) = \frac{1 - \cos \theta_R - \frac{1}{3 \sin^2 \theta_0} [\cos \theta_R \sin^2 \theta_R + 2 \cos \theta_R - 2]}{1 - \cos \theta_0 - \frac{1}{3 \sin^2 \theta_0} [\cos \theta_0 \sin^2 \theta_0 + 2 \cos \theta_0 - 2]} \quad (3-43a)$$

$$\text{and } f(\theta_0, \theta_R) = 1, \text{ for } \theta_R = \theta_0. \quad (3-43b)$$

Using Equations (3-42), (3-44) and (3-39) results in the evaluation of the instantaneous optical power in terms of all the other models.

3.4 MODEL UNCERTAINTIES

The sub-models contained in Section 3.3 have a number of uncertainties, due to the lack of available experimental data.

3.4.1 Energy Transmission

The clear atmosphere transmission is well understood at all zenith angles of interest, so the model in Section 3.3.1 has negligible uncertainty.

The cloud energy transmission is not well understood. Areas of uncertainty, not directly treated in the present one-month planned experiment*, include the transition value from thick to thin clouds, the incident zenith angle dependence, the very-thick cloud (optical thickness >50) behavior, and the impact of the single scatter albedo being less than 0.9999. Therefore, future work may modify the model in Section 3.3.2.

The cloud-to-water energy transmission is a small effect and the model in Section 3.3.3 should stand.

The air water interface transmission model in Section 3.3.4 and 3.3.6 has little experimental verification, and may require modification in the high wind speed/large zenith angle regime.

The water energy transmission is not well understood. There are uncertainties with regard to the correct characterization of water loss (absorption with a large fraction of scattering), to thick cloud effects (is there extra water loss here if the water loss coefficient is given by the diffuse attenuation coefficient?). Experimental results support the difference (up to 7 dB) between thick and thin cloud received energy over a particular field-of-view for one type of water at less than operational depths, but no absolute results exist. This area of uncertainty needs to be resolved for the depths of interest and different water types. Therefore, the model in Section 3.3.7 may be modified in the future.

3.4.2 Angular Effects

The SPDPH model in Section 3.3.5 and 3.3.8 is uncertain in two key areas: the shape of the received radiance distribution (including its zenith angle dependency which may be a small effect), and the angular extent of this radiance in clear and cloudy conditions. The present model is based on experimental results at shallow

* To be performed in August/September, 1979.

3.4.2 (Continued)

depths, with one type of water and for small beams incident on the water (clear weather), or the sun (thin to medium cloudy weather). This model assumes that the in-water, air-water interface, and incident angular distributions add in a root sum of squares fashion, which is highly suspect when comparable values arise from more than one contributor, e.g., the thick cloud contribution (modelled as diffuse light hitting the water) and the in-water scattering.

This uncertainty has a large effect on SNR and hardware (the field-of-view requirements interact strongly with the filter size and optical bandpass) and needs to be resolved for the depths of interest, different water types and clear through cloudy weather.

3.4.3 Temporal Effects

The model in Section 3.3.9 for pulse shape and pulse width in the SPDPM is uncertain for both thin and thick cloud conditions, and needs to be experimentally verified.

Consider the zenith angle/field-of-view dependence of the received pulse width in clear weather/thin cloud condition. It may be that pulses more than a few attenuation lengths in duration are unlikely, or that far longer pulses may arise in clearer water conditions. (A related issue is the manner in which the varied temporal effects add up.) This implies a large spread in values, for the pulsewidth, resulting in large signal-to-noise ratio effects (up to $\sqrt{10}$, at least), and needs to be resolved for a receiver at operational depths and in varied water types.

A further uncertainty involves an interaction among energy transmission, field-of-view and time-of-arrival. Does the energy arriving from the "edge" of the field arrive late enough to be useless in signal demodulation? This should also be experimentally ascertained, since no time-resolved underwater experimental results (i.e., for short-pulse sources) presently exist.

(We do not consider here a filter which causes additional pulse distortion. If such a filter does become the leading candidate for OSCAR implementation, the model for both thin and thick clouds would have to be changed.)

Table 3-12 summarizes the uncertainty status of the signal portion of the SPDPM.

3.5 "PARAMETER VALUE" UNCERTAINTIES

There are two level of parameter uncertainties: the details of the input parameters to the SPDPM submodels, and the overall data base developments. This section only considers the details of the input parameters; the overall data bases are discussed in Section 5.6 and 6.6*.

3.5.1 Cloud

There are numerous uncertainties in SPDPM inputs.

The inputs to the SPDPM include:

$\langle \cos \theta \rangle$ = mean value of cosine of the single scattering angle. NOSC has set it = 0.875 in their data base, but it is an inferred, not a measured, result. It is uncertain, but has a small impact.

σ = rms angle for single scattering within the cloud. NOSC has set this = 0.64 radian. Again it is an inferred and not measured result, but appears to have little impact.

ω_0 (Single scattering albedo) = 0.9999, but 0.999 or even 0.99 may be more appropriate for some clouds. The impact of the smaller value, for very thick clouds, is less pulse stretching and less energy transmission.

σ_c = average extinction coefficient of the cloud. This depends both on ω_0 and the particle density (as a function of particle size) in the cloud, $n(r)$. ω_0 is not completely known as discussed above, while $n(r)$ is measured by instruments which may have errors from 20% to 100%. Therefore, σ_c for a given cloud type must be considered as uncertain.

T = geometric thickness of the cloud (note, optical thickness = $\sigma_c T$). This is uncertain for a given cloud type (all stratus clouds do not have the same thickness, of course) and poorly defined if the cloud surface is non-uniform. In addition, according to the SPDPM model, it has a greater impact on pulse stretching than does σ_c .

* Moreover only the uncertainties of the environmental parameter are considered here. The system design parameters are described in Section 5.6.

3.5.2 Air Water Interface

There are uncertainties in the values of wind speed to use, and this may have significant impact in bad conditions. For winds less than 20 kts, any uncertainty in the value has a negligible impact.

3.5.3 Water

There are many uncertainties in the water parameters. The inputs to the SPDPM include:

k_i = diffuse attenuation coefficient of the i 'th water layer. The values presented by NOSC are uncertain in absolute magnitude, but the wavelength trend is correct.

D_i = thickness of the i 'th water layer. It is uncertain and has a significant impact on the system if the upper dirty water layer is thin compared to the operational depth.

s_i = RMS angle for a single scattering event in the water. The value provided by NOSC is uncertain since it is based on an empirical fit to data at shallow depths and for one type of water. This uncertainty could have a large impact on the required clear weather receiver field of view.

S = Scattering coefficient for the entire path. It is uncertain whether its value should be taken independent of depth, and in its absolute value for all water types.

n = water index of refraction. No uncertainty.

Table 3-13 summarizes the uncertainty status of all the parameters for the signal portion of the SPDPM.

Table 3-13. Status of "Input Parameters" to the Signal Portion of the SPDPM

PARAMETER	STATUS	COMMENTS ON EXPERIMENTAL WORK REQUIRED
Clear Atmosphere	OK	None
Cloud:		
$\cos \theta$	OK	None
θ	OK	None
τ_0	Partially known	No direct experiment possible
ρ_c	Partially known	Some work is planned during first cloud experiment. Equipment may be too innacurate for good results
T	Partailly known	Interpretation of data required
Cloud-to-Water	OK	None
Air Water Interface	OK, for low wind speed	Some required for bad conditions.
Water:		
k_1	Partially known	Required if not done by other contractors
D_1	Partially known	Required if available data not able to be interpreted.
s_1	Partially known	Required as a function of depth and water type.
S	Partially known	May become available for surface water from ongoing work. Needed for water at depth.
n	OK	None

Section 4

SINGLE PULSE DOWNLINK PROPAGATION MODEL - NOISE

This section discusses the model for the propagation of the noise relative to a single signal pulse. The section is organized as follows:

4.1 Model Philosophy and Flow Chart - Noise

4.1.1 Philosophy of Approach - Noise

4.1.2 Model Flow Chart - Noise

4.2 Input Information for Noise Calculations

4.2.1 Sources

4.2.2 Clear Atmosphere

4.2.3 Cloud

4.2.4 Cloud to Water

4.2.5 Water

4.2.6 Air/Water Interface

4.2.7 Receiver

4.2.8 Signal Characteristics

4.3 Sub-Models

4.3.1 Clear Atmosphere Transmission - Noise

4.3.2 Cloud Energy Transmission - Noise

4.3.3 Cloud to Water Energy Transmission - Noise

4.3.4 Air-Water Interface Transmission - Noise

4.3.5 Air-Water Interface Angular Effects - Noise

4.3.6 Relative Surface Foam Coverage

4.3.7 Water Energy Transmission - Noise

4.3.8 Water Distribution of Radiance - Noise

4.3.9 Detection Bandwidth

4.3.10 Average Background Power due to Sunlight

4.3.11 Average Background Power due to Moonlight

4.3.12 Average Background Power due to Blue Skylight

4.3.13 Average Background Power due to Stellar/Zodiacal Light

4. (Continued)

4.3.14 Average Background Power due to Bioluminescence

4.3.15 Noise Equivalent Optical Power Dependence on Noise Sources

4.4 Computer Program for Complete SPDPH

4.4.1 Introduction

4.4.2 Names of Variables

4.4.3 Listing

4.5 Model Uncertainties

4.5.1 Average Power Transmission

4.5.2 Angular Effects

4.5.3 Temporal Effects

4.6 Parameter Value Uncertainties

4.1 Model Philosophy and Flow Chart-Noise

This section considers the basic approach used in the detailed models presented in Section 4.3, and presents flow charts showing the inter-relationship of the sub-models and their required inputs. (These inputs are discussed in more detail in Section 4.2).

4.1.1 Philosophy of Approach - Noise

Since all the background sources that must propagate through clouds are continuous in time, that part of the modeling related to the temporal effects is not present here. This simplifies the noise modeling.

On the other hand, the sources of the noise are so different (sun, moon, sky-light, star-light, bioluminescence, shot noise in the receiver amplifier, detector dark current, etc.), that it has been difficult to develop a single unified approach to all of them. The approach, therefore, is to:

- (1) Express the noise contribution as a noise-equivalent-optical-power, (NEP_{TOT}) which is the root sum of squares of all the noise-equivalent-optical power contributions of the individual noise components. The NEP_{TOT} is then directly comparable to the instantaneous received optical power $P_R(t)$ developed in Section 3, and the signal-to-noise ratio is \hat{P}_R/NEP_{TOT} ; for \hat{P}_R the peak value of the received signal power;
- (2) Take the out-of-water background sources in terms of equivalent exo-atmospheric radiances, and then their propagation through the atmosphere and water path is treated in parallel with the signal energy transmission of Section 3.3. The angular effects and noise radiance distribution are also treated in a manner similar to that of the signal in Section 3;
- (3) Take the noise contributions of the background sources as the 1-sigma point in the fluctuations generated in the signal current by their steady presence, and express their contributions in terms of an equivalent optical power;
- (4) Treat the amplifier shot noise, detector dark current and signal shot noise in the standard way, and express their contributions in terms of an equivalent optical power;

4.1.1 (Continued)

- (5) Present the modeling in a modular fashion, so that the effect of each portion of the path is evident. In addition, as further experiments and analyses are undertaken, pieces of the model may be upgraded without requiring extensive modifications to the total model;
- (6) Separate the cloud conditions into clear/thin cloud corresponding to an optical thickness (τ_{OPT}) < 10, and thick cloud for τ_{OPT} > 10. Below τ_{OPT} = 10 one set of sub-models is assumed to apply, while above it a different set applies. In many cases these sub-models do not correspond at τ_{OPT} = 10, and so the overall model should only be used for τ_{OPT} < 10 and τ_{OPT} >> 10. (Further analysis and experiments on the "multiple forward scattering" region should enable the sub-models to be upgraded, and this inconsistency removed).
- (7) Assume appropriate and simple analytic forms for at-present unknown functions such as the radiance distributions. This enables us to present analytic results (except for the receiver axis offset from the beam axis of the incident radiation), which is an aid to a physical understanding of the situation.

4.1.2 Model Flow Chart-Noise

A schematic of the overall downlink single pulse noise equivalent power propagation model is shown in Figure 4-1. Given the input parameters, the path energy transmission and angular and radiance distributions are derived for the four "exo-atmospheric" background sources. Then, using additional input data, the average background power for all background sources is derived, and the noise-equivalent optical power for all the noise components.

Figure 4-2 is a detailed flow diagram of the direct sunlight contribution, showing the calculations that must occur to arrive at the required output. (The flow charts for the moonlight, blue sky-light and starlight/zodiacal light are identical to this one, while the simpler one for the bioluminescence is shown in Figure 4-3):

- (I) The input parameters are listed in the eight ellipses on the left hand side of the figure, including source, clear atmosphere, cloud, cloud to water, air/water interface, water, receiver and signal characteristic parameters. (The symbols are defined in the glossary in Section 2, and also in the input discussion in Section 4.2):
- (II) The calculation equations are represented by the rectangular boxes. Within each box is the symbol for the parameter to be calculated and the equation number (from Section 4.3) for the equation to be used to calculate that parameter.

The first quantity calculated is the cloud optical thickness, τ_{OPT} , since this determines which equation should be used to calculate many other parameters. Whenever // appears in a rectangular box, the equation number preceeding it refers to $\tau_{OPT} > 10$, while the equation number following it refers to $\tau_{OPT} < 10$. Hence, given the value of τ_{OPT} , the rest of the models to be used are specifically determined.

- (III) The second set of calculations performed are of two types:
 - (a) Path transmission, including τ_a' , τ_c' , τ_{cw}' , τ_{aw}' , and τ_w' ;
 - (b) Angular and radiance distribution including f_a , f_{aw} , f_w , ϕ_0 and $f' (A_R \phi_0')$:

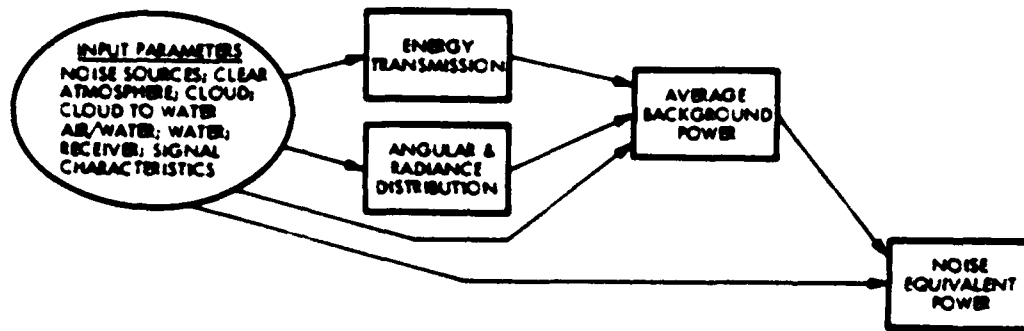
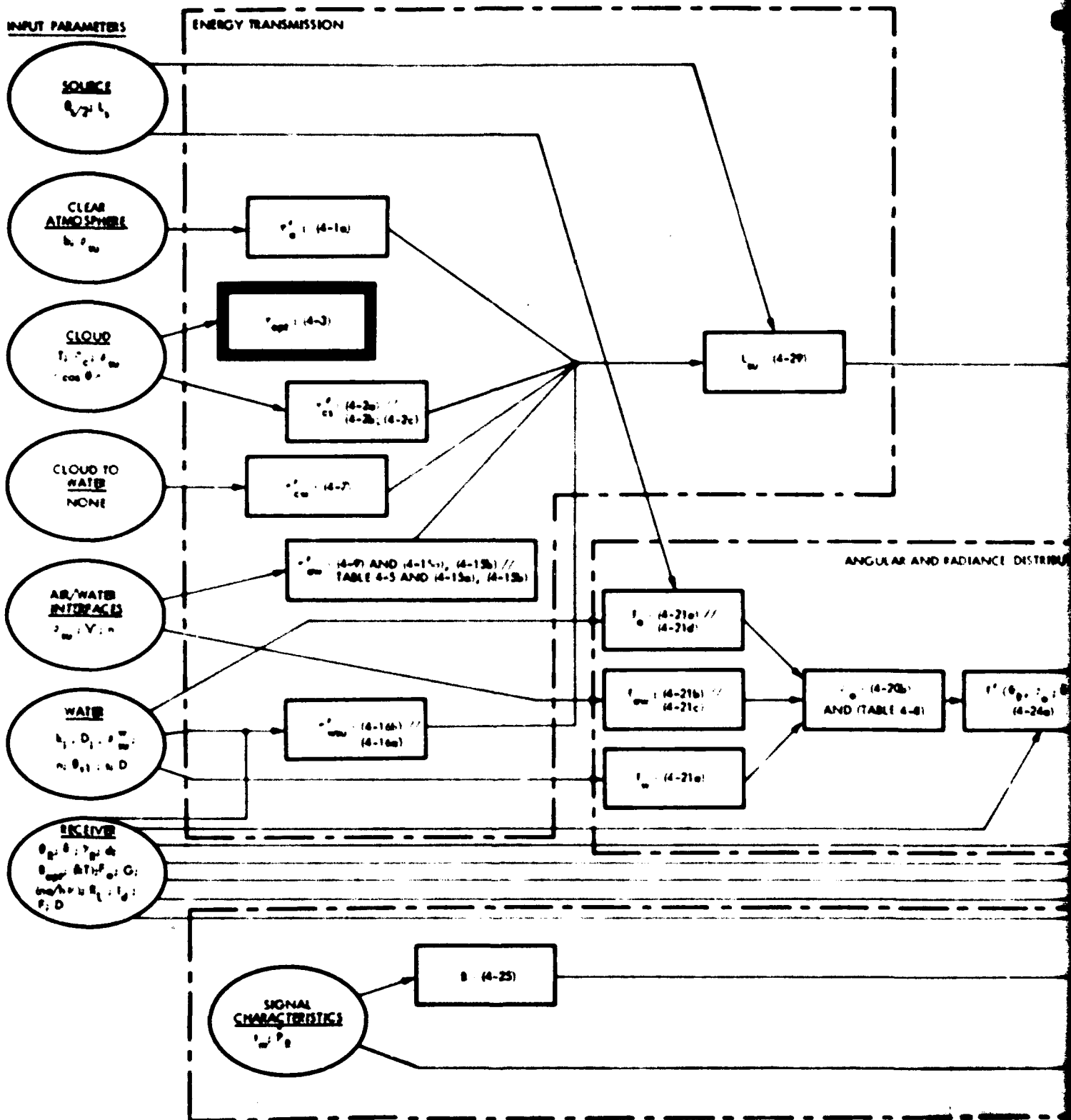


Figure 4-1. Schematic of Typical Single-Pulse Noise Equivalent Power Downlink Propagation Model

4.1.2 (Continued)

- (IV) The path transmission, angular and radiance distribution, source and receiver parameters are then used to calculate the average background power due to that source.
- (V) The total average background power due to all sources is then calculated;
- (VI) The total average background power, receiver and signal characteristics are then used to calculate the total noise equivalent optical power.

Figure 4-3 shows the flow chart for calculating the average background power due to bioluminescence, P_{BL} . This value of P_{BL} enter into Figure 4-2 in the $\bar{\epsilon}P_B^1$ calculations.



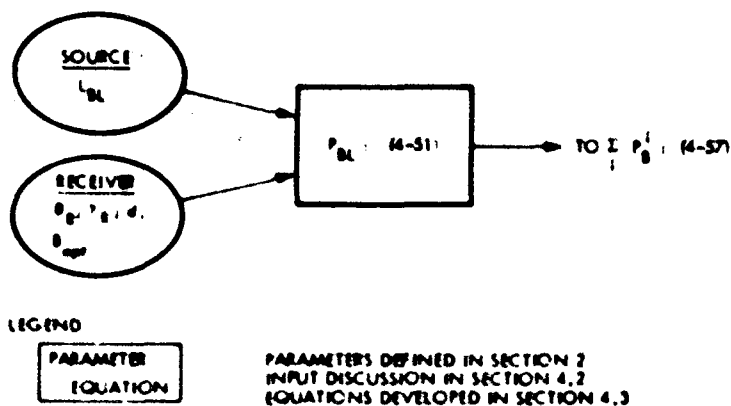


Figure 4-3. Flow Diagram of Single-Pulse Downlink Propagation Model Noise due to Bioluminescence

4.2 Input Information for Noise Calculation

This section discusses the form (and values in some cases) of the required inputs to the noise model, in terms of the eight categories: source, clear atmosphere, cloud, cloud to water, air/water interface, water, receiver and signal characteristics.

4.2.1 Source

There are five sources of the average background, which are treated here as independent. These sources are: sunlight; moonlight; blue sky-light; starlight/zodiacal light; and bioluminescence.

It is expected that these sources will be treated rationally when using them as inputs, so that when sunlight is present, only the blue-skylight will be expected with a non-zero value; and when moonlight is considered to be non-zero, only the starlight/zodiacal light and bioluminescence will be used with non-zero values.

We consider each of the five sources separately.

Sun

<u>Symbol</u>	<u>Description</u>	<u>Units</u>
$\theta_{s/2}$	The half-angle subtended by the sun at the earth. Its value is taken as ¹ $4.65 \cdot 10^{-3}$ radians.	Radians
L_s	Effective exo-atmospheric spectral radiance of the sun. This is the result of taking the exo-atmospheric irradiance of the sun and treating it as a hemispherical source. The result is ² $(2000/\pi) = 635.62$ watts/(meters) ² (steradians)(micron) over the blue-green region.	Watts/(meters) ² (steradians)x(microns)

4.2.1 (Continued)

Moon

<u>Symbol</u>	<u>Description</u>	<u>Units</u>
$\theta_{m/2}$	The half-angle subtended by the moon at the earth. Its value is equal to $\theta_{s/2} = 4.65 (10^{-3})$ radians.	Radians
L_m	Effective exo-atmospheric spectral radiance of the moon. As for the sun, this is the result of taking the exo-atmospheric irradiance of the moon and taking it as a hemispherical source. The result is $4 (4.3/\pi) (10^{-3}) = 1.37 (10^{-3})$ watts/(meters) ² (Steradians) (microns) for a full moon in the blue-green region.	<u>Watts</u> (Meters) ² (Steradians) (Microns)

Blue Skylight

<u>Symbol</u>	<u>Description</u>	<u>Units</u>
L_b	Effective exo-atmospheric spectral radiance of the blue-sky light. This is estimated from a private communication (from L. Stotts of NOSC) to be 100 watts/[(meter) ² (srad) (micron)].	<u>Watts</u> (Meters) ² (Steradians) (Microns)

4.2.1 (Continued)

Starlight/Zodiacal Light

<u>Symbol</u>	<u>Description</u>	<u>Units</u>
L_z	Effective exo-atmospheric spectral radiance due to all non-lunar night time sources. The value ⁶ is $3 (10^{-6})$ [watts/(meters) ² (srad)(micron)] in the blue-green spectral region.	[Watts/(meters) ² (Steradians)(microns)]

Bioluminescence

<u>Symbol</u>	<u>Description</u>	<u>Units</u>
L_{BL}	Spectral irradiance of the ambient bioluminesce sources at the aperture of the submarine receiver. The value for this parameter is least well known of all the background contributors. We use the values provided in the SAOCS RFP, so that ⁷ $L_{BL} = (10^{-3})$ watts/m ² microns.	[Watts/(meters) ² (microns)]

4.2.2 Clear Atmosphere

The required parameters are:

<u>Symbol</u>	<u>Description</u>	<u>Units</u>
b	Effective clear atmospheric optical thickness. For a zenith transmission of 70%; $b = 0.357$	
θ_{su}	In-air solar zenith angle	Radians
θ_{lu}	In-air lunar zenith angle	Radians

4.2.3 Cloud

The required parameters are:

<u>Symbol</u>	<u>Description</u>	<u>Units</u>
T	Geometric or physical thickness of the cloud.	Meters
σ_c	Average extinction coefficient of the cloud.	(Meters) ⁻¹
θ_{su}	In-air solar zenith angle	Radians
θ_{mu}	In-air lunar zenith angle	Radians
$\langle \cos \theta \rangle$	The average value of the cosine of the scattering angle for single scattering within the cloud.	
ω_0	Single scattering albedo of a cloud particle	

4.2.4 Cloud to Water

No parameters in this area affect the noise properties.

4.2.5 Water

The required parameters are:

<u>Symbol</u>	<u>Description</u>	<u>Units</u>
k_i	Diffuse attenuation coefficient of the i'th water layer.	(Meters) ⁻¹
D_i	Thickness of the i'th water layer	(Meters)
θ_{su}^w	In-water Solar Zenith Angle	Radians
θ_{mu}^w	In-water Lunar Zenith Angle	Radians
n	Water Index of refraction	
θ_{SI}	Root-Mean-Square angle for a single scattering event in the water.	Radians
s	Scattering coefficient for the entire water path	(Meters) ⁻¹
D	Depth of the submarine receiver	Meters

4.2.6 Air/Water Interface

The required parameters are:

<u>Symbol</u>	<u>Description</u>	<u>Units</u>
θ_{su}	In-air solar zenith angle	Radians
θ_{mu}	In-air lunar zenith angle	Radians
V	Surface Wind Speed	Meters/Second
n	Water Index of Refraction	

4.2.7 Receiver

The required parameters are:

<u>Symbol</u>	<u>Description</u>	<u>Units</u>
θ_R	Half-angle of the receiver field of view	Radians
ϵ	Off-set angle between the in-water noise source beam and the receiver optical axis	Radians
T_R	Transmission of the receiver optical chain	
d	Diameter of the receiver optical aperture	Meters
B_{opt}	Passband of the optical filter	Microns
(kT)	Thermal Noise contribution in the amplifier	Joules
F_a	Excess amplifier noise over thermal noise	
G	Gain of the photo-detector	
$(-e/h \cdot)$	Responsivity of the photo-surface	Amps/Watts
R_L	Load Resistance following the photo-detector	Ohms
I_d	Dark current at the detector cathode	Amps
F	Excess noise in the photo-detector gain	
D	Depth of the submarine receiver	Meters

4.2.8 Signal Characteristics

Two parameters from the signal characteristics which enter into the Noise calculations are:

<u>Symbol</u>	<u>Description</u>	<u>Unit</u>
t_M	Time after pulse initiation at which it peaks, for a $t \exp - (t/t_M)$ shape.	Seconds
\hat{P}_R	Peak value of the received optical signal power.	Watts

References for Section 4.2

1. Handbook of Geophysics, Revised Edition (The MacMillan Co., New York, 1960) pp 17-1, 17-2.
2. Reference 1, p 16-15, Figure 16-10.
3. R.C. Haynes, Introduction to Space Science, John Wiley and Sons, (New York, 1971) pp 4-5.
4. W.K. Pratt, Laser Communication Systems, John Wiley and Sons (New York, 1969) p. 123, Figure 6-9.
5. Reference 4, p 121, Figure 6-6.
6. Reference 4, p 122, Figure 6-7.
7. T. Flom, P.J. Titterton, et al, "Optical Submarine Communication by Aerospace Relay (OSCAR)," Secret Report, Interim Report No. 2, May 1, 1978, Contract No. N00039-77-C-0100, p 3-22 to 3-24.

4.3 SUB-MODELS

This section develops all the equations used in the calculation of the noise contribution to the total noise equivalent optical power.

Sections 4.3.1, 4.3.2, 4.3.3, 4.3.4, 4.3.6, and 4.3.7 consider the path transmission of the energy.

Sections 4.3.5 and 4.3.8 consider the angular effects and the distribution of the received radiance.

Section 4.3.9 considers the electrical detection bandwidth in terms of the received pulse width.

In each of these sections, after the equations are developed they are evaluated for typical cases in both tables and figures.

Sections 4.3.10 through 4.3.14 then derive the average background optical power for the five types of background sources, and Section 4.3.15 presents the expression for the total noise equivalent optical power due to all noise sources.

4.3.1 Clear Atmospheric Transmission-Noise

In the absence of any clouds or aerosols, the clear atmospheric transmission is described by the term τ_a' . Using the approximate AFCRL model¹, the solar (or lunar) zenith angle dependence is given by:

$$\tau_a' = \exp(-b \sec \theta_{su}), \quad (4-1a, b)$$

for τ_a' = solar (or lunar) clear atmospheric transmission

b = effective clear atmosphere optical thickness

θ_{su} = solar zenith angle.

(For the lunar case, θ_{su} is replaced by θ_{mu} = lunar zenith angle.)

The typical value of b is determined by

$$\tau_a'(\theta_{su} = 0) = 0.7 = \exp(-b),$$

or $b = 0.357$.

Table 4-1 and Figure 4-4 show the values of τ_a' as a function of solar zenith angle.

The other two out-of-water sources of background radiation are taken as uniformly distributed over the hemisphere. Then the effective atmospheric transmission is weighted by the transmission at each zenith angle, or, for the blue-sky and the stellar sources,

$$\tau_a' = \frac{\int_0^{2\pi} d\phi \int_0^{\pi/2} \sin \theta d\theta \exp[-b \sec \theta]}{\int_0^{2\pi} d\phi \int_0^{\pi/2} \sin \theta d\theta}$$

$$\tau_a' = E_2(b) \quad \text{for blue sky or stellar background,}$$

(4-1c, d)

Table 4-1. Typical Clear Atmospheric Transmission ($b=0.357$)

θ_{su} , Solar Zenith Angle	τ_a , Clear Atmospheric Transmission
0	0.7
10	0.7
20	0.68
30	0.66
40	0.63
50	0.57
60	0.49
70	0.35
80	0.13

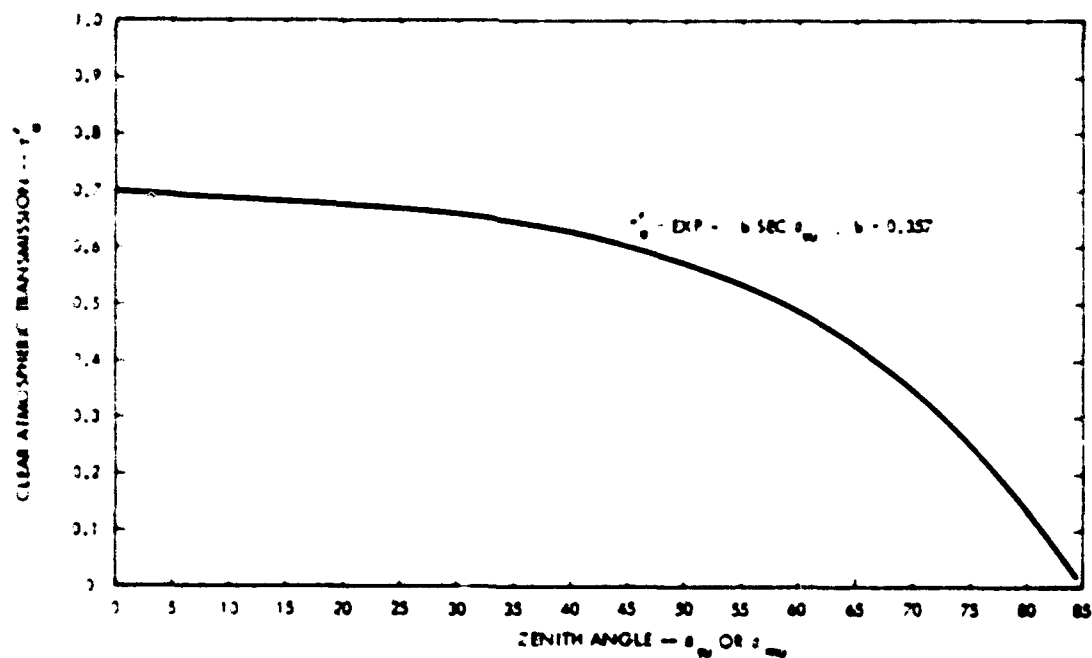


Figure 4-4. Typical Clear Atmospheric Transmission ($b = 0.357$)

with $E_2(b)$ = exponential integral².

For $b = 0.357$, $E_2(0.357) = 0.42$.

References for Section 4.3.1

1. R. A. McClatchey, R. W. Fenn, J. E. A. Selby, F. E. Volz and J. S. Garing
"Optical Properties of the Atmosphere (Revised)" AFCRL-71-0279, 10 May 1971.
2. M. Abramowitz and I. A. Stegun, editor, Handbook of Mathematical Functions.
NBS Applied Mathematics Series 35, Government Printing Office, November 1970.
p 228.

4.3.2 Cloud Energy Transmission - Noise

The transmission of sunlight or moonlight by clouds does not have an experimentally verified expression. Most work in cloud transmission has been a broadband treatment of transmitted irradiance (watts/m²), and there have been no experiments which collected the total energy emerging from thick or thin clouds.

We propose to adopt a number of different (but consistent) models, depending on the characteristics of the noise source.

For the sun and moon we shall adopt the same model as for the signal (Section 3.3.2) with the exception that both the sunlight and moonlight do spread out with zenith angle, and thus the extra cosine factor is always present.

Therefore, for the sun

$$\begin{aligned} \tau'_{cs} = & \left\{ \frac{1}{\tau_{opt} (1 - \langle \cos \theta \rangle + 1.42)} \right\} \left\{ \cos \theta_{su} \right\} \left\{ 1.69 - 0.5513 \theta_{su} \right. \\ & + 2.7173 \theta_{su}^2 - 6.9866 \theta_{su}^3 + 7.1446 \theta_{su}^4 - 3.4249 \theta_{su}^5 \\ & + 0.6155 \theta_{su}^6 \left. \right\} \times \left\{ 2 \sqrt{3(1 - \langle \cos \theta \rangle) (1 - \omega_0)} \right\} \left\{ \tau_{opt} + \frac{1.42}{1 - \langle \cos \theta \rangle} \right\} \\ & \times \left\{ \frac{\exp \left[- \sqrt{3(1 - \langle \cos \theta \rangle) (1 - \omega_0)} \right] \left\{ \tau_{opt} + \frac{1.42}{1 - \langle \cos \theta \rangle} \right\}}{1 - \exp \left[- 2 \sqrt{3(1 - \langle \cos \theta \rangle) (1 - \omega_0)} \right] \left\{ \tau_{opt} + \frac{1.42}{1 - \langle \cos \theta \rangle} \right\}} \right\} \\ & \text{for } \tau_{opt} \geq 10; \end{aligned} \quad (4-2a)$$

$$\begin{aligned} \tau'_{cs} = & \left\{ 1 - 0.085 \tau_{opt} \left[\frac{1.69}{10(1 - \langle \cos \theta \rangle + 1.42)} \right] \right\} \left[\cos \theta_{su} \right]^2, \\ & \text{for } \tau_{opt} \leq 10; \end{aligned} \quad (4-2b)$$

$$\tau'_{cs} = \cos \theta_{su}, \quad \text{for } \tau_{opt} = 0. \quad (4-2c)$$

4.3.2 (Continued)

where

τ'_{cs} = cloud energy transmission of direct sunlight,

τ_{opt} = optical thickness of the cloud

$\langle \cos \theta \rangle$ = mean cosine of the scattering angle

and

θ_{su} = solar zenith angle

As before,

$$\tau_{opt} = T \kappa_c \quad (4-3)$$

for T = geometrical thickness of the cloud, and κ_c = mean extinction of the cloud.

For the moon

$$\begin{aligned} \tau'_{cm} = & \left\{ \frac{1}{\tau_{opt} (1 - \langle \cos \theta \rangle) + 1.42} \right\} \left\{ \cos \theta_{mu} \right\} \left\{ 1.69 - 0.5513 \theta_{mu} + 2.7173 \theta_{mu}^2 \right. \\ & - 6.9866 \theta_{mu}^3 + 7.1446 \theta_{mu}^4 - 3.4249 \theta_{mu}^5 + 0.6155 \theta_{mu}^6 \left. \right\} \\ & \times \left\{ 2 \sqrt{3 (1 - \langle \cos \theta \rangle) (1 - \omega_0)} \right\} \left\{ \tau_{opt} + \frac{1.42}{1 - \langle \cos \theta \rangle} \right\} \\ & \times \left\{ \frac{\exp - \left[\sqrt{3 (1 - \langle \cos \theta \rangle) (1 - \omega_0)} \right] \left\{ \tau_{opt} + \frac{1.42}{1 - \langle \cos \theta \rangle} \right\}}{(1 - \exp - \left[2 \sqrt{3 (1 - \langle \cos \theta \rangle) (1 - \omega_0)} \right] \left\{ \tau_{opt} + \frac{1.42}{1 - \langle \cos \theta \rangle} \right\})} \right\} \\ & \text{for } \tau_{opt} \geq 10; \end{aligned} \quad (4-4a)$$

and

$$\tau'_{cm} = \left\{ 1 - 0.085 \tau_{opt} \right\} \left\{ \frac{1.69}{10 (1 - \langle \cos \theta \rangle) + 1.42} \right\} (\cos \theta_{mu})^2$$

for $\tau_{opt} \leq 10;$ (4-4b)

and

$$\tau'_{cm} = \cos \theta_{mu} \quad \text{for } \tau_{opt} = 0. \quad (4-4c)$$

4.3.2 (Continued)

where

τ_{cm} = cloud energy transmission of direct moonlight,

and θ_{mu} = lunar zenith angle.

The typical energy transmission (for $\langle \cos \theta \rangle = 0.83$) described by Equations (4-2) and (4-4) is shown in Table 4-2 and Figure 4-5.

The zenith angle dependence for both regimes of τ_{opt} is shown in Table 4-3 and Figure 4-6.

Again there is a discontinuity in the zenith angle dependence at $\tau_{opt} = 10$ which we shall ignore, pending a verified model of cloud energy transmission.

The other two out-of-water sources of the ambient background are approximated as uniform sources distributed across the full hemisphere. Then an extra factor arises due to their distribution in angle of incidence upon the cloud. This extra factor is given by

$$\int_0^{\pi/2} f(\theta) \sin \theta d\theta.$$

Table 4-2. Typical Energy Transmission for Sunlight and Moonlight at Zenith ($\langle \cos \theta \rangle = 0.83$, $\omega_0 = 1$).

τ_{opt} , Optical Thickness	τ_{cs} , τ_{cm} , Cloud Energy Transmission
0	1
2	0.91
4	0.82
6	0.72
8	0.63
10	0.54
20	0.35
30	0.26
40	0.21
50	0.17
60	0.15
70	0.13
80	0.11
90	0.10
100	0.09

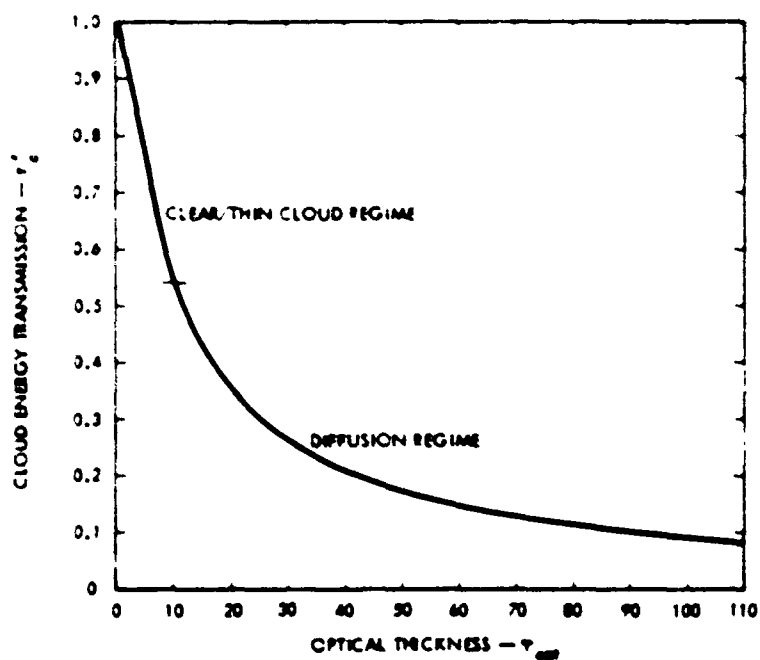


Figure 4-5. Thick and Thin Cloud Energy Transmission Versus Optical Thickness, for $\langle \cos \theta \rangle = 0.83$, $\omega_0 = 1$.

Table 4-3. Zenith Angle Dependence of Sun and Moon Cloud Energy Transmission (Normalized to $\theta_{su} = 0$ and $\theta_{mu} = 0$)

$\vartheta_{su}, \vartheta_{mu}$ Zenith Angle	Thick Cloud Dependence ($\tau_{opt} \geq 10$)	Thin Cloud Dependence ($\tau_{opt} \leq 10$)
0	1	1
10	0.96	0.97
20	0.90	0.88
30	0.79	0.75
40	0.66	0.59
50	0.50	0.41
60	0.34	0.25
70	0.20	0.12
80	0.08	0.03
85	0.03	0.008

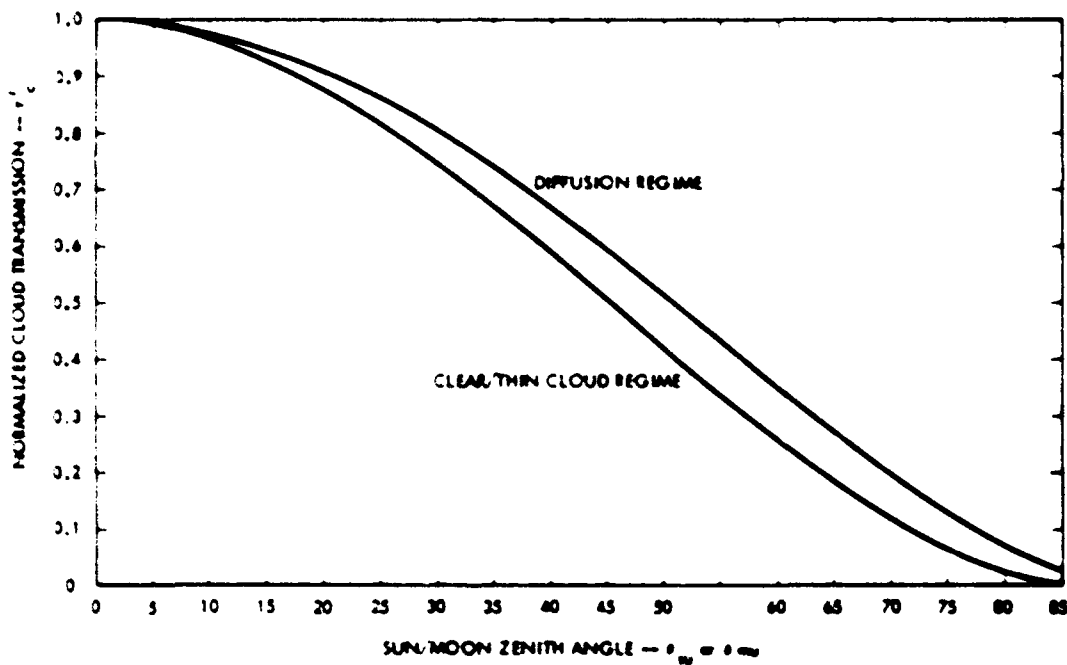


Figure 4-6. Thin and Thick Cloud Zenith Angle Dependence of Cloud Transmission Normalized to Zenith

4.3.2 (Continued)

for $f(\mu) = 1 - 0.3262 \mu + 1.608 \mu^2 - 4.1341 \mu^3 + 4.2276 \mu^4 - 2.0266 \mu^5 + 0.3642 \mu^6$
 $\mu = \cos \theta$ for thin clouds
 $\theta =$ zenith angle of the incident light.

Evaluating this integral we find it equals approximately 2/3 for thick clouds and 1/2 for thin ones.

Therefore, for the blue sky background, the cloud energy transmission is given by

$$\tau_{CB} = \frac{2}{3} \left\{ \frac{1.69}{\tau_{opt} (1 - \langle \cos \theta \rangle) + 1.42} \left\{ 2 \sqrt{3(1 - \langle \cos \theta \rangle) (1 - \tau_{opt})} \right\} \tau_{opt} + \frac{1.42}{1 - \langle \cos \theta \rangle} \right\} \times \left\{ \frac{\exp - \left[\sqrt{3(1 - \langle \cos \theta \rangle) (1 - \tau_{opt})} \right] \tau_{opt} + \frac{1.42}{1 - \langle \cos \theta \rangle}}{1 - \exp - \left[2 \sqrt{3(1 - \langle \cos \theta \rangle) (1 - \tau_{opt})} \right] \tau_{opt} + \frac{1.42}{1 - \langle \cos \theta \rangle}} \right\} \quad \text{for } \tau_{opt} \geq 10. \quad (4-5a)$$

$$\text{and } \tau_{CB} = \frac{1}{2} \left\{ 1 - 0.085 \tau_{opt} \left[\frac{1.69}{10 (1 - \langle \cos \theta \rangle) + 1.42} \right] \right\} \quad \text{for } \tau_{opt} < 10. \quad (4-5b)$$

$$\text{and } \tau_{CB} = 1 \text{ for } \tau_{opt} = 0. \quad (4-5c)$$

4.3.2 (Continued)

The discontinuity at $\tau_{opt} = 10$ is again present, and again neglected until a better experimentally-verified model is derived.

Note Equations (4-5a, b) are independent of solar zenith angle. However, the strength of the radiance incident from the blue sky does depend on solar zenith angle.

For the moonless night case, the stellar/zodiacal light cloud energy transmission is given by

$$\tau_{CZ} = \frac{2}{3} \left\{ \frac{1.69}{\tau_{opt} (1 - \langle \cos \theta \rangle) + 1.42} \right\} \left\{ 2 \sqrt{3(1 - \langle \cos \theta \rangle) (1 - \omega_0)} \right\} \left\{ \tau_{opt} + \frac{1.42}{1 - \langle \cos \theta \rangle} \right\} \\ \times \left\{ \frac{\exp - \left[\sqrt{3(1 - \langle \cos \theta \rangle) (1 - \omega_0)} \left\{ \tau_{opt} + \frac{1.42}{1 - \langle \cos \theta \rangle} \right\} \right]}{1 - \exp - \left[2 \sqrt{3(1 - \langle \cos \theta \rangle) (1 - \omega_0)} \left\{ \tau_{opt} + \frac{1.42}{1 - \langle \cos \theta \rangle} \right\} \right]} \right\} \quad (4-6a)$$

and

$$\tau_{CZ} = \frac{1}{2} \left\{ 1 - 0.085 \tau_{opt} \left[\frac{1.69}{10 (1 - \langle \cos \theta \rangle) + 1.42} \right] \right\} \\ \text{for } \tau_{opt} > 10, \quad (4-6b)$$

and

$$\tau_{CZ} = 1, \quad \text{for } \tau_{opt} = 0 \quad (4-6c)$$

Table 4-4 and Figure 4-7 show a typical cloud energy transmission as a function of cloud optical thickness for these uniform sources of ambient background.

Table 4-4. Typical Cloud Energy Transmission for Blue Skylight and Stellar/Zodiacal Light ($\langle \cos \theta \rangle = 0.83$, $\omega_0 = 1$.)

τ_{opt} Optical Thickness	τ_{cb} , τ_{cz} Cloud Energy Transmission
0	1
2	0.46
4	0.41
6	0.36
8	0.32
10	0.27 (thin); 0.36 (thick)
20	0.23
30	0.17
40	0.14
50	0.11
60	0.1
70	0.087
80	0.073
90	0.067
100	0.06

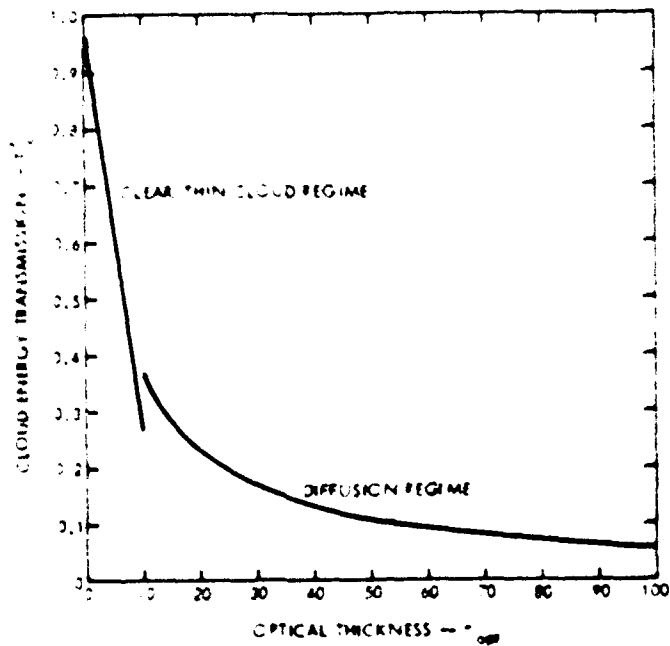


Figure 4-7. Typical Cloud Energy Transmission for Blue Skylight and Stellar Light ($\langle \cos \theta \rangle = 0.83$, $\omega_0 = 1$.)

4.3.3 Cloud to Water Energy Transmission - Noise

Because the sun and moon are effectively sources of infinite plane waves, and the blue sky and stellar background cover the entire hemisphere, there is no "spot" or "beam" enlargement in propagating from the cloud base to the water surface. Therefore, the transmission of noise energy from cloud base to the water surface is given by:

$$T_{CW} = 1,$$

(4-7)

for all cloud conditions.

4.3.4 Air-Water Transmission - Noise

The energy transmission of the air-water interface is composed of two factors:

$$\tau'_{aw} = (\tau'_{aw1}) \times (\tau'_{aw2}) \quad (4-8)$$

for τ'_{aw} = Total energy transmission of air-water interface

τ'_{aw1} = air-water interface transmission due to index of refraction discontinuity

τ'_{aw2} = air water interface transmission due to foam and streaks on the sea surface.

This section treats τ'_{aw1} , while τ'_{aw2} is discussed in Section 4.3.b. For thin clouds and clear weather ($\tau_{opt} \leq 10$) the solar and lunar energy transmission is again given as a function of wind speed and solar/lunar zenith angle in Table 4-5 and Figure 4-6.

For diffuse or uniform radiation incident on the sea-surface, we use the approximation in Section 3.3.4 (which neglects wave effects) and take $\tau'_{aw1} = 0.83$.

$$\tau'_{aw1s} = 0.83, \tau_{opt} \geq 10; \quad (4-9)$$

$$\tau'_{aw1m} = 0.83, \tau_{opt} \geq 10; \quad (4-10)$$

and for blue sky

$$\tau'_{aw1B} = 0.83, \text{ all values of } \tau_{opt}. \quad (4-11)$$

and for stellar, zodiacal light,

$$\tau'_{aw1Z} = 0.83, \text{ all values of } \tau_{opt}. \quad (4-12)$$

Table 4-5. τ_{awls}/τ_{awlm} Time Averaged Downlink Air Sea Interface Transmittance (for Thin Clouds, $\tau_{opt} \leq 10$)

θ Signal Zenith Angle in Air	V_1 Wind Speed								
	0	103	206	412	721	103	134	165	19.6 m/sec
	0	2	4	8	14	20	26	32	38 knots
0	0.978	0.977	0.976	0.974	0.970	0.967	0.963	0.960	0.956
5	0.975	0.974	0.972	0.970	0.966	0.963	0.959	0.956	0.952
10	0.964	0.962	0.961	0.959	0.955	0.951	0.948	0.944	0.941
15	0.945	0.944	0.943	0.940	0.936	0.933	0.929	0.926	0.922
20	0.920	0.918	0.917	0.914	0.910	0.907	0.903	0.899	0.896
25	0.887	0.885	0.884	0.881	0.877	0.873	0.870	0.866	0.863
30	0.847	0.845	0.844	0.841	0.837	0.833	0.829	0.826	0.822
35	0.800	0.798	0.797	0.794	0.790	0.786	0.782	0.779	0.775
40	0.747	0.745	0.743	0.741	0.738	0.733	0.729	0.725	0.722
45	0.687	0.686	0.684	0.681	0.677	0.673	0.668	0.666	0.663
50	0.620	0.619	0.617	0.615	0.611	0.608	0.605	0.602	0.599
55	0.548	0.546	0.545	0.543	0.540	0.538	0.536	0.534	0.532
60	0.488	0.486	0.485	0.483	0.480	0.478	0.476	0.474	0.473
65	0.385	0.385	0.385	0.386	0.387	0.389	0.391	0.393	0.396
70	0.295	0.298	0.299	0.303	0.310	0.315	0.321	0.325	0.329
75	0.203	0.208	0.214	0.224	0.236	0.247	0.255	0.262	0.268
80	0.113	0.126	0.136	0.153	0.172	0.186	0.197	0.206	0.213
85	0.0361	0.0610	0.0751	0.0988	0.119	0.135	0.148	0.157	0.166
90	0	0.0266	0.0390	0.0584	0.0888	0.0961	0.108	0.117	0.124

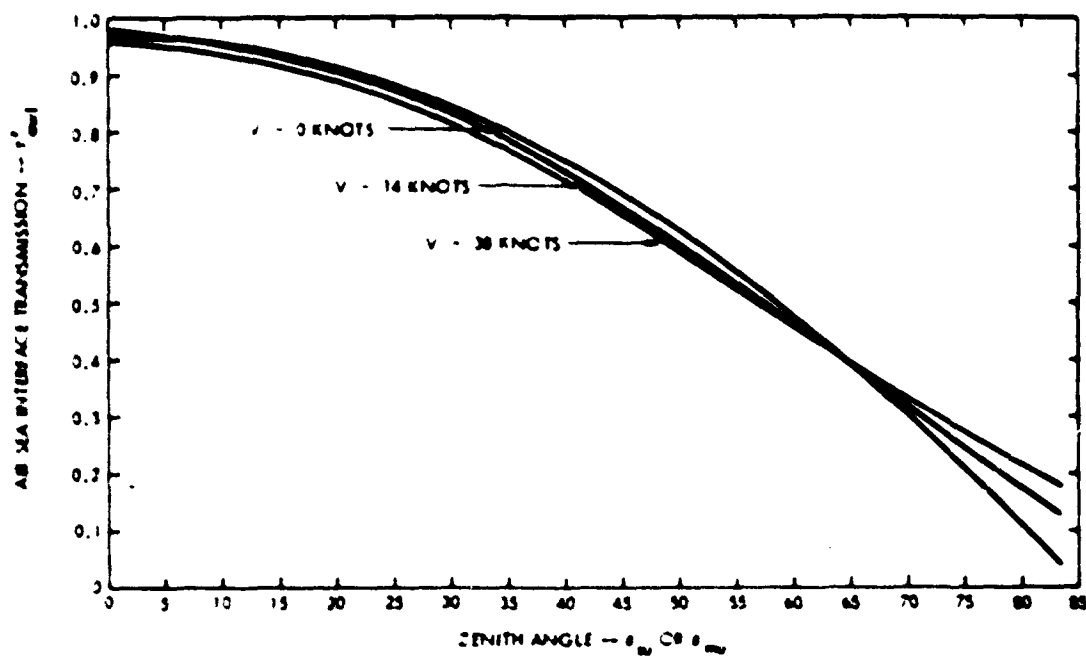


Figure 4-8. Air-Sea Interface Transmittance as a Function of Sun or Moon Zenith Angle and Surface Wind Speed V

4.3.5 Air-Water Interface Angular Effects - Noise

The wave slopes on the sea surface cause an overall increase in the beam divergence of an incident beam, or, equivalently, the apparent angular size of the source as viewed from an underwater point-of-view. With regard to the background sources, only the sun and moon for clear weather conditions ($\tau_{opt} \leq 10$) will be appreciably affected.

Again, using the Karp model discussed in Section 3.3.5,

$$\Delta \theta_{aw}^{su, mu} = 0.0103 V^{1/2}, (\tau_{opt} \leq 10) \quad (4-13a)$$

for $\Delta \theta_{aw}^{su}$ = RMS induced half-angle spread for the sun;

$\Delta \theta_{aw}^{mu}$ = RMS induced half-angle spread for the moon.

V = surface wind speed in knots.

For all τ_{opt} ,

$$\Delta \theta_{aw}^{B, Z} = 0, \quad (4-14)$$

for $\Delta \theta_{aw}^B$ = effect on blue sky source;

$\Delta \theta_{aw}^Z$ = effect on stellar/zodiacal source

Also $\Delta \theta_{aw}^{su, mu} = 0, (\tau_{opt} \geq 10) \quad (4-13b)$

since the light is diffuse after emerging from the thick clouds.

Tables 4-6 and Figure 4-9 evaluate (4-13a) for V in knots (and meters per second).

Since the full angular subtense of the sun (and the moon) is ≈ 0.5 degrees, this effect will substantially increase its apparent size. The relative contribution of $\Delta \theta_{aw}$ to the distribution of noise radiance at the receiver is discussed in Section 4.3.8. Except for the clearest water it is a small effect, and so the impact of neglecting zenith angle effects, and dissimilar wave slopes in the downwind and crosswind direction, may be negligible. We therefore adopt this model until better information is available.

Table 4-b. RMS Air-Water Interface Induced Half-Angle Effects ($r_{opt} \leq 10$)
Sun and/or Moon

V, Wind Speed		$\Delta \theta_{aw}$ su or mu	
Knots	Meters/Second	Milliradians	Degrees
0	0	0	0
2	1.03	14.6	0.84
4	2.06	20.7	1.18
8	4.12	29.2	1.67
14	7.21	38.6	2.21
20	10.3	46.2	2.65
26	13.4	52.6	3.0
32	16.5	58.4	3.35
38	19.6	63.6	3.64

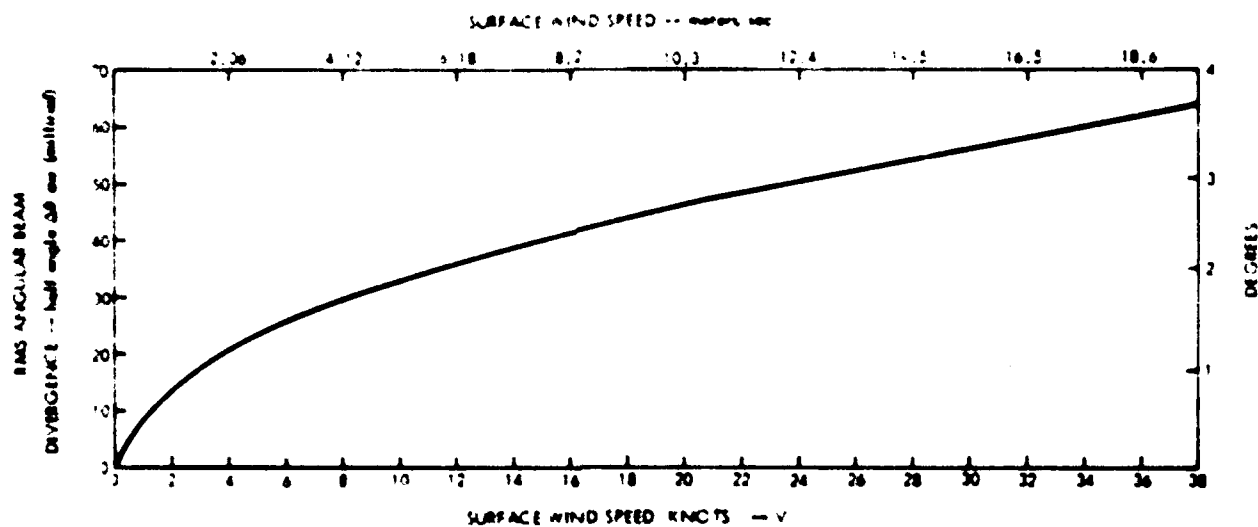


Figure 4-9. RMS Air-Water Interface Effect as a Function of Wind Speed V

4.3.6 Relative Surface Foam Coverage

The energy transmission of the air-water interface is composed of two factors:

$$\tau'_{aw} = (\tau'_{aw1}) \times (\tau'_{aw2}).$$

for τ'_{aw} = Total energy transmission of the air-water interface

τ'_{aw1} = air water interface transmission due to index of refraction discontinuity

and τ'_{aw2} = air water interface transmission due to foam and streaks on the water surface.

This section treats τ'_{aw2} , while τ'_{aw1} has been treated in Section 4.3.4.

The surface foam coverage and its effects are taken to be independent of the noise source and cloud conditions. As discussed in Section 3.3.6, for a foam albedo = 1,

$$\tau'_{aw2} = 1 - (1.2 (10^{-5})) V^{3.3}, V \leq 9 \text{ m/sec.} \quad (4-15a)$$

$$\text{and } \tau'_{aw2} = 1 - (1.2 (10^{-5})) V^{3.3} (0.225V - 0.99), V \geq 9 \text{ m/sec.} \quad (4-15b)$$

for V = surface wind speed in meters/sec.

Equation (4-15a,b) is evaluated in Table 4-7 and Figure 4-10 for V in knots (and meters/second).

Although this model neglects zenith angle effects we shall adopt it pending further experimental work.

Table 4-7. Air Water Energy Transmission Due to Surface Foam and Streaks
(Assuming a Foam/Streak Albedo = 1)

V, Wind Speed		τ'_{aw2}
Knots	Meters/Second	
0	0	1
2	1.03	1
4	2.06	1
8	4.12	1
14	7.21	0.99
20	10.3	0.96
26	13.4	0.87
32	16.5	0.66
38	19.6	0.25

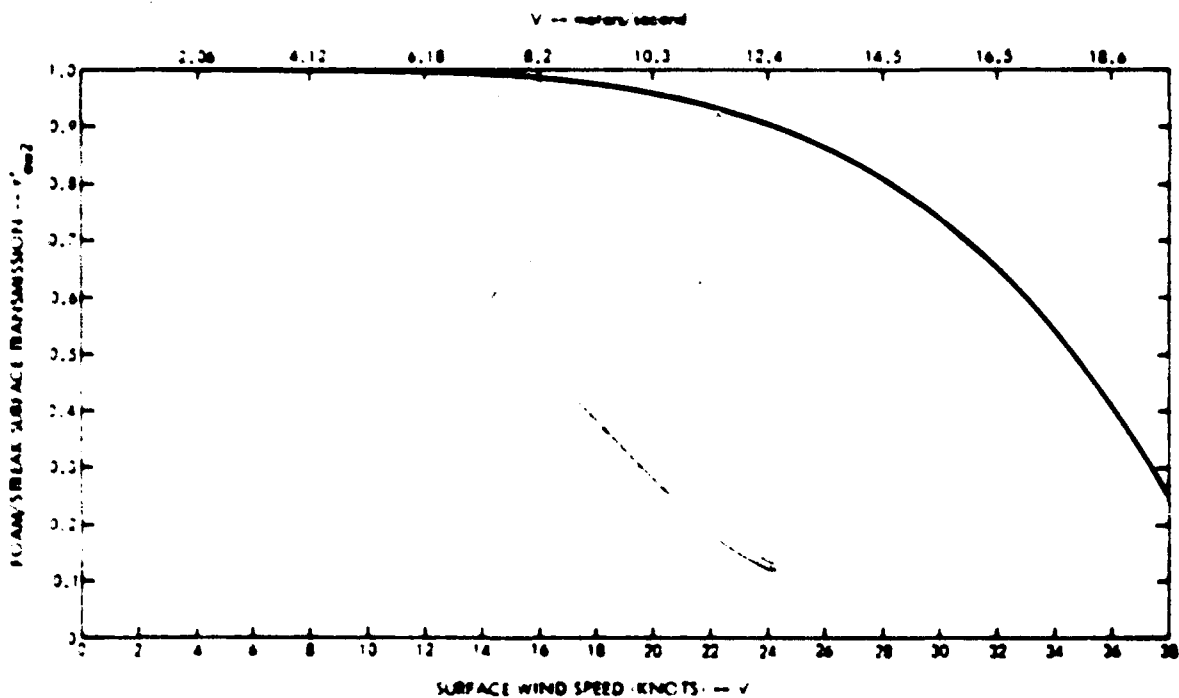


Figure 4-10. Foam/Streak Surface Coverage Transmission Versus Surface Wind Speed

4.3.7 Water Energy Transmission - Noise

The energy transmission of the water is denoted by τ_w' . The angularly localized noise sources (sun and moon) behave similarly to the signal energy transmission discussed in Section 3.3.7, thus we take:

$$\tau_{wsu}' = \exp - \left\{ \frac{\sum_{i=1}^J (k_i D_i)}{\cos \theta_{su}^w} \right\} \quad (4-16a)$$

for $\theta_{su}^w = \sin^{-1} \left(\frac{1}{n} \sin \theta_{su} \right)$

and $\sum_{i=1}^J D_i = D, \tau_{opt} \leq 10.$

where k_i = diffuse attenuation coefficient for the i 'th water layer;

D_i = thickness of the i 'th water layer

D = receiver depth

n = sea-water index of refraction

θ_{su}^w = in-water solar zenith angle

θ_{su} = in-air solar zenith angle;

$$\tau_{mwu}' = \exp - \left\{ \frac{\sum_{i=1}^J (k_i D_i)}{\cos \theta_{mwu}^w} \right\} \quad (4-17a)$$

for $\theta_{mwu}^w = \sin^{-1} \left(\frac{1}{n} \sin \theta_{mwu} \right)$

and $\sum_{i=1}^J D_i = D, \tau_{opt} \leq 10.$

where θ_{mwu}^w = in-water lunar zenith angle;

θ_{mwu} = in-air lunar zenith angle.

4.3.7 (Continued)

Moreover for the thick cloud conditions,

$$\tau_{wsu}^i = \exp - \left\{ \sum_{i=1}^j k_i D_i \right\}, \text{ for } \tau_{opt} > 10. \quad (4-16b)$$

and, in the same way

$$\tau_{wru}^i = \exp - \left\{ \sum_{i=1}^j k_i D_i \right\}, \text{ for } \tau_{opt} > 10. \quad (4-17b)$$

For the blue sky and starlight/zodiacal light background sources, the same models should approximately apply for all τ_{opt} . Therefore,

$$\tau_{wb}^i = \exp - \left\{ \sum_{i=1}^j k_i D_i \right\}, \text{ for all } \tau_{opt}. \quad (4-18)$$

and

$$\tau_{wz}^i = \exp - \left\{ \sum_{i=1}^j k_i D_i \right\}, \text{ for all } \tau_{opt}. \quad (4-19)$$

This model is uncertain in

- (1) The values of k_i to use;
- (2) The values of D_i ;
- (3) its applicability in very clear water and/or at shallow receiver depths.

It is the best model available now and it will be revised when better information becomes available.

4.3.8 Water Distribution of Radiance - Noise

There is no experimentally verified expression for the in-water distribution of background radiance as a function of source character, source zenith angle, water properties and receiver depth. As discussed in Section 3.3.8, we therefore adopt the expression

$$1 - \left(\frac{\sin \theta^w}{\sin \theta_0} \right)^2$$

as an estimate of the angular distribution, with

θ^w = in-water angle measured from the axis, or principal ray of the noise source.

θ_0 is related to the half power point of the received radiance by the equation

$$\frac{1}{2} = \frac{1 - (\cos \theta_{1/2})^2 \left\{ \frac{-1}{3 \sin^2 \theta_0} \left(\cos \theta_{1/2} \sin^2 \theta_{1/2} + 2 \cos \theta_{1/2} - 2 \right) \right\}}{1 - \cos \theta_0 - \frac{1}{3 \sin^2 \theta_0} \left(\cos \theta_0 \sin^2 \theta_0 + 2 \cos \theta_0 - 2 \right)} \quad (4-20a)$$

Equation (4-20a) is evaluated in Table 4-8. Values between those shown are obtained by linear interpolation.

Again assuming that the in-air incident beam spread, air-water beam spread and in-water scattering induced spread are statistically independent effects, we adopt the NOSC¹ model:

$$\theta_{1/2} = \left[f_w + f_{aw} + f_a \right]^{1/2} \quad (4-20b)$$

for all four out-of-water background sources. For solar and lunar sources

$$\begin{aligned} f_w &= \text{water contribution} \\ &= \frac{2}{s_1} \frac{s_0}{\cos \theta_{su}^w} \quad \text{all } \theta_{OPT} \end{aligned} \quad (4-21a)$$

Table 4-8. Relation of radiance zero point, θ_0 , and received radiance half-power point, $\theta_{1/2}$, for $1 - (\sin \theta^w / \sin \theta_0)^2$ radiance distribution

$\theta_{1/2}$ (degrees)	θ_0 (degrees)
3.8	5
7.6	10
11.4	15
15.2	20
19.0	25
22.7	30
26.5	35
30.2	40
33.9	45
37.5	50
41.1	55
44.6	60
48.1	65
51.6	70
54.9	75
58.2	80

4.3.8 (Continued)

and

$$f_w = \frac{1}{2} \frac{s D}{\cos \theta_{su}^w} \cdot \text{all } \theta_{mu}^w$$

(4-22a)

while for the distributed background sources of blue sky and stellar/zodiacal light,

$$f_w = \frac{1}{2} s D \cdot \text{all } \theta_{mu}^w$$

(4-23a)

for $\frac{1}{2} s$ = mean square single scattering angle in water

s = scattering coefficient in water

D = receiver depth

θ_{su}^w = in-water solar zenith angle

θ_{mu}^w = in-water lunar zenith angle.

4.3.8 (Continued)

Again, for solar and lunar sources

$$f_{aw} = (0.0103 V^2)^2; \tau_{OPT} \leq 10$$

(4-21b), (4-22b)

$$= 0; \tau_{OPT} \geq 10.$$

(4-21c), (4-22c)

V = surface wind speed (knots), as discussed in Section 4.3.5.

For the distributed sources,

$$f_{aw} = 0, \text{ all } \tau_{OPT}$$

(4-23b)

Finally, for the sun and moon,

$$f_a = \left(\frac{1}{n}\right)^2 \left(\theta_s/2\right)^2; \tau_{OPT} \leq 10$$

(4-21d)

$$= (33.8^\circ)^2; \tau_{OPT} \geq 10$$

(4-21e)

and $f_a = \left(\frac{1}{n}\right)^2 \left(\theta_m/2\right)^2; \tau_{OPT} \leq 10;$

(4-22d)

$$= (33.8^\circ)^2; \tau_{OPT} \geq 10.$$

(4-22e)

for n = water index of refraction.

$\theta_s/2$ = half the angular subtense of the sun ($\sim (1/4)^\circ$)

and $\theta_m/2$ = half the angular subtense of the moon ($\sim (1/4)^\circ$)

These equations have been discussed and derived in Section 3.3.8. For the distributed sources,

$$f_a = (33.8^\circ)^2, \text{ all } \tau_{OPT}.$$

4.3.8 (Continued)

In general, the receiver will be directly viewing the signal, while the background source enters at an off-axis angle. Then the fraction of the noise radiance which enters the receiver is given by

$$f(\theta_0, \theta_R) = \frac{\int_0^{2\pi} d\phi \int_0^{\theta_R} d\theta \sin \theta \left[1 - \left(\frac{\sin \theta}{\sin \theta_0} \right)^2 \right]^2}{\int_0^{2\pi} d\phi \int_0^{\theta_0} d\theta \sin \theta \left[1 - \left(\frac{\sin \theta}{\sin \theta_0} \right)^2 \right]} \quad (4-24a)$$

for $\theta' = \cos^{-1} \left[\cos \theta \cos \theta_0 + \sin \theta \sin \theta_0 \sin \phi \right]$,

for θ_R = half-angle of the receiver field of view

θ_0 = off-set angle between axis of noise source and receiver optical axis.

This expression will be used further in Section 4.2.10 and 4.2.11.

(4-24a) applies to the background sources in thin cloud conditions. Under thick cloud conditions, both signal and background will appear to arrive from the zenith, and so $\theta_0 = 0$. For this case,

$$f(\theta_0, \theta_R) = \frac{1 - \cos \theta_R - \frac{1}{3 \sin^2 \theta_0} \left[\cos \theta_0 \sin^2 \theta_R + 2 \cos \theta_R - 2 \right]}{1 - \cos \theta_0 - \frac{1}{3 \sin^2 \theta_0} \left[\cos \theta_0 \sin^2 \theta_0 + 2 \cos \theta_0 - 2 \right]} \quad (4-24b)$$

References for Section 4.3.8

1. R.E. Howarth, M.E. Hyde and W.R. Stone, "Submarine-Aircraft and Submarine-Satellite Optical Communications System Model (U)," Confidential Report, MELC-TR-2021, 1977.

4.3.9 Detection Bandwidth

The required electrical detection bandwidth to optimally detect the pulses discussed in Section 3.3.9 is not known at present. In lieu of such a result we assume:

- 1) The receiver has foreknowledge of the expected pulse width;

$$2) \quad B = \frac{0.4}{(2.45 \tau_m)} \quad (4-25)$$

for B = electrical detection bandwidth

τ_m = time at which pulse peak value occurs after pulse start, for a pulse shape $f(t) = t \exp - (t/\tau_m)$.

For gaussian shaped pulses and detection filter, (4-25) is the nearly optimum match.* As further work is done in the area of the real pulses to be expected here, (4-25) may be revised.

Equation 4-25 is evaluated in Table 4-9 and Figure 4-11 for the pulse-widths and optical thicknesses developed in Section 3.3.9.

Table 4-9. Typical Detection Bandwidths for Pulse Width Conditions of Table 3-11

τ_{opt} Optical thickness	T Geom. Thickness (km)	Δt_c Pulsewidth (μ sec)	Δt_m Peak Time (μ sec)	B Detection Bandwidth (kHz)
10	0.25	1.15	0.47	348
20	0.5	3.55	1.49	110
30	0.75	7.08	2.89	56.5
40	1.00	11.27	4.6	35.5
50	1.25	16.13	6.58	24.8
60	1.50	21.55	8.8	18.6
70	1.75	27.48	11.22	14.6
80	2.00	33.93	13.85	11.8
90	2.25	40.88	16.69	9.8
100	2.50	48.25	19.7	8.3

*H.P. Westman, Editor, Reference Data for Radio Engineer, Fifth Edition, p. 29-5, (H. W. Sams & Co., New York, 1969).

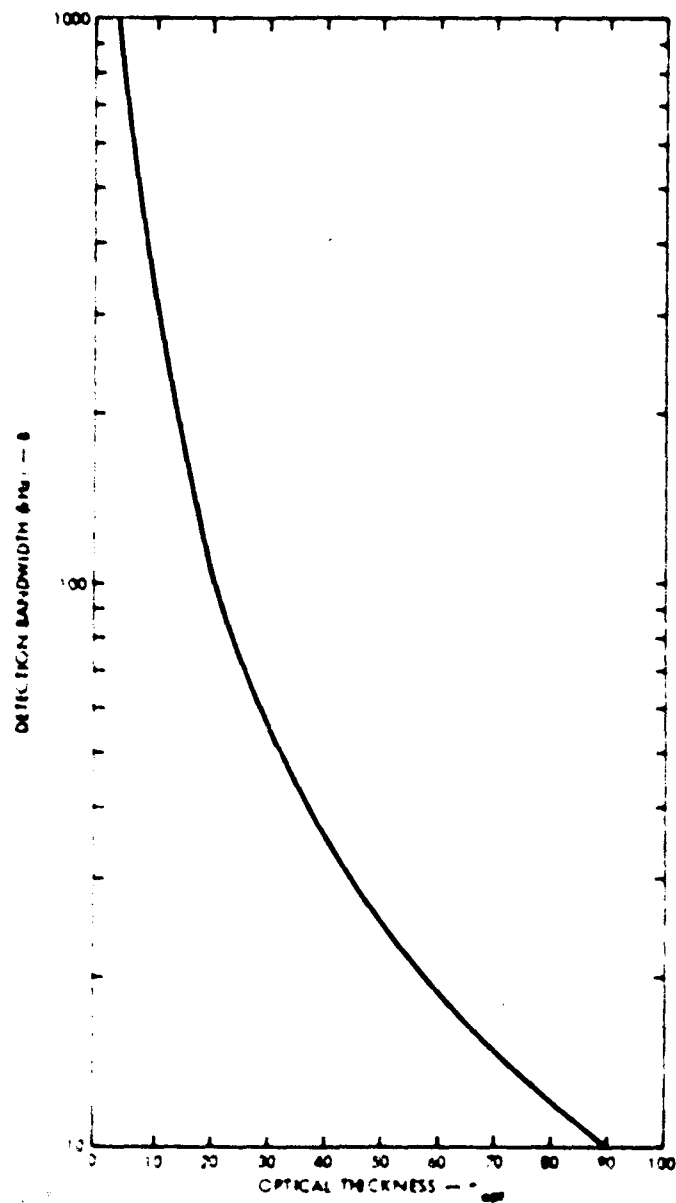


Figure 4-11. Detection Bandwidth for Pulse-Widths of Table 3-11

4.3.10 Average Background Power Due to Sunlight

The average optical background power in the receiver due to the sun is given by an equation analogous to that developed in Section 3.3.10 for the received optical signal energy. We therefore take

$$P_{SU} = (\text{Spectral Radiance at Receiver Aperture Due to Sun}) \times (\text{Receiver optics transmission}) \times (\text{Receiver Area}) \times (\text{Receiver optical filter bandpass}) \times (\text{Receiver Solid Angle}) \times (\text{Fraction of incident radiance in this receiver field of view}).$$

(4-26)

We take

$$\tau_R = \text{Receiver optics transmission}$$

$$d = \text{Receiver aperture diameter}$$

$$\frac{\pi d^2}{4} = \text{Area of receiver aperture}$$

$$B_{opt} = \text{Receiver optical filter bandpass}$$

$$\theta_p = \text{Half-Angle of the receiver field of view}$$

$$2\pi(1 - \cos \theta_R) = \text{Receiver field of view solid angle}$$

$$L_{SU} = \text{Spectral Radiance at Receiver aperture due to the sun}$$

and

$$f'(\theta_0, \theta_R) = \text{fraction of incident radiance within receiver field of view.}$$

Then

$$P_{SU} = L_{SU} \left(\tau_R \frac{\pi d^2}{4} \right) B_{opt} \left(2\pi(1 - \cos \theta_R) \right) f'(\theta_0, \theta_R). \quad (4-27)$$

Because the sun is a CW source, we use the energy transmission formalism to develop the expression:

4.3.10 (Continued)

$$L_{su} = (\text{Exo-atmospheric effective solar radiance}) \times$$

$$(\text{Clear Atmosphere Energy Transmission}) \times (\text{Cloud Energy Transmission}) \times$$

$$(\text{Cloud to Water Energy Transmission}) \times$$

$$(\text{Air-Water Interface Energy Transmission}) \times (\text{Water Energy Transmission}),$$

(4-28)

and we use

- L_s = Exo-atmospheric effective solar radiance
- τ_a = Clear atmosphere energy transmission, as discussed in Section 4.3.1;
- τ_{cs} = Cloud energy transmission, as discussed in Section 4.3.2;
- τ_{cw} = Cloud to water energy transmission, as discussed in Section 4.3.3;
- τ_{aws} = Air-water energy transmission, as discussed in Sections 4.3.4 and 4.3.6;
- τ_{wsu} = Water energy transmission, as discussed in Section 4.3.7.

Gathering these expressions we find

$$L_{su} = L_s \tau_a \tau_{cs} \tau_{cw} \tau_{aws} \tau_{wsu}$$

(4-29)

The fraction of incident radiance within the receiver field of view depends on the angular separation between the axis of the receiver field of view and the in-water solar zenith angle, as developed in Section 4.3.8.

4.3.10 (Continued)

$$f'(\theta_R, \theta_0, \theta) = \frac{\int_0^{2\pi} d\phi \int_0^{\theta_R} d\theta^w \sin \theta^w \left[1 - \left(\frac{\sin \theta^{w'}}{\sin \theta_0} \right)^2 \right]}{\int_0^{2\pi} d\phi \int_0^{\theta_0} d\theta^w \sin \theta^w \left[1 - \left(\frac{\sin \theta^w}{\sin \theta_0} \right)^2 \right]} \quad (4-30)$$

$$\text{for } \theta^{w'} = \cos^{-1} \left\{ \cos \theta^w \cos \theta_{SUR} + \sin \theta^w \sin \theta_{SUR} \sin \theta \right\} \quad (4-31)$$

and θ_{SUR} = angular separation between solar beam axis and receiver optical axis,

θ_0 = off solar beam axis angle at which the solar radiance goes to zero.

These expressions will be used in the development of the Noise Equivalent Power expression in Section 4.3.15.

4.3.11 Average Background Power Due to Moonlight

The average optical background power in the receiver due to the moon is completely analogous to that for the sun discussed in Section 4.3.10. We therefore take

$$P_{mu} = (\text{Spectral Radiance at Receiver Aperture Due to Moon}) \times \\ (\text{Receiver optics transmission}) \times (\text{Receiver area}) \times \\ (\text{Receiver optical filter bandpass}) \times (\text{Receiver Solid Angle}) \times \\ (\text{Fraction of incident radiance within the receiver field of view}).$$

(4-32)

We take τ_R = Receiver optics transmission,

d = Receiver aperture diameter,

$\frac{\pi d^2}{4}$ = Area of receiver aperture,

B_{opt} = Receiver optical filter bandpass,

θ_R = Half-Angle of the Receiver Field of View

$2 - (1 - \cos \theta_R)$ = Receiver field of view solid angle

L_{mu} = Spectral radiance at receiver aperture due to moon

and

$f'(\theta_0, \theta_R, \theta)$ = Fraction of incident radiance within receiver field of view.

Then

$$P_{mu} = L_{mu} \left(\tau_R \frac{\pi d^2}{4} \right) (B_{opt}) \left(2 - (1 - \cos \theta_R) \right) f'(\theta_0, \theta_R, \theta) \quad (4-33)$$

4.3.11 (Continued)

Because the moon is a CW source, we use the energy transmission formalism to develop the expression:

$$L_{mu} = \begin{aligned} & \text{(Exo-atmospheric effective lunar radiance)} \times \\ & \text{(Clear atmosphere energy transmission)} \times \text{(Cloud energy transmission)} \times \\ & \text{(Cloud to water energy transmission)} \times \\ & \text{(Air-Water interface energy transmission)} \times \\ & \text{(Water energy transmission)}. \end{aligned} \quad (4-34)$$

and we use

L_m = Exo-atmospheric effective lunar radiance;

τ_a = Clear atmosphere energy transmission, as discussed in Section 4.3.1

τ_{cm} = Cloud energy transmission, as discussed in Section 4.3.2.

τ_{cw} = Cloud to water energy transmission, as discussed in Section 4.3.3

τ_{awm} = Air-Water energy transmission as discussed in Section 4.3.4, and 4.3.6.

and

τ_{wm} = Water energy transmission, as discussed in Section 4.3.7.

Gathering the various expressions we find

$$L_{mu} = L_m \tau_a \tau_{cm} \tau_{cw} \tau_{awm} \tau_{wm} \quad (4-35)$$

As for the sunlight, the fraction of incident lunar radiance within the receiver field of view depends on the angular separation between the optical axis of the receiver field of view and the in-water lunar zenith angle. As developed in Section 4.3.8,

4.3.11 (Continued)

$$f'(\vartheta_R, \vartheta_0, \delta) = \frac{\int_0^{2\pi} d\theta \int_0^{\vartheta_R} d\vartheta^W \sin \vartheta^W \left[1 - \left(\frac{\sin \vartheta^W}{\sin \vartheta_0} \right)^2 \right]}{\int_0^{2\pi} d\theta \int_0^{\vartheta_0} d\vartheta^W \sin \vartheta^W \left[1 - \left(\frac{\sin \vartheta^W}{\sin \vartheta_0} \right)^2 \right]} \quad (4-36)$$

for

$$\vartheta^{W'} = \cos^{-1} \left\{ \cos \vartheta^W \cos \vartheta_{MUR} + \sin \vartheta^W \sin \vartheta_{MUR} \sin \theta \right\} \quad (4-37)$$

and

ϑ_{MUR} = Angular separation between lunar beam axis and receiver optical axis

ϑ_0 = Off lunar beam axis angle at which the lunar radiance goes to zero.

These expressions will be used in the development of the Noise Equivalent Power expression in Section 4.3.15.

4.3.12 Average Background Power Due to Blue Skylight

The average optical background power in the receiver due to the blue skylight is partially analogous to that for the sun and moon discussed in Sections 4.3.10 and 4.3.11. We therefore take, for the average optical background power due to blue skylight:

$$P_{BS} = (\text{Spectral Radiance at Receiver Aperture due to the Blue Sky}) \times (\text{Receiver optics transmission}) \times (\text{Receiver area}) \times (\text{Receiver optical filter bandpass}) \times (\text{Receiver solid angle}) \times (\text{Fraction of incident radiance within the receiver field of view}).$$

(4-38)

We take

τ_R = Receiver optics transmission;

d = Receiver aperture diameter;

$\frac{\pi d^2}{4}$ = Area of receiver aperture;

B_{opt} = Receiver optical filter bandpass

θ_R = Half-Angle of the Receiver field of view

$2\pi(1 - \cos \theta_R)$ = Receiver field of view solid angle

L_{BS} = Spectral radiance at receiver aperture due to the blue skylight,

$f'(\theta_0, \theta_R, \dots)$ = Fraction of incident radiance within receiver field of view,

and

$$P_{BS} = L_{BS} \left(\tau_R \left(\frac{\pi d^2}{4} \right) \right) B_{opt} 2\pi(1 - \cos \theta_R) f'(\theta_0, \theta_R, \dots) \quad (4-39)$$

Because the blue skylight is a cw source, we use the energy transmission formalism to develop the expression:

$$L_{BS} = (\text{Clear sky exo-atmospheric effective radiance}) \times (\text{Clear atmospheric transmission}) \times (\text{Cloud energy transmission}) \times (\text{Cloud to Water Energy Transmission}) \times (\text{Air-Water Interface Energy Transmission}) \times (\text{Water Energy Transmission})$$

(4-40)

4.3.12 (Continued)

and we use

- L_B = Clear sky exo-atmospheric effective radiance,
- τ_a' = Clear atmospheric transmission, as discussed in Section 4.3.1,
- τ_{CB} = Cloud energy transmission, as discussed in Section 4.3.2,
- τ_{CW} = Cloud to water energy transmission as discussed in Section 4.3.3,
- τ_{awB} = Air-water energy transmission, as discussed in Sections 4.3.4 and 4.3.6,
- τ_{WB} = Water energy transmission, as discussed in Section 4.3.7.

Gathering the expressions we find

$$L_{BS} = L_B \tau_a' \tau_{CB} \tau_{CW} \tau_{awB} \tau_{WB} \quad (4-41)$$

Again, the fraction of blue-sky radiance within the receiver field of view is given by

$$f'(\theta_R, \phi_0, \psi) = \frac{\int_0^{2\pi} d\alpha \int_0^{\theta_R} d\psi \sin \psi \left[1 - \left(\frac{\sin \psi'}{\sin \psi_0} \right)^2 \right]}{\int_0^{2\pi} d\alpha \int_0^{\psi_0} d\psi \sin \psi \left[1 - \left(\frac{\sin \psi}{\sin \psi_0} \right)^2 \right]} \quad (4-42)$$

$$\text{for } \psi' = \cos^{-1} \left[\cos \psi \cos \psi_{BR} + \sin \psi \sin \psi_{BR} \sin \phi_0 \right] \quad (4-43)$$

4.3.12 (Continued)

and θ_{BR} = Off zenith pointing angle of the receiver axis,
while

θ_0 = Off-zenith angle at which the blue sky radiance goes to zero.

These expressions will be used in the development of the Noise Equivalent Optical Power expression in Section 4.3.15.

4.3.13 Average Background Power Due to Stellar/Zodiacal Light

The average optical background power in the receiver due to the nighttime distributed sources of stellar and zodiacal light follows the patterns established in the previous three sections. We take, for the average optical background power due to these sources:

$$P_Z = (\text{Spectral radiance at receiver aperture due to the stellar/Zodiacal light}) \times (\text{Receiver optics transmission}) \times (\text{Receiver Area}) \times (\text{Receiver optical filter bandpass}) \times (\text{Receiver solid angle}) \times (\text{Fraction of incident radiance within the receiver field-of-view}). \quad (4-44)$$

We again take

τ_R = Receiver optics transmission,

d = Receiver aperture diameter,

$\frac{\pi d^2}{4}$ = Area of receiver aperture,

B_{OPT} = Receiver optical filter bandpass;

θ_R = Half-Angle of the receiver field-of-view;

$2\pi(1 - \cos \theta_R)$ = Receiver field-of-view solid angle;

L_{ZS} = Spectral radiance at receiver aperture due to the stellar/zodiacal light;

$f'(\theta_0, \theta_R, \theta)$ = Fraction of incident radiance within the receiver field-of-view;

θ_0 = Off-axis angle at which the received radiance goes to zero, as discussed in Section 4.3.8.

Then,

$$P_Z = L_{ZS} \left(\tau_R \left(\frac{\pi d^2}{4} \right) \right) B_{OPT} (2\pi(1 - \cos \theta_R)) f'(\theta_0, \theta_R, \theta) \quad (4-45)$$

4.3.13 (Continued)

Because this background source is cw, we use the energy transmission formalism to develop the expression:

$$L_{ZS} = (\text{Stellar/Zodiacal Light Clear Sky Effective Exo-Atmospheric Radiance}) \times (\text{Clear Atmospheric Transmission}) \times (\text{Cloud Energy Transmission}) \times (\text{Cloud to Water Energy Transmission}) \times (\text{Air-Water Interface Energy Transmission}) \times (\text{Water Energy Transmission}) \quad (4-46)$$

and we use

- L_Z = Stellar/Zodiacal Light Clear Sky Effective Exo-Atmospheric Radiance,
- τ_a = Clear Atmospheric Transmission, as discussed in Section 4.3.1,
- τ_{cz} = Cloud Energy Transmission, as discussed in Section 4.3.2,
- τ_{cw} = Cloud to Water Energy Transmission, as discussed in Section 4.3.3,
- τ_{awz} = Air-Water Interface Energy Transmission, as discussed in Sections 4.3.4 and 4.3.6,
- τ_{wz} = Water Energy Transmission, as discussed in Section 4.3.7.

Gathering the expressions we find:

$$L_{ZS} = L_Z \tau_a \tau_{cz} \tau_{cw} \tau_{awz} \tau_{wz} \quad (4-47)$$

Again, the fraction of stellar/zodiacal radiance within the receiver field-of-view is given by

$$f(\theta_r, \phi_r) = \frac{\int_0^{2\pi} d\phi \int_0^{\theta_0} d\theta \sin \theta \left[1 - \left(\frac{\sin \theta'}{\sin \theta_0} \right)^2 \right]}{\int_0^{2\pi} d\phi \int_0^{\theta_0} d\theta \sin \theta \left[1 - \left(\frac{\sin \theta}{\sin \theta_0} \right)^2 \right]} \quad (4-48)$$

4.3.13 (Continued)

$$\text{for } \theta^W = \cos^{-1} \left[\cos \theta^W \cos \delta_{zr} + \sin \theta^W \sin \delta_{zr} \sin \phi \right]$$

and δ_{zr} = Off-zenith pointing angle of the receiver axis.

These expressions will be used in the development of the Noise Equivalent Optical Power expression in Section 4.3.15.

4.3.14 Average Background Power Due to Bioluminescence

The final source of optical background power is the local bioluminescent sources which are stimulated to emit by the submarine motion, or other disturbances in the water. This is modelled in a slightly different way than the previous four sources, and cloud and water properties have only an indirect effect on this source strength. We therefore write for the average background power due to bioluminescence,

$$P_{BL} = (\text{Spectral irradiance at receiver aperture due to bioluminescence}) \times (\text{Receiver Optics Transmission}) \times (\text{Receiver Area}) \times (\text{Receiver Optical Filter Bandpass}). \quad (4-50)$$

and we set

L_{BL} = Spectral irradiance at receiver aperture due to bioluminescence,

T_R = Receiver Optics Transmission,

d = Diameter of Receiver Aperture,

$\frac{\pi d^2}{4}$ = Area of Receiver Aperture,

B_{OPT} = Optical Filter Bandpass.

Therefore,

$$P_{BL} = L_{BL} \left(T_R \left(\frac{\pi d^2}{4} \right) \right) B_{OPT} \quad (4-51)$$

4.3.15 Noise Equivalent Optical Power Dependence on Noise Sources

In general, a direct detection optical communication system has four independent noise contributions, which include thermal (or amplifier) noise, dark current detector noise, signal shot noise and background shot noise. These are noise sources insofar as they generate fluctuations in the electrical current present in the detection system. It is conventional to write the "noise" as the 1-σ point of the fluctuating electrical current, assuming the noise sources add independently and are steady in character.

Because we have derived a signal level in terms of the instantaneous received optical power, it is appropriate to describe the noise components in terms of a Noise Equivalent (Optical) Power, as derived from the post-detection electrical power.

We write, for a photomultiplier tube type of detector,

$$NEP_{tot} = \left[NEP_{th}^2 + NEP_{dc}^2 + NEP_{ss}^2 + NEP_B^2 \right]^{1/2} \quad (4-52)$$

for

NEP_{tot} = Total Noise Equivalent (Optical) Power due to all sources

NEP_{th} = Noise equivalent optical power due to thermal or amplifier noise

NEP_{dc} = Noise equivalent optical power due to photo-detector dark current

NEP_{ss} = Noise equivalent optical power due to shot-noise generated by the signal

NEP_B = Noise equivalent optical power due to shot-noise generated by the Background.

Then

$$NEP_{TH} = \left[\frac{4 (kT) B F_a}{G^2 \left(\frac{e}{h\nu} \right)^2 R_L} \right]^{1/2} \quad (4-53)$$

4.3.15 (Continued)

for

(kT) = thermal noise energy = (Boltzman's constant) X (Absolute Temperature)

B = electrical detection bandwidth, as discussed in Section 4.3.9

G = Detection gain

η = Photo surface quantum efficiency

e = charge on the electron

h ν = energy per signal photon

e/h ν = photo-surface responsivity

R_L = load resistance

F_a = Amplifier noise figure.

For the dark current contribution,

$$NEP_{DC} = \left[\frac{2 e B F G^2 I_d R_L}{G^2 (\eta e/h\nu)^2 R_L} \right]^{1/2} = \left[\frac{2 e B F I_d}{(\eta e/h\nu)^2} \right]^{1/2} \quad (4-54)$$

for

F = excess noise in the detector gain

and I_d = dark current at the photo-cathode.

For the signal shot noise contribution,

$$NEP_{ss} = \left[\frac{2 e B F (\eta e/h\nu) G^2 \hat{P}_R R_L}{G^2 (\eta e/h\nu)^2 R_L} \right]^{1/2} = \left[\frac{2 e B F \hat{P}_R}{(\eta e/h\nu)} \right]^{1/2} \quad (4-55)$$

for \hat{P}_R = peak received optical signal power at the photo surface, as discussed in Section 3.3.10.

Finally, the CW background contributes

4.3.15 (Continued)

$$NEP_B = \left[\frac{2 e B F G^2 (ne/h\nu) R_L (\sum P_B^i)}{G^2 (ne/h\nu)^2 R_L} \right]^{1/2} = \left[\frac{2 e B F \sum P_B^i}{(ne/h\nu)} \right]^{1/2} \quad (4-56)$$

for

$$\sum P_B^i = P_{su} + P_{mu} + P_{BS} + P_z + P_{BL} \quad (4-57)$$

for

P_{su} = Average background power due to sunlight, as discussed in Section 4.3.10;

P_{mu} = Average background power due to moonlight, as discussed in Section 4.3.11;

P_{BS} = Average background power due to blue skylight, as discussed in Section 4.3.12;

P_z = Average background power due to stellar/zodiacal light, as discussed in Section 4.3.13;

and P_{BL} = Average background power due to bioluminescence, as discussed in Section 4.3.14.

Two comments are in order at this point:

1. If the signal shot noise dominates the noise components, the formulation should be re-examined to insure that enough photo-electrons are being generated to make it applicable;
2. Not all the average background contributors will be present at any one time, which will be accounted for in the time-of-day modeling of the respective spectral radiances.

4.4 COMPUTER PROGRAM FOR COMPLETE SPDPM

4.4.1 Introduction

Figures 3-2 and 4-2 provided the basis for the computer program to perform calculations for the Single Pulse Downlink Propagation Model (SPDPM). The program is blocked out as shown in Figure 4-12.

Parameters which may be varied often are read from a data file, SPPM DATA. The values can be changed by editing this file.

The main program, SPPM, will display all parameter values prior to execution, then read parameter values for its use. Initial calculations are followed by a branch to one of the three cases: thin cloud, thick cloud, and clear atmosphere.

Within each case, signal calculations are performed first. This is followed by noise contributions from sun, moon, blue sky, stellar and zodiacal light, and bioluminescence. The final calculations include NEP's and the output follows.

There is a limited error message capability, primarily to handle cases where certain variables fall outside allowable limits.

Special functions can be used by all three cases. These include lookup tables and a numerical double integral.

4.4.2 Names of Variables

Because of the limitation of available characters in the FORTRAN IV programming language, many variables used in previous sections of this document required redefinition. Wherever possible, names were kept the same or very similar:

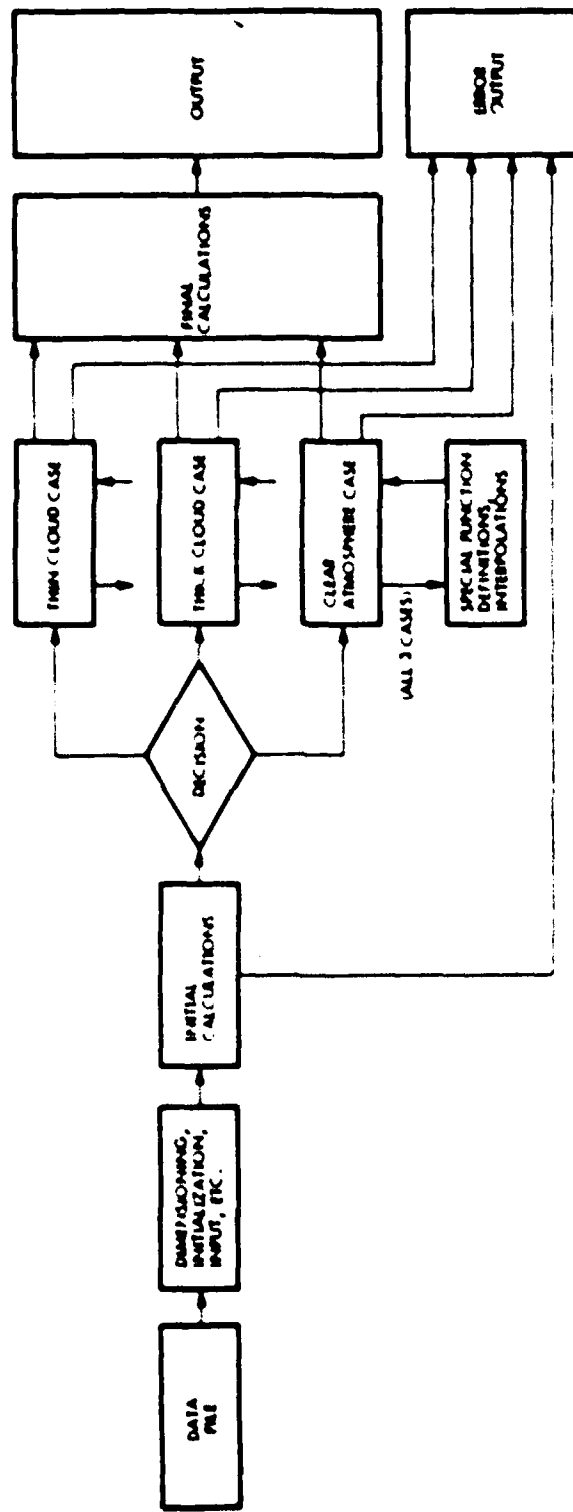


Figure 4-12. Complete SPDPH Computer Program Block Diagram

<u>TEXT</u>	<u>PROGRAM</u>	<u>DEFINITION</u>
c	C	Speed of light
I_d	ID	Photocathode dark current

Other variables were changed to a greater extent, but an attempt was made to make the new name easily understandable and relatable to the text name:

<u>TEXT</u>	<u>PROGRAM</u>	<u>DEFINITION</u>
B	BWE	Electrical Detection Bandwidth
B_{OPT}	BWOPT	Receiver Optical Filter Bandpass (Bandwidth)
D	DEPR	Receiver Depth

Because of the large number of text variables involving T, τ and θ , many of these required redefinition. First all angles () were redefined to start with letters other than T (see below). Most program T variables are transmissions, with the following exceptions:

<u>TEXT</u>	<u>PROGRAM</u>	<u>DEFINITION</u>
T	TABS	Absolute Temperature
D_i	THWCi	i^{th} water layer thickness
T	THGC	Geometrical Cloud thickness
b	THOPTA	Effective Clear Atmosphere Optical Thickness
τ_{OPT}	THOPTC	Cloud Optical Thickness
t	TI	Time Variable
t_m	TIPEAK	Time of pulse peak, relative to pulse start

There are also several program internal variables beginning with T which have no counterpart in the text.

The large number of transmissions have led to a systematization of these. They are all of the following form:

4.4.2 (Continued)

$$T \begin{pmatrix} A \\ \text{or} \\ AA \end{pmatrix} \begin{pmatrix} B \\ \text{or} \\ BB \end{pmatrix} \begin{pmatrix} C \\ \text{or} \\ \text{Nothing} \end{pmatrix}$$

where T signifies transmission; A or AA is a one or two letter designation for the energy source; B or BB, for the medium or interface; C, a further description if necessary.

A, AA

SG - signal

S - Sun

M - moon

BS - Blue Sky

Z - Stellar/Zodiacal
Light

B, BB

A - air

C - Cloud

CW - Cloud to water N - index of refraction

AW - Air Water
Interface

W - water

C

F - foam + streaks on
surface

Thus TSGAWN is transmission of the signal through the air-water interface considering refractive index effects; TZC is stellar/zodiacal light transmission through clouds. Text variables which correspond are τ_{aw} and τ_{cz} .

Angle variables have been renamed to begin with A for non-referenced angles, and ZA for Zenith Angles:

TEXT

A

θ_{SU}

PROGRAM

ASCAT

ZASA

DEFINITION

Cloud particle mean
Scattering Angle

Solar in-air zenith
angle

Unfortunately, some variables had to be defined quite differently from text variables:

TEXT

$\langle \cos \theta \rangle$

$\tau_{z/h}$

d

PROGRAM

COSACS

RESP

DIAR

DEFINITION

Mean Cosine of in-
Cloud Scattering
Angle

Responsivity

Receiver aperture
diameter

A list relating text and program variables follows:

A

ADLTA = δ	Offset angle between receiver optical axis and axis of the incoming light (signal section)
ACSCAT = θ	Cloud particle mean scattering angle
ATBWF = θ_T	Full angle exp (-2) transmitter beamwidth
AMSW = θ_{S1}^2	Mean square single scattering angle in water
ANSWI or ANSW(I) = θ_{S11}^2	Mean square single scattering angle in water for i'th layer
ARFOV = θ_R	Half angle of the receiver field of view
AS = $\theta_S/2$	Half of the angle subtended by the sun
AM = $\theta_M/2$	Half of the angle subtended by the moon
ARDWSG = θ_0	Off-axis angle at which in-water radiance goes to zero
ABKHP =	Half-power angle of the background radiance
ADLTAS = θ	Offset angle between receiver optical axis and axis of the incoming light
ADLTAM = θ	
ADLTAB = θ	
ADLTAZ = θ	
ARDWNS,M,B,Z = θ_0	Off-axis angle at which in-water radiance goes to zero (noise section)

B

BWE = B	Electrical detection bandwidth
BWOPT = B_{OPT}	Receiver optical filter bandpass

C

CF = C_f	Fraction of sea surface covered by foam and streaks
C = C	Speed of light
COSACS = $\cos \theta$	mean cosine of the in-cloud scattering angle

D

DEPR = D =	Receiver depth
DIAR = d =	Diameter of receiver aperture
DPWW = Δt_w =	Pulse width due to water portion of the path
DPWCW = Δt_{cw} =	Pulse width due to cloud to water portion of the path
DPWC = Δt_c =	pulse width due to cloud portion of the path

E

EPNORM = A_E =	Energy to instantaneous power normalization parameter
ER = E_R =	Total received energy per pulse
E2 = E_2 =	Exponential integral
ET = E_p =	Transmitted energy per pulse
EXTC = γ_c =	Mean extinction coefficient of the cloud

F

FW = f_w =	Water contribution to received beam half-angle
FAW = f_{aw} =	Air/water interface contribution to received beam half-angle
FA = f_a =	Atmospheric contribution to received beam half-angle
FWI or FW(I) = f_{wi} =	Contribution of i'th water layer to received beam half-angle
FSG = $\frac{f'(\theta_0, \theta_R)}{f'(\theta_0, \theta_R, \theta_{SL})}$ =	Fraction of incident radiance within receiver field of view
FWSQ, FWQ, = f_w =	Noise water contribution to received beam half-angle
FWBSQ, FWZQ	
FAS, FAM, = f_f	Noise atmospheric contribution to received beam half-angle
FABS, FAZ	

F (Continued)

FAWS, FAWM, $= f_{aw}$ = Noise-air-water contribution to received beam half-angle
FAWBS, FAWZ
FNS, FNM, (noise) = Fraction of incident radiance within receiver field of view
FNBS, FNZ

G

G = G = Detection gain
GAMT = γ_T = Transmitter optics transmission
GAMR = γ_R = Receiver optics transmission

H

HCW = H Distance from cloud base to water surface
HNU = $h\nu$ = Energy per signal photon

I

IRADM = $I(:^M)$ = Water radiance distribution
ID = I_d = Dark current at the photo cathode

J

J = j = Number of water layers present from surface to submarine receiver

K

K \emptyset = k = Diffuse attenuation coefficient of the water
KI or K(I) = k_i = Diffuse attenuation coefficient of the i'th water layer
KT = (kt) = Thermal noise energy - (Boltzmann's constant) x (absolute temperature)
KBOLTZ = Boltzmann's constant

L

$LSR = L_{SU} =$	Spectral radiance at receiver aperture due to the sun
$LSX = L_S =$	Exo-atmospheric effective solar radiance
$LMR = L_{MU} =$	Spectral radiance at receiver aperture due to the moon
$LMX = L_M =$	Exo-atmospheric effective lunar radiance
$LBSR = L_{BS} =$	Spectral radiance at receiver aperture due to blue sky light
$LBSX = L_B =$	Clear sky exo-atmospheric effective radiance due to blue sky light
$LZR = L_{ZS} =$	Spectral radiance at receiver aperture due to stellar and zodiacal light
$LZX = L_Z =$	Clear sky exo-atmospheric effective radiance due to stellar and zodiacal light
$LBLR = L_{BL} =$	Spectral irradiance at receiver aperture due to bioluminescence

M

N

$NOISF = F =$	Excess noise in detector gain
$NOISFA = F_a =$	Amplifier noise figure
$NDEX = n =$	Water index of refraction
$NEPTOT = NEP_{TOT} =$	Total noise equivalent optical power due to all sources
$NEPTH = NEP_{TH} =$	Noise equivalent optical power due to thermal or amplifier noise
$NEPID = NEP_{DC} =$	Noise equivalent optical power due to photo-detector dark current
$NEPSS = NEP_{SS} =$	Noise equivalent optical power due to shot-noise generated by the signal
$NEPSB = NEP_B =$	Noise equivalent optical power due to shot-noise generated by the background

O

OMEG θ = ω_0 = Cloud particle single scatter albedo
OMEG R = Ω_R = Solid angle of the receiver
OMEG W = Ω_0 = Full solid angle containing the incoming in-water radiance

P

PR = $P_R(t)$ = Instantaneous received signal power
PRS = P_{SU} = Average optical power at receiver due to the sun
PRM = P_{MU} = Average optical power at receiver due to the moon
PRBS = P_{BS} = Average optical power at receiver due to the blue sky
PRZ = P_Z = Average optical power at receiver due to stellar and zodiacal light
PRBL = P_{BL} = Average optical power at receiver due to bioluminescence
PRPEAK = P_R = Peak received signal power
PHILF = ϕ_f = $\frac{f_a + f_{aw} + f_w}{f_a + f_{aw} + f_w}$

Q

Q = q = Parameter describing ability of satellite transmitter to correct for zenith
QE = e = Charge on electron

R

RANGE = R = Range from satellite to submarine
RL = R_L = Load resistance
RFLW = $R(\cdot_s)$ = Sea surface reflectance
RESP = $(ne/h\cdot)$ = Responsivity
RPS = $f(t)$ = Received pulse shape

S

SCAT0 = S = Water scattering coefficient

SCATI or SCAT(I) = s_i = Scattering coefficient of i'th water layer

T

THOPTA = b = Effective clear atmosphere optical thickness

TABS = Absolute temperature

THGC = T = Geometrical thickness of the cloud

TI = t = Time

TIPEAK = t_m = Time after pulse start at which peak value occurs

TSGA = τ_a = Signal clear atmospheric energy transmission

TSGC = τ_c = Signal cloud energy transmission

THOPTC = τ_{OPT} = Optical thickness of the cloud

TSGCW = τ_{cw} = Signal cloud to water energy transmission

TSGAW = τ_{aw} = Signal total energy transmission of air/water interface

TSGAWI = τ_{aw2} = Signal air-water interface energy transmission due to the index of refraction discontinuity

TSGAWF = τ_{aw2} = Signal air-water interface energy transmission due to foam and streaks on the sea surface

TSGW = τ_w = Signal water energy transmission

TSBKA, TSBKA^w

TMBKA

TBSBKA = τ'_a = Background clear atmospheric energy transmission

TSC = τ'_{CS} = Cloud energy transmission of the direct sunlight

TMC = τ'_{CM} = Cloud energy transmission of the direct moonlight

TBSC = τ'_{CB} = Cloud energy transmission of the blue skylight

TZC = τ'_{CZ} = Cloud energy transmission of the stellar and zodiacal light

TBKCW = τ_{cw} = Background cloud to water energy transmission

T (Continued)

TSAW			
TMAW			
TBSAW	τ_{AW}		Total background energy transmission of the air-water interface
TZAW			
TBKAWF	τ_{AW2}		Background air/water interface transmission due to foam and streaks on the sea surface
TSAWN	τ_{AWIS}		Solar air/water interface transmission due to index of refraction discontinuity
TMAWN	τ_{AWIM}		Lunar air/water interface transmission due to index of refraction discontinuity
TBSAWN	τ_{AWIS}		Blue skylight air/water interface transmission due to index of refraction discontinuity
TZAWN	τ_{AWIZ}		Stellar and zodiacal light air/water interface transmission due to index of refraction discontinuity
TSW	τ_{WSU}		Solar water energy transmission
TMW	τ_{WMU}		Lunar water energy transmission
TBSW	τ_{WB}		Blue sky water energy transmission
TZW	τ_{WZ}		Stellar and zodiacal light water energy transmission

TABLE 1 - Table of τ_{AW1} for THOPTC = 10

TABLE 2 - Table of E_2

U

V

V = V =

Surface wind speed

W

X

Y

Z

ZASGA = θ_S

Signal in-air zenith angle

ZASGW = θ_S^W

Signal in-water zenith angle

ZASA = θ_{SU}

Solar in-air zenith angle

ZAMA = θ_{MU}

Lunar in-air zenith angle

ZASW = θ_{SU}^W

Solar in-water zenith angle

ZAMW = θ_{MU}^W

Lunar in-water zenith angle

1000 1774

1901. 03.04. 10.00
05.07.14 00.10.10

[illegible]

4.4.3 (Continued)

PAGE 0003

ISSUE J.051802.0001
 05/02/79 09:02:04

```

C CHECK TO SEE IF PARAMETERS ARE WITHIN RANGE(S) SPECIFIED
C
C
C 10 J=2:1
C   IF (A(J)-FM.FA12320.20.10
C     FIND NECESSARY RANGE FOR INTERPOLATION BY A(J)
C
C 20 J=1:1
C   CALCULATE VALUE BY FORMULATION FOR INTERPOLATION
C   IF (A(J)-FM.FA12320.20.10
C     FIND NECESSARY RANGE FOR INTERPOLATION
C
C 30 DO 40 J=1:5
C   A(J)=A(J)+1
C   IF (A(J)-FM.FA12320.20.10
C     FIND NECESSARY RANGE FOR INTERPOLATION
C
C 40 CONTINUE
C
C 1000 NUM=5.-FM.FA12320.20.10
C   IF (A(J)-FM.FA12320.20.10
C     FIND NECESSARY RANGE FOR INTERPOLATION
C
C 1500 IF (A(J)-FM.FA12320.20.10
C   THIS STATEMENT PERFORMS ACTUAL INTERPOLATION
C
C   RETURN
C
C 2000 IF (A(J)-FM.FA12320.20.10
C   THIS STATEMENT PERFORMS ACTUAL INTERPOLATION
C
C   RETURN
C
C 3000 IF (A(J)-FM.FA12320.20.10
C   THIS STATEMENT PERFORMS ACTUAL INTERPOLATION
C
C   RETURN
C
C 4000 IF (A(J)-FM.FA12320.20.10
C   THIS STATEMENT PERFORMS ACTUAL INTERPOLATION
C
C   RETURN
C
C 5000 IF (A(J)-FM.FA12320.20.10
C   THIS STATEMENT PERFORMS ACTUAL INTERPOLATION
C
C   RETURN
C
C 6000 IF (A(J)-FM.FA12320.20.10
C   THIS STATEMENT PERFORMS ACTUAL INTERPOLATION
C
C   RETURN
C
C 7000 IF (A(J)-FM.FA12320.20.10
C   THIS STATEMENT PERFORMS ACTUAL INTERPOLATION
C
C   RETURN
C
C 8000 IF (A(J)-FM.FA12320.20.10
C   THIS STATEMENT PERFORMS ACTUAL INTERPOLATION
C
C   RETURN
C
C 9000 IF (A(J)-FM.FA12320.20.10
C   THIS STATEMENT PERFORMS ACTUAL INTERPOLATION
C
C   RETURN
C
C 10000 IF (A(J)-FM.FA12320.20.10
C   THIS STATEMENT PERFORMS ACTUAL INTERPOLATION
C
C   RETURN
C

```

4.5 MODEL UNCERTAINTIES

The sub-models contained in Section 4.3 have a number of uncertainties, due to a lack of experimental work. (The uncertainties in the signal models was discussed in Section 3.3.)

4.5.1 Average Power Transmission

Two additional uncertainties arise in the models in Sections 4.3.1, 4.3.2, 4.3.3, 4.3.4, 4.2.6, and 4.2.7, in addition to those present in the signal energy transmission models.

Clear atmosphere transmission for solar or lunar zenith angles greater than 85° is not correctly given in the SPDPM.

Air-water interface transmission for solar or lunar zenith angles greater than 85° is also not correctly given in the SPDPM.

The importance of these two inaccuracies is undetermined, until we estimate how often such conditions apply to the scenario. This will be done in future work.

4.5.2 Angular Effects

The same uncertainty effects apply here as for the signal angular effects.

4.5.3 Temporal Effects

At present all the background sources in the SPDPM are taken as steady state. The bioluminescent background may have enough temporal structure to invalidate this model, but no definitive results exist at present.*

Table 4-10 summarizes the uncertainty status of the noise portion of the SPDPM.

*Again, a pulse distorting filter is not treated in these sub-models. Should it become the leading candidate for the optical filter, the temporal sub-model would need modification.

Table 4-10. Status of Noise Portion Models of SPDPM

	THIN CLOUD	THICK CLOUD	COMMENTS ON EXPERIMENTAL WORK REQUIRED
<u>AVERAGE POWER TRANSMISSION</u>			
Clear Atmosphere	Partially verified	Not applicable	Large zenith angle prob- lems. Impact TBD.
Cloud	Unknown but small effect	Unknown	Signal experiment applicable. Large zenith angle effects TBD.
Cloud to Water	Not applicable	OK	None
Air-Water Interface	Partially verified	OK	Large zenith problems. Impact TBD.
Water	Unknown	Unknown	A signal experiment would be applicable.
<u>ANGULAR EFFECTS</u>			
Shape	Partially verified	Partially verified	Should be done.
Out-of-Water Contribution	OK	Partially verified	Should be done if other related work is planned.
Air-Water Interface	OK	OK	None
In-Water Contribution	Partially verified	Partially verified	Needed for depth and water type.
Combination of Effects	Partially verified	Unknown	Needed
<u>TEMPORAL EFFECTS</u>			
Bioluminescence	Temporal character unknown as a function of depth, loca- tion, submarine speed, season. Some experimental work is needed.		

4.6 PARAMETER VALUE UNCERTAINTIES

In addition to those parameter value uncertainties discussed in Section 3.5 for the signal portion of the SPDPM, the noise portion parameters are uncertain with regard to background levels.

The solar and lunar parameters are not uncertain. The effective strength of the blue skylight background (and its solar zenith angle dependence) is uncertain and requires clarification. It has a significant impact since for thick cloud conditions the system may be skylight limited at high latitudes.

The starlight/zodiacal light parameters are not in question.

The strength of the bioluminescence is very uncertain, as is its distribution in depth, season, time of night, location, and its response to stimulation such as submarine motion. This is important since for the value of 10^{-3} watts/(m²-micron) used in the SPDPM the system is bioluminescent limited for many water and cloud conditions.

Table 4-11 summarizes the uncertainty status of the "parameter" values for the noise portion of the channel characterization.

Table 4-11. Status of "Input Parameters" to the Noise Portion of the SPDPM

PARAMETER	STATUS	COMMENTS ON EXPERIMENTAL WORK REQUIRED
Clear Atmosphere	OK	None
<u>Cloud:</u>		
$\cos \theta$	OK	None
ρ	OK	None
τ_0	Partially known	No direct experiment possible
τ_c	Partially known	Some work is planned during first cloud experiment. Equipment may be too inaccurate for good results.
T	Partially known	Interpretation of data required.
Cloud-to-Water	OK	None
Air Water Interface	OK, for low wind speeds	Some required for bad conditions.
<u>Water:</u>		
k_i	Partially known	Required if not done by other contractors.
D_i	Partially known	Required if available data not able to be interpreted.
σ_i	Partially known	Required as a function of depth and water type.
S	Partially known	May become available for surface water from ongoing work. Needed for water at depth.
n	OK	None
<u>Background Levels:</u>		
Blue Skylight	Partially known	Needed
Bioluminescence	Unknown	Needed

Section 5

DOWNLINK COMMUNICATION MODEL

This section discusses the model for the optical communication link from a satellite to a submerged submarine. The section is organized as follows:

- 5.1 Downlink Communications Model-Philosophy and Flow Chart
 - 5.1.1 Philosophy of Approach - Downlink Communication Model
 - 5.1.2 Model Flow Chart - Downlink Communication Model
- 5.2 Input Information
 - 5.2.1 Environment
 - 5.2.2 Requirements
 - 5.2.3 System Design
- 5.3 Sub-Models
 - 5.3.1 Area Relationships
 - 5.3.2 Temporal Relationships
 - 5.3.3 Message
 - 5.3.4 Modulation/Demodulation
 - 5.3.5 Scanning Relationships
 - 5.3.6 Receiver and Source
 - 5.3.7 Availability/System Effectiveness and Adaptive Scanning
- 5.4 Computer Program for the DCM
 - 5.4.1 Introduction
 - 5.4.2 Names of Variables
 - 5.4.3 Listing
- 5.5 Model Uncertainties
 - 5.5.1 Area Relationships
 - 5.5.2 Temporal Relationships
 - 5.5.3 Message

5. (Continued)

- 5.5.4 Modulation/Demodulation
- 5.5.5 Scanning Relationships
- 5.5.6 Receiver and Source
- 5.5.7 Availability/System Effectiveness
- 5.5.8 Included SPDPM Sub Models

5.6 Parameter Value Uncertainties

- 5.6.1 Environment
- 5.6.2 Requirements
- 5.6.3 System Design

5.1 Downlink Communications Model-Philosophy and Flow Chart

This section explains the basic approach used in the detailed models presented in Section 5.3, and presents flow charts showing the interrelationships of the sub-models and their required inputs. (These inputs are discussed in more detail in Section 5.2.)

5.1.1 Philosophy of Approach-Downlink Communications Model

This model is an intermediate step between the Single Pulse Downlink Propagation Model (SPDPM) and the Full OSCAR Communication System architecture. We have therefore used the approach that:

1. The SPDPM is fully available for use;
2. This Downlink Communication Model (DCM) treats the problem of communicating to a specific area by a single satellite within a single time interval. It does not consider the entire OSCAR coverage area, a complete satellite constellation suitable for covering that area, the system effectiveness of any part but the downlink communication link of the OSCAR system, etc. As such it is a building block in the complete system architecture just as the SPDPM is a building block within this Downlink Communication Model.
3. For a given interval of time, the full OSCAR system requirements must be met. During this time interval, the satellite location, sun location, and moon location are completely specified. In addition, the area which must be communicated with is described both geometrically and with regard to its complete propagation environment;
4. The coverage area is resolved into equal-area resolution elements, each with a uniform value of the environmental parameters and each small enough so that signal and background zenith angle effects vary negligibly across the element. Then each element is represented by a mean value of latitude and longitude and the SPDPM is evaluated at that point, with results which apply throughout the resolution element.
5. A single system design is tested to see how well it meets OSCAR requirements. Besides all the normal transmitter and receiver hardware parameters, this system design considers:

5.1.1 (Continued)

- a. The satellite location
 - b. The choice of demodulation technique(s)
 - c. The choice of post-detection processing for anti-jam of time-of-peak demodulation
 - d. The choice of scan technique.
6. This system design includes consideration of all the times involved, including source warm-up time, dead-time between frames, slot widths, and time to slew to a new spot.
 7. The minimum spot dimensions are dependent on their overlap, the adjacent spot revisit time, the satellite short and long term pointing jitter, the scan technique and the total time allowed to cover the area.

5.1.2 Model Flow Chart-Downlink Communication Model

A schematic of the overall Downlink Communication Model is shown in Figure 5-1. The input parameters are designated as environment, requirements, and system design. Using these inputs, area relationships and receiver parameters (chiefly the value of δ , the angle between receiver axis and the incoming beam) are developed. In parallel, source parameters (like required prime power), message, and modulation/demodulation equations are evaluated. The modulation/demodulation and area relationship results are used to determine the scanning parameters, and then all the parameters are used as inputs to the availability analysis. Finally, temporal relationships (like the source on-time) are evaluated from the source and availability results.

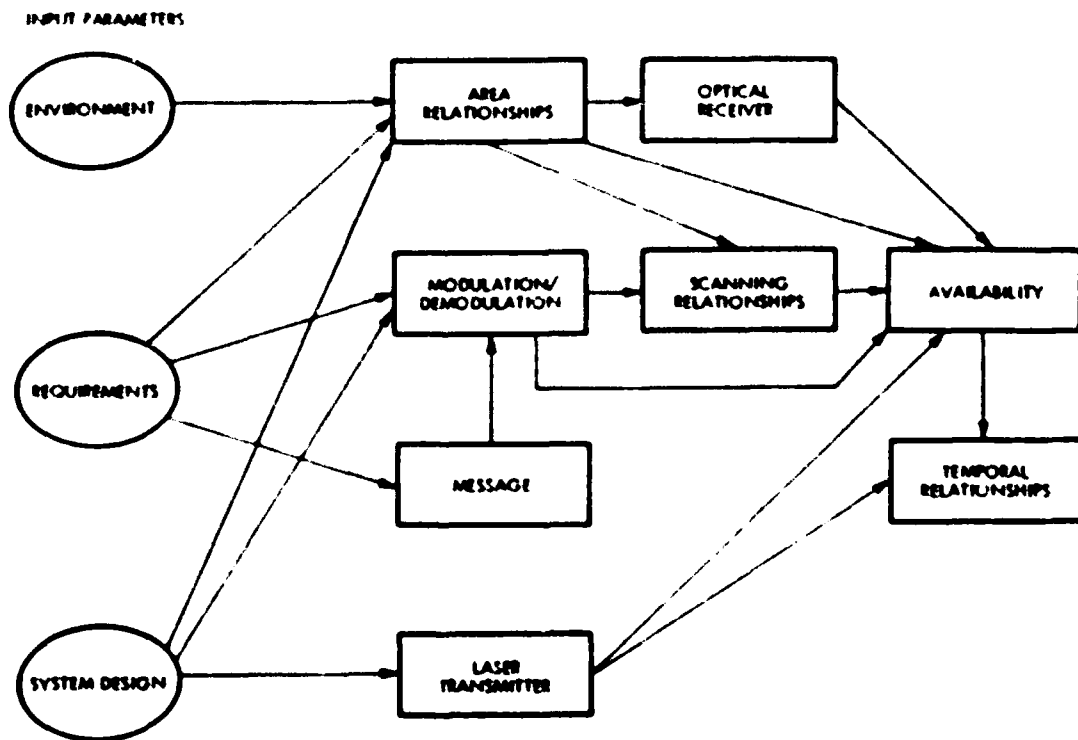


Figure 5-1. Schematic of Downlink Communication Model

5.1.2 (Continued)

Figure 5-2 is a detailed flow chart showing all the calculations to be performed in this model:

- (I) The input parameters are listed in the three ellipses on the left hand side of the figure, including environment, requirements, and system design. (The symbols are defined in the glossary in Section 2, and also in the input discussions in Section 5.2).
- (II) The only additional input is the nominal $\tau_{OPT} = 50$ value, shown in the ellipse near the center, and used in the partially adaptive scanning analysis.
- (III) The calculation equations are represented by the rectangular boxes. Within each box is the symbol for the parameter to be calculated and the equation number (from Section 5.3) for the equation to be used to calculate the parameter.
- (IV) SPDPM within a rectangular box refers to the full single pulse downlink propagation model.
- (V) The diamond shaped boxes represent branch points. Only one of the two (or three) paths coming out of the diamond are followed, depending on the value of the parameters (or input choice). The branching parameters include τ_{OPT} , Threshold or Time-of-Peak Demodulation, Anti-Jam Processing for Time-of-Peak Demodulation, q , T_{TOT} vis-a-vis T_A , and scan technique.
- (VI) Key outputs of the program include P_{TOT} , total satellite prime power; A_{VL} , availability or system effectiveness; N_{SP} , the number of spoofing events per year; N_J (or N'_J), the number of jamming events per year; and N_{PL} , the number of pulses used by a given laser transmitter to achieve the A_{VL} .

(FIGURE LOCATED IN ENVELOPE IN REAR OF BOOK)

Figure 5-2. Flow Diagram of Downlink
Communication Model

5-7/5-8

5.2 Input Information

This section discusses the form and units of the required inputs to the downlink communication model. These inputs are divided into three categories, as seen in the computer flow charts: Environment, Requirements, and System Design.

5.2.1 Environment

All the Single Pulse Downlink Propagation Model (SPDPM) environmental inputs are required here since the SPDPM will be extensively utilized. These inputs include b , T , σ_c , $\langle \cos \theta \rangle$, ω_0 , θ , H , V , n , k_1 , D_1 , θ_{S1} , s , $\theta_{S/2}$, L_S , $\theta_{m/2}$, L_m , L_B , L_Z , and L_{BL} .

Other and new environmental parameters are:

<u>SYMBOL</u>	<u>DESCRIPTION</u>	<u>UNITS</u>
A_{RE}	Area of a single resolution element	(Meter) ²
R_{SU}	Distance from sun to receiver	Meters
λ_{SU}	Solar latitude	Degrees
β_{SU}	Solar longitude	Degrees
R_E	Mean Earth Radius	Meters
R_{MU}	Distance from moon to receiver	Meters
λ_{MU}	Lunar latitude	Degrees
β_{MU}	Lunar longitude	Degrees

5.2.2 Requirements

All the Statement of Work requirements are entered here in their most elemental form:

<u>SYMBOL</u>	<u>DESCRIPTION</u>	<u>UNITS</u>
T_A	Coverage Time	Seconds
Coverage Area	That area for which a given satellite is assigned responsibility for the time interval T_A . The boundaries should be specified in latitude and longitude.	-

5.2.2 (Continued)

<u>SYMBOL</u>	<u>DESCRIPTION</u>	<u>UNITS</u>
M_{LO}	The message length, i.e., the number of bits which must be broadcast to the entire coverage area within T_A .	Bits
N_M	The number of missed messages per year. (This is the quality of service requirement)	$(\text{Year})^{-1}$
N_{SPi}	The number of spoofing events per year.	$(\text{Year})^{-1}$
N_{Ji}	The number of jamming events per year.	$(\text{Year})^{-1}$
g	The ratio of threat "cost" to our system "cost."	-
D	Submarine Depth	Meters

5.2.3 System Design

All the SPDPM system design inputs are required here since it will be extensively utilized. These inputs include q , γ_T , θ_R , γ_R , d , B_{OPT} , (kT) , F_A , G , $(ne/h\nu)$, R_L , I_d and F .

Other and new system design parameters are:

<u>SYMBOL</u>	<u>DESCRIPTION</u>	<u>UNITS</u>
t_{Si}	Slew time, scan time or dead time between illuminated spots.	Seconds
t_W	Source warm-up time, before it is ready for full operation.	Seconds
PRF	Source repetition frequency	$(\text{Seconds})^{-1}$, or Hz
G_{EL}	Off-zenith in-water receiver pointing angle, which may be different in each resolution element.	Degrees
G_{AZ}	Azimuth receiver pointing angle, relative to the local longitude.	Degrees

5.2.3 (Continued)

<u>SYMBOL</u>	<u>DESCRIPTION</u>	<u>UNITS</u>
m	Number of simultaneously active lasers aboard the satellite.	-
E_p	Energy per pulse of each active laser aboard the satellite.	Joules
F_L	"Wallplug" laser efficiency	-
P_{HO}	Prime-power on the satellite required for all non-laser functions.	Watts
R_S	Satellite altitude	Meters
λ_S	Satellite latitude	Degrees
β_S	Satellite longitude	Degrees
t_f	Dead time between frames	Seconds
t_s	Slot width	Seconds
z	Number of bits per pulse	-
ϕ	Overlap factor between illuminated spots	-
σ_{TS}	Satellite rms short term angular jitter	Radians
σ_{TDR}	Satellite rms long term angular drift	Radians
Demodulation Approach	Choice of threshold exceedance or time-of-peak demodulation approach	-
Post Detection Processing for Time-of-Peak Demodulation	Choice of post-detection processing approach to provide anti-jamming capability for time-of-peak demodulation approach.	-
Scanning Approach	Choice of totally non-adaptive scan, one partially adaptive scan, or fully adaptive scan technique.	-

5.3 Sub-Models

This section develops all the equations used in the calculation of the performance of the communication downlink.

Section 5.3.1 considers the area relationship and develops the concept of resolution elements.

Section 5.3.2 considers the temporal relationships and Section 5.3.3 considers relationships derived from the message parameters.

Section 5.3.4 develops the modulation/demodulation relationships for pulse position modulation, both threshold and time-of-peak demodulation, and derives signal to noise and message structure requirements for quality of service, spoofing and jamming.

Section 5.3.5 develops scanning relationships while Section 5.3.6 considers new receiver and laser transmitter parameters.

Section 5.3.7 develops equations for system availability, for non-adaptive and adaptive scanning.

5.3.1 Area Relationships

The input to the downlink communication system model will include the location of the satellite terminal and the location and extent of the area it is responsible for communicating with. All the angular information will be input in terms of latitude and longitude. We therefore define, as exemplified in Figure 5-3:

- R_S Satellite altitude
- R_E Mean earth radius
- λ_S Satellite latitude
- λ_{SU} Sun's latitude
- λ_{MU} Moon's latitude
- λ_{AI} Latitude of point within coverage area
- λ_S Satellite longitude
- λ_{SU} Sun's longitude
- λ_{MU} Moon's longitude
- λ_{AJ} Longitude of point within coverage area.

From these input parameters we need to derive

- R Range from satellite to submarine
- θ_S Signal zenith angle into the water
- θ_{SU} Solar zenith angle into the water
- θ_{MU} Lunar zenith angle into the water.

It is straightforward to derive the range by expressing the satellite location and submarine location in cartesian coordinates with the origin at the center of the earth.

$$R^2 = (X_S - X_E)^2 + (Y_S - Y_E)^2 + (Z_S - Z_E)^2 \quad (5-1)$$

5.3.1 (Continued)

for

$$x_E = R_E \cos \alpha_{Ai} \cos \beta_{Ai}, \quad (5-1a)$$

$$x_S = (R_E + R_S) \cos \alpha_S \cos \beta_S, \quad (5-1d)$$

$$y_E = R_E \cos \alpha_{Ai} \sin \beta_{Ai}, \quad (5-1b)$$

$$y_S = (R_E + R_S) \cos \alpha_S \sin \beta_S, \quad (5-1e)$$

$$z_E = R_E \sin \alpha_{Ai}, \quad (5-1c)$$

$$z_S = (R_E + R_S) \sin \alpha_S, \quad (5-1f)$$

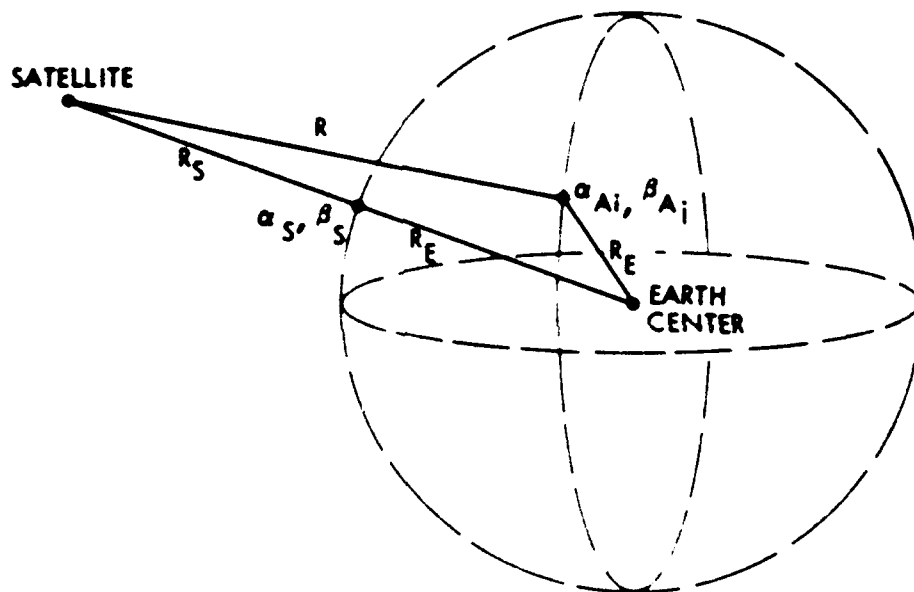


Figure 5-3. Latitude and Range Satellite to Earth Geometry

5.3.1 (Continued)

The expression becomes, after substitution and manipulation,

$$R_{IJ} = \left[(R_E + R_S)^2 + R_E^2 - R_E(R_E + R_S) \left\{ \cos(\lambda_{A1} + \lambda_S) \left(\cos(\beta_{AJ} - \beta_S) - 1 \right) + \cos(\lambda_{A1} - \lambda_S) \left(\cos(\beta_{AJ} - \beta_S) + 1 \right) \right\} \right]^{1/2} \quad (5-2)$$

From Figure 5-4, the zenith angle into the water for the signal is given by

$$\beta_S = \dots \quad (5-3)$$

$$\text{for } R^2 = (R_E + R_S)^2 - R_E^2 + 2 R_E R \cos \dots \quad (5-4)$$

Comparing (5-3) and (5-4) it is evident that

$$\beta_{S_{IJ}} = \cos^{-1} \left\{ \frac{1}{R} \left[\left(\frac{R_E + R_S}{2} \right) \left\{ \cos(\lambda_{A1} + \lambda_S) [\cos(\beta_{AJ} - \beta_S) - 1] + \cos(\lambda_{A1} - \lambda_S) [\cos(\beta_{AJ} - \beta_S) + 1] \right\} - R_E \right] \right\} \quad (5-5)$$

By analogy, for the solar zenith angle (since $R_{SU} \gg R_E$)

$$\beta_{SU_{IJ}} = \cos^{-1} \left\{ \frac{1}{2} \left\{ \cos(\lambda_{A1} + \lambda_{SU}) [\cos(\beta_{AJ} - \beta_{SU}) - 1] + \cos(\lambda_{A1} - \lambda_{SU}) [\cos(\beta_{AJ} - \beta_{SU}) + 1] \right\} \right\} \quad (5-6)$$

and for the lunar zenith angle (since $R_{MU} \gg R_E$)

$$\beta_{MU_{IJ}} = \cos^{-1} \left\{ \frac{1}{2} \left\{ \cos(\lambda_{AJ} + \lambda_{MU}) [\cos(\beta_{AJ} - \beta_{MU}) - 1] + \cos(\lambda_{A1} - \lambda_{MU}) [\cos(\beta_{A1} - \beta_{MU}) + 1] \right\} \right\} \quad (5-7)$$

These angular expressions must also be interpreted in terms of an area to be covered. We assume the following propagation path inputs over the coverage area:

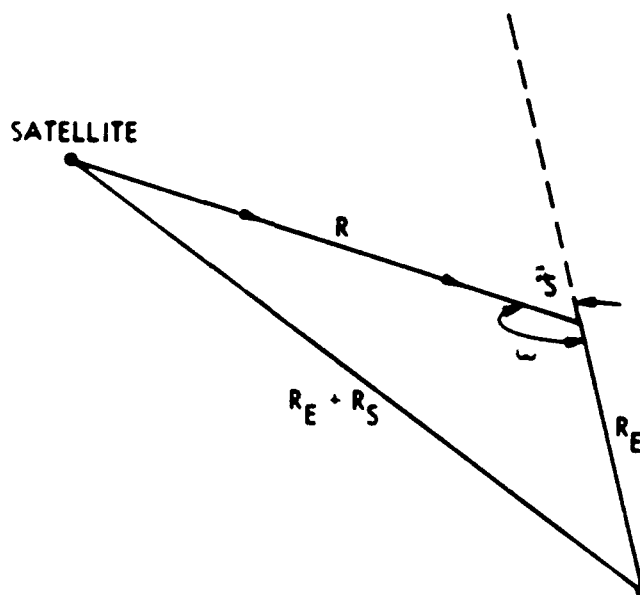


Figure 5-4. Signal Zenith Entrance Angle Geometry

5.3.1 (Continued)

1. There are four areas of importance in the OSCAR scenario:
 - a. The total area in the OSCAR requirement which must be communicated with during the time interval;
 - b. The area which a single satellite is assigned to cover during a single time interval. It is this area which is considered in this Downlink Communication Model (DCM), and which we designate A_1 ;
 - c. The single satellite/single time interval coverage area A_1 is divided into environmental resolution elements, of area A_{RE} , each of which has a uniform value of all parameters related to the environment's effects on both the signal and background propagation;
 - d. The area of a single illuminated spot, which will ordinarily be much less than A_{RE} , and which will be determined in later sections.

These four areas are illustrated in Figure 5-5.

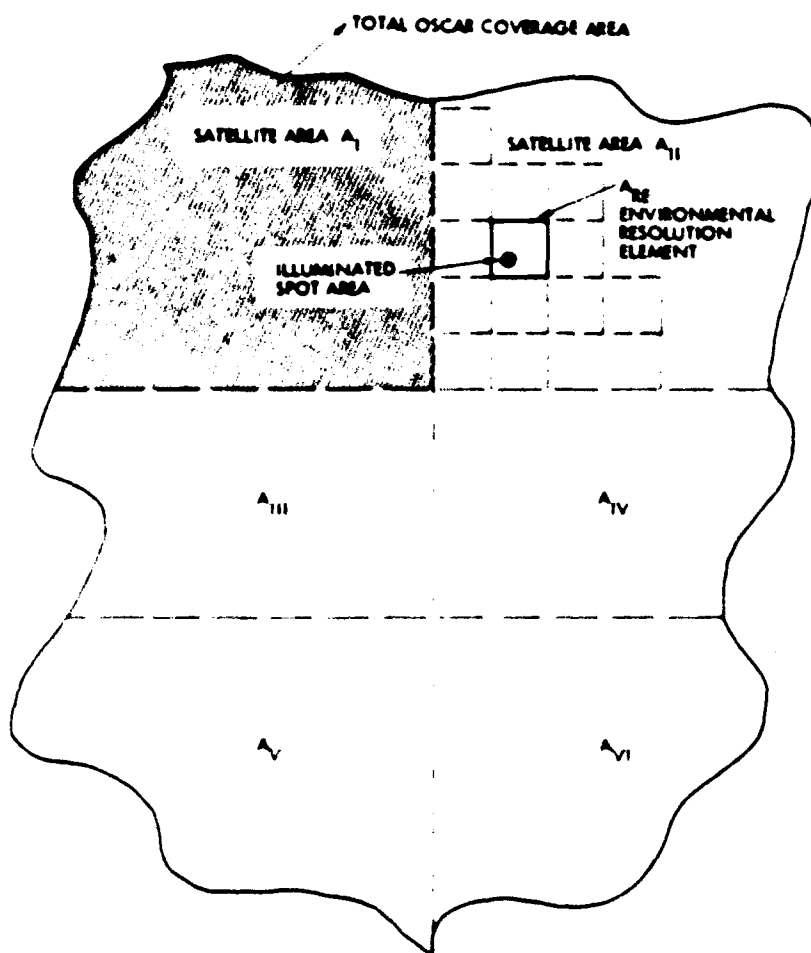


Figure 5-5. Illustration of Four Area Relations

5.3.1 (Continued)

2. Each resolution element is much larger than the smallest possible illuminated spot area, but small enough to allow for essential signal level equality due to signal and/or background zenith angle alone within the element, if the environmental effects are uniform over the entire coverage area;

5.3.1 (Continued)

3. Each resolution element is bounded by constant latitude/constant longitude lines. The four corners of resolution element are then given by (for the first element in the coverage area, for example)

$$1^{\alpha}A, 1^{\beta}A; 1^{\alpha}A, 2^{\beta}A;$$

$$2^{\alpha}A, 1^{\beta}A; 2^{\alpha}A, 2^{\beta}A.$$

4. The entire resolution element is characterized by its mean value of latitude and longitude, and it is this value (α_A, β_A) which is used in all Single Pulse Propagation Model calculations. The mean values are defined by

$$\alpha_1 = \frac{1}{2} \left(1^{\alpha}A + 1+1^{\alpha}A \right) \quad (5-8)$$

and

$$\beta_j = \frac{1}{2} \left(j^{\beta}A + j+1^{\beta}A \right) \quad (5-9)$$

In this way the number of calculations (required to characterize operation over the full area with possible adaptive scan coverage) are minimized.

5. Each resolution element within the coverage area contains the same area.
6. This area shall have the same width in longitude, independent of latitude. Its angular dimension in latitude shall be varied to maintain equal areas.

The approximate area of a figure bounded by constant latitude and longitude is given by

$$A_{RE} = [R_E (\alpha_2 - \alpha_1)] \left[R_E (\beta_2 - \beta_1) \cos\left(\frac{\alpha_2 + \alpha_1}{2}\right) \right] \quad (5-10)$$

5.3.1 (Continued)

To insure that the resulting resolution elements will not assume distorted shapes at either latitude extreme, we demand that it be approximately symmetric at the mid-latitude value, or

$$R_E (\lambda_2 - \lambda_1) = R_E (\lambda_2 - \lambda_1) \cos \left(\frac{\lambda_2 + \lambda_1}{2} \right) \text{ at } \frac{\lambda_2 + \lambda_1}{2} = 45^\circ,$$

$$\text{or, } \Delta \lambda = \Delta \lambda \cos \left(\frac{\lambda_2 + \lambda_1}{2} \right) \text{ at } \frac{\lambda_2 + \lambda_1}{2} = 45^\circ,$$

$$\text{or } \Delta \lambda = \frac{\Delta \lambda}{2} \quad (5-11a)$$

Putting (5-11a) into (5-10) at $\frac{\lambda_2 + \lambda_1}{2} = 45^\circ$ we find

$$\frac{(\Delta \lambda)^2}{2} = \frac{A_{RE}}{R_E^2}.$$

$$\text{or } \Delta \lambda = \frac{[2 A_{RE}]^{1/2}}{R_E} \quad (5-11b)$$

We have solved (5-11b) for $A_{RE} = 3(10^{11})\text{m}^2$, $2(10^{11})\text{m}^2$, $1(10^{11})\text{m}^2$ and $5(10^{10})\text{m}^2$ and listed the results in Table 5-1. Also shown in Table 5-1 are the values of the corresponding latitude boundaries as the latitude is stepped off from 0° to 70° , and the length of each side of the resolution element.

The spot sizes themselves are much smaller than these resolution elements. If we maintain a circular spot independent of signal zenith angle, its diameter will be given by

$$D_{SP} = R \theta_T \quad (5-11c)$$

Table 5-1. Resolution Element Angular Coordinates

α_i
 [Vertical Dimension (m)]
 [Horizontal Dimension (m)]

A_{RE}

$3(10^{11})m^2$	$2(10^{11})m^2$	$1(10^{11})m^2$	$5(10^{10})m^2$
$\Delta\theta = 0.1215 (6.96^\circ)$	$\Delta\theta = 0.0891 (5.68^\circ)$	$\Delta\theta = 0.0701 (4.01^\circ)$	$\Delta\theta = 0.0438 (2.84^\circ)$
3.48 [3.868×10^3] 7.7	2.84 [3.158×10^3] 6.3	2.01 [2.232×10^3] 4.46	1.41 [1.577×10^3] 3.157
6.97 [3.88] 7.72	5.68 [3.166] 6.3	4.028 [2.23] 4.4	2.84 [1.578] 3.16
10.49 [3.9] 7.69	8.556 [3.18] 6.287	6.0 [2.24] 4.456	4.28 [1.58] 3.15
14.048 [3.95] 7.656	11.44 [3.206] 6.266	8.06 [2.25] 4.45	5.88 [1.58] 3.15
17.685 [4.017] 7.6	14.358 [3.239] 6.24	10.1 [2.26] 4.44	7.1 [1.58] 3.15
21.355 [4.089] 7.536	17.3 [3.262] 6.2	12.146 [2.275] 4.425	8.55 [1.58] 3.14
25.14 [4.2] 7.45	20.3 [3.336] 6.158	14.2 [2.29] 4.41	9.98 [1.598] 3.14
29.046 [4.34] 7.35	23.375 [3.4] 6.1	16.29 [2.31] 4.39	11.43 [1.6] 3.13
33.31 [4.5] 7.23	26.5 [3.46] 6.046	18.4 [2.34] 4.37	12.88 [1.61] 3.128
37.385 [4.73] 7.08	29.73 [3.58] 5.97	20.5 [2.36] 4.35	14.3 [1.62] 3.12
41.88 [5.02] 6.93	33.06 [3.7] 5.89	22.88 [2.4] 4.32	15.8 [1.63] 3.11

Table 5-1. Resolution Element Angular Coordinates (Continued)

A_{RE}

$3(10^{11})m^2$ λ = 0.1215 (6.96°)	$2(10^{11})m^2$ λ = 0.0901 (5.68°)	$1(10^{11})m^2$ λ = 0.0701 (4.01°)	$5(10^{10})m^2$ λ = 0.0486 (2.84°)
46.74° [5.4 6.78]	36.5° [3.84 5.8]	24.89° [2.44 4.29]	17.3° [1.6 3.1]
52.0° [5.94 6.49]	40.1° [4.025 5.89]	27.12° [2.48 4.26]	18.79° [1.65 3.08]
58.1° [6.76 6.197]	43.97° [4.25 5.57]	29.4 [2.53 4.22]	20.8° [1.67 3.08]
65.54° [8.19 5.82]	48.0° [4.547 5.43]	31.74° [2.59 4.183]	21.8° [1.69 3.06]
76.14° [11.8 5.25]	52.5° [4.94 5.26]	34.13° [2.66 4.14]	23.36° [1.71 3.05]
	57.47° [5.50 5.06]	36.6° [2.74 4.08]	24.9° [1.73 3.03]
	63.21° [6.38 4.8]	39.14 [2.8 4.04]	26.48° [1.75 3.02]
	70.427° [8.02 4.49]	41.78° [2.93 3.98]	28.08° [1.78 3.0]
		44.54° [3.06 3.9]	29.71° [1.8 2.98]
		47.42° [3.21 3.84]	31.38° [1.83 2.96]
		50.49° [3.4 3.76]	33.03° [1.86 2.94]
		53.8° [3.64 3.67]	34.7° [1.9 2.92]
		57.3° [3.94 3.66]	36.48° [1.94 2.89]
		61.24° [4.37 3.44]	38.26° [1.99 2.86]
		66.7° [5.0 3.3]	40.1° [2.04 2.83]

Table 5-1. Resolution Element Angular Coordinates (Continued)

ARE			
$3(10^{11})\text{m}^2$	$2(10^{11})\text{m}^2$	$1(10^{11})\text{m}^2$	$5(10^{10})\text{m}^2$
$\Delta\theta = 0.1215 (0.96^\circ)$	$\Delta\theta = 0.0801 (0.68^\circ)$	$\Delta\theta = 0.701 (4.01^\circ)$	$\Delta\theta = 0.0486 (2.84^\circ)$
		71.2° [6.08 3.11]	41.90° [2.00 2.804]
			43.83° [2.156 2.77]
			45.94° [2.23 2.74]
			48.02° [2.31 2.7]
			50.19° [2.41 2.66]
			52.46° [2.52 2.6]
			54.86° [2.66 2.56]
			57.40° [2.83 2.51]
			60.14° [3.04 2.4]
			63.13° [3.32 2.38]
			66.47° [3.70 2.30]
			70.32° [4.28 2.21]

5.3.1 (Continued)

for θ_T = full angle exp (-2) transmitter beam width (irradiance). Using, for example, a square in circle for overlap from spot to spot, the square coverage area has a side

$$D_{SQ} = 0.707 D_{SP} \quad (5-11d)$$

Then the total number of spots within a resolution element is given by

$$N_{SRE} = \frac{A_{RE}}{(D_{SQ})^2} \quad (5-11e)$$

Using $D_{SP} = 30$ km, Table 5-2 shows the number of spots within each resolution element area.

Table 5-2. Number of Illuminated Spots Per Resolution Elements for Square in Circle Overlap

$A_{RE} (m^2)$	$N_{SRE} \text{ (for } D_{SP} = 30 \text{ km)}$
$3(10^{11})$	667
$2(10^{11})$	446
$1(10^{11})$	223
$5(10^{10})$	112

5.3.2 Temporal Relationships

A basic system requirement is that the total coverage area be communicated to within a time T_A , the area coverage time. This is accomplished by a spot scan. Therefore, if we define

M_D = Time to communicate to each spot, or

= Message duration, and

t_{sL} = dead time between messages, or,

= time to scan to a new spot and develop the appropriate beam width, and

N_{TOTSP} = total number of spots within the coverage area, and finally,

t_w = source turn-on/warm-up time, then the total on time for a single source, during a given T_A interval, is given by

$$T_{ON} = t_w + N_{TOTSP} M_D + (N_{TOTSP} - 1)t_{sL} = t_w + T_{TOT} \quad (5-12a)$$

If the calculated $T_{TOT} > T_A$, and no adaptive techniques work to reduce it, then

$$T_{ON} = t_w + T_A \quad (5-12b)$$

If the source has a pulse repetition rate given by PRF, then the total number of pulses used to communicate to the area during a given T_A is given by

$$N_{PL} = (T_{ON})(PRF). \quad (5-13a)$$

Naturally there should be a check that

$$(N_{TOTSP} - 1)t_{sL} + N_{TOTSP} M_D \leq T_A \quad (5-13b)$$

or the system will not meet the requirement.

5.3.3 Message

The fundamental message length to be delivered over the time T_A to the coverage area is defined as M_{Lo} , with units "bits." In some cases, the total number of bits that must be communicated to each spot exceeds M_{Lo} because of the quality of service, jamming, spoofing, or practical hardware considerations. We therefore define

$$M_L = M_{Lo} + M_{OV} \quad (5-15)$$

for M_L = total message length (bits), and M_{OV} = overhead bits added to each message.

One key requirement is the number of missed messages per year, defined as N_M . Evidently the total number of messages per year is given by

$$\frac{\# \text{ Messages}}{\text{Year}} = \frac{\# \text{ Seconds per year}}{T_A} = \frac{3.15576 (10^7)}{T_A}$$

Then if N_M is the number of missed messages per year, the probability of a missed message is given by

$$P_M = \frac{N_M T_A}{3.15576 (10^7)} \quad (5-16)$$

5.3.4 Modulation/Demodulation

There are three system requirements which interact with/determine the modulation/demodulation approach:

N_M = # of missed messages per year per boat;

N_J = # of jammed messages per year per boat;

N_{SP} = # of spoofed messages per year per boat.

This section considers these requirements in terms of the M'ary modulation format and various demodulation approaches.

5.3.4.1 Modulation

The PPM (pulse position modulation) format is used here to minimize required optical (average) power and to maximize the data transfer rate for a given source pulse repetition rate.

The building blocks of the format are slots and frames, as shown in Figure 5-6.

Defining t_s = slot width, and

i = # of bits/pulse,

then if 2^i resolvable slots are included in one frame, the location of a pulse in any one of these slots will denote the i bits.

Therefore, frame width = $(2^i) t_s$ seconds.

If in addition we define t_f = dead time between frames,

then a message containing a total of M_L (bits) will have a message duration M_D (seconds) given by

$$M_D = \left(\frac{M_L}{i} \right) \left(\frac{2^i t_s}{1} \right) + \left(\frac{M_L}{i} - 1 \right) t_f.$$

or,

$$M_D = \left(\frac{M_L 2^i t_s}{i} \right) + \left(\frac{M_L}{i} - 1 \right) t_f. \quad (5-17)$$

The message length is determined partially by the demodulation technique, since the format and the requirements (N_M , N_J , and N_{SP}) determine the required number of overhead bits to be added to M_{L0} , the fundamental message length.

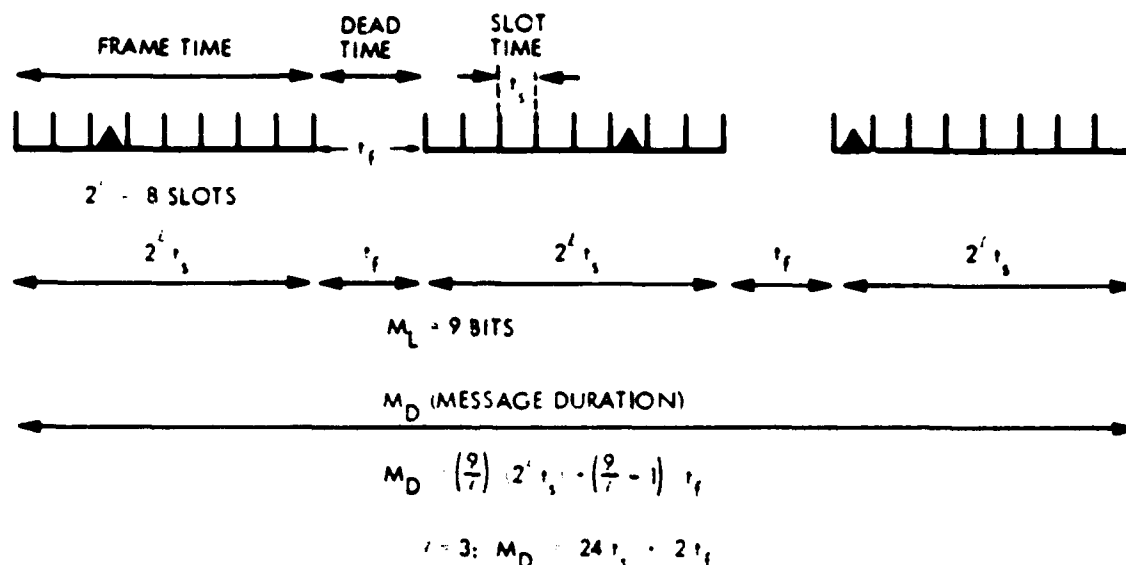


Figure 5-6. $L=3$, $M_L=9$ PPM Example

5.3.4.2 Demodulation

Given the fundamental message length, M_{L0} , the requirements (N_M , N_J , N_{SP}) and the demodulation technique, the required signal to noise ratio per pulse and the number of overhead bits are determined.

5.3.4.2.1 Threshold Detection

The first demodulation technique considered is threshold detection, i.e., the pulse will be said to occur at a given time (within a given slot) if the received power exceeds a preset level, as shown in Figure 5-7.

Errors occur when the noise exceeds this threshold or the signal + noise falls below this threshold.

We define P_E = bit error probability:

and P_P = pulse error probability:

$$\text{so that } P_E = \frac{P_P}{2} \quad (5-18)$$

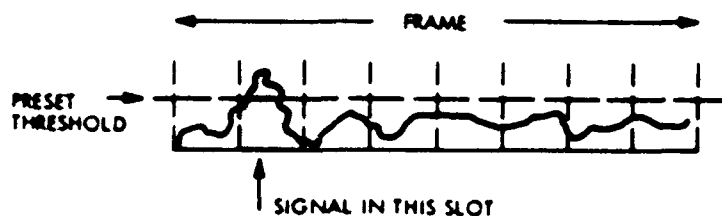


Figure 5-7. Threshold Demodulation for PPM Format

5.3.4.2.1 (Continued)

The probability of a pulse error is composed of the probability of a missing pulse, P_m , and the probability (P_N) that at least one of the $(2^i - 1)$ time slots contain a noise spike, so that

$$P_p = P_m + P_N. \quad (5-19)$$

Since there are $2^i - 1$ opportunities for a noise spike, the allowable single pulse probability of false alarm, P_{FA} , is

$$P_{FA} = \frac{P_N}{2^i - 1}. \quad (5-20)$$

We arbitrarily assume

$$P_m = \frac{P_p}{2} \text{ and } P_N = \frac{P_p}{2}. \quad (5-21)$$

which means

$$P_m = \frac{P_p}{2} = P_E. \quad (5-21)$$

5.3.4.2.1 (Continued)

and
$$P_{FA} = \frac{P_N}{2^L - 1} = \frac{P_E}{(2^L - 1)} \quad (5-22)$$

From gaussian detection theory¹,

$$P_{FA} = \frac{1}{2.3} \exp - \left(\frac{I_t^2}{2 I_n^2} \right) \quad (5-23)$$

and
$$P_m = \frac{1}{2.3} \exp - \left(\frac{(I - I_t)^2}{2 I_n^2} \right) \quad (5-24)$$

for I = Peak signal current = $(ne/h\nu) P_R$.

I_n = rms noise current = $(ne/h\nu) (NEP_{TOT})$.

and I_t = threshold current.

We can therefore rewrite these equations as

$$\frac{I_t}{I_n} = (TNR) = [-2.3 \ln (2.3 P_{FA})]^{1/2} \quad (5-25)$$

and
$$\frac{I}{I_n} = \left(\frac{S}{N} \right) = \left[-2.3 \ln (2.3 P_E) \right]^{1/2} + \left[-2.3 \ln \left(\frac{2.3 P_E}{(2^L - 1)} \right) \right]^{1/2} \quad (5-26)$$

Recall equation (5-16)

$$P_m = \frac{N_m T_A}{3.15576 (10^9)}$$

* Due to large background levels, the Gaussian regime applies almost always in the OSCAR scenario.

5.3.4.2.1 (Continued)

for $N_M = \#$ of missed messages per year,

T_A = time to deliver each message to the coverage area,

P_M = probability of a missed message.

If we take the probability of a missed pulse to be the same as the probability of a missed message, then

$$P_M = \frac{P_P}{2} = \frac{N_M T_A}{3.15576 (10^7)} \quad (5-27)$$

and re-using $P_{FA} = \frac{P_P}{2(2^L-1)} = \frac{N_M T_A}{2(2^L-1) 3.15576 (10^7)} \quad (5-28)$

and $P_E = \frac{P_P}{2} = \frac{N_M T_A}{3.15576 (10^7)} \quad (5-29)$

then the threshold-to-noise ratio becomes

$$TNR = \left[-2 \ln \left(\frac{\sqrt{3} N_M T_A}{(2^L-1) 3.15576 (10^7)} \right) \right]^{1/2} \quad (5-30)$$

while the signal-to-noise ratio becomes

$$\frac{S}{N} = \left[-2 \ln \left(\frac{\sqrt{3} N_M T_A}{[3.15576 (10^7)]} \right) \right]^{1/2} + \left[-2 \ln \left(\frac{2 \sqrt{3} N_M T_A}{(2^L-1) (3.15576 (10^7))} \right) \right]^{1/2} \quad (5-31)$$

These expressions yield the required single pulse (TNR) and S/N in terms of the requirements, N_M and T_A , and a parameter of the modulation format, L .

In considering the jamming (N_J) and spoofing (N_{SP}) requirements and their effects on the system parameters, we start with the following assumptions:

5.3.4.2.1 (Continued)

- (1) Frame times, slot times, average PRF and scanning patterns are all unknown to the Spoofer/Jammer;
- (2) "g" times as many spoof/jam pulses occur on the average in any given time period as do signal pulses;
- (3) Spoof/jam pulses are of amplitude equivalent to the signal pulses, and will cross the threshold;
- (4) Submarine position is unknown to the spoofer/jammer;
- (5) The scanning of the spoofer/jammer is random.

In effect, then, the submarine is fixed in space during the scanning time, and the received spoof/jam pulses will occur randomly in time because of both random scanning and random timing.

The number of signal pulses received in every period T_A will be

$$N_{si} = \frac{M_L}{T_A} \quad (5-32)$$

while the number of spoof/jam pulses will be

$$SPN_{si} = \frac{g M_L}{T_A} \quad (5-33)$$

Then the probability of a spoof/jam pulse occurring in any particular time slot of width t_s within the time T_A is

$$P_i = 1 - \left(1 - \frac{t_s}{T_A}\right)^{SPN_{si}} = \left(\frac{g M_L}{T_A}\right) \left(\frac{t_s}{T_A}\right) \quad (5-34)$$

for $\frac{t_s}{T_A} \ll 1.$

To spoof the receiver we will assume that one and only one pulse will occur in each of the M_L/i frames. Then the probability of one and only one pulse occurring in a frame of 2^i slots is

$$2^i P_1 (1-P_1)^{2^i-1},$$

and the joint probability that M_L/i frames are satisfied is

$$P_{SP} = \left\{ 2^i P_1 (1-P_1)^{2^i-1} \right\}^{M_L/i} \quad (5-35)$$

For the message duration given by M_D in (5-17), the number of message durations per year are given by

$$\frac{3.15576 (10^7)}{M_D},$$

so that the number of successful spoofing events per year is

$$N_{SP} = P_{SP} \frac{3.15576 (10^7)}{M_D} \quad (5-36)$$

Using (5-17), (5-34) and (5-35),

$$N_{SP} = \left\{ 2^i \left(\frac{g M_L}{i} \right) \left(\frac{t_s}{T_A} \right) \left[1 - \left(\frac{g M_L}{i} \right) \left(\frac{t_s}{T_A} \right) \right]^{2^i-1} \right\}^{M_L/i} [3.15576 (10^7)] \times \left\{ \left(\frac{M_L 2^i t_s}{i} \right) + t_f \left(\frac{M_L}{i} - 1 \right) \right\}^{-1} \quad (5-37)$$

5.3.4.2.1 (Continued)

This expression is used to calculate N_{SP} as a function of the requirements (g, M_L, T_A), hardware parameters (t_s, t_p) and modulation format (i). The result is to be compared with the inputted requirement for spoofing:

$$N_{SP1} \leq N_{SP} \quad (5-38)$$

Jamming is defined here as either inserting one extra pulse in any signal frame, or inserting at least one pulse in a frame immediately preceding or following the signal frames.

The probability of at least one extra pulse in the M_L/i frames is

$$P_{J1} = 1 - \left[(1 - p_1)^{2^i - 1} \right]^{\frac{M_L}{i}} \quad (5-39)$$

while the probability that at least one pulse exists in either adjacent frame is

$$P_{J2} = 1 - \left[(1 - p_1)^{2^i} \right]^2 \quad (5-40)$$

The total jamming probability is then

$$\begin{aligned}
 P_J &= 1 - (1 - P_{J1}) (1 - P_{J2}) \\
 &= 1 - [1 - p_1]^{(2^i - 1) \frac{M_L}{i} + 2^{i+1}} \quad (5-41)
 \end{aligned}$$

Since there are $\frac{3.15576 (10^7)}{T_A}$ messages received per year per boat, the number of jammed messages per boat is given by

$$N_J = P_J \frac{3.15576 (10^7)}{T_A} \quad (5-42)$$

5.3.4.2.1 (Continued)

Using (5-34) and (5-41),

$$N_j = \left\{ 1 - \left[1 - \left(\frac{g M_L}{l} \right) \left(\frac{t_s}{T_A} \right) \right]^{(2^l - 1) \frac{M_L}{l} + 2^{i+1}} \right\} \frac{3.15576 (10^7)}{T_A} \quad (5-43)$$

This expression is used to calculate the number of jammed messages per boat per year, N_j , as a function of the other requirements (g , M_L , T_A), a hardware parameter (t_s) and a property of the modulation format (l). The result is to be compared with the inputted requirements for jamming:

$$N_{ji} \leq N_j \quad (5-44a)$$

Note that no additional bits were added to obtain suitable operation, and so for threshold demodulation,

$$M_L = M_{Lo} \quad (5-44b)$$

5.3.4.2.2 Time-of-Peak Detection

The second demodulation technique considered is time-of-peak detection, i.e., the pulse is determined to occur at that time within the frame at which the maximum value of received energy occurs, as shown in Figure 5-8. This determination is made following a filter matched to the pulse width.

The probability of error is now taken as the probability of at least one noise peak exceeding the signal peak and in an incorrect time slot. This is done using the bound on this probability²,

$$P(x) \leq \frac{y-1}{\sqrt{2-(1+1/I_n)}} \exp - \left[2 \left(\frac{1}{I_n} \right)^2 \right] \quad (5-45)$$

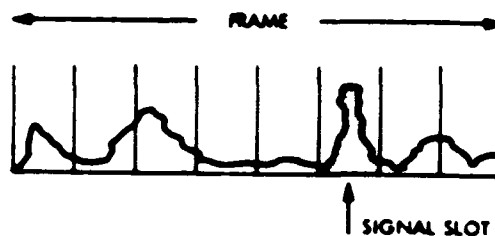


Figure 5-8. Time-of-Peak Demodulation for PPM Format

5.3.4.2.2 (Continued)

for y = number of slots in the frame = 2^i

$$\left(\frac{1}{T_n}\right)^2 = \left(\frac{S}{N}\right)^2.$$

x = the event corresponding to one peak exceeding the signal level at a given S/N .

Therefore, $P(x) = P_p = P_E \frac{2(2^i)}{(2^i - 1)}$

and $P_E \leq \frac{2^i - 1}{2 \cdot 2^i \cdot S/N} \exp - \left[\frac{1}{2} \left(\frac{S}{N} \right)^2 \right].$

and using (5-29) again,

$$\frac{N_M T_A}{3.15576 (10^7)} \leq \frac{2^i - 1}{2 \cdot 2^i \cdot (S/N)} \exp - \left[\frac{1}{2} \left(\frac{S}{N} \right)^2 \right]. \quad (5-46)$$

This equation cannot be inverted to yield the S/N required to satisfy a given $N_M T_A$ requirement for a given modulation format, i . Instead, for the given i and $N_M T_A$, values of (S/N) are inserted until the equation is satisfied, and that value is

5.3.4.2.2 (Continued)

taken as the required (S/N). S/N = 5 is the lowest value considered, and it is incremented in steps of 0.1 until (5-46) is satisfied for the value of i selected.

The time-of-peak demodulation technique provides an extreme problem for the signal processor, since every frame will have a peak and therefore every group of frames of appropriate length will have to be processed to search for a signal.

To relieve this problem and meet the N_m (# of missed messages per year per boat) requirement, we consider the addition of w extra frames, each containing a pulse in its own preselected slot. If we then state that the receipt of a false message (due to ambient noise sources) is equivalent to the loss of a true message, we may proceed as follows:

If the signature pulse may be in any one of the 2^i slots of a given frame, and w signature pulses (in w frames) are used, then the probability that the total signature will be duplicated is approximately given by

$$P_{FS} = \frac{1}{(2^i)^w} = \frac{1}{2^{iw}}. \quad (5-47)$$

Since the first frame of a false signature may be any frame in a year, the expected number of false signatures per year is the same as the number of missed messages per year, or,

$$N_M = P_{FS} \left\{ \frac{3.15576 (10^7)}{2^i t_s} \right\} = \frac{3.15576 (10^7)}{t_s 2^i (w+1)}. \quad (5-48)$$

Solving for w we find

$$2^{i(w+1)} = \frac{3.15576 (10^7)}{t_s N_M}.$$

or,

$$w = \frac{1}{i} \left\{ 24.91 - 1.44 \ln (t_s N_M) \right\} - 1.$$

5.3.4.2.2 (Continued)

with the provision that the result of (5-49) is always rounded off to the next highest integer if it is non-integer, since the # of additional signal frames must be an integer.

This procedure results in a number of overhead bits per message,

$$M_{OV} = w_i, \quad (5-50)$$

and a total message length

$$M_L = M_{LO} + w_i. \quad (5-51)$$

In considering the jamming (N_j) and spoofing (N_{sp}) requirements, the same 5 assumptions as in Section 5.3.4.2.1 are again made. In particular, "g" times as many spoof/jam pulses occur on the average in any given time period as do signal pulses.

Consider spoofing:

The number of signal pulses received during area coverage time T_A is

$$N_{s1} = \frac{M_L}{t}, \quad (5-52)$$

while the average number of threat pulses during the same time is

$$SP^{N_{s1}} = \frac{g M_L}{t}. \quad (5-53)$$

Then the probability that one threat pulse will occupy any particular slot (of width t_s) within the time T_A is

$$P_1 = 1 - \left(1 - \frac{t_s}{T_A}\right)^{SP^{N_{s1}}} = \frac{gt_s M_L}{t T_A}, \quad (5-54)$$

for $t_s \ll T_A$.

5.3.4.2.2 (Continued)

To spoof a message using the w signature pulse approach requires that all w pulse positions be duplicated. Therefore, the probability of spoofing is

$$P_{SP} = (P_1)^w = \left(\frac{g t_s M_L}{2 T_A} \right)^w \quad (5-55)$$

Since the message duration is

$$M_D = \left(\frac{M_L 2^i t_s}{i} \right) + \left(\frac{M_L}{i} - 1 \right) t_f \quad (5-56)$$

for t_f = interframe dead time,

and there are $\frac{3.15576 (10^7)}{M_D}$ opportunities for messages per year,

then the number of spoof events per year are

$$N_{SP} = P_{SP} \frac{3.15576 (10^7)}{M_D} .$$

or,
$$N_{SP} = 3.15576 (10^7) \left(\frac{g t_s M_L}{2 T_A} \right)^w \left\{ \frac{1}{\left(\frac{M_L}{i} t_s 2^i \right) + \left(\frac{M_L}{i} - 1 \right) t_f} \right\} \quad (5-57)$$

Once w is determined by (5-49), (5-57) is evaluated to determine if the spoofing requirement is met, so that (5-57) is compared to the inputted spoofing requirement:

$$N_{SP1} \leq N_{SP} \quad (5-58)$$

With regard to jamming, we assume initially that jamming occurs whenever a threat pulse falls within a signature frame in any unoccupied slot, since then the

5.3.4.2.2 (Continued)

signature will not be recognized. Since there are $2^i - 1$ unoccupied slots within each signature frame, the probability of jamming is

$$P_J = 1 - (1 - P_1)^{w(2^i-1)} = w(2^i-1) \frac{g t_s M_L}{T_A} \quad (5-59)$$

again for $t_s \ll T_A$.

Since there are $\frac{3.15576 (10^7)}{A}$ messages sent per year, the number of jammed messages is

$$N_J = 3.15576 (10^7) \frac{w(2^i-1) g t_s M_L}{T_A} \quad (5-60)$$

Again, after evaluation the comparison is made

$$N_{J1} > N_J \quad (5-61)$$

However, many values of the parameters exist for which $N_J < N_{J1}$, for all other requirements easily met. We therefore consider an alternative post-detection processing scheme, which will accept a frame with two peaks, one of which is in the correct slot, as a valid signature frame. Then to jam the link, two threat pulses would have to occur in the signature frames.

Since the probability that a single threat pulse occurs within a given frame in an unoccupied slot is

$$P_F = 1 - (1 - P_1)^{2^i-1} = (2^i-1) P_1 \quad (5-62a)$$

(for $P_1 \ll 1$, true for $t_s \ll T_A$). Then the probability that two threat pulses occur in a given frame is

$$P_{2F} = (P_F)^2 = [1 - (1 - P_1)^{2^i-1}]^2 = (2^i-1)^2 P_1^2 \quad (5-62b)$$

5.3.4.2.2 (Continued)

Then the jamming probability is the probability that two pulses occur in any of w frames, so that

$$P_J = 1 - (1 - P_{2F})^w = wP_{2F} = w(2^i - 1)^2 P_1^2$$

or,
$$P_J = w(2^i - 1)^2 \left(\frac{g t_s M_L}{i T_A} \right)^2 \quad (5-63)$$

and
$$N_J = 3.15576 (10^7) \frac{w(2^i - 1)^2}{T_A} \left(\frac{g t_s M_L}{i T_A} \right)^2 \quad (5-64a)$$

and the comparison equation is

$$N_{J1} \geq N_J \quad (5-64b)$$

In running this program, then, the post-detection processing must be specified before it can be determined if the jamming requirement is satisfied.

References for Section 5.3.4

1. RCA Electro-Optics Handbook, Section 8, RCA - 1968
2. J. M. Wozencraft and I. M. Jacobs, "Principles of Communication Engineering," John Wiley and Sons, 1965, p 629.

5.3.5 Scanning Relationships

The area to be covered is illuminated by spots of relatively small diameter. Each spot is illuminated for a length of time given by the message duration (M_D) of equation (5-17), and then the transmitter is redirected to a new spot. If we define this slewing time as t_{sL} , then the total time devoted to each spot may be taken as,

$$T_{SP} = M_D + t_{sL} \quad (5-65)$$

To determine the total time to scan the entire area of responsibility, we define

A_{SP} = area of spot

and A_{SC} = area of useful coverage within the illuminated spot.

As a baseline we take the square in circle pattern defined in Figure 5-9a.

The effective area covered by the inside square is given by

$$A_{SC} = c^2 D_{sp}^2 = D_{sq}^2$$

where:

D_{sp} = spot diameter,

D_{sq} = square side,

c = overlap factor, defined by

$$D_{sq} = c D_{sp}$$

Since $A_{sp} = \frac{\pi}{4} D_{sp}^2$

$$A_{SCMIN} = \frac{4}{\pi} A_{sp} = c^2 D_{spMIN}^2 \quad (5-68)$$

and $(4/\pi)$ is the general efficiency factor of the scan pattern. For $c = 0.707$, this efficiency factor = $(2/\pi) = 0.637$, which is the highest possible for any square inside a circle.

5.3.5 (Continued)

There is a finite probability that the motion of a submarine may allow it to escape communication (connectivity failure) if its initial position and velocity value are unfavorably related to the scan pattern. We will here estimate the probability of these positions and velocity vectors occurring if the submarine is randomly positioned relative to the scan pattern.

The baseline "square-in-a-circle" scan is assumed and the squares are offset in succeeding lines. The worst case for timing is assumed: the adjacent spots are visited with the maximum elapsed time. It is also assumed that the submarine velocity magnitude is constant and that the velocity vector direction is constant during the intermessage times.

The square in a circle pattern is as shown in Figure 5-9.

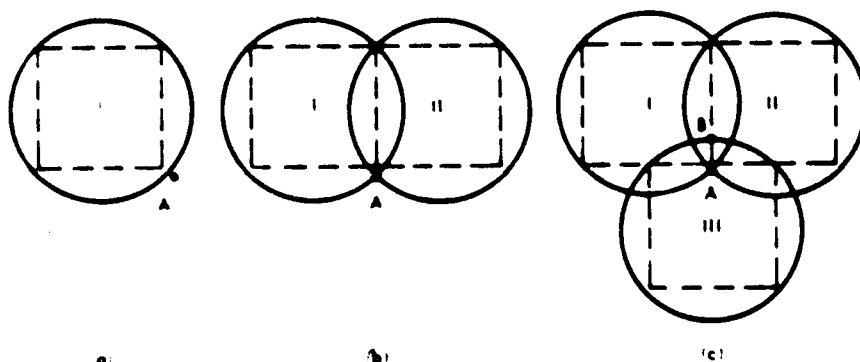


Figure 5-9. Square-in-Circle Overlap Scan Pattern

We will concentrate on area II' which receives the message during the last spot of revisit time with areas I and II being first spots illuminated.

If a submarine is in area III during the first spot time, and moves out of circle 3 during revisit time, it will escape communication.

5.3.5 (Continued)

Because of the symmetry of the problem, we will consider only one eighth of the square as shown in Figure 5-9d.

The square side is D_{SQ} and the circle radius is $\frac{D_{sp}}{2}$. Thus $D_{SQ} = \sqrt{\frac{2}{2}} D_{sp}$.

If VT_A is the distance the submarine moves during revisit time, there is an area, A, within which the submarine cannot escape communication. There is also an area B within which the submarine will have been communicated to during the first frame.

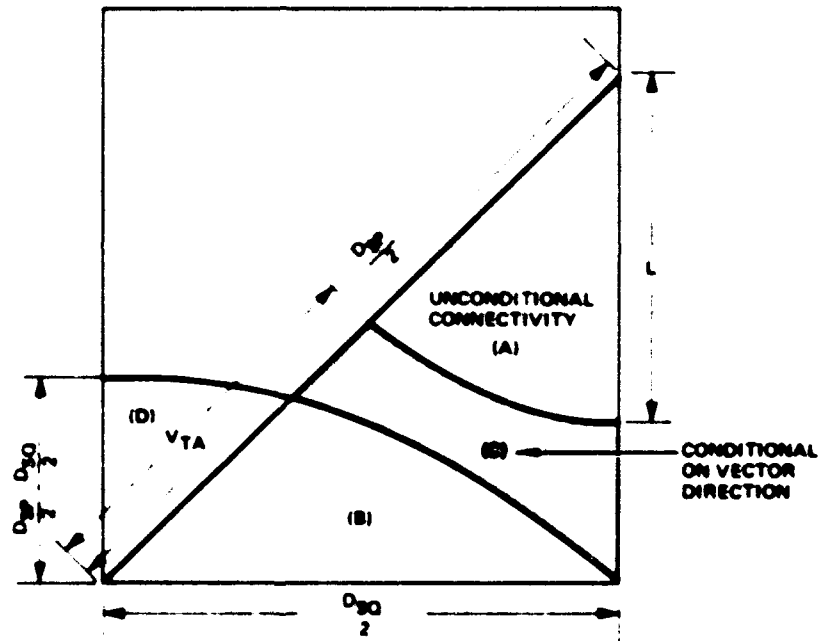


Figure 5-9d. Escape Geometry

The area C is an area within which the submarine may escape if the velocity direction is within bounds.

5.3.5 (Continued)

It is difficult to write an analytical expression for area C but it can be approximated by the following approach:

$$\text{Area A} = \frac{-(D_{sp}/2 - vT_A)^2}{8}$$

$$\text{Area (B+D)} = \frac{\pi R^2 - S^2}{8} = \frac{\pi R^2}{8} - \frac{2R^2}{8} = \frac{R^2(\pi - 2)}{8} = \frac{-(\frac{D_{sp}}{2})^2 - D_{SQ}}{8} = \frac{(\frac{D_{sp}}{2})^2(\pi - 2)}{8}$$

$$\text{Area D} = \frac{(R - \frac{S}{2})^2}{2} = \frac{R^2(1 - \frac{\sqrt{2}}{2})^2}{2} = \frac{(\frac{D_{sp}}{2} - \frac{D_{SQ}}{2})^2}{2} = \frac{(\frac{D_{sp}}{2})^2(1 - \frac{\sqrt{2}}{2})^2}{2}$$

$$\text{Area B} = \left(\frac{D_{sp}}{2}\right) \left[\frac{\pi}{8} - \frac{1}{4} - \frac{1}{2} + \frac{2}{2} - \frac{1}{4} \right] = 0.0998 \left(\frac{D_{sp}}{2}\right)^2$$

$$\text{Area A+B+C} = \frac{S^2}{8} = \frac{R^2}{4} = \frac{D_{SQ}^2}{8} = \frac{1}{4} \left(\frac{D_{sp}}{2}\right)^2$$

The probability of conditional escape is:

$$P_{CE} = \frac{C}{(A+B+C)} = \frac{(A+B+C) - A - B}{(A+B+C)} = 1 - 0.171 = \frac{1 - vT_A}{\left(\frac{D_{sp}}{2}\right)^2}$$

Note that the probability can never be less than zero, therefore:

$$\frac{vT_A}{\frac{D_{sp}}{2}} \geq 0.274 \quad \text{for conditional escape.}$$

Therefore for the condition

$$D_{sp} \geq 7.3 vT_A \quad \text{there will be no connectivity failure.}$$

5.3.5 (Continued)

However, this is unnecessarily restrictive. Consider a particular case with the following assumed values:

1. Spot size (minimum) $D_{SQ} = 20$ Km, $\frac{D_{sp}}{2} = 14.1$ Km
2. Submarine velocity x time = 6 Km

Therefore $\frac{vT}{D_{sp}} = 0.424$ which exceeds the limit above. This area is the darker shaded area in Figure 5-9e.

This area is estimated graphically as two small triangles with areas of 7 squares and 3 squares, respectively, where the total area (A+B+C) is 128 squares

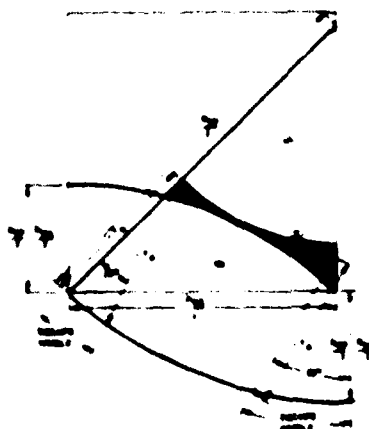


Figure 5-9e. Escape Geometry

The direction of possible escape from the larger triangle is any angle less than an estimated 35° from the radius line. Therefore, assuming uniform probability of direction, the probability of escape direction is

$$\frac{35^\circ}{180^\circ} = 0.1944$$

From the smaller triangle the escape direction must be less than 20° from radius vectors which leads to a probability of 0.111.

Therefore the overall probability of escape with these conditions is:

$$P = \frac{7}{128} \times 0.1944 + 3 \times 0.111 = 0.0106 \times 0.026 = 1.3\%$$

5.3.5 (Continued)

Note that if $vT_A \leq 4$ km, there is no escape. Thus, if the time is random, there is only a 1/3 probability that vT is greater than 4 for the particular velocity.

Therefore the probability of escape is less than

$$P_E \leq 0.4\%$$

especially considering the narrower escape angles which have not been included in the approximation and that other worst-case assumptions have been made.

It should also be noted that on a purely statistical basis one would estimate that the probability of two consecutive connectivity failures would be $(.004)^2 = 1.6 \times 10^{-5}$. However, by studying the geometry, one realizes that if the direction is not abruptly changed, the submarine is in an unconditional area at the start of the second period and will not escape communication.

Therefore, it is concluded that the probability of connectivity failure is considered negligibly small if

$$D_{SP} \geq 4.7 vT_A.$$

For the OSCAR requirements, this condition is nearly always met, so we shall not consider this as a limit in the DCM analysis. (Section 4.3 of Volume 4 discusses this point further.)

Returning now to our basic discussion of scanning, and the number of spots per resolution element, recall A_{RE} = area of resolution element. Thus the number of illuminated spots within a resolution element is given by

$$N_{SREMAX} = \frac{A_{RE}}{A_{SCMIN}} \quad (5-69)$$

If there are $N_{TOT RE}$ resolution elements within the area of responsibility of the satellite, then the total number of spots (assuming equal beam diameters throughout) is given by

$$N_{TOT SP} = (N_{TOT RE}) (N_{SRE}) \quad (5-70)$$

5.3.5 (Continued)

and the total time required to cover the entire area of responsibility is

$$T_{TOT} = (N_{TOT \text{ sp}}) (T_{sp}) - t_{sl} \quad (5-71a)$$

$$T_{TOT} = (N_{TOT \text{ sp}}) (M_D) + (N_{TOT \text{ sp}} - 1) t_{sl} \quad (5-71b)$$

If $T_{TOT} > T_A$, then another terminal located on the satellite is required. We shall discuss this further in Section 5.3.7 on Adaptive Scanning.

For an elliptical spot, the area is given by

$$A_{sp} = \frac{\pi}{4} D_{sp} D_{sp} (\cos \theta_s)^q \quad (5-73)$$

for θ_s = signal zenith angle

q = factor between 0 and 1 related to the satellite transmitter's ability to correct for the zenith angle spreading.

From the properties of ellipses, any rectangle within an ellipse which touches all sides has the area

$$A_{RECTIJMIN} = D_{spMIN} D_{spMIN} (\cos \theta_{slj})^q \approx (1 - e^2)^{1/2} \quad (5-74)$$

which leads to the area efficiency coverage factor

$$\frac{A_{RCT}}{A_{sp}} = \frac{A}{\pi} \approx (1 - e^2)^{1/2} \quad (5-75)$$

and the same condition on t_{ARV} as (5-67) if the ellipses are overlapped as the circles are in Figure 5-9. This efficiency factor is maximized for $e = 0.707$, just as for the square in the circle approach, and again = 0.637.

5.3.5 (Continued)

The number of spots per resolution element would now be

$$N_{SREij} = \frac{A_{RE}}{A_{RCTij}} \quad (5-76)$$

and (5-70) and (5-71) are then useable for the new value of N_{SREij} when summed over ij .

The final key parameter of the scan pattern is the allowable minimum size of D_{sp} determined by satellite stability. This diameter is related to the satellite range and beam divergence by

$$D_{sp} = R\theta_T \quad (5-77)$$

for the assumed small angles involved here.

θ_T , in turn, must be greater than a minimum determined by

- (1) The satellite's induced pointing jitter during a single message duration, which we characterize by its rms value θ_{TS} .
- (2) The satellite long term angular drift, so that a spot position adjacent to a previously illuminated spot is precisely located. This effect is characterized by its rms value θ_{TDR} .

Negligible pointing induced signal loss is encountered if

$$\theta_{TMIN} = 10 (\theta_{TS}^2 + \theta_{TDR}^2)^{1/2} \quad (5-78)$$

which implies

$$D_{spMIN} = 10 R_{ijMAX} (\theta_{ts}^2 + \theta_{TDR}^2)^{1/2} \quad (5-79)$$

This point will be further discussed in Section 5.3.7 on Adaptive Scanning.

5.3.6 Receiver and Source

Some particular aspects of the laser transmitter and receiver must be modelled in order to provide a full downlink communications model.

5.3.6.1 Receiver

We need to derive the in-water angle, δ , between the optical axis of the receiver and the signal beam, the sun, the moon, and the local vertical, respectively.

We first consider the signal beam. The input to the model is the latitude (λ_s), longitude (β_s) and altitude (R_s) of the satellite, and the latitude (λ_{Aj}) and longitude (β_{Aj}) of the receiver. From these, in Section 5.3.1 we derived the range from satellite to receiver [R , equation (5-2)], and the signal zenith angle into the water [γ_s , equation (5-5)]. Since γ_{SR} is the in-water angle between receiver optical axis and signal principal direction, we must transform the input information into the local coordinate system centered on the receiver and oriented to local vertical. It is also useful to align an axis with the local longitude.

We therefore perform the following coordinate transformations (cf Figure 5-10):

1. (x_1, y_1, z_1) is the earth centered system
2. (x_2, y_2, z_2) is the system whose origin is at the receiver, but whose three axes are parallel to the earth-centered axis.
3. (x_3, y_3, z_3) is a system resulting from the rotation of the (x_2, y_2, z_2) system about the z_2 axis by an angle β_j .
4. (x_4, y_4, z_4) is a system resulting from the rotation of the (x_3, y_3, z_3) system about the y_3 axis by an angle $(\frac{\pi}{2} - \lambda_j)$, resulting in z_4 along the local vertical and x_4 along the direction of constant longitude.

In the (x_1, y_1, z_1) system, x_E and x_S are given by the equation immediately following equation (5-1) [equation (5-1a) through (5-1f)]. For the satellite, then, the transformation of its coordinates into the (x_2, y_2, z_2) system is given by

$$x_2 = x_s - x_E; \quad (5-80a)$$

$$y_2 = y_s - y_E; \quad (5-80b)$$

$$z_2 = z_s - z_E. \quad (5-80c)$$

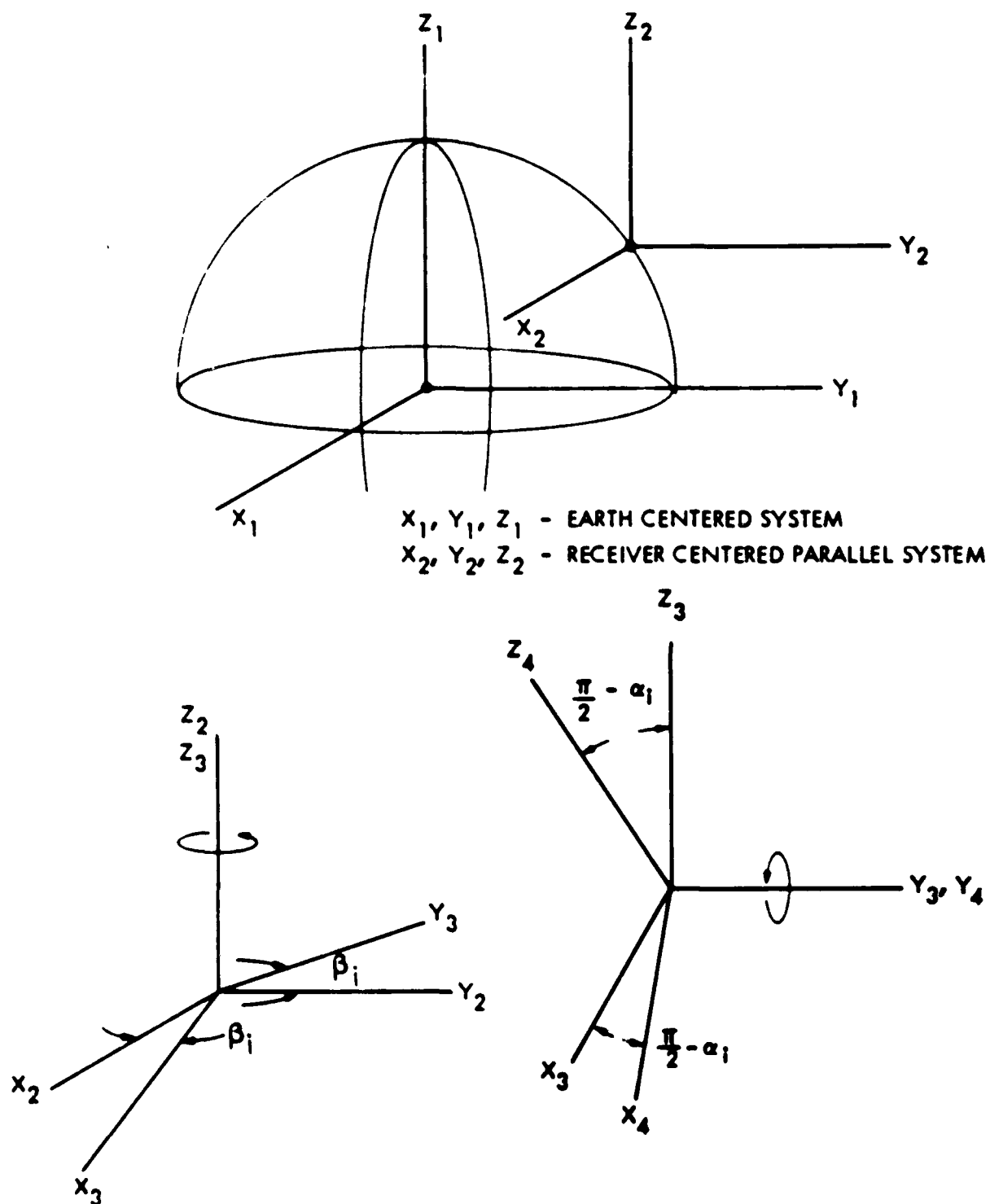


Figure 5-10. OSCAR Coordinate Transformation

5.3.6.1 (Continued)

Rotation about the z_2 axis by an angle β_j results in the transformation equation,

$$x_3 = x_2 \cos \beta_j + y_2 \sin \beta_j; \quad (5-81a)$$

$$y_3 = y_2 \cos \beta_j - x_2 \sin \beta_j; \quad (5-81b)$$

$$z_3 = z_2. \quad (5-81c)$$

Finally, rotation about the x_3 axis by the angle $(\frac{\pi}{2} - \alpha_1)$ results in the transformation equations

$$x_4 = x_3 \sin \alpha_1 - z_3 \cos \alpha_1; \quad (5-82a)$$

$$y_4 = y_3; \quad (5-82b)$$

$$z_4 = z_3 \sin \alpha_1 + y_3 \cos \alpha_1. \quad (5-82c)$$

The signal zenith angle in the last coordinate system is given by

$$\hat{\theta}_s = \cos^{-1} \left\{ \frac{z_4}{[x_4^2 + y_4^2 + z_4^2]^{1/2}} \right\} \quad (5-83a)$$

which is equivalent to the result in equation (5-5).

The signal azimuth (relative to β_j because of the coordinate transformation) is given by

$$\theta_{sA1j} = \tan^{-1} \left(\frac{y_4}{x_4} \right) = \tan^{-1} \left\{ \frac{(y_s - y_E) \cos \beta_j - (x_s - x_E) \sin \beta_j}{[(x_s - x_E) \cos \beta_j + (y_s - y_E) \sin \beta_j] \sin \alpha_1 - (z_s - z_E) \cos \alpha_1} \right\} \quad (5-83b)$$

5.3.6.1 (Continued)

The in-water azimuth is the same expression, while the in-water zenith angle is given by

$$\phi_{s1j}^w = \sin^{-1} \left(\frac{1}{n} \sin \phi_{s1j} \right), \quad (5-84)$$

for n = sea-water index of refraction.

If the receiver pointing angle is characterized by

G_{EL1j} = zenith pointing angle

G_{AZ1j} = azimuth pointing angle (in the x_4, y_4, z_4 system), then the in-water angle between the signal and receiver axis is

$$\phi_{SR1j} = \cos^{-1} \left\{ \sin G_{EL1j} \sin \phi_{s1j}^w [\cos (G_{AZ1j} - \phi_{SA1j})] + \cos G_{EL1j} \cos \phi_{s1j}^w \right\} \quad (5-85)$$

The solar and lunar off-receiver axis in-water pointing angles are derived in a like manner, using equation (5-6) for ϕ_{su} and equation (5-7) for ϕ_{mu} . Equations (5-1a through 5-1f) are the same form with

$R_s \rightarrow R_{su}$ (sun range),

and $R_s \rightarrow R_{mu}$ (moon range).

However, since $R_{su} \gg R_E$ and $R_{mu} \gg R_E$, the first (translation) transformation for the sun and moon becomes

$$x_2 = x_{su} \text{ (or } x_{mu}), \quad (5-86a)$$

$$y_2 = y_{su} \text{ (or } y_{mu}), \quad (5-86b)$$

$$z_2 = z_{su} \text{ (or } z_{mu}), \quad (5-86c)$$

5.3.6.1 (Continued)

Moreover,

$$x_{su} = R_{su} \cos \alpha_{su} \cos \beta_{su}, \quad (5-87a)$$

$$y_{su} = R_{su} \cos \alpha_{su} \sin \beta_{su}, \quad (5-87b)$$

$$\text{and } z_{su} = R_{su} \sin \alpha_{su}. \quad (5-87c)$$

Then $x_2 \rightarrow x_3$ and $x_3 \rightarrow x_4$ proceed in the same manner as (5-81) and (5-82) with the results

$$\alpha_{suA} = \tan^{-1} \left(\frac{y_4}{x_4} \right),$$

or

$$\phi_{suA1j} = \tan^{-1} \left\{ \frac{y_{su} \cos \beta_j - x_{su} \sin \beta_j}{(x_{su} \cos \beta_j + y_{su} \sin \beta_j) \sin \alpha_i - z_{su} \cos \alpha_i} \right\} \quad (5-88)$$

Also,

$$\alpha_{suij}^w = \sin^{-1} \left(\frac{1}{n} \sin \alpha_{suij} \right) \quad (5-89)$$

and

$$\alpha_{suR1j} = \cos^{-1} \left\{ \sin G_{EL1j} \sin \alpha_{suij}^w [\cos (G_{AZ1j} - \phi_{suA1j})] + \cos G_{EL1j} \cos \alpha_{suij}^w \right\} \quad (5-90)$$

In like manner,

$$x_{mu} = R_{mu} \cos \alpha_{mu} \cos \beta_{mu}; \quad (5-91a)$$

$$y_{mu} = R_{mu} \cos \alpha_{mu} \sin \beta_{mu}; \quad (5-91b)$$

$$\text{and } z_{mu} = R_{mu} \sin \alpha_{mu}. \quad (5-91c)$$

5.3.6.1 (Continued)

and

$$\phi_{\mu Aij} = \tan^{-1} \left\{ \frac{y_{\mu} \cos \beta_j - x_{\mu} \sin \beta_j}{(x_{\mu} \cos \beta_j + y_{\mu} \sin \beta_j) \sin \alpha_i - z_{\mu} \cos \alpha_i} \right\}$$

(5-92)

and

$$\phi_{\mu ij}^w = \sin^{-1} \left(\frac{1}{n} \sin \phi_{\mu ij} \right) .$$

(5-93)

so that

$$\phi_{\mu Rij} = \cos^{-1} \left\{ \sin G_{ELij} \sin \phi_{\mu ij}^w [\cos (G_{AZij} - \phi_{\mu Aij})] + \cos G_{ELij} \cos \phi_{\mu ij}^w \right\}$$

(5-94)

Note that the parameters R_{su} and $R_{\mu u}$ do not appear in the final result since they cancel out of (5-88) and (5-92) respectively.

For the diffuse sources, it is evident that

$$\phi_{BRij} = \phi_{ZRij} = G_{ELij}$$

(5-95)

5.3.6.2 Laser Transmitter(s)

The transmitter is described by a much simpler model. We define

θ_T = full angle e^{-2} irradiance beam divergence;

E_p = energy per pulse at the laser transmitter;

PRF = pulse repetition frequency of the laser transmitter.

Then

$$P_{AV} = (E_p) (PRF),$$

(5-96a)

for P_{AV} = average power of the laser transmitter.

Since there may be more than one laser on a given satellite, we define

m = number of lasers (or terminals) per satellite, so that

mP_{AV} = total optical power capability of the satellite,

and

$$E_{TOT} = mE_p.$$

(5-96b)

If we then define

F_L = efficiency of the laser ("wall plug"), then

$$P_L F_L = mP_{AV}; \quad P_L = \frac{mP_{AV}}{F_L}$$

(5-96c)

for P_L = total prime power required on the satellite to sustain the lasers aboard.

In general, additional prime power will be required for other subsystems on the satellite, so we define

5.3.6.2 (Continued)

P_{HO} = prime power on the satellite required for all non-laser functions,
and

$$P_{TOT} = P_L + P_{HO} \quad (5-97)$$

for P_{TOT} = total prime power capability required on the satellite.

5.3.7 Availability/System Effectiveness and Adaptive Scanning

The final requirement to be covered is the availability or system effectiveness. This is a calculated value, depending on the system and propagation path inputs, and is compared to the requirement at the end of the entire calculation.

Availability of the communications downlink depends on both time and area, i.e., a part of the required area will be unavailable if the SNR is too low to communicate to it, or, if the system takes all the allotted time (T_A) communicating to the rest of the area.

This approach to availability suggests that if more than one active laser exists on each satellite, and if its characteristics could be modified to aid on other resolution elements, that availability might be thereby increased.

There are numerous possible variations of adaptive scanning, and we shall treat only three extremes here:

1. The totally non-adaptive system, which uses a single transmit beam divergence and energy per pulse over the entire area of responsibility;
2. A system which does not compensate for the environmental condition; but does compensate for zenith angle effects by varying its transmit beam width;
3. A system which compensates for all conditions.

5.3.7.1 Non-Adaptive Scanning

If the satellite has no information about the area it must communicate to, it will be assumed to meet the temporal aspects of availability first, and let the successful communications to a given spot be moot.

The first determinant of any scan pattern is the minimum angular spot size. We have previously developed the criterion for its selection:

The long and short term angular jitter of the spacecraft, as expressed in (5-78) and (5-79).

We will investigate this constraint, and determine the minimum value of θ_T possible, and denote it as θ_{T1} .

5.3.7.1 (Continued)

Now, θ_{T1} will apply over the entire coverage area (for this totally non-adaptive scan). Then, within a given resolution element, all spots will have the useful area given by

$$A_{RCT1JMIN} = R_{1J}^2 \theta_{T1}^2 (\cos \phi_{s1J})^2 (1 - \epsilon^2)^{1/2}, \quad (5-98)$$

which is (5-74) with $D_{sp} = R_{1J} \theta_{T1}$ and $q = 1$.

The number of spots within the resolution element is given by

$$N_{SRE1JMAX} = \frac{A_{RE}}{A_{RCT1J}} \quad (5-99)$$

and the total number of spots within the coverage area is given by

$$N_{TOTSPMAX} = \sum_{1J} N_{SRE1JMAX} \quad (5-100)$$

Then, using (5-71b), the time it takes to cover the entire area with a single terminal is given by

$$T_{TOTMAX} = (N_{TOTSPMAX}) (M_D) + (N_{TOTSPMAX} - 1) t_{SL} \quad (5-101)$$

If $T_{TOTMAX} > T_A$, the only recourse left to the totally non-adaptive scan is to either increase θ_{T1} or to add more terminals which simultaneously use the old θ_{T1} .

Combining (5-98), (5-99), (5-100) and (5-101) we see that

$$T_{TOT} \propto \frac{1}{(\theta_{T1})^2}$$

5.3.7.1 (Continued)

and from the SPDPM,

$$\left(\frac{S}{N}\right)_{ij} = \frac{E_p}{(\tau_{T1})^2}$$

Therefore, increasing τ_{T1} will decrease T_{TOT} and $\left(\frac{S}{N}\right)_{ij}$ equally, unless E_p is proportionately increased. So, adding a second terminal of equal energy onto the same spot means τ_{T1} may be increased by $\sqrt{2}$ for the same $\left(\frac{S}{N}\right)_{ij}$, while T_{TOT} is reduced by a factor of 2. Alternatively, adding a second terminal which operates independently will also maintain $\left(\frac{S}{N}\right)_{ij}$ and, by partitioning the resolution elements so that each terminal is responsible for half the total area, will result in the T_{TOT} for a given terminal being reduced by a factor of 2 from its previous value.

Evidently, then, the effect of adding a second terminal is independent of its actual mode of operation. We therefore assume that the temporal availability requirement is satisfied by the increase of

$$\tau_{T1} = \tau_{T2} \text{ so that}$$

$$T_{TOT} = T_A \text{ in (5-101).}$$

The calculation procedure is to calculate (5-98) - (5-101), and if

$$T_{TOT} = T_A \text{ define}$$

$$\tau_{T2} = \tau_{T1} \left(\frac{T_{TOTMAX}}{T_A} \right)^{1/2} \quad (5-102)$$

Using τ_{T2} we now develop

$$FOM_{ij} = \left(\frac{S}{N}\right)_{ij} / \left(\frac{S}{N}\right)_{REQ} \quad (5-103)$$

5.3.7.1 (Continued)

for
$$\left(\frac{S}{N}\right)_{REQ} = (MARG) \times \left(\frac{S}{N}\right). \quad (5-104a)$$

and $\left(\frac{S}{N}\right)$ in (5-104) is derived from the quality of service requirements for a given demodulation approach in Section 5.3.4.

MARG = system margin used to compensate for unmodelled noise sources, and

$$\left(\frac{S}{N}\right)_{ij} = \frac{P_{R1j}}{NEP_{TOT1j}}, \text{ for the } ij \text{ resolution element from the SPDPM.} \quad (5-104b)$$

The availability is then simply given by the ratio of the areas for which $FOM_{ij} \geq 1$ to the total area responsibility, or,

$$A_{VL} = \frac{\sum_{ij} A_{RE1j} \text{ (all } ij \text{ such that } FOM_{ij} \geq 1)}{\sum_{ij} A_{RE1j}} \quad (5-105)$$

For diagnostic purposes, it is also useful to print out the minimum value of the FOM_{ij} , T_{TOT} if $T_{TOT} = T_A \cdot T_1$ and T_2 .

5.3.7.2 One Partially Adaptive-Scanning Approach

We now consider a system which knows all the zenith angle aspects of its coverage area, but none of the environmental conditions. We assume that

- (1) It controls the transmit beam divergence to compensate for the known zenith angle effects;
- (2) Therefore it always uses circular spots;
- (3) It compensates for zenith angle effects as if thick clouds were present, not clear weather, to assure maximum availability if thick clouds are indeed present.

5.3.7.2 (Continued)

The first determinant again is the minimum angular spot size, as discussed in Section 5.3.7.1. Use is also made of the FOM_{ij} defined in (5-103).

Given θ_{T1} , the minimum angular dimension, FOM_{ij} is evaluated for all the resolution elements for a nominal value of $\tau_{OPT} = 50$ throughout the coverage area. The smallest value of FOM_{ij} will normally occur at the largest zenith angle, and we denote it by FOM_{ss} . The transmit beam widths of each and every other FOM_{ij} are increased until

$$FOM_{ij} = FOM_{ss}.$$

In general the smallest values of θ_s will correspond to the largest increase in the transmit beam divergence. Since $FOM_{ij} \propto \frac{1}{(\theta_{Tij})^2}$, the increase in each transmit beam divergence is given by

$$\theta_{Tij} = \theta_{T1} \left(\frac{FOM_{ij} (\theta_T = \theta_{T1})}{FOM_{ss}} \right)^{1/2}. \quad (5-106)$$

Now θ_{Tij} will apply within a given resolution element, and will result in a useful coverage area

$$A_{SCij} = c^2 R_{ij}^2 \theta_{Tij}^2. \quad (5-107)$$

where we have used $D_{sp} = R_{ij} \theta_{Tij}$. The number of spots within this resolution element is given by

$$N_{SREij} = \frac{A_{RE}}{A_{SCij}}. \quad (5-108)$$

and the total number of spots within the coverage area is

$$N_{TOTsp} = \sum_{ij} N_{SREij}. \quad (5-109)$$

5.3.7.2 (Continued)

The time it takes to cover the entire area with a single terminal is

$$T_{TOT} = (N_{TOTsp}) (M_D) + (N_{TOTsp} - 1) t_{sl}. \quad (5-110)$$

If $T_{TOT} > T_A$, we may again consider either increasing θ_{T1} or adding a second terminal. As for the totally non-adaptive scan, the net effect of adding a second terminal is independent of whether it is used to illuminate the same spot as the first terminal (allowing θ_{T1} to increase by $\sqrt{2}$), or separately illuminates spots of diameter θ_T .

We therefore assume that the temporal availability is satisfied by an increase of $\theta_{T1} \rightarrow \theta_{T2}$ so that $T_{TOT} = T_A$ in 5-110. The calculational procedure is to calculate (5-107) - (5-110) and if $T_{TOT} > T_A$, define

$$\theta_{T2} = \theta_{T1} \left(\frac{T_{TOT}}{T_A} \right)^{1/2}. \quad (5-111)$$

since inspection of (5-107) - (5-110) shows that

$$T_{TOT} = \frac{1}{(\theta_{T1})^2}.$$

Given θ_{T2} , then, new values of θ_{T+j} are derived from

$$\theta_{T2+j} = (\theta_{T1+j}) \left(\frac{\theta_{T2}}{\theta_{T1}} \right). \quad (5-112)$$

In order to calculate the actual downlink availability, the FOM_{ij} are calculated for θ_{T2+j} and the actual environmental conditions present in each resolution element. The availability is then simply given by the ratio of the areas for which $FOM_{ij} \geq 1$ to the total area responsibility, or

5.3.7.2 (Continued)

$$A_{VL} = \frac{\sum_{ij} A_{REij}}{\sum_{ij} A_{REij} \text{ (all } ij \text{ for which } FOM_{ij} \geq 1)} .$$

(5-112)

For diagnostic purposes it is also useful to print out the value of T_{TOT} if $T_{TOT} < T_A + T_1 + T_2$ and the maximum value of θ_{T2ij} .

5.3.7.3 Availability for Fully Adaptive Scanning

In general, the resolution elements will present wildly varying values of $\left(\frac{S}{N}\right)_{ij}$ because of the differing environmental and angular properties present. It therefore makes sense to design a system which utilizes the excess signal in one area to compensate for a signal deficit in another area, if all conditions are known in advance to the satellite.

This adaptation of the scan parameters might be performed by

- (1) Reducing the slot width, t_s , in clear weather areas. This would reduce the message duration, and allow more time for communicating to covered areas. However, it requires a source that could operate efficiently in widely differing modes, and a receiver with a foreknowledge of the slot width being used. For these reasons we discard this possibility.
- (2) Increasing the spot diameter to the limit imposed by the $\left(\frac{S}{N}\right)_{REQ} = \left(\frac{S}{N}\right)_{ij}$. Thus the A_{RE} would be covered in less time, allowing extra time to cover the "bad" areas:
- (3) Using multiple terminals to illuminate the same spot, so that the $\left(\frac{S}{N}\right)_{ij}$ is increased.
- (4) Reducing the spot diameter in "bad" areas, to increase the $\left(\frac{S}{N}\right)_{ij}$. This is inadvisable since the minimum spot diameter is constrained by
 - (A) Long and short term satellite jitter;
 - (B) Submarine motion (equation 5-67)
 - (C) Enlargement in passing through the cloud.

5.3.7.3 (Continued)

Therefore we cannot arbitrarily reduce the D_{sp} to aid in bad weather communications⁺.

- (5) Reducing submarine depth (smaller $|D|$). This should only be considered after all other expedients fail, since it does relieve a significant requirement.

In analyzing the adaptive scan, then, we assume

- (1) The $\left(\frac{S}{N}\right)_{ij}$ will always be adjusted to be equal to $\left(\frac{S}{N}\right)_{REQ}$ by enlarging the spot diameter, and by adding additional terminals onto the same spot, as required.
- (2) Only circular spots are considered, since the optical complexity is like that required for spot variation among resolutions elements.

We then begin, as before, by defining a minimum beam divergence θ_{T1} , based on the satellite jitter or submarine motion constraints. Given this θ_{T1} , a FOM_{ij} is derived for each resolution element, via

$$FOM_{ij} = FOM_{ij} (\alpha_T = \theta_{T1}). \quad (5-114)$$

We again note that for $FOM_{ij} (\alpha_T = \theta_{T1}) \geq 1$ for a single terminal, then if m terminals of equal energy per pulse are available on the satellite, the system performance cannot tell whether they are combined onto a single spot (enlarging θ_T) or separately used to illuminate spots of α_{T1} size. For resolution elements with $FOM_{ij} (\alpha_T = \theta_{T1}) < 1$ for a single terminal input of E_p , the optimum approach* is to use all available terminals to increase FOM_{ij} until it is > 1 , and then increase the α_{Tij} until $FOM_{ij} = 1$.

⁺However, it might be possible to use in-cloud spreading to reduce the required spot overlap.

*Or else, during some portion of T_A the total prime power capability of the satellite would be under-utilized while some areas were coverable but uncovered.

5.3.7.3 (Continued)

This implies that the very fact that there are m terminals is irrelevant to the availability analysis for this optimum adaptive scanning. Instead, FOM_{ij} should be evaluated as if all the available energy per pulse were present in a single beam.

When this is done, and FOM_{ij} evaluated in (5-114), for $FOM_{ij} < 1$ the resolution elements will not be covered. Hence the fundamentally unavailable area is

$$A_{UNAV} = \frac{\sum_{ij} A_{REij} (for all FOM_{ij} (\alpha_T = \alpha_{T1}) < 1)}{\sum_{ij} A_{REij}} \quad (5-115)$$

On the other hand, for $FOM_{ij} > 1$, excess energy is being delivered, and the source being suboptimally utilized. We correct this by deriving

$$\alpha_{Tij} = \alpha_{T1} \left[\frac{FOM_{ij} (\alpha_T = \alpha_{T1})}{1} \right]^{1/2} \quad (5-116)$$

((since this means $FOM_{ij} (\alpha_T = \alpha_{Tij}) = 1$)), for all $FOM_{ij} (\alpha_T = \alpha_{T1}) \geq 1$.

We again use the effective coverage area of

$$A_{scij} = \epsilon^2 R_{ij}^2 \alpha_{Tij}^2 \quad (5-117)$$

so that the number of spots per resolution element is

$$N_{SREij} = \frac{A_{RE}}{A_{scij}} \quad (5-118)$$

5.3.7.3 (Continued)

and the total number of spots is

$$N_{TOTSP} = \sum_{ij} N_{SREij} \quad \text{(for all } ij \text{ such that } FOM_{ij} (\theta_T = \theta_{T1}) \geq 1 \text{)} \quad (5-119)$$

Then the total time required to cover the entire coverable area is

$$T_{TOT} = N_{TOTSP} M_D + (N_{TOTSP} - 1) t_{Si} \quad (5-120)$$

However, now if it happens that $T_{TOT} > T_A$, there is no recourse short of adding additional energy capability to the satellite, since there is no excess energy arriving at any submarine receiver. Indeed $T_{TOT} > T_A$ means that part of the area able to be covered from the SNR point of view is temporally unavailable.

To determine the availability, then, the time to scan each resolution element must be calculated. Moreover, since availability is a measure of area coverage, it makes sense to cover the resolution elements with the largest values of $FOM_{ij} (\theta_T = \theta_{T1})$ first, since they are using the largest spot diameter, θ_{T1j} .

We define the time to cover a given resolution element by

$$T_{ij} = N_{SREij} (M_D + t_{Si}) \quad (5-121)$$

and calculate

$$\sum_{ij} T_{ij} = T_{PART} \quad \text{(for } FOM_{ij} (\theta_T = \theta_{T1}) \geq 1 \text{)} \quad (5-122)$$

in order of largest to smallest)

until

$$T_{PART} > T_A \quad (5-122a)$$

5.3.7.3 (Continued)

The resolution element for which T_{PART} changes from $\sim T_A$ to $\sim T_A$ is denoted by the subscript o, t , and the fraction of its area covered is given by the fraction

$$\frac{T_A - T_{\text{PART}}(y_j = o, t - 1)}{T_{o, t}}$$

Then the availability is given by

$$A_{\text{VL}} = \frac{\sum_{ij}^{o, t-1} A_{\text{RE}ij}}{\sum_{ij} A_{\text{RE}ij}} + \left\{ \frac{T_A - T_{\text{PART}}(ij = o, t - 1)}{T_{o, t}} \right\} \quad (5-123)$$

It is also useful to print out A_{UNVL} (from 5-115), T_{TOT} (if $T_{\text{TOT}} \cdot T_A$), θ_{T1} and the maximum value of T_{ij} , and the minimum and maximum values of $N_{\text{SRE}ij}$.

Note if $T_{\text{TOT}} \leq T_A$.

$$A_{\text{VL}} = 1 - A_{\text{UNAV}} \quad (5-124)$$

5.4 COMPUTER PROGRAM FOR THE DCM

5.4.1 Introduction

The downlink communication program is arranged as shown in Figure 5-11. There are eleven subroutines used in the program. These include the eight shown in the Figure; a general sorting subroutine (SORT); the single pulse model which has been incorporated into a subroutine (DSPDPM) called by FADAPT, PADAPT, and NADAPT; and a look-up table and interpolation subroutine (DSTRD2) called by DSPDPM.

There are four data files read into the program. The file SPPM contains that input data which is only used by the single pulse subroutine. The file ENVDATA contains the data from the environmental data bases, as well as the input data on the solar and lunar positions. Files DATAB and DATAC contain the input data concerning the satellite, laser, and signal processing and scanning requirements.

DMAIN is the mainline program used to read in the input data from the data files and to call the other subroutines. Subroutine DNCOMM is used to calculate all zenith angles, azimuthal angles, and receiver axis offset angles needed for the DCM. The range calculations from the satellite to the environmental resolution elements are also handled in this subroutine. The next subroutine called, SGPROC, is the subroutine that handles all signal-to-noise, jamming, spoofing, and message length computations for the downlink model. Subroutine POWER is used to perform the necessary energy and power calculations for the satellite and laser.

After these subroutines have been called and the necessary computation completed, a branch follows to one of three cases: fully adaptive scanning (FADAPT), partially adaptive scanning (PADAPT), or a non-adaptive scan (NADAPT). In these subroutines, the single pulse model subroutine (DSPDPM) is called upon to make signal-to-noise calculations for each environmental resolution element in the coverage area of that particular satellite. From these results, and temporal availability considerations, these subroutines perform the beam divergence, number of spots, and availability calculations that correspond to that particular mode of scanning.

The final subroutine called, ARYRIT, does all the printing and labeling of the output data.

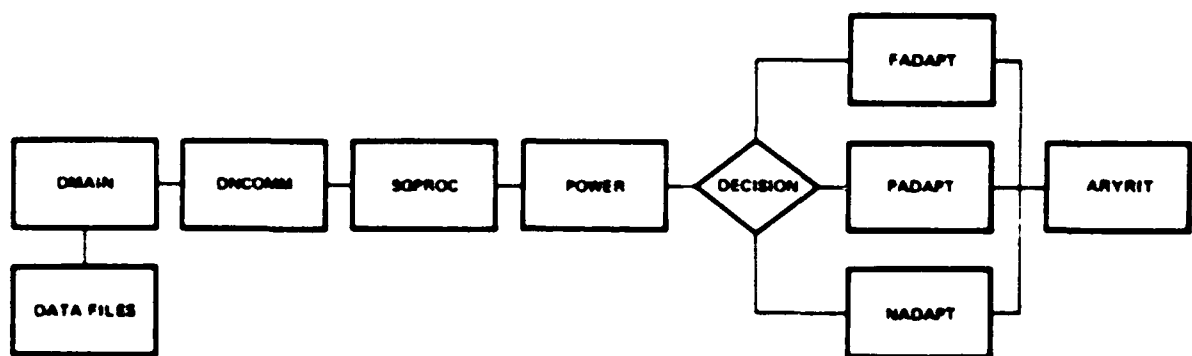


Figure 5-11. Layout of the DCM Program

5.4.2 Names of Variables

This section lists the Fortran terminology and definition of all variables used in the DCM which were not previously used and listed for the SPDPM.

A

ACARE =	Total area with signal-to-noise ratio greater than required signal-to-noise ratio
APAE = G_{AZ} =	Azimuthal pointing angle of receiver
ARE = A_{RE} =	Area of resolution elements
ASC = A_{SC} =	Area of square in spot
AUNAV = A_{UNAV} =	Fraction of the area that cannot be covered
AVL = A_{VL} =	Fraction of the area that can be covered
AZMUA = θ_{MUA} =	Azimuthal lunar angles
AZSGA = θ_{SA} =	Azimuthal signal angle
AZSUA = θ_{SUA} =	Azimuthal solar angles
AZMIN = $\theta_{SP_{min}}$ =	Minimum azimuthal angle from satellite

B

BITSP = i =	Number of message bits per laser pulse
BMDIV = θ_T =	Beam divergence

C

COFOV = θ_R =	Half-angle of receiver field of view
----------------------	--------------------------------------

D

DEADT = t_d =	Dead time between frames
DEADTS = t_{dS} =	Dead time between spots
DIVAD = θ_{TOR} =	Beam Divergence required due to satellite angular drift

5.4.2 (Continued)

$DIVMIN = \theta_{TMN}$ = Minimum beam divergence required due to satellite restrictions.

$DIVPJ = \theta_{\epsilon_s}$ = Minimum beam divergence required due to satellite pointing jitter

$DIVSAT$ = Minimum beam divergence required due to satellite restrictions

E

$EFF = F_L$ = "Wall plug" efficiency of the laser

$ETOT = E_{TOT}$ = Total energy transmitted from all lasers per pulse

F

$FOM = FOM$ = Figure of merit, ratio of S/N in resolution element to S/N required for quality of service requirement

G

$GAINSP = g$ = "Gain" of spoof pulses relative to regular pulses

LATS	= θ_s	} = Latitude of the satellite, sun, and moon in degrees and radians
LATSR		
LATSU	= θ_{su}	
LATSUR		
LATMU	= θ_{mu}	
LATMUR		
LNGS	= θ_s	} = Longitude of the satellite, sun and moon in degrees and radians
LNGSR		
LNGSU	= θ_{su}	
LNGSUR		
LNGMU	= θ_{mu}	
LNGMUR		

5.4.2 (Continued)

$\left. \begin{array}{l} \text{LATMR}(I) = \alpha_i \\ \text{LATMRR}(I) \\ \text{LNGMR}(J) = \beta_j \\ \text{LNGMRR}(J) \end{array} \right\} = \text{Mean latitude and longitude of the environmental resolution elements in degrees and radians}$

M

$\text{MARG} = \text{MARG} = \text{System margin used to compensate for unmodelled noise source}$
 $\text{MAXR} = R_{ij_{\max}} = \text{Maximum range from satellite to any resolution element}$
 $\text{MBITS} = M_{LO} = \text{Number of message bits}$
 $\text{MESDUR} = M_D = \text{Total message duration}$
 $\text{MLBITS} = M_L = \text{Total message length in bits}$
 $\text{MAXZA} = \text{Maximum zenith angle from satellite to any resolution element}$

N

$\text{NCOL} = \text{Number of resolution elements along a line of constant latitude around the earth}$
 $\text{NROW} = \text{Number of resolution elements in the northern hemisphere along a line of constant longitude}$
 $\text{NJAM} = N_J = \text{Number of jammed pulses in threshold detection}$
 $\text{NLASER} = m = \text{Number of lasers used on the satellite}$
 $\text{NMISM} = (N_m') = \text{Number of missed messages per year}$
 $\text{NPULSE} = \text{Number of pulses used to communicate to the coverage area}$
 $\text{NRE} = N_{\text{TOTRE}} = \text{Number of resolution elements in the coverage area}$
 $\text{NSPOOF} = N_{SD} = \text{Number of spoofing events per year}$
 $\text{NSPOT}(I,J) = N_{\text{SRE}_{ij}} = \text{Number of spots needed to cover the } i, j \text{ resolution element}$
 $\text{NTSPOT} = N_{\text{TOTSP}} = \text{Number of spots needed to cover the entire coverage area}$

5.4.2 (Continued)

NUMEF = w	Number of extra frames needed in message to reduce duplication probability to acceptable level
NJTOP2 =	Number of jammed pulses using TOP processing
O	
OV LAP = λ	Spot overlap factor
OVHBTS = $\sqrt{V_0}$	Number of overhead bits
P	
PROP =	Number of resolution elements in northern hemisphere
PAVG = P_{AV}	Average power output from laser
PI = π	3.1416
PLRE =	Fraction of last resolution element that can be covered in the fully adaptive scan
PMISSM = P_M	Probability of missing a transmitted message
PNOLAS = P'_{HO}	Prime power (satellite) required for non-laser functions
PRF = PRF	Pulse repetition frequency of the laser
PTOT = P'_{TOT}	Prime power on satellite required
R	
RE = R_E	Radius of the earth
RMU = R_{MU}	Distance from earth to the moon
RSU = R_{SU}	Distance from earth to the sun
RITOP1 =	An option to print (1.) or withhold printing (0.) of the output data from DNCOMP
RITOP2 =	An option to print (1.) or withhold printing (0.) of the output data from DSPDPM

5.4.2 (Continued)

RNTYPE =	A decision variable. If it equals 1 a non-adaptive scan is employed, 2 is a partially adaptive scan, 3 is a fully adaptive scan
S	
SATSD = $D_{sp_{min}}$ =	Minimum spot diameter due to scanning restrictions
SDMIN =	Minimum spot diameter
SFOM =	The sorted array of FOM values
SN = S/N =	The signal to noise ratio
SNREQ = $(S/N)_{REQ}$ =	Signal to noise ratio required by quality of service requirement
STIMRE =	The sorted array of TIMRE values
SUM1 =	$\sum_1 D_i$
SPOPT =	A decision variable used to tell whether threshold detection or time-of-peak detection is to be used
T	
THW =	Thickness of first water layer
TIMAVL = T_A =	Time available to deliver message to coverage area
TIMEON = T_{on} =	Amount of time that laser is turned on
TIMRE(I,J) = T_{ij} =	Time necessary to cover a given resolution element
TSLOT = t_s =	Slot width
TTOTAL = T_{tot} =	Total time required to cover area of responsibility
TPART = T_{PART} =	The $\sum T_{ij}$ in order of largest to smallest FOM_{ij} until it is greater than T_A
TSGNR = TNR =	Threshold signal to noise ratio

5.4.2 (Continued)

W

WARMUP = t_w = Time necessary for the laser to warmup

X

* $X_E = X_E$ = X coordinate of the submarine

* $X_S = X_S$ = X coordinate of the satellite

* $X_{MU} = X_{MU}$ = X coordinate of the moon

* $X_{SU} = X_{SU}$ = X coordinate of the sun

*In the earth centered system

Y

* $Y_E = Y_E$ = Y coordinate of the submarine

* $Y_S = Y_S$ = Y coordinate of the satellite

* $Y_{MU} = Y_{MU}$ = Y coordinate of the moon

* $Y_{SU} = Y_{SU}$ = Y coordinate of the sun

*In the earth centered system

Z

* $Z_E = Z_E$ = Z coordinate of the submarine

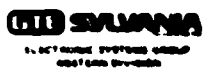
* $Z_S = Z_S$ = Z coordinate of the satellite

* $Z_{SU} = Z_{SU}$ = Z coordinate of the sun

* $Z_{MU} = Z_{MU}$ = Z coordinate of the moon

ZPAR = G_{EL} = Zenith pointing angle of the receiver

*In the earth centered system



5.4.3 DMC Listing

This section lists the complete DCM program. The order of the subroutines listed is

DMAIN
DNCOMM
SGPROC
POWER
FADAPT
PADAPT
NAVAPT
ARYRIT
DSPDPM
SORT
DSTRD2

1070 1748

91152162 41/780/56
1531-417807-60051

[illegible]

1000 374

05/02/19 04:11:07

[illegible]

4000 1374

[illegible][illegible]

5-28

1000

11081-7048-1041
3119193 61/78/56
09/07/19 09:14:16

```

00000010  SUBROUTINE POWERSUM(IQ, ITHROW, IJ, PWR, NLSM, OFF, PWRG, AS)
00000020  IMPLICIT REAL (8, /)
00000030  GO TO (1, 2, 3, 4, 5, 6, 7, 8, 9, 10, 11, 12, 13, 14, 15, 16, 17, 18, 19, 20, 21, 22, 23, 24, 25, 26, 27, 28, 29, 30, 31, 32, 33, 34, 35, 36, 37, 38, 39, 40, 41, 42, 43, 44, 45, 46, 47, 48, 49, 50, 51, 52, 53, 54, 55, 56, 57, 58, 59, 60, 61, 62, 63, 64, 65, 66, 67, 68, 69, 70, 71, 72, 73, 74, 75, 76, 77, 78, 79, 80, 81, 82, 83, 84, 85, 86, 87, 88, 89, 90, 91, 92, 93, 94, 95, 96, 97, 98, 99, 100)
00000040  PWRG = PWRG + PWR
00000050  GO TO 100
00000060  PWRG = PWRG + PWR
00000070  GO TO 100
00000080  PWRG = PWRG + PWR
00000090  GO TO 100
00000100  PWRG = PWRG + PWR
00000110  GO TO 100
00000120  PWRG = PWRG + PWR
00000130  GO TO 100
00000140  PWRG = PWRG + PWR
00000150  GO TO 100
00000160  PWRG = PWRG + PWR
00000170  GO TO 100
00000180  PWRG = PWRG + PWR
00000190  GO TO 100
00000200  PWRG = PWRG + PWR
00000210  GO TO 100
00000220  PWRG = PWRG + PWR
00000230  GO TO 100
00000240  PWRG = PWRG + PWR
00000250  GO TO 100
00000260  PWRG = PWRG + PWR
00000270  GO TO 100
00000280  PWRG = PWRG + PWR
00000290  GO TO 100
00000300  PWRG = PWRG + PWR
00000310  GO TO 100
00000320  PWRG = PWRG + PWR
00000330  GO TO 100
00000340  PWRG = PWRG + PWR
00000350  GO TO 100
00000360  PWRG = PWRG + PWR
00000370  GO TO 100
00000380  PWRG = PWRG + PWR
00000390  GO TO 100
00000400  PWRG = PWRG + PWR
00000410  GO TO 100
00000420  PWRG = PWRG + PWR
00000430  GO TO 100
00000440  PWRG = PWRG + PWR
00000450  GO TO 100
00000460  PWRG = PWRG + PWR
00000470  GO TO 100
00000480  PWRG = PWRG + PWR
00000490  GO TO 100
00000500  PWRG = PWRG + PWR
00000510  GO TO 100
00000520  PWRG = PWRG + PWR
00000530  GO TO 100
00000540  PWRG = PWRG + PWR
00000550  GO TO 100
00000560  PWRG = PWRG + PWR
00000570  GO TO 100
00000580  PWRG = PWRG + PWR
00000590  GO TO 100
00000600  PWRG = PWRG + PWR
00000610  GO TO 100
00000620  PWRG = PWRG + PWR
00000630  GO TO 100
00000640  PWRG = PWRG + PWR
00000650  GO TO 100
00000660  PWRG = PWRG + PWR
00000670  GO TO 100
00000680  PWRG = PWRG + PWR
00000690  GO TO 100
00000700  PWRG = PWRG + PWR
00000710  GO TO 100
00000720  PWRG = PWRG + PWR
00000730  GO TO 100
00000740  PWRG = PWRG + PWR
00000750  GO TO 100
00000760  PWRG = PWRG + PWR
00000770  GO TO 100
00000780  PWRG = PWRG + PWR
00000790  GO TO 100
00000800  PWRG = PWRG + PWR
00000810  GO TO 100
00000820  PWRG = PWRG + PWR
00000830  GO TO 100
00000840  PWRG = PWRG + PWR
00000850  GO TO 100
00000860  PWRG = PWRG + PWR
00000870  GO TO 100
00000880  PWRG = PWRG + PWR
00000890  GO TO 100
00000900  PWRG = PWRG + PWR
00000910  GO TO 100
00000920  PWRG = PWRG + PWR
00000930  GO TO 100
00000940  PWRG = PWRG + PWR
00000950  GO TO 100
00000960  PWRG = PWRG + PWR
00000970  GO TO 100
00000980  PWRG = PWRG + PWR
00000990  GO TO 100
00001000  PWRG = PWRG + PWR
00001010  GO TO 100
00001020  PWRG = PWRG + PWR
00001030  GO TO 100
00001040  PWRG = PWRG + PWR
00001050  GO TO 100
00001060  PWRG = PWRG + PWR
00001070  GO TO 100
00001080  PWRG = PWRG + PWR
00001090  GO TO 100
00001100  PWRG = PWRG + PWR
00001110  GO TO 100
00001120  PWRG = PWRG + PWR
00001130  GO TO 100
00001140  PWRG = PWRG + PWR
00001150  GO TO 100
00001160  PWRG = PWRG + PWR
00001170  GO TO 100
00001180  PWRG = PWRG + PWR
00001190  GO TO 100
00001200  PWRG = PWRG + PWR
00001210  GO TO 100
00001220  PWRG = PWRG + PWR
00001230  GO TO 100
00001240  PWRG = PWRG + PWR
00001250  GO TO 100
00001260  PWRG = PWRG + PWR
00001270  GO TO 100
00001280  PWRG = PWRG + PWR
00001290  GO TO 100
00001300  PWRG = PWRG + PWR
00001310  GO TO 100
00001320  PWRG = PWRG + PWR
00001330  GO TO 100
00001340  PWRG = PWRG + PWR
00001350  GO TO 100
00001360  PWRG = PWRG + PWR
00001370  GO TO 100
00001380  PWRG = PWRG + PWR
00001390  GO TO 100
00001400  PWRG = PWRG + PWR
00001410  GO TO 100
00001420  PWRG = PWRG + PWR
00001430  GO TO 100
00001440  PWRG = PWRG + PWR
00001450  GO TO 100
00001460  PWRG = PWRG + PWR
00001470  GO TO 100
00001480  PWRG = PWRG + PWR
00001490  GO TO 100
00001500  PWRG = PWRG + PWR
00001510  GO TO 100
00001520  PWRG = PWRG + PWR
00001530  GO TO 100
00001540  PWRG = PWRG + PWR
00001550  GO TO 100
00001560  PWRG = PWRG + PWR
00001570  GO TO 100
00001580  PWRG = PWRG + PWR
00001590  GO TO 100
00001600  PWRG = PWRG + PWR
00001610  GO TO 100
00001620  PWRG = PWRG + PWR
00001630  GO TO 100
00001640  PWRG = PWRG + PWR
00001650  GO TO 100
00001660  PWRG = PWRG + PWR
00001670  GO TO 100
00001680  PWRG = PWRG + PWR
00001690  GO TO 100
00001700  PWRG = PWRG + PWR
00001710  GO TO 100
00001720  PWRG = PWRG + PWR
00001730  GO TO 100
00001740  PWRG = PWRG + PWR
00001750  GO TO 100
00001760  PWRG = PWRG + PWR
00001770  GO TO 100
00001780  PWRG = PWRG + PWR
00001790  GO TO 100
00001800  PWRG = PWRG + PWR
00001810  GO TO 100
00001820  PWRG = PWRG + PWR
00001830  GO TO 100
00001840  PWRG = PWRG + PWR
00001850  GO TO 100
00001860  PWRG = PWRG + PWR
00001870  GO TO 100
00001880  PWRG = PWRG + PWR
00001890  GO TO 100
00001900  PWRG = PWRG + PWR
00001910  GO TO 100
00001920  PWRG = PWRG + PWR
00001930  GO TO 100
00001940  PWRG = PWRG + PWR
00001950  GO TO 100
00001960  PWRG = PWRG + PWR
00001970  GO TO 100
00001980  PWRG = PWRG + PWR
00001990  GO TO 100
00002000  PWRG = PWRG + PWR
00002010  GO TO 100
00002020  PWRG = PWRG + PWR
00002030  GO TO 100
00002040  PWRG = PWRG + PWR
00002050  GO
```

100-774

616014 91/70/50
1001-147074-10051

[illegible]

5.4.3 (Continued)

PAGE 0003

15003.540001.1001
05/02/79 1515133

```

C 110 11003.540001.1001
C 111 CALCULATE TOTAL TIME LATER IS TURNED ON
C 112
C 113
C 114
C 115
C 116
C 117
C 118
C 119
C 120
C 121
C 122
C 123
C 124
C 125
C 126
C 127
C 128
C 129
C 130
C 131
C 132
C 133
C 134
C 135
C 136
C 137
C 138
C 139
C 140
C 141
C 142
C 143
C 144
C 145
C 146
C 147
C 148
C 149
C 150
C 151
C 152
C 153
C 154
C 155
C 156
C 157
C 158
C 159
C 160
C 161
C 162
C 163
C 164
C 165
C 166
C 167
C 168
C 169
C 170
C 171
C 172
C 173
C 174
C 175
C 176
C 177
C 178
C 179
C 180
C 181
C 182
C 183
C 184
C 185
C 186
C 187
C 188
C 189
C 190
C 191
C 192
C 193
C 194
C 195
C 196
C 197
C 198
C 199
C 200
C 201
C 202
C 203
C 204
C 205
C 206
C 207
C 208
C 209
C 210
C 211
C 212
C 213
C 214
C 215
C 216
C 217
C 218
C 219
C 220
C 221
C 222
C 223
C 224
C 225
C 226
C 227
C 228
C 229
C 230
C 231
C 232
C 233
C 234
C 235
C 236
C 237
C 238
C 239
C 240
C 241
C 242
C 243
C 244
C 245
C 246
C 247
C 248
C 249
C 250
C 251
C 252
C 253
C 254
C 255
C 256
C 257
C 258
C 259
C 260
C 261
C 262
C 263
C 264
C 265
C 266
C 267
C 268
C 269
C 270
C 271
C 272
C 273
C 274
C 275
C 276
C 277
C 278
C 279
C 280
C 281
C 282
C 283
C 284
C 285
C 286
C 287
C 288
C 289
C 290
C 291
C 292
C 293
C 294
C 295
C 296
C 297
C 298
C 299
C 300
C 301
C 302
C 303
C 304
C 305
C 306
C 307
C 308
C 309
C 310
C 311
C 312
C 313
C 314
C 315
C 316
C 317
C 318
C 319
C 320
C 321
C 322
C 323
C 324
C 325
C 326
C 327
C 328
C 329
C 330
C 331
C 332
C 333
C 334
C 335
C 336
C 337
C 338
C 339
C 340
C 341
C 342
C 343
C 344
C 345
C 346
C 347
C 348
C 349
C 350
C 351
C 352
C 353
C 354
C 355
C 356
C 357
C 358
C 359
C 360
C 361
C 362
C 363
C 364
C 365
C 366
C 367
C 368
C 369
C 370
C 371
C 372
C 373
C 374
C 375
C 376
C 377
C 378
C 379
C 380
C 381
C 382
C 383
C 384
C 385
C 386
C 387
C 388
C 389
C 390
C 391
C 392
C 393
C 394
C 395
C 396
C 397
C 398
C 399
C 400
C 401
C 402
C 403
C 404
C 405
C 406
C 407
C 408
C 409
C 410
C 411
C 412
C 413
C 414
C 415
C 416
C 417
C 418
C 419
C 420
C 421
C 422
C 423
C 424
C 425
C 426
C 427
C 428
C 429
C 430
C 431
C 432
C 433
C 434
C 435
C 436
C 437
C 438
C 439
C 440
C 441
C 442
C 443
C 444
C 445
C 446
C 447
C 448
C 449
C 450
C 451
C 452
C 453
C 454
C 455
C 456
C 457
C 458
C 459
C 460
C 461
C 462
C 463
C 464
C 465
C 466
C 467
C 468
C 469
C 470
C 471
C 472
C 473
C 474
C 475
C 476
C 477
C 478
C 479
C 480
C 481
C 482
C 483
C 484
C 485
C 486
C 487
C 488
C 489
C 490
C 491
C 492
C 493
C 494
C 495
C 496
C 497
C 498
C 499
C 500
C 501
C 502
C 503
C 504
C 505
C 506
C 507
C 508
C 509
C 510
C 511
C 512
C 513
C 514
C 515
C 516
C 517
C 518
C 519
C 520
C 521
C 522
C 523
C 524
C 525
C 526
C 527
C 528
C 529
C 530
C 531
C 532
C 533
C 534
C 535
C 536
C 537
C 538
C 539
C 540
C 541
C 542
C 543
C 544
C 545
C 546
C 547
C 548
C 549
C 550
C 551
C 552
C 553
C 554
C 555
C 556
C 557
C 558
C 559
C 560
C 561
C 562
C 563
C 564
C 565
C 566
C 567
C 568
C 569
C 570
C 571
C 572
C 573
C 574
C 575
C 576
C 577
C 578
C 579
C 580
C 581
C 582
C 583
C 584
C 585
C 586
C 587
C 588
C 589
C 590
C 591
C 592
C 593
C 594
C 595
C 596
C 597
C 598
C 599
C 600
C 601
C 602
C 603
C 604
C 605
C 606
C 607
C 608
C 609
C 610
C 611
C 612
C 613
C 614
C 615
C 616
C 617
C 618
C 619
C 620
C 621
C 622
C 623
C 624
C 625
C 626
C 627
C 628
C 629
C 630
C 631
C 632
C 633
C 634
C 635
C 636
C 637
C 638
C 639
C 640
C 641
C 642
C 643
C 644
C 645
C 646
C 647
C 648
C 649
C 650
C 651
C 652
C 653
C 654
C 655
C 656
C 657
C 658
C 659
C 660
C 661
C 662
C 663
C 664
C 665
C 666
C 667
C 668
C 669
C 670
C 671
C 672
C 673
C 674
C 675
C 676
C 677
C 678
C 679
C 680
C 681
C 682
C 683
C 684
C 685
C 686
C 687
C 688
C 689
C 690
C 691
C 692
C 693
C 694
C 695
C 696
C 697
C 698
C 699
C 700
C 701
C 702
C 703
C 704
C 705
C 706
C 707
C 708
C 709
C 710
C 711
C 712
C 713
C 714
C 715
C 716
C 717
C 718
C 719
C 720
C 721
C 722
C 723
C 724
C 725
C 726
C 727
C 728
C 729
C 730
C 731
C 732
C 733
C 734
C 735
C 736
C 737
C 738
C 739
C 740
C 741
C 742
C 743
C 744
C 745
C 746
C 747
C 748
C 749
C 750
C 751
C 752
C 753
C 754
C 755
C 756
C 757
C 758
C 759
C 760
C 761
C 762
C 763
C 764
C 765
C 766
C 767
C 768
C 769
C 770
C 771
C 772
C 773
C 774
C 775
C 776
C 777
C 778
C 779
C 780
C 781
C 782
C 783
C 784
C 785
C 786
C 787
C 788
C 789
C 790
C 791
C 792
C 793
C 794
C 795
C 796
C 797
C 798
C 799
C 800
C 801
C 802
C 803
C 804
C 805
C 806
C 807
C 808
C 809
C 810
C 811
C 812
C 813
C 814
C 815
C 816
C 817
C 818
C 819
C 820
C 821
C 822
C 823
C 824
C 825
C 826
C 827
C 828
C 829
C 830
C 831
C 832
C 833
C 834
C 835
C 836
C 837
C 838
C 839
C 840
C 841
C 842
C 843
C 844
C 845
C 846
C 847
C 848
C 849
C 850
C 851
C 852
C 853
C 854
C 855
C 856
C 857
C 858
C 859
C 860
C 861
C 862
C 863
C 864
C 865
C 866
C 867
C 868
C 869
C 870
C 871
C 872
C 873
C 874
C 875
C 876
C 877
C 878
C 879
C 880
C 881
C 882
C 883
C 884
C 885
C 886
C 887
C 888
C 889
C 890
C 891
C 892
C 893
C 894
C 895
C 896
C 897
C 898
C 899
C 900
C 901
C 902
C 903
C 904
C 905
C 906
C 907
C 908
C 909
C 910
C 911
C 912
C 913
C 914
C 915
C 916
C 917
C 918
C 919
C 920
C 921
C 922
C 923
C 924
C 925
C 926
C 927
C 928
C 929
C 930
C 931
C 932
C 933
C 934
C 935
C 936
C 937
C 938
C 939
C 940
C 941
C 942
C 943
C 944
C 945
C 946
C 947
C 948
C 949
C 950
C 951
C 952
C 953
C 954
C 955
C 956
C 957
C 958
C 959
C 960
C 961
C 962
C 963
C 964
C 965
C 966
C 967
C 968
C 969
C 970
C 971
C 972
C 973
C 974
C 975
C 976
C 977
C 978
C 979
C 980
C 981
C 982
C 983
C 984
C 985
C 986
C 987
C 988
C 989
C 990
C 991
C 992
C 993
C 994
C 995
C 996
C 997
C 998
C 999
C 1000

```


9000 6782

8175015 91720160
1001-140000-70001

[illegible]

2008-2009

1308 J. P. A. 1. 1001
05/02/19 09:47:49

[illegible]

5.4.3 (Continued)

1000 3572

1306J.PADAP1.F001
05/02/19 09:47:49

```

00001110
00001120
00001130
00001140
00001150
00001160
00001170
00001180
00001190
00001200
00001210
00001220
00001230
00001240
00001250
00001260
00001270
00001280
00001290
00001300
00001310
00001320
00001330
00001340
00001350
00001360
00001370
00001380
00001390
00001400
00001410
00001420
00001430
00001440
00001450
00001460
00001470
00001480
00001490
00001500
00001510
00001520
00001530
00001540
00001550
00001560
00001570
00001580
00001590
00001600
00001610
00001620
00001630
00001640
00001650
00001660
00001670
00001680
00001690
00001700
00001710
00001720
00001730
00001740
00001750
00001760
00001770
00001780
00001790
00001800
00001810
00001820
00001830
00001840
00001850
00001860
00001870
00001880
00001890
00001900
00001910
00001920
00001930
00001940
00001950
00001960
00001970
00001980
00001990
00002000
00002010
00002020
00002030
00002040
00002050
00002060
00002070
00002080
00002090
00002100
00002110
00002120
00002130
00002140
00002150
00002160
00002170
00002180
00002190
00002200
00002210
00002220
00002230
00002240
00002250
00002260
00002270
00002280
00002290
00002300
00002310
00002320
00002330
00002340
00002350
00002360
00002370
00002380
00002390
00002400
00002410
00002420
00002430
00002440
00002450
00002460
00002470
00002480
00002490
00002500
00002510
00002520
00002530
00002540
00002550
00002560
00002570
00002580
00002590
00002600
00002610
00002620
00002630
00002640
00002650
00002660
00002670
00002680
00002690
00002700
00002710
00002720
00002730
00002740
00002750
00002760
00002770
00002780
00002790
00002800
00002810
00002820
00002830
00002840
00002850
00002860
00002870
00002880
00002890
00002900
00002910
00002920
00002930
00002940
00002950
00002960
00002970
00002980
00002990
00003000
00003010
00003020
00003030
00003040
00003050
00003060
00003070
00003080
00003090
00003100
00003110
00003120
00003130
00003140
00003150
00003160
00003170
00003180
00003190
00003200
00003210
00003220
00003230
00003240
00003250
00003260
00003270
00003280
00003290
00003300
00003310
00003320
00003330
00003340
00003350
00003360
00003370
00003380
00003390
00003400
00003410
00003420
00003430
00003440
00003450
00003460
00003470
00003480
00003490
00003500
00003510
00003520
00003530
00003540
00003550
00003560
00003570
00003580
00003590
00003600
00003610
00003620
00003630
00003640
00003650
00003660
00003670
00003680
00003690
00003700
00003710
00003720
00003730
00003740
00003750
00003760
00003770
00003780
00003790
00003800
00003810
00003820
00003830
00003840
00003850
00003860
00003870
00003880
00003890
00003900
00003910
00003920
00003930
00003940
00003950
00003960
00003970
00003980
00003990
00004000
00004010
00004020
00004030
00004040
00004050
00004060
00004070
00004080
00004090
00004100
00004110
00004120
00004130
00004140
00004150
00004160
00004170
00004180
00004190
00004200
00004210
00004220
00004230
00004240
00004250
00004260
00004270
00004280
00004290
00004300
00004310
00004320
00004330
00004340
00004350
00004360
00004370
00004380
00004390
00004400
00004410
00004420
00004430
00004440
00004450
00004460
00004470
00004480
00004490
00004500
00004510
00004520
00004530
00004540
00004550
00004560
00004570
00004580
00004590
00004600
00004610
00004620
00004630
00004640
00004650
00004660
00004670
00004680
00004690
00004700
00004710
00004720
00004730
00004740
00004750
00004760
00004770
00004780
00004790
00004800
00004810
00004820
00004830
00004840
00004850
00004860
00004870
00004880
00004890
00004900
00004910
00004920
00004930
00004940
00004950
00004960
00004970
00004980
00004990
00005000
00005010
00005020
00005030
00005040
00005050
00005060
00005070
00005080
00005090
00005100
00005110
00005120
00005130
00005140
00005150
00005160
00005170
00005180
00005190
00005200
00005210
00005220
00005230
00005240
00005250
00005260
00005270
00005280
00005290
00005300
00005310
00005320
00005330
00005340
00005350
00005360
00005370
00005380
00005390
00005400
00005410
00005420
00005430
00005440
00005450
00005460
00005470
00005480
00005490
00005500
00005510
00005520
00005530
00005540
00005550
00005560
00005570
00005580
00005590
00005600
00005610
00005620
00005630
00005640
0000565
```

1000 3542

1508 J. MADARI. 1001
03/02/19 09:09:20

[illegible]

[illegible]

PAGE 0001

36:06157 31770750
1906-1907-1908-1909-1910-1911-1912-1913-1914-1915-1916-1917-1918-1919-1920-1921-1922-1923-1924-1925-1926-1927-1928-1929-1930-1931-1932-1933-1934-1935-1936-1937-1938-1939-1940-1941-1942-1943-1944-1945-1946-1947-1948-1949-1950-1951-1952-1953-1954-1955-1956-1957-1958-1959-1960-1961-1962-1963-1964-1965-1966-1967-1968-1969-1970-1971-1972-1973-1974-1975-1976-1977-1978-1979-1980-1981-1982-1983-1984-1985-1986-1987-1988-1989-1990-1991-1992-1993-1994-1995-1996-1997-1998-1999-2000-2001-2002-2003-2004-2005-2006-2007-2008-2009-2010-2011-2012-2013-2014-2015-2016-2017-2018-2019-2020-2021-2022-2023-2024-2025-2026-2027-2028-2029-2030-2031-2032-2033-2034-2035-2036-2037-2038-2039-2040-2041-2042-2043-2044-2045-2046-2047-2048-2049-2050-2051-2052-2053-2054-2055-2056-2057-2058-2059-2060-2061-2062-2063-2064-2065-2066-2067-2068-2069-2070-2071-2072-2073-2074-2075-2076-2077-2078-2079-2080-2081-2082-2083-2084-2085-2086-2087-2088-2089-2090-2091-2092-2093-2094-2095-2096-2097-2098-2099-2100-2101-2102-2103-2104-2105-2106-2107-2108-2109-2110-2111-2112-2113-2114-2115-2116-2117-2118-2119-2120-2121-2122-2123-2124-2125-2126-2127-2128-2129-2130-2131-2132-2133-2134-2135-2136-2137-2138-2139-2140-2141-2142-2143-2144-2145-2146-2147-2148-2149-2150-2151-2152-2153-2154-2155-2156-2157-2158-2159-2160-2161-2162-2163-2164-2165-2166-2167-2168-2169-2170-2171-2172-2173-2174-2175-2176-2177-2178-2179-2180-2181-2182-2183-2184-2185-2186-2187-2188-2189-2190-2191-2192-2193-2194-2195-2196-2197-2198-2199-2200-2201-2202-2203-2204-2205-2206-2207-2208-2209-2210-2211-2212-2213-2214-2215-2216-2217-2218-2219-2220-2221-2222-2223-2224-2225-2226-2227-2228-2229-2230-2231-2232-2233-2234-2235-2236-2237-2238-2239-2240-2241-2242-2243-2244-2245-2246-2247-2248-2249-2250-2251-2252-2253-2254-2255-2256-2257-2258-2259-2260-2261-2262-2263-2264-2265-2266-2267-2268-2269-2270-2271-2272-2273-2274-2275-2276-2277-2278-2279-2280-2281-2282-2283-2284-2285-2286-2287-2288-2289-2290-2291-2292-2293-2294-2295-2296-2297-2298-2299-2300-2301-2302-2303-2304-2305-2306-2307-2308-2309-2310-2311-2312-2313-2314-2315-2316-2317-2318-2319-2320-2321-2322-2323-2324-2325-2326-2327-2328-2329-2330-2331-2332-2333-2334-2335-2336-2337-2338-2339-2340-2341-2342-2343-2344-2345-2346-2347-2348-2349-2350-2351-2352-2353-2354-2355-2356-2357-2358-2359-2360-2361-2362-2363-2364-2365-2366-2367-2368-2369-2370-2371-2372-2373-2374-2375-2376-2377-2378-2379-2380-2381-2382-2383-2384-2385-2386-2387-2388-2389-2390-2391-2392-2393-2394-2395-2396-2397-2398-2399-2400-2401-2402-2403-2404-2405-2406-2407-2408-2409-2410-2411-2412-2413-2414-2415-2416-2417-2418-2419-2420-2421-2422-2423-2424-2425-2426-2427-2428-2429-2430-2431-2432-2433-2434-2435-2436-2437-2438-2439-2440-2441-2442-2443-2444-2445-2446-2447-2448-2449-2450-2451-2452-2453-2454-2455-2456-2457-2458-2459-2460-2461-2462-2463-2464-2465-2466-2467-2468-2469-2470-2471-2472-2473-2474-2475-2476-2477-2478-2479-2480-2481-2482-2483-2484-2485-2486-2487-2488-2489-2490-2491-2492-2493-2494-2495-2496-2497-2498-2499-2500-2501-2502-2503-2504-2505-2506-2507-2508-2509-2510-2511-2512-2513-2514-2515-2516-2517-2518-2519-2520-2521-2522-2523-2524-2525-2526-2527-2528-2529-2530-2531-2532-2533-2534-2535-2536-2537-2538-2539-2540-2541-2542-2543-2544-2545-2546-2547-2548-2549-2550-2551-2552-2553-2554-2555-2556-2557-2558-2559-2560-2561-2562-2563-2564-2565-2566-2567-2568-2569-2570-2571-2572-2573-2574-2575-2576-2577-2578-2579-2580-2581-2582-2583-2584-2585-2586-2587-2588-2589-2590-2591-2592-2593-2594-2595-2596-2597-2598-2599-2600-2601-2602-2603-2604-2605-2606-2607-2608-2609-2610-2611-2612-2613-2614-2615-2616-2617-2618-2619-2620-2621-2622-2623-2624-2625-2626-2627-2628-2629-2630-2631-2632-2633-2634-2635-2636-2637-2638-2639-2640-2641-2642-2643-2644-2645-2646-2647-2648-2649-2650-2651-2652-2653-2654-2655-2656-2657-2658-2659-2660-2661-2662-2663-2664-2665-2666-2667-2668-2669-2670-2671-2672-2673-2674-2675-2676-2677-2678-2679-2680-2681-2682-2683-2684-2685-2686-2687-2688-2689-2690-2691-2692-2693-2694-2695-2696-2697-2698-2699-2700-2701-2702-2703-2704-2705-2706-2707-2708-2709-2710-2711-2712-2713-2714-2715-2716-2717-2718-2719-2720-

[illegible]

[illegible]

[illegible]

0100 2704

0670(15) 417076
1601-40450-7001

[illegible]

5.4.3 (Continued)

PAGE 0011

1500J.D5P00P.0091
05/02/76 15:10:58

```

2475 10100-10100015CANF 0005710
2480 1000-001-10011 0005720
C 10100 ENERGY TRANSMISSION 2410-2400 0005730
2490 1000-0101000000000000000000 0005740
C 10100 ENERGY TRANSMISSION DUE TO BLUE SKY 0005750
C 10100 ENERGY TRANSMISSION DUE TO BLUE SKY 0005760
C 10100 ENERGY TRANSMISSION DUE TO BLUE SKY 0005770
2495 1005-1005-00057 0005780
2500 1005-1005-00057 0005790
2505 1005-1005-00057 0005800
2510 1005-1005-00057 0005810
2515 1005-1005-00057 0005820
2520 1005-1005-00057 0005830
C 1005-1005-00057 0005840
C 1005-1005-00057 0005850
C 1005-1005-00057 0005860
C 1005-1005-00057 0005870
C 1005-1005-00057 0005880
C 1005-1005-00057 0005890
C 1005-1005-00057 0005900
C 1005-1005-00057 0005910
C 1005-1005-00057 0005920
C 1005-1005-00057 0005930
C 1005-1005-00057 0005940
C 1005-1005-00057 0005950
C 1005-1005-00057 0005960
C 1005-1005-00057 0005970
C 1005-1005-00057 0005980
C 1005-1005-00057 0005990
C 1005-1005-00057 0006000
C 1005-1005-00057 0006010
C 1005-1005-00057 0006020
C 1005-1005-00057 0006030
C 1005-1005-00057 0006040
C 1005-1005-00057 0006050
C 1005-1005-00057 0006060
C 1005-1005-00057 0006070
C 1005-1005-00057 0006080
C 1005-1005-00057 0006090
C 1005-1005-00057 0006100
C 1005-1005-00057 0006110
C 1005-1005-00057 0006120
C 1005-1005-00057 0006130
C 1005-1005-00057 0006140
C 1005-1005-00057 0006150
C 1005-1005-00057 0006160
C 1005-1005-00057 0006170
C 1005-1005-00057 0006180
C 1005-1005-00057 0006190
C 1005-1005-00057 0006200
C 1005-1005-00057 0006210
C 1005-1005-00057 0006220
C 1005-1005-00057 0006230
C 1005-1005-00057 0006240
C 1005-1005-00057 0006250
C 1005-1005-00057 0006260
C 1005-1005-00057 0006270

```


[illegible]

0100 4943

06101193 01/20/60
1804-440430-72071

[illegible]

[illegible]

5.4.3 (Continued)

PAGE 0019

TSDB J. D. SODPH. FOR
 05/02/75 CS10151

00010270
 00010280
 00010290
 00010300
 00010310
 00010320
 00010330
 00010340
 00010350
 00010360
 00010370
 00010380
 00010390

C FIND INTERVAL FOR B
 1-0
 7510 1-101
 1718-YAM(1-11) 7520-7600-7510
 C INTERPOLATION CALCUS
 7520 11-YAM(11-1,21-110-YAM(11-1,11)-YAM(11-1,11))
 1704-111-1,21-YAM(11,1,1)
 RETURN
 C NO INTERPOLATION NEEDED
 7600 11-YAM(11,1,21)
 RETURN
 END

5.4.3 (Continued)

PAGE 0001

1500J-S001.F001
05/02/74 05134107

00000013
00000020
00000030
00000040
00000050
00000060
00000070
00000080
00000090
00000100
00000110
00000120
00000130
00000140
00000150
00000160
00000170
00000180
00000190
00000200

```

SUBROUTINE SUB1(ARRAY1,ARRAY2,IS)
  INTEGER I,J,N,NUMP
  LOGICAL DONE
  DIMENSION ARRAY1(100),ARRAY2(100)
  DO 100 I=2,N
    CONTINUE
    DONE IS .FALSE.
    DO 100 J=1,NUMP
      ARRAY1(I)=ARRAY2(J)
      ARRAY2(J)=ARRAY1(I)
    CONTINUE
    DONE IS .TRUE.
  CONTINUE
  RETURN
END SUBROUTINE SUB1

```


2008 7943

15003.051002.1101
05/02/19 04:42:06

[illegible]

PAGE 0003

00174140 41180150
10011700150-100151

[illegible]

5.5 MODEL UNCERTAINTIES

The sub-models developed in Section 5.3 have very few uncertainties, and should require little future revision.

5.5.1 Area Relationships

The only uncertainty here involves the size and shape of environmental resolution elements (ERE's). The ERE concept itself is too useful to be neglected, but future cloud and water data base work may reveal that ERE's of a different size or shape are more appropriate in the OSCAR applications.

5.5.2 Temporal Relationships

There are no uncertainties in the models for the temporal relationships in Section 5.3.2.

5.5.3 Message

There are no uncertainties in the models for the message in Section 5.3.3.

5.5.4 Modulation/Demodulation

The only uncertainties in the models developed in Section 5.3.4 concern their completeness. There may be other demodulation and message processing approaches which will change the required Signal-to-Noise ratio and/or Message Lengths (Overhead bits) from the present formulation. GTE-Sylvania will continue to search for these improved demodulation techniques in related work.

A second-order uncertainty concerns our model for jamming/spoofing, and the five assumptions made there-in. If those assumptions were altered by the NAVY, the related sub-models would also require modification.

5.5.5 Scanning Relationships

There is no uncertainty in the model developed in Section 5.3.5. However, as the hardware design progresses, the formulation of the satellite pointing accuracy may be changed to better reflect the attitude stabilization and pointing technique actually employed. This will probably be a minor analytic change.

5.5.6 Receiver and Source

There are no uncertainties in the models developed in Section 5.3.6.

5.5.7 Availability/System Effectiveness and Adaptive Scanning

The sub-models for adaptive scanning may be modified as more is learned about:

1. The precision of the information obtainable from remote scanning;
2. The practicality of the angular expansion/elliptical correction optics.

It may happen that only relatively crude information is available concerning the clouds in the coverage area, and that a continuously variable beam size is not practical, so that some straightforward model modification should occur.

5.5.8 Included SPDPM Sub-Models

The propagation related SPDPM sub-models were discussed in Sections 3.4 and 4.5. The SPDPM system design sub-models are well understood. The only one requiring possible modification is the pulse-shape/detection bandwidth, if the atomic resonance optical filter becomes the leading candidate, since this filter adds an additional pulse stretching/distortion to that caused by the propagation path/field-of-view effects.

Table 5-3 summarizes the status of the DCM sub-models.

5.5.8 (Continued)

TABLE 5-3. STATUS OF SUB-MODELS OF THE DCM
 (SPDPM models are discussed in Sections 3.4 and 4.5)

SUB-MODEL	STATUS	COMMENT
Area Relationship	O.K. in principle	Size and shape of environmental resolution elements may be modified in future.
Temporal Relationships	O.K.	-
Message	O.K.	-
Modulation/Demodulation	O.K. as written	Further work on better schemes continues, and may modify these models. Changing the "threat" assumptions would change the spoofing/jamming models.
Scanning Relationships	O.K. as written	Satellite design work may redefine the pointing accuracy sub-model.
Receiver and Source	O.K.	-
Availability/Adaptive Scanning	O.K. as written	Probably will be modified as the remote sensing precision and practical optical designs are better understood.
SPDPM - Environmental	Partially Verified	See discussion in Sections 3.4 and 4.5
SPDPM - System Design	O.K. as written	Will require modification if atomic resonance filter becomes the leading candidate.

5.6 "PARAMETER VALUE" UNCERTAINTIES

The parameter value uncertainties for the DCM are of quite a different type than those for the SPDPM. Here the uncertainties primarily relate to those hardware parameters which are actually achievable.

5.6.1 Environment

Those environmental inputs unique to the DCM include:

- A_{RE} = area of a single environmental resolution element. This is uncertain and will remain so until sufficient cloud and water data base development occurs to uniquely define it.
- R_{SU} = distance from sun to receiver. This is well known to the required accuracy.
- λ_{SU} = solar latitude is also well known to the required accuracy.
- β_{SU} = solar longitude is also well known to the required accuracy.
- R_E = mean earth radius is well known.
- R_{MU} = distance from moon to receiver. This is well known to the required accuracy.
- λ_{MU} = lunar latitude is well known to the required accuracy.
- β_{MU} = lunar longitude is also well known to the required accuracy.

The environmental SPDPM inputs were discussed in Sections 3.5 and 4.6 from the point-of-view of the values existing along a single propagation path. Use of the SPDPM in the DCM requires the additional information of their simultaneous values throughout a satellite coverage area. The cloud properties are particularly uncertain when such correlated information is desirable, and the water properties are only approximately known over large stretches of the coverage area.

Better data base development must occur in order to provide adequate inputs to the DCM.

5.6.2 Requirements

There is no uncertainty in any of the requirements inputs listed in Section 5.2.2.

5.6.3 System Design

Considering the present state-of-the-art in laser and filter technology, it is not surprising that there are significant uncertainties in many aspects of the system design inputs. These inputs and their uncertainties include:

- t_{st} ▪ slew time, scan time or dead time between illuminated spots. The value of this parameter depends on the details of the transmitter optics design and the scan technique used, both of which remain to be determined.
- t_w ▪ source warm-up time. Since the laser source is unknown, so is a precise value for this parameter.
- PRF ▪ source repetition frequency. This parameter depends on the most efficient laser operating point, the choice of λ , the minimum slot width achievable and the number of lasers aboard the space-craft, all of which are not precisely determined at this time.
- G_{EL} ▪ Off-zenith in-water receiver pointing angle. The optimum value of this parameter will remain uncertain until water propagation experiments and water data base development work is accomplished.
- G_{AZ} ▪ Azimuth receiver pointing angle. The same comments apply as for G_{EL} .
- m ▪ Number of simultaneously active lasers aboard the satellite. This is unknown until a particular laser candidate is selected, and its optimal operating point is determined.
- E_p ▪ Energy per pulse of each active laser aboard the satellite. The same comments apply as for m .
- F_L ▪ Wall plug laser efficiency. Same comments as for m .
- P'_{HO} ▪ prime power on the satellite required for all non-laser functions. This parameter depends on future satellite design.

5.6.3 (Continued)

- R_S ▪ satellite altitude. This will be sufficiently known for all candidate orbits.
- α_S ▪ Satellite latitude. This will be sufficiently known for all candidate orbits.
- β_S ▪ Satellite longitude. This will be sufficiently known for all candidate orbits.
- t_f ▪ dead time between frames. This again depends on the details of the laser, and its minimum time-to-refire.
- t_S ▪ slot width. This depends on the pulse stretching encountered in the environment, and so will remain uncertain until extensive cloud propagation experiments and cloud data base development occurs.
- i ▪ number of bits per pulse. This parameter depends on slot width and minimum achievable spot size, both of which remain to be determined.
- c ▪ overlap factor between illuminated spots. This is not uncertain so long as a random spot scan is employed.
- θ_{TS} ▪ Satellite short term angular jitter. This parameter is unknown until further design is accomplished.
- θ_{TDR} ▪ Satellite long term angular drift. Same comment as for θ_{TS} .

The system design inputs for the SPDPM were not discussed previously, since Section 3.5 and 4.6 emphasized the environmental parameters. The primary uncertainty, beyond those discussed above, lies in the receiver; in particular:

- θ_R ▪ Receiver half angle field-of-view. This will not be known until adequate water propagation experiments and water data base development occur
- γ_R ▪ Receiver (primarily filter) transmission. This will not be known until the filter type and receiver field-of-view are known.

5.6.3 (Continued)

B_{OPT} = filter bandpass. This will not be known until the filter type and receiver field-of-view are known.

Table 5-4 summarizes the status of the input parameters of the DCM.

5.6.3 (Continued)

Table 5-4. Status of "Input Parameters" to DCM

PARAMETER	STATUS	COMMENT
ENVIRONMENT	PARTIAL	cf SPDPM discussion in Section 3.5 and 4.6. Distribution/Correlation of environmental parameters is unknown.
REQUIREMENTS	O.K.	—
SYSTEM DESIGN		
t_{s2}	TBD	Depends on system design details.
t_w	TBD	Depends on laser selected.
PRF	TBD	Depends on laser and slotwidth.
G_{EL}, G_{AZ}	TBD	Depends on water propagation experiment
m	TBD	Depends on laser characteristics
E_p	TBD	Depends on laser characteristics
F_L	TBD	Depends on laser characteristics
P_{HO}	TBD	Depends on details of satellite design
R_S, α_S, β_S	O.K.	Known for each candidate orbit.
t_f	TBD	Depends on laser characteristics.
t_s	TBD	Depends on extensive cloud propagation results.
z	TBD	Depends on slot width and spot size.
c	O.K.	Known so long as random scan is used.
$\theta_{TS}, \theta_{TDR}$	Partially known	Depends on details of satellite design.
θ_R	TBD	Depends on water propagation experiment.
γ_R	TBD	Depends on filter characteristics.
B_{OPT}	TBD	Depends on filter characteristics.

Section 6

FULL OSCAR SYSTEM MODEL

This section discusses the model for the full OSCAR system, including the ground stations, microwave uplink, satellite orbits, optical downlink and submarine terminal. The section is organized as follows:

- 6.1 Full OSCAR Systems Model -- Philosophy and Flow Charts
 - 6.1.1 Philosophy of Approach -- Full OSCAR System Model
 - 6.1.2 Model Flow Chart -- Full OSCAR Model
- 6.2 Input Information
 - 6.2.1 Environment
 - 6.2.1.1 Fixed Data Bases
 - 6.2.1.2 Data Bases with Predictable Variations
 - 6.2.1.3 Data Bases with Unpredictable Variations
 - 6.2.2 Requirements
 - 6.2.3 System Design
 - 6.2.3.1 Ground Station
 - 6.2.3.2 Satellites
 - 6.2.3.3 Submarine Terminals
- 6.3 Environment, Requirements, System Design Considerations
 - 6.3.1 Environment
 - 6.3.1.1 Data Bases with Predictable Variation
 - 6.3.1.1.1 Solar Location
 - 6.3.1.1.2 Lunar Location/Brightness
 - 6.3.1.1.3 Ice Location
 - 6.3.2 Requirements
 - 6.3.2.1 System Effectiveness
 - 6.3.2.1.1 Basic Definitions
 - 6.3.2.1.2 Downlink Availability

6. (Continued)

6.3.2.1.3 Crosslink Availability

6.3.2.1.4 Penalty

6.3.2.1.5 Sample Calculation

6.3.2.2 Life Cycle Cost

6.3.3 System Design Considerations

6.3.3.1 Orbits

6.3.3.2 Dynamic Efforts

6.3.3.3 Line-of-Sight

6.3.3.4 RF Link Analysis

6.3.3.5 Area Allocations

6.3.3.6 Remote Sensor Performance

6.3.3.6.1 Submarine Remote Sensors

6.3.3.6.2 Satellite Remote Sensors

6.4 Model Implementation

6.5 Discussion of Analysis

6.5.1 Environmental Models

6.5.2 System Design Analysis

6.6 Parameter Value Uncertainties

6.6.1 Environment

6.1 FULL OSCAR SYSTEM MODEL -- PHILOSOPHY AND FLOW CHARTS

This section explains the basic approach used in developing the architecture for the Full OSCAR System Model (FOSM), and presents a flow chart showing the overall interrelationship of the analysis discussed in Section 6.3 and its required inputs. (These inputs are discussed in more detail in Section 6.2.)

6.1.1 Philosophy of Approach -- Full OSCAR System Model (FOSM)

This model, when fully implemented and verified, will be a model of the complete OSCAR system. At this time, only the overall architecture of the FOSM has been developed. In developing this architecture we have used the following approach:

- a. The SPDPM is fully available for use as a building block;
- b. The DCM is fully available for use as a building block;
- c. The baseline option in the DCM is the one most favorable for OSCAR implementation -- i.e., fully adaptive scan;
- d. The FOSM requires inputs in the categories of environment, requirements and system design.
- e. The environmental inputs include the time varying data bases of cloud parameters, air-water interface parameters, and water parameters.
- f. The requirements inputs include system effectiveness parameters.
- g. The system design parameters include the details of all aspects of the system, from ground station through satellite orbits through submarine terminals.
- h. The system performance over a given set of time intervals is calculated for a given system design using the sub-models included herein. If suitable system performance is not achieved, the system design is modified and the system performance calculated again. If suitable system performance is achieved over a given set of time intervals, then the results are combined with those over other time intervals, so that the system performance over the system lifetime is estimated. If this lifetime performance is not suitable, the system design is iterated, and the process repeated until the system performance matches the requirements.

6.1.1 (Continued)

- i. The downlink availability is the driver of total system effectiveness. At this stage of the overall OSCAR program, the SPDPM is composed of unverified propagation models, the DCM inputs include uncertain parameters, and the technology to be used in the OSCAR system is in the R&D stage. Therefore, the downlink availability is calculated to the limits of our present day knowledge, and reasonable requirements are imposed on the remaining contributors to system effectiveness so that the system specification is met.

Implementation of this approach is discussed in Section 6.4, and exemplary results are presented in Section 3 of Volume IV of this final report.

6.1.2 Model Flow Chart -- Full OSCAR System Model

A top level schematic of the Full OSCAR System Model (FOSM) is shown in Figure 6-1. The input parameters are designated as environment, requirements and system design. All three inputs are used to calculate the downlink performance over many time intervals, which requires a multiple application of the DCM. The environment and system design parameters are used to estimate uplink/crosslink availability, and the system design inputs are then used to calculate equipment availability.* All availabilities are then used to calculate system effectiveness over the same time intervals, and, if no system design iteration is necessary, then performance over the system lifetime is calculated.

*But from (i) above, at present the uplink and equipment availability are not calculated from first principles, but are assigned from the downlink result.

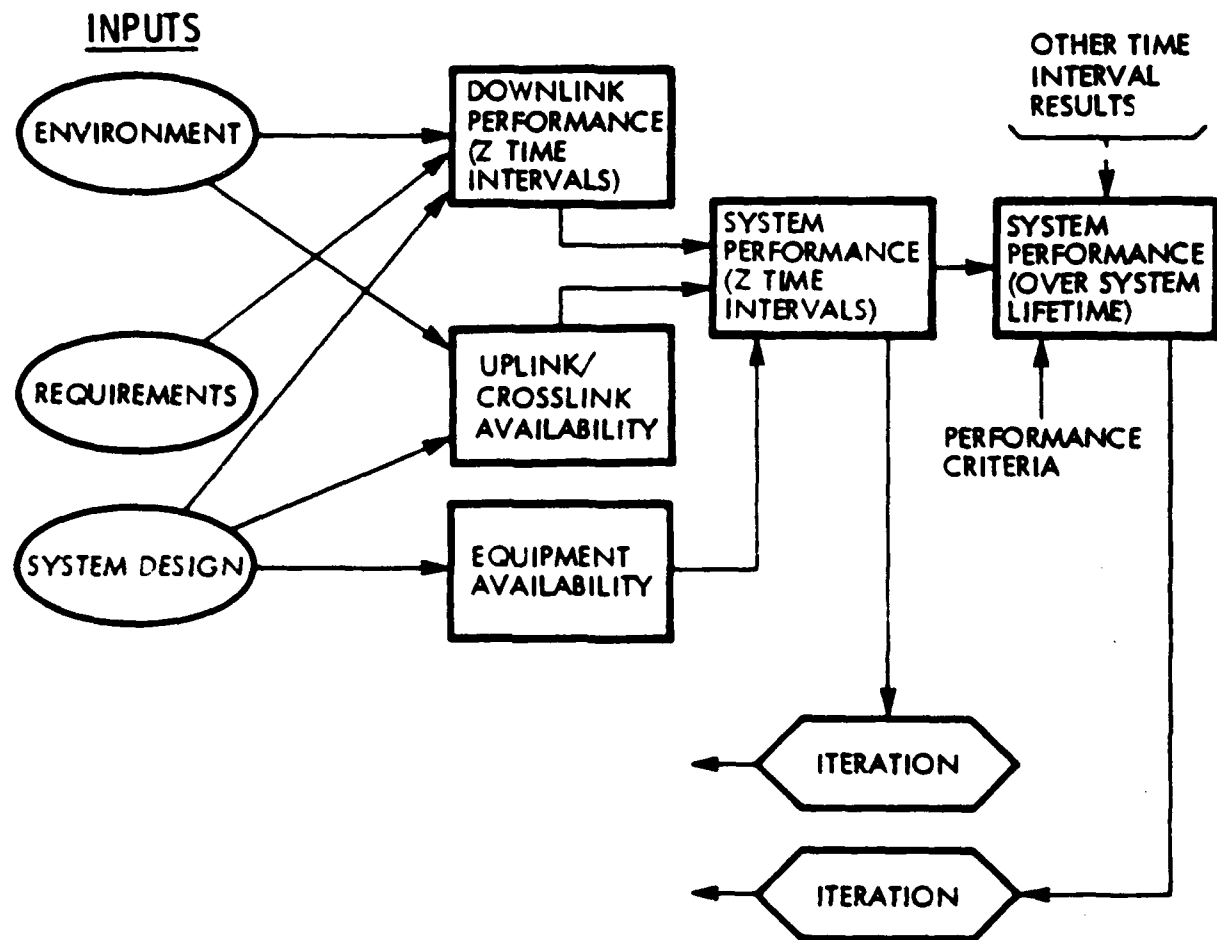


Figure 6-1. Complete Model-Flow Chart

6.2 INPUT INFORMATION

The inputs to the FOSM are divided into Environment, Requirements and System Design. This section discusses each of these three kinds of inputs.

6.2.1 Environment

The Environmental inputs to the FOSM are composed of fixed data bases, data bases with predictable variations and data bases with unpredictable variations. Each type has extensive inputs for the Full OSCAR System Model.

6.2.1.1 Fixed Data Bases

The fixed data bases include the operational area coverage, the astronomical distances (since we ignore monthly and seasonal changes in R_{SU} and R_{MU}), the choice of Environmental Resolution Elements, the Skylight/Starlight strength, and ocean depth within the coverage area. Some of these data bases were previously used in the SPDPM. Other and new environmental parameters include:

<u>SYMBOL</u>	<u>DESCRIPTION</u>	<u>UNITS</u>
α_i, β_j	Mean latitude and longitude of all the ERE's within the coverage area.	degrees
$D_{oc\ ij}$	Mean ocean depth of ij^{th} ERE. This enters in when $D_{oc\ ij} > D$.	meters

6.2.1.2 Data Bases with Predictable Variations

The data bases with predictable variations include the solar latitude and longitude, the lunar latitude, longitude and phase, and the locations of the ice. Some of these data bases were previously used in the SPDPM and DCM, including L_s , L_m , α_{SU} , β_{SU} , α_{MU} , and β_{MU} .

Other and new environmental parameters include:

<u>SYMBOL</u>	<u>DESCRIPTION</u>	<u>UNITS</u>
ϕ_{PM}	Phase of the moon, which determines its relative strength.	degrees
t	Time of day at Greenwich (0 degrees longitude)	hours

6.2.1.2 (Continued)

<u>SYMBOL</u>	<u>DESCRIPTION</u>	<u>UNITS</u>
	TIME AFTER WINTER SOLSTICE	days
t_{mo}	Time after full moon	days
t_{rm}	Time after sunset	hours
θ_0	Lunar latitude at sunset of a given day	degrees
IC_{ij}	Fraction of the ij^{th} resolution element which is covered by ice.	--

6.2.1.3 Data Bases with Unpredictable Variations

The data bases with unpredictable variations include the cloud conditions, the air-water interface conditions, the water conditions and the strength of the bioluminescence. Parts of these data bases have been used in the SPDPH and DCM, including: T , σ_c , $\langle \cos \theta \rangle$, ω_0 , θ and H for the clouds for each ERE; n and V for the air-water interface for each ERE; n , k_i , D_i , θ_{S1} , and S for the water for each ERE; and L_{BL} for the bioluminescence for each ERE.

Of these thirteen parameters, the most important ones with unpredictable temporal and spatial variations are T and σ_c for the clouds, V for the air-water interface, k_i and D_i for the water, and L_{BL} itself for the bioluminescence.

New inputs include:

<u>SYMBOL</u>	<u>DESCRIPTION</u>	<u>UNITS</u>
$MTBF_c$	Mean time between environmental conditions which are sufficient to cause an outage.	hours
$MTTR_c$	Mean time for outage-causing conditions to clear.	hours

6.2.2 Requirements

The Full OSCAR System Model uses the complete OSCAR requirement set as its requirements inputs. Some of these have previously been used in the SPDPM and DCM, including T_A , M_{LO} , N_M , N_{SPI} , N_{J1} , g and D . The rest of the requirements are:

- Full operational area coverage, specified in terms of α_i , β_j , for the ERE's.
- No submarine motion constraint (speed or direction);
- System Effectiveness, specified in terms of a total system availability $E_{ff}(\text{syst})$. Also important are T_{AV} , the time over which the availabilities are averaged in order to obtain $E_{ff}(\text{SYST})$, and P_{EN} , the penalty time for an outage of any portion of the link.

6.2.3 System Design Inputs

The required system design inputs include Ground Station, Satellite, and Submarine Terminal information.

6.2.3.1 Ground Station

The microwave ground stations were not considered at all in the SPDPM nor the DCM because those models only involve the downlink. Therefore, all the inputs are new, and consist of:

<u>SYMBOL</u>	<u>DESCRIPTION</u>	<u>UNITS</u>
B_U	Number of bits to be conveyed on the uplink, per single time interval	bits
B_C	Number of bits to be conveyed on the crosslink, per single time interval	bits
B_B	Number of bits to be conveyed on the backlink, per single time interval	bits
t_U	Time allowed for uplink delivery of bits	seconds
t_C	Time allowed for crosslink delivery of bits	seconds
t_B	Time allowed for backlink delivery of bits	seconds
λ_{RF}	Wavelength corresponding to center RF frequency	meters
P_S	Satellite transmitter power	watts
P_G	Ground station transmitter power	watts

6.2.3.1 (Continued)

<u>SYMBOL</u>	<u>DESCRIPTION</u>	<u>UNITS</u>
P_{JG}	Effective jammer radiated power	watts
η_s	Satellite antenna efficiency	--
η_G	Ground station antenna efficiency	--
λ_J	Latitude of jammer	degrees
λ_J	Longitude of Jammer	degrees
λ_{GS}	Latitude of ground station	degrees
λ_{GS}	Longitude of ground station	degrees
T_{SUN}	Noise temperature of the sun	$^{\circ}$ Kelvin
T_{EARTH}	Noise temperature of the earth	$^{\circ}$ Kelvin
$T_{RECEIVER}$	Noise temperature of the receiver	$^{\circ}$ Kelvin
T_{RAIN}	Noise temperature of the rain	$^{\circ}$ Kelvin
W	Extent of Spread Spectrum	Hz
$\left(\frac{E_{RF}}{N_0} \right)_c$	Critical $\left(\frac{\text{Energy per bit}}{\text{Noise Power per Hertz}} \right)$	$\frac{\text{cycles}}{\text{bit}}$
n_{RF}	Number of ground sites per satellite	--
D_s	Satellite antenna diameter	meters
D_G	Ground Station antenna diameter	meters
R_{JG}	Distance from jammer to Ground Station	meters
A_{UL}	Uplink availability	--
$MTBF$	Mean time between failure	hours
$MTTR$	Mean time to repair	hours

6.2.3.2 Satellites

Some inputs for the satellites were previously used in the SPDPH and the DCM, but primarily for a single time interval. The invariant satellite inputs are R_{SU} , R_{MU} , t_{S1} , t_w , PRF, m, E_p , F_L , R_e , P_L , H_O , t_f , L , q , γ_T , ϵ , MARG, $\Delta\lambda$, θ_{TS} , θ_{TDR} and choice of the scanning approach.

Additional, and new inputs are:

<u>SYMBOL</u>	<u>DESCRIPTION</u>	<u>UNITS</u>
P_{TOT}^i	Total prime power capability of the satellite	watts
T_{ORB}	Period of the orbits	hours
e_e	Eccentricity of the (elliptical) orbit	--
t_p	Time when perigee of the orbit was traversed	hours
ω	Argument of perigee	degrees
i	Inclination angle	degrees
α	Right ascension of the ascending node	degrees
ω_{OR}	Rotation rate of the earth	degrees/second (radians/second)
n	Number of satellites in single ground track	--
ν	Optical frequency	Hz
λ	Optical wavelength	meters
ϕ_{GS}	Latitude of Ground Station	degrees
λ_{GS}	Longitude of Ground Station	degrees
ϕ_S	Latitude of jammer	degrees
λ_S	Longitude of jammer	degrees
Revisits	Number of times a given spot is revisited	--
MTBF	Mean time between failures	hours
MTTR	Mean time to repair (or replace)	hours

6.2.3.3 Submarine Terminals

Most of the system design inputs for the submarine terminal have already been listed in the SPDPM and DCM sections, including θ_R , D , γ_R , d , B_{OPT} , (kT) , F_a , G , $(ne/h\nu)$, R_L , I_d , F , G_{EL} , G_{AZ} , t_{SL} , demodulation approach, and post-detection processing for time-of-peak demodulation.

Other and new inputs are:

<u>SYMBOL</u>	<u>DESCRIPTION</u>	<u>UNITS</u>
$MTBF_{SUB}$	Mean Time Between Failure	hours
$MTTR_{SUB}$	Mean Time to Repair	hours

6.3 ENVIRONMENT, REQUIREMENTS AND SYSTEM DESIGN CONSIDERATIONS

This section discusses the analysis to be used in the Full Oscar System Model architecture, except for those previously developed in Sections 3 and 4 (the SPDPH), and Section 5 (the DCM).

Section 6.3.1 considers models for the predictable environmental data bases, including sun, moon and ice location.

Section 6.3.2 discusses models for system effectiveness and life cycle cost.

Section 6.3.3 describes the system design analyses relating to the orbits, dynamic effects, line-of-sight, RF link analysis, area allocations, and remote sensor performance for both the submarine and the satellite.

6.3.1 Environment

The sub-models for the data bases only correspond to data bases with predictable spatial and temporal variations. (The fixed data bases are numbers input to other models, while the unpredictable data bases are not suitable for modeling due to their unpredictability.*)

6.3.1.1 Solar Location

The solar contribution to the optical background is characterized by:

$\theta_{S/2}$: The half-angle subtended by the sun at the earth,

L_S : Effective exo-atmospheric radiance of the sun;

R_{SU} : Distance from the sun to the receiver;

λ_{SU} : Solar latitude;

β_{SU} : Solar longitude.

To the accuracies required by the SPDPM, DCM and FOSM, the first three parameters are taken as invariable, and equal to:

$$\theta_{SU} = 4.65 (10^{-3}) \text{ radians}$$

$$L_S = 635.62 \text{ watts}/((m^2 (\text{srad}) \mu m))$$

$$R_{SU} = 1.497 (10^{11}) \text{ meters.}$$

The solar latitude and longitude are key to estimates of the solar zenith angle for a given environmental resolution element, as shown in equation (5-6) of Section 5.3.1 of this report. However, they do not have to be modelled with extreme accuracy since the P_{SU} and NEP_B are fairly insensitive to changes in solar zenith angle of $\pm 2.5^\circ$.

We therefore consider simple models, and separate the latitude and longitude.

*Future work may change the categorization of some of these unpredictable data bases to predictable, and hence model-suitable, ones.

6.3.1.1 (Continued)

For the longitude (degrees east of Greenwich), the sun is modelled as going around the earth once in 24-hours (to our accuracy), so we take

$$\beta_{SU} = 360 \left[1 - \frac{t}{24} \right] \quad (6-1)$$

for t = time, measured in hours after high noon at 0° longitude (Greenwich).

For the latitude, the extreme and mean are well known, so that

- $\alpha_{SU} = 0^\circ$, vernal equinox
- $\alpha_{SU} = 23.5^\circ$, summer solstice
- $\alpha_{SU} = 0^\circ$, autumnal equinox
- $\alpha_{SU} = -23.5^\circ$, winter solstice.

Considering the accuracy required (and to minimize computational time), we use Table 6-1 as the solar latitude model.

Table 6-1. Solar Latitude Model

DAYS AFTER WINTER SOLSTICE	α_{SU} (DEGREES)
0	-23.5
30	-21
61	-12
91 (Equinox)	0
121	+12
152	+21
192 (Summer Solstice)	+23.5
222	+21
253	+12
283 (Equinox)	0
314	-12
335	-21

Values between those shown are linearly interpolated.

6.3.1.2 Lunar Location and Phase

The lunar contribution to the optical background is characterized by:

- $\theta_{m/2}$: The half-angle subtended by the moon at the earth;
- L_m : Effective exo-atmospheric spectral radiance of the moon;
- R_{mu} : Distance from the moon to the receiver;
- α_{mu} : Lunar latitude;
- β_{mu} : Lunar longitude.

To the accuracies required by the SPDPM, DCM and FOSM, the first and third parameters are taken as invariable, and equal to:

$$\begin{aligned}\theta_{m/2} &= 4.65 (10^{-3}) \text{ radians;} \\ R_{mu} &= 3.83 (10^8) \text{ meters.}\end{aligned}$$

The value of L_m used in the SPDPM was $1.37 (10^{-3}) \text{ watts/((meters)}^2 \text{ (srad) (meter))}$, corresponding to a full moon in the blue-green spectral region. For any but a full moon the magnitude of L_m is reduced. The magnitude of L_m depends on the phase angle, α_{pm} , as defined in Figure 6-2.

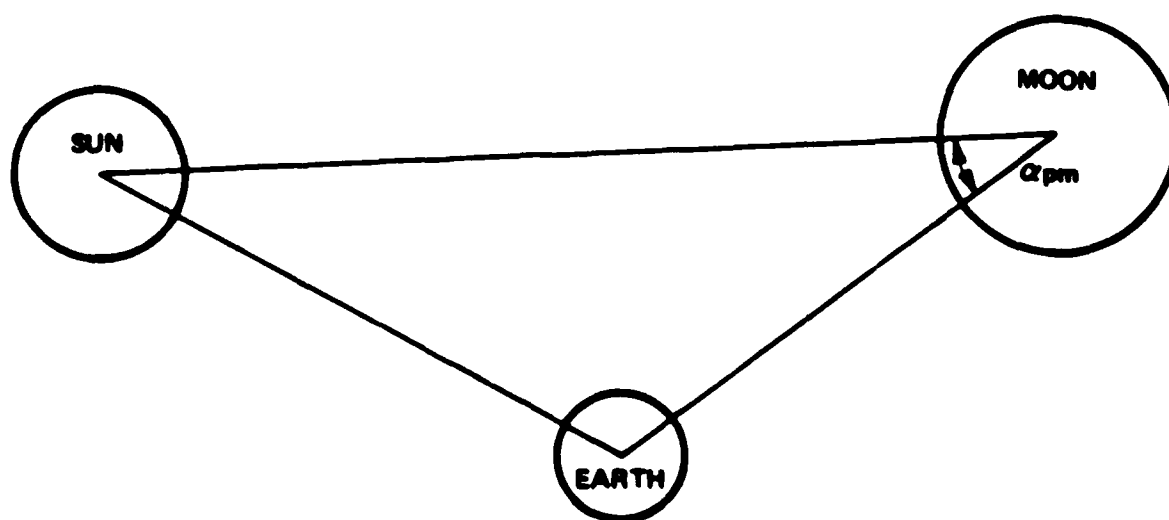


Figure 6-2. Definition of Lunar Phase Angle, α_{pm}

6.3.1.2 (Continued)

To the accuracy required here, we take α_{pm} to linearly go through 360° in 27.5 days, so that

$$\alpha_{pm} = 360 \left(\frac{t_{mo}}{27.5} \right) \quad (6-2)$$

for t_{mo} measured in days, and corresponding to time after full moon.

No analytic model* exists to relate L_m to α_{pm} , so we use the empirically derived result in Table 6-2, and the equation:

$$L_m = 1.37 (10^{-3}) \bar{I}_m \quad (6-3)$$

Table 6-2. Lunar Brightness as a Function of Phase Angles

LUNAR BRIGHTNESS AS A FUNCTION OF PHASE ANGLE			
α_{pm} (DEGREES)	\bar{I}_m	α_{pm}	\bar{I}_m
0	1		
5	0.88	75	0.12
10	0.78	80	0.1
15	0.69	85	0.09
20	0.61	90	0.08
25	0.55	95	0.07
30	0.48	100	0.06
35	0.43	105	0.05
40	0.37	110	0.045
45	0.33	115	0.04
50	0.28	120	0.035
55	0.24	130	0.025
60	0.2	140	0.01
65	0.17	150	0
70	0.14		

*2. Kopal, "An Introduction to the Study of the Moon," Gordon and Breach, (New York, 1966) Chapter 17.

6.3.1.2 (Continued)

The lunar latitude and longitude are key to estimates of the lunar zenith angle for a given environmental resolution element, as shown in equation (5-7) of Section 5.3.1 of this report. However, they do not have to be modelled with extreme accuracy since the P_{mu} and NEP_B are fairly insensitive to changes of lunar zenith angles.

We therefore consider simple models, and separate the latitude and longitude.

For the longitude, again in degrees east of Greenwich, the earth rotates 360° while the moon is moving approximately $1/28 (360) = 12.9^\circ$ in its orbit around the earth. Over one night, the inaccuracy in completely neglecting lunar motion is taken as negligible and for each night we take

$$\beta_{mu} = \beta_0 \left(1 - \frac{t_{nm}}{24} \right) \quad (6-4)$$

for β_0 = initial longitude of the moon at sunset,* and

t_{nm} = time after sunset, measured in hours.

For the latitude, we use the fact that the plane of the moon-earth orbit is inclined at approximately 5.1° to the ecliptic, the plane of the earth-sun orbit. Therefore, we take

$$\gamma_{mu} = \gamma_{su} + 5.1^\circ \quad (6-5)$$

as our approximate model for the lunar latitude.

6.3.1.3 Ice Locations

A few of the environmental resolution elements are far enough North that a fraction of their area is covered by ice during the winter and spring months. We model this as completely blanking the OSCAR communication downlink for that fraction of the area. The key parameter is:

* β_0 should be provided by a separate input, so that the approximation errors in equation (6-4) are not compounded from night to night.

6.3.1.3 (Continued)

IC_{ij} : Fraction of ij th resolution element covered by ice. IC_{ij} will be provided in a look-up table in Volume IV of this final report. We do not present it here so that the unclassified nature of this volume may be sustained.

6.3.2 System Effectiveness and Life Cycle Cost Models

This section discusses models for the system effectiveness in terms of link availability, and the life cycle cost model.

6.3.2.1 System Effectiveness

The full OSCAR system may be depicted as a communication tree where the message originates at the ground stations (relatively few in number), is transmitted through the uplink to the satellite, and then through downlinks to the submarines.* Such a tree is represented in Figure 6-3, with the system elements shown.

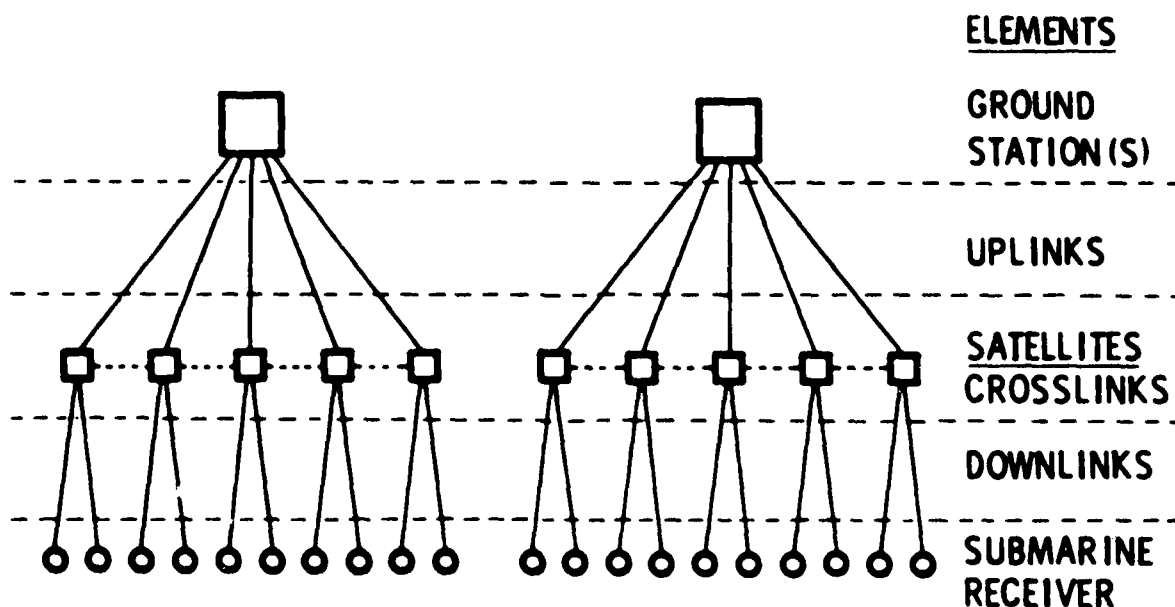


Figure 6-3. System Effectiveness Communication Tree

*Crosslinks between satellites, if used, would not destroy this analogy.

6.3.2.1.1 Basic Definition

Using the communication tree, it is seen that an end-to-end link can be traced from each submarine back to a ground station. Therefore, the number of complete links will equal the number of submarines, and the r^{th} link will have an availability:

$$A_L(r) = A_{GS}^{(r)} A_{UL}^{(r)} A_{SAT}^{(r)} A_{CL}^{(r)} A_{DL}^{(r)} A_{SB}^{(r)}. \quad (6-6)$$

The availabilities used are for the appropriate element in the link e.g., that of the ground station and that of the satellite which services that particular submarine, and are defined as:

A_{GS} = ground station availability,

A_{UL} = Uplink availability,

A_{SAT} = satellite availability,

A_{CL} = crosslink availability, including relay equipment on satellites,

A_{DL} = downlink availability,

A_{SB} = submarine receiver availability.

System effectiveness is defined as the average end-to-end link availability:

$$E_{ff}(\text{syst}) \triangleq \bar{A}_L. \quad (6-7)$$

This can be written in the expanded form.

$$E_{ff}(\text{syst}) = \frac{1}{N_L} \sum_{r=1}^{N_L} A_{GS}^{(r)} A_{UL}^{(r)} A_{SAT}^{(r)} A_{CL}^{(r)} A_{DL}^{(r)} A_{SB}^{(r)} \quad (6-8)$$

Because of the construction of the tree, this equation can be expanded in the following form:

6.3.2.1.1 (Continued)

$$E_{ff}(\text{syst}) = \frac{1}{N_L} \left\{ A_{GS}(1) \left[A_{UL}(1) A_{SAT}(1) A_{CL}(1) (A_{DL}(1) A_{SB}(1) + A_{DL}(2) A_{SB}(2) + \dots) \right. \right. \\ + A_{UL}(2) A_{SAT}(2) A_{CL}(2) (A_{DL}(1) A_{SB}(1) + A_{DL}(1+1) A_{SB}(1+1) + \dots) \\ + A_{UL}(j) A_{SAT}(j) A_{CL}(j) (A_{DL}(k) A_{SB}(k) + A_{DL}(k+1) A_{SB}(k+1) + \dots) \left. \right] \\ + A_{GS}(2) \left[A_{UL}(m) A_{SAT}(m) A_{CL}(m) (A_{DL}(n) A_{SB}(n) + A_{DL}(n+1) A_{SB}(n+1) + \dots) \right. \\ \left. \left. + A_{UL}(m+1) A_{SAT}(m+1) A_{CL}(m+1) (A_{DL}(p) A_{SB}(p) + \dots) \right] \right\} \quad (6-9)$$

If the availability of any individual system element is the same as any other element of the same type, then the expression for system effectiveness reverts to the much simpler form:

$$E_{ff}(\text{syst}) = \bar{A}_{GS} \bar{A}_{UL} \bar{A}_{SAT} \bar{A}_{CL} \bar{A}_{DL} \bar{A}_{SB} \quad (6-10)$$

Moreover, if the availability of like elements is identical, then the mean link availability is equivalent to any individual element availability.

6.3.2.1.2 Downlink Availability

The "downlink" availability requires special mention. Although at any time the number of downlinks equals the number of boats, the specific location of the boats is not known, even to the appropriate environmental resolution element. Therefore, the downlink availability is averaged over all possible boat locations, which in particular will be the satellite area of responsibility, but in sum would be the entire FBM operational area.

Also since the downlink is tied intimately to weather conditions, water conditions, and signal and background conditions, it is reasonable to average over a time interval sufficient to include a range of these conditions. A one month interval would allow for seasonal variations and permit systems' strategies which optimize for seasonal variations. However, in order to meet the system

6.3.2.1.2 (Continued)

effectiveness specification, the availability should be averaged over at least a year (or multiple seasonal periods, including the appropriate system strategies).

6.3.2.1.3 Crosslink Availability

The crosslink availabilities are most likely to be those elements which do not have identical values. This is seen from the fact that some end-to-end links may include crosslinks while other end-to-end links may not require them. Therefore a weighted mean is used in the equation for \bar{A}_{CL} :

$$\bar{A}_{CL} = \frac{N_{CL} A_{CL} + (N_L - N_{CL})(1)}{N_L} \quad (6-11)$$

where N_{CL} is the number of crosslinks used in the entire system, and the crosslink availability is taken as unity for those links not using crosslinks.

In general, the number of end-to-end links using crosslinks may change during a cycle of the satellite orbits. Therefore, N_{CL} may be a dynamic number, and the average value over a complete cycle will be used.

6.3.2.1.4 Penalty

The specification requires that a penalty be imposed for each outage. This penalty is imposed on the average element availabilities in accordance with the following rule:

$$A_{XX} = \frac{1}{1+X} \quad (6-12)$$

where X is the larger of either

$$(MTTR/MTBF)_{XX}$$

or

$$\frac{T_{av} P_{en}}{(MTBF)_{XX}^2}$$

6.3.2.1.4 (Continued)

where T_{av} is the time over which the system effectiveness is averaged, P_{en} is the penalty, MTTR is the mean time to repair, and MTBF is the mean time between failures.

In the case of the downlink, the nomenclature "mean time between failures" and "mean time to repair" is meaningless. The same statistical concepts are retained by assigning the following definitions for links that do not have equipment:

$MTBF_C \equiv$ mean time between conditions which are sufficient to cause outage.

$MTTR_C \equiv$ mean time for these conditions to clear.

For the uplink and downlink, this information must be provided by the environmental data bases, either implicitly or explicitly.

6.3.2.1.5 Sample Calculation

A sample calculation of availability has been performed using the values in Table 6-3, and choosing T_{av} = 8700 hours (1 year), P_{en} = 1 hour.

TABLE 6-3
 Inputs for Sample System Effectiveness Calculations

	GS	UL	SAT	DL	SB
MTBF (hours)	5000	10,000	50,000	400	5000
MTTR (hours)	1	.5	100	12	1

6.3.2.1.5 (Continued)

The mean element availabilities are:

$$\begin{aligned}\bar{A}_{GS} &= 0.9965 \\ \bar{A}_{UL} &= 0.99991 \\ \bar{A}_{SAT} &= 0.998 \\ \bar{A}_{DL} &= 0.948 \\ \bar{A}_{SB} &= 0.9965\end{aligned}$$

The system effectiveness is then 0.945.

In this example the downlink availability dominates the system effectiveness, as would seem reasonable.

6.3.2.2 Life Cycle Cost Model

The life cycle cost models to be used in the FOSM are

NAVWESA, WEAPON SYSTEM LCC, FLEX 9B and NAVWESA, EQUIPMENT LCC, FLEX 4B
--

They have been used by GTE-Sylvania on other NAVY programs.

6.3.3 System Design Analyses

The new system design analyses includes Orbits, Dynamic Effects, Line-of-Sight, RF link analysis, Area Allocation and Remote Sensor Performance.

6.3.3.1 Orbits

The OSCAR satellites are assumed to travel in circular or elliptical orbits around a spherical earth. Any perturbations to these orbits caused by the sun, the moon, atmospheric drag, or the asphericity of the Earth's gravitation field are to be corrected by periodic thrusts from station-keeping rockets. The orientations of the elliptical orbits remain fixed in inertial space (Figure 6-4), and are referenced to the Earth's equatorial plane (Figure 6-5).

6.3.3.1 (Continued)

Time is referenced to the sidereal day, which represents one rotation of the Earth relative to inertial space, rather than to the sun. This differs from a solar day by a factor of 364/365, since the Earth rotates one more time during this year than the number of days in the year. The "hour" used for time is defined as one twentieth-fourth of a sidereal day, and the time origin corresponds to the earth's prime meridian pointing in the direction of the vernal equinox. The satellite positions are determined by six orbital parameters (See Figure 6-5 and 6-6):

- T_{orb} , the period of the orbit
- e , the eccentricity of the ellipse.
- t_p , time when perigee of the orbit was traversed,
- ω , argument of perigee (angle)
- i , inclination angle
- Ω , right ascension of the ascending node (angle).

For any given time, these are used to obtain the position (R_s, α_s, β_s) and velocity ($\dot{R}_s, \dot{\alpha}_s, \dot{\beta}_s$) of the satellite in the spherical fixed earth coordinate system. (This is the system used in the DCM.)

The position and velocity of a satellite moving in a spherically symmetric gravitational field were derived by Kepler:

$$E = \frac{2(t - t_p) + r_e \sin E}{T_{orb}} \quad (6-13a)$$

$$a = \left(5080 \frac{\text{km}}{\text{hr}^{2/3}} \right) T_{orb}^{2/3} \quad (6-13b)$$

The diagram illustrates the geometry of a satellite orbit around Earth. The Earth is represented by a sphere with a vertical axis passing through the North Pole (NP) and South Pole (SP). The Equator is shown as a horizontal line. A satellite is shown in orbit, with its position relative to the Earth's center and the observer's horizon indicated. Key points and lines include:

- NP**: North Pole
- SP**: South Pole
- EQUATOR**: The horizontal line representing the Earth's equator.
- SATELLITE**: The satellite in orbit.
- ORBIT**: The path of the satellite around Earth.
- AP**: Apogee (the point in the orbit furthest from Earth).
- PERIGEE**: The point in the orbit closest to Earth.
- P₀**: A point on the orbit, likely the perigee.
- Q**: A point on the orbit.
- ASCENDING NODE**: The point where the orbit crosses the equator from south to north.
- DECLINATION OF VECTORS EQUATOR**: A label indicating the angle between the vector and the equator.
- S**: Points on the orbit, likely representing the satellite's position at different times.
- P₀**: A point on the orbit, likely the perigee.
- Q**: A point on the orbit.
- ASCENDING NODE**: The point where the orbit crosses the equator from south to north.
- DECLINATION OF VECTORS EQUATOR**: A label indicating the angle between the vector and the equator.

6-26

6.3.3.1 (Continued)

To translate to equatorial plane coordinates requires the following sequence (see Figure 6-5):

- A rotation of ω about the 1Z axis.
- A rotation of i about the 2X axis.
- A rotation of $\Omega + \Omega_{\text{or}} t$ about the 3Z axis.

These operations are accomplished by successive multiplication of both the position and velocity vectors by the standard rotational matrices of linear algebra:

$$\begin{bmatrix} 2x & 2\dot{x} \\ 2y & 2\dot{y} \\ 2z & 2\dot{z} \end{bmatrix} = \begin{bmatrix} R_3(\Omega + \Omega_{\text{or}} t) \\ R_1(i) \\ R_3(\omega) \end{bmatrix} \begin{bmatrix} 1x_W & 1\dot{x}_W \\ 1y_W & 1\dot{y}_W \\ 1o_W & 1\dot{o}_W \end{bmatrix} \quad (6-14)$$

$$\text{where } R_1(\alpha) = \begin{bmatrix} 1 & 0 & 0 \\ 0 & \cos \alpha & \sin \alpha \\ 0 & -\sin \alpha & \cos \alpha \end{bmatrix} \quad (6-15a)$$

is a rotation about the X axis (or axis 1) through an angle of α .

$$R_2(\alpha) = \begin{bmatrix} \cos \alpha & 0 & -\sin \alpha \\ 0 & 1 & 0 \\ \sin \alpha & 0 & \cos \alpha \end{bmatrix} \quad (6-15b)$$

is a rotation about the Y axis (or axis 2), and

$$R_3(\alpha) = \begin{bmatrix} \cos \alpha & \sin \alpha & 0 \\ -\sin \alpha & \cos \alpha & 0 \\ 0 & 0 & 1 \end{bmatrix} \quad (6-15c)$$

is a rotation about the Z axis (or axis 3).

6.3.3.1 (Continued)

The satellite state vector is now referenced to the rotating geocentric fixed earth rectangular coordinate system. The following transformation is used to convert between this system and the spherical coordinate system of longitude and latitude:

$$R_s = \sqrt{3_x^2 + 3_y^2 + 3_z^2} - R_e \quad (6-20a)$$

$$\alpha_s = \tan^{-1} \frac{3_z}{\sqrt{3_x^2 + 3_y^2}} \quad (6-20b)$$

$$\beta_s = \tan^{-1} \frac{3_y}{3_x} \quad (6-20c)$$

$$\dot{R}_s = \frac{3_x \dot{3}_x + 3_y \dot{3}_y + 3_z \dot{3}_z}{\sqrt{3_x^2 + 3_y^2 + 3_z^2}} \quad (6-20d)$$

$$\dot{\alpha}_s = \frac{3_z(3_x \dot{3}_x + 3_y \dot{3}_y) - 3_z(3_x \dot{3}_x + 3_y \dot{3}_y)}{\sqrt{3_x^2 + 3_y^2} (3_x^2 + 3_y^2 + 3_z^2)} \quad (6-20e)$$

$$\dot{\beta}_s = \frac{3_x \dot{3}_y - 3_y \dot{3}_x}{3_y^2 + 3_x^2} \quad (6-20b)$$

where R_s is the distance from the earth's center to the satellite, α_s is the longitude, and β_s is the latitude. Application of the foregoing transformation from the orbital plane for successive times traces out the ground track of the satellite.

If a stationary ground track is shared by several satellites, it is assumed that the optimal configuration has them equally spaced in time. This requires:

$$t_{pj} = t_{pj-1} - \frac{24}{n} \quad (6-21)$$

and
$$\alpha_j = \alpha_{j-1} + \frac{360}{n} \quad (6-21)$$

6.3.3.1 (Continued)

where n is the number of satellites, 2π is the orbital period, and t_{pj} and α_j are the time of perigee passage and the ascending node angle for the j^{th} satellite.

6.3.3.2 Dynamic Effects

The effects of satellite motion in the FOSM are summarized by the following parameters:

$\theta_s, \dot{\theta}_s$: zenith angle and rate at the earth's surface;

$\phi_{SA}, \dot{\phi}_{SA}$: azimuth angle and rate at the earth's surface;

θ^{SLEW} : angle between 2 satellites as viewed from the earth's surface;

R : range from a satellite to a point on the earth's surface;

θ^{SLEW} : angle between two points on the earth's surface as viewed from the satellite;

$\left(\frac{\Delta\nu}{\nu}\right)$: the relative Doppler frequency shift for a signal between the satellite and the earth's surface;

θ^{SLEW} : angle between a point on the earth's surface and a satellite as viewed from another satellite;

$\left(\frac{\Delta\nu}{\nu}\right)_s$: the relative Doppler frequency shift for signal between two satellites;

$\theta_s, \dot{\theta}_s$: zenith angle and rate for a point on the earth's surface as viewed from inertially oriented satellite-centered coordinate system with its Z axis parallel to the earth's axis and its X axis pointing in the direction of the vernal equinox (See Figure 6-8).

6.3.3.2 (Continued)

$\dot{\alpha}_{SA}, \dot{\beta}_{SA}$: azimuth angle and rate for a point on the earth's surface in the satellite's system (See Figure 6-8).

R_{SS} : distance between 2 satellites.

R_{JS} : distance from jammer to satellite.

These parameters are obtained by conversion of position and velocity from the geocentric fixed earth system to coordinate systems centered on either the satellites or the earth's surface (Figures 6-7 & 6-8). The positions and velocities constitute state vectors for the satellites, submarines, ground stations, jammers, sun, and moon. The satellite state vector in the rectangular fixed earth system, were derived in Section 6.3.3.1 as $(^3x_3, ^3y_3, ^3z_3, \dot{^3x_3}, \dot{^3y_3}, \dot{^3z_3})_3$.

The submarines, ground stations, and jammers are at the earth's surface and the submarines are assumed to have negligible speed compared to the satellites. Their state vectors in the spherical fixed earth system are therefore $(R_e, \alpha_{SUB}, \beta_{SUB}, 0, 0, 0)$ for the submarines, $(R_e, \alpha_{GS}, \beta_{GS}, 0, 0, 0)$ for the ground station, and $(R_e, \alpha_J, \beta_J, 0, 0, 0)$ for the jammer. The sun and moon coordinates in the spherical system are $(R_{SU}, \alpha_{SU}, \beta_{SU}, 0, 0, 0)$ and $(R_{MU}, \alpha_{MU}, \beta_{MU}, 0, 0, 0)$.

To determine $\dot{\alpha}_S, \dot{\beta}_S, \dot{\alpha}_{SA}, \dot{\beta}_{SA}, \dot{\alpha}_{SLEW}, \dot{\beta}_{SLEW}, \dot{R}$ and $\frac{\Delta v}{v}$ for a submarine or a ground station located at longitude α and latitude β , the satellite state vector is converted to a system centered at (α, β) , in which the Z axis is pointing away from the earth's center, the X axis is pointing South along the meridian, and the Y axis is pointing East (See Figure 6-7). To convert to this system from the rectangular fixed earth system of Section 6.3.3.1, the following operations are required.

- Rotation of position and velocity through an angle of β about axis 3 using matrix (6-15c) of Section 6.3.3.1.
- Rotation of position and velocity through an angle of $(\pi/2) - \alpha$ about axis 2 using matrix (6-15b) of Section 6.3.3.1.
- Translation from earth centered to topo-centered:

$$Z = Z - R_e$$

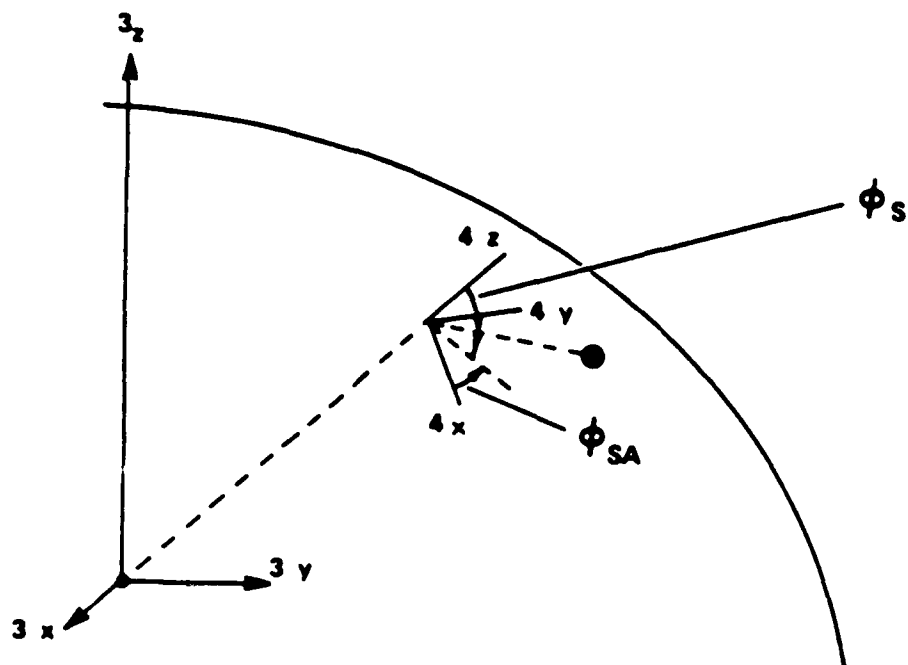


Figure 6-7. Ground Station and Submarine Coordinate System

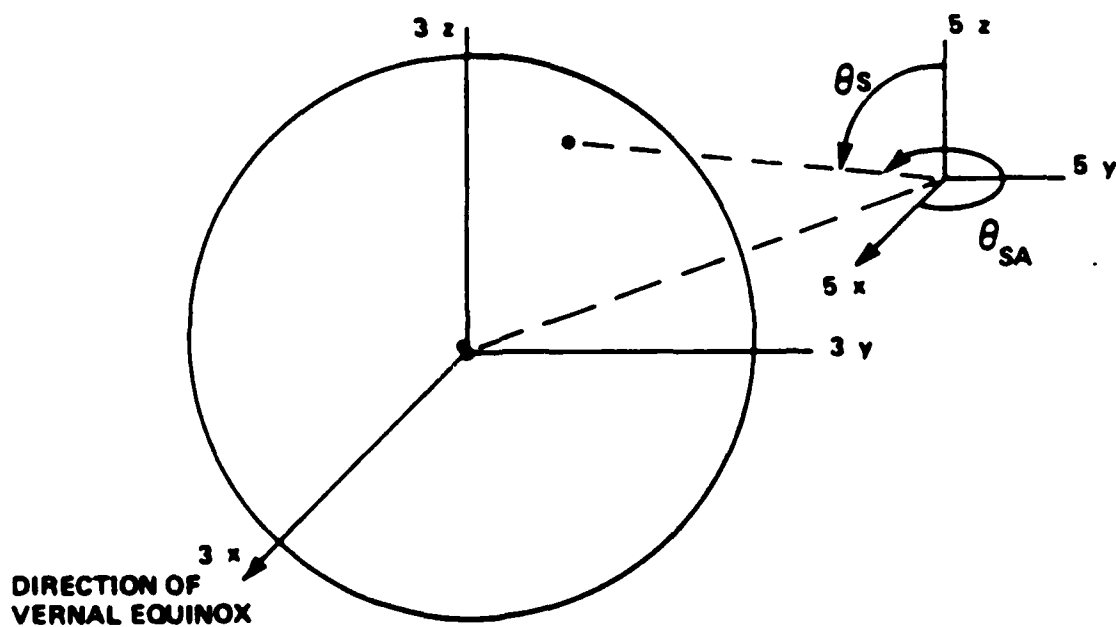


Figure 6-8. Satellite Coordinate System

6.3.3.2 (Continued)

The resulting transformation equations are:

$$\begin{aligned} 4X &= 3X \sin i \cos B + 3Y \sin i \sin B - 3Z \cos i \\ 4Y &= -3X \sin i + 3Y \cos i \end{aligned} \quad \begin{matrix} (6-23 \\ a,b,c) \end{matrix}$$

$$4Z = 3X \cos i \cos B + 3Y \cos i \sin B + 3Z \sin i - R_3$$

$$\begin{aligned} 4\dot{X} &= 3\dot{X} \sin i \cos B + 3\dot{Y} \sin i \sin B - 3\dot{Z} \cos i \\ 4\dot{Y} &= -3\dot{X} \sin i + 3\dot{Y} \cos i \end{aligned} \quad \begin{matrix} (6-24 \\ a,b,c) \end{matrix}$$

$$4\dot{Z} = 3\dot{X} \cos i \cos B + 3\dot{Y} \cos i \sin B + 3\dot{Z} \sin i$$

where $3R$ state vector is derived in Section 6.3.3.1.

The slew angle, ϕ_{SLEW} , at this latitude, i , and longitude, B , between two satellites is now calculated from the vector dot product of the satellite's positions:

$$\phi_{SLEW} = \cos^{-1} \left[\frac{4X_1 4X_2 + 4Y_1 4Y_2 + 4Z_1 4Z_2}{\sqrt{4X_1^2 + 4Y_1^2 + 4Z_1^2} \sqrt{4X_2^2 + 4Y_2^2 + 4Z_2^2}} \right] \quad (6-25)$$

The rectangular coordinates are converted to the spherical coordinate system shown in Figure (6-9) by using the following equations:

$$R = \sqrt{4X^2 + 4Y^2 + 4Z^2}, \quad \phi_S = \cot^{-1} \frac{4Z}{\sqrt{4X^2 + 4Y^2}}, \quad \phi_{SA} = \tan^{-1} \frac{4Y}{4X} \quad \begin{matrix} (6-26 \\ a,b,c) \end{matrix}$$

$$\begin{aligned} \dot{R} &= \frac{4\dot{X} 4X + 4\dot{Y} 4Y + 4\dot{Z} 4Z}{\sqrt{4X^2 + 4Y^2 + 4Z^2}} \\ \dot{\phi}_S &= \frac{(4\dot{X} 4\dot{X} + 4\dot{Y} 4\dot{Y}) 4Z - 4\dot{Z} (4\dot{X}^2 + 4\dot{Y}^2)}{\sqrt{4X^2 + 4Y^2} (4\dot{X}^2 + 4\dot{Y}^2 + 4\dot{Z}^2)} \end{aligned} \quad \begin{matrix} (6-27 \\ a,b,c) \end{matrix}$$

$$\phi_{SA} = \frac{4\dot{X} 4\dot{Y} - 4\dot{Y} 4\dot{X}}{4\dot{X}^2 + 4\dot{Y}^2}$$

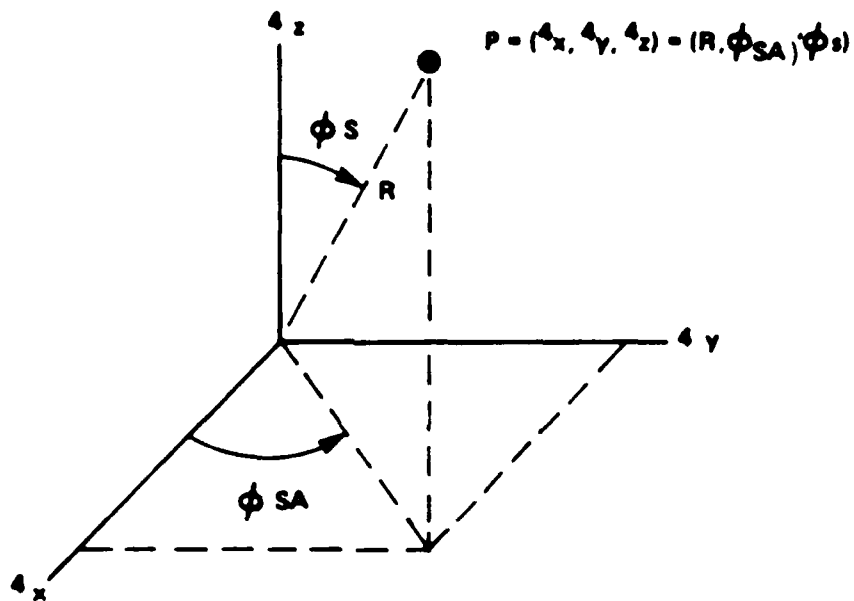


Figure 6-9. Rectangular and Spherical Coordinate Systems Centered on Earth's Surface.

6.3.3.2 (Continued)

The relative Doppler frequency, $(\Delta\nu/\nu)$, is calculated from \dot{R} , the rate of change of the range between the satellite and the point on the earth's surface:

$$\left(\frac{\Delta\nu}{\nu}\right) = \frac{\Delta\lambda}{\lambda} = \frac{\dot{R}}{C} \quad (6-28)$$

where $\Delta\nu$ and $\Delta\lambda$ are the frequency and wavelength shifts,
 ν and λ are the carrier frequency and wavelengths,
and C is the speed of light.

This effect limits the minimum useful bandwidth of nontunable filter and laser combinations to:

$$\Delta\lambda_{\min} = \frac{\lambda}{C} \left| (\dot{R})_{\max} - (\dot{R})_{\min} \right| \quad (6-29)$$

where \dot{R}_{\max} is the radial velocity leading to the highest Doppler shifted optical frequency,

and \dot{R}_{\min} is the radial velocity leading to the lowest Doppler shifted optical frequency,

and the algebraic sign of the velocities are preserved.

To determine \dot{S} , \dot{S}_A , \dot{S}_B , \dot{S}_C , \dot{S}_D , \dot{S}_E , \dot{S}_F , \dot{S}_G , \dot{S}_H , \dot{S}_I , \dot{S}_J , \dot{S}_K , \dot{S}_L , \dot{S}_M , \dot{S}_N , \dot{S}_O , \dot{S}_P , \dot{S}_Q , \dot{S}_R , \dot{S}_S , \dot{S}_T , \dot{S}_U , \dot{S}_V , \dot{S}_W , \dot{S}_X , \dot{S}_Y , \dot{S}_Z for the satellite, the state vectors of the ground sites, jammers and submarines are converted to a coordinate system centered on the satellite. The fixed earth state vectors $(R_e, \phi, \lambda, 0, 0, 0)$ in the latitude, longitude system are first converted to rectangular coordinates:

$$\left. \begin{aligned} x_{GS} &= R_e \cos \alpha_{GS} \cos \beta_{GS} \\ y_{GS} &= R_e \cos \alpha_{GS} \sin \beta_{GS} \end{aligned} \right\} \quad (6-30 \text{ a,b,c})$$

$$z_{GS} = R_e \sin \alpha_{GS}$$

$$\dot{x}_{GS} = \dot{y}_{GS} = \dot{z}_{GS} = 0 \quad (6-31 \text{ a,b,c})$$

$$\begin{aligned} {}^3x_J &= R_e \cos \alpha_J \cos \beta_J \\ {}^3y_J &= R_e \cos \alpha_J \sin \beta_J \\ {}^3z_J &= R_e \sin \alpha_J \end{aligned} \quad \left. \begin{array}{l} \\ \\ \end{array} \right\} \begin{array}{l} (6-32 \\ a,b,c) \end{array}$$

$$\dot{{}^3x}_J = \dot{{}^3y}_J = \dot{{}^3z}_J = 0 \quad \left. \begin{array}{l} \\ \end{array} \right\} \begin{array}{l} (6-33 \\ a,b,c) \end{array}$$

$$\begin{aligned} {}^3x_{SUB} &= R_e \cos \alpha_{SUB} \cos \beta_{SUB} \\ {}^3y_{SUB} &= R_e \cos \alpha_{SUB} \sin \beta_{SUB} \\ {}^3z_{SUB} &= R_e \sin \alpha_{SUB} \end{aligned} \quad \left. \begin{array}{l} \\ \\ \end{array} \right\} \begin{array}{l} (6-34 \\ a,b,c) \end{array}$$

$$\dot{{}^3x}_{SUB} = \dot{{}^3y}_{SUB} = \dot{{}^3z}_{SUB} = 0 \quad \left. \begin{array}{l} \\ \end{array} \right\} \begin{array}{l} (6-35 \\ a,b,c) \end{array}$$

The satellite state vector is then subtracted. The resulting vectors are in the system centered at the satellite and rotating with the earth. Since the solar cells must always point toward the sun, the satellite's orientation is assumed to remain (relatively) motionless in inertial space ($\frac{360}{365}$ degrees of rotation per day). Therefore the orientation of the basic satellite system is assumed to be inertial. To convert to this system the state vectors are rotated $-\omega_{or}t$ about axis 3 using matrix 6-15c of Section 6.3.3.1 and $\hat{\omega}_{or} \times \hat{r}$ is added to the velocity components, $\dot{\hat{r}}$, where ω_{or} is the rate of rotation of the earth. The transformation equations are:

6.3.3.2 (Continued)

$${}^5x_{GS} = ({}^3x_{GS} - {}^3x_S) \cos \omega_{or} t - ({}^3y_{GS} - {}^3y_S) \sin \omega_{or} t$$

$${}^5y_{GS} = ({}^3x_{GS} - {}^3x_S) \sin \omega_{or} t + ({}^3y_{GS} - {}^3y_S) \cos \omega_{or} t$$

$${}^5z_{GS} = {}^3z_{GS} - {}^3z_S$$

(6-36
a,b,c)

$$\dot{{}^5x}_{GS} = (\dot{{}^3x}_{GS} - \dot{{}^3x}_S) \cos \omega_{or} t - (\dot{{}^3y}_{GS} - \dot{{}^3y}_S) \sin \omega_{or} t$$

$$\dot{{}^5y}_{GS} = (\dot{{}^3x}_{GS} - \dot{{}^3x}_S) \sin \omega_{or} t + (\dot{{}^3y}_{GS} - \dot{{}^3y}_S) \cos \omega_{or} t$$

$$\dot{{}^5z}_{GS} = \dot{{}^3z}_{GS} - \dot{{}^3z}_S$$

(6-37
a,b,c)

$${}^5x_J = ({}^3x_J - {}^3x_S) \cos \omega_{or} t - ({}^3y_J - {}^3y_S) \sin \omega_{or} t$$

$${}^5y_J = ({}^3x_J - {}^3x_S) \sin \omega_{or} t + ({}^3y_J - {}^3y_S) \cos \omega_{or} t$$

$${}^5z_J = {}^3z_J - {}^3z_S$$

(6-38
a,b,c)

$$\dot{{}^5x}_J = (\dot{{}^3x}_J - \dot{{}^3x}_S) \cos \omega_{or} t - (\dot{{}^3y}_J - \dot{{}^3y}_S) \sin \omega_{or} t$$

$$\dot{{}^5y}_J = (\dot{{}^3x}_J - \dot{{}^3x}_S) \sin \omega_{or} t + (\dot{{}^3y}_J - \dot{{}^3y}_S) \cos \omega_{or} t$$

$$\dot{{}^5z}_J = \dot{{}^3z}_J - \dot{{}^3z}_S$$

(6-39
a,b,c)

$${}^5x_{SUB} = ({}^3x_{SUB} - {}^3x_S) \cos \omega_{or} t - ({}^3y_{SUB} - {}^3y_S) \sin \omega_{or} t$$

$${}^5y_{SUB} = ({}^3x_{SUB} - {}^3x_S) \sin \omega_{or} t + ({}^3y_{SUB} - {}^3y_S) \cos \omega_{or} t$$

$${}^5z_{SUB} = {}^3z_{SUB} - {}^3z_S$$

(6-40
a,b,c)

6.3.3.2 (Continued)

$$\left. \begin{aligned} \dot{x}_{SUB}^5 &= (\dot{x}_{SUB}^3 - \dot{x}_S^3) \cos \Omega_{or} t - (\dot{y}_{SUB}^3 - \dot{y}_S^3) \sin \Omega_{or} t \\ \dot{y}_{SUB}^5 &= (\dot{x}_{SUB}^3 - \dot{x}_S^3) \sin \Omega_{or} t + (\dot{y}_{SUB}^3 - \dot{y}_S^3) \cos \Omega_{or} t \\ \dot{z}_{SUB}^5 &= \dot{z}_{SUB}^3 - \dot{z}_S^3 \end{aligned} \right\} \quad (6-41 \text{ a,b,c})$$

where $(\dot{x}_S^3, \dot{y}_S^3, \dot{z}_S^3, \dot{x}_S^3, \dot{y}_S^3, \dot{z}_S^3)$ is the state vector of the satellite in the rectangular geocentric fixed earth coordinate system derived in Section 6.3.3.1.

θ_{SLEW} is calculated using the vector dot product:

$$\theta_{SLEW} = \cos^{-1} \frac{\dot{x}_{SUB1}^5 \dot{x}_{SUB2}^5 + \dot{y}_{SUB1}^5 \dot{y}_{SUB2}^5 + \dot{z}_{SUB1}^5 \dot{z}_{SUB2}^5}{\sqrt{\dot{x}_{SUB1}^2 + \dot{y}_{SUB1}^2 + \dot{z}_{SUB1}^2} \sqrt{\dot{x}_{SUB2}^2 + \dot{y}_{SUB2}^2 + \dot{z}_{SUB2}^2}} \quad (6-42)$$

$\theta_S, \theta_{SA}, \theta_{SA}$ are obtained using the equations for conversion to spherical coordinates:

$$\theta_S = \cot^{-1} \left[\frac{\dot{z}_{SUB}}{\sqrt{\dot{x}_{SUB}^2 + \dot{y}_{SUB}^2}} \right] \quad (6-43)$$

$$\theta_S = \frac{(\dot{x}_{SUB}^5 \dot{x}_{SUB}^5 + \dot{y}_{SUB}^5 \dot{y}_{SUB}^5) \dot{z}_{SUB}^5 - \dot{z}_{SUB}^5 (\dot{x}_{SUB}^2 + \dot{y}_{SUB}^2)}{\sqrt{\dot{x}_{SUB}^2 + \dot{y}_{SUB}^2} (\dot{x}_{SUB}^2 + \dot{y}_{SUB}^2 + \dot{z}_{SUB}^2)} \quad (6-44)$$

$$\theta_{SA} = \tan^{-1} \frac{\dot{y}_{SUB}}{\dot{x}_{SUB}} \quad (6-45)$$

$$\theta_{SA} = \frac{\dot{x}_{SUB}^5 \dot{y}_{SUB}^5 - \dot{y}_{SUB}^5 \dot{x}_{SUB}^5}{\dot{x}_{SUB}^2 + \dot{y}_{SUB}^2} \quad (6-46)$$

6.3.3.2 (Continued)

γ_{SLEW} is most easily calculated using the vector dot product in rectangular fixed earth coordinates:

$$\gamma_{SLEW} = \cos^{-1} \frac{({}^3x_{S2} - {}^3x_{S1})({}^3x_J - {}^3x_{S1}) + ({}^3y_{S2} - {}^3y_{S1})({}^3y_J - {}^3y_{S1}) + ({}^3z_{S2} - {}^3z_{S1})({}^3z_J - {}^3z_{S1})}{\sqrt{({}^3x_{S2} - {}^3x_{S1})^2 + ({}^3y_{S2} - {}^3y_{S1})^2 + ({}^3z_{S2} - {}^3z_{S1})^2} \sqrt{({}^3x_J - {}^3x_{S1})^2 + ({}^3y_J - {}^3y_{S1})^2 + ({}^3z_J - {}^3z_{S1})^2}} \quad (6-47)$$

where γ_{SLEW} is the angle between satellite 2 and the jammer on the earth's surface as viewed from satellite 1.

R_{SS} , the distance between 2 satellites, and R_{SJ} , the distance between satellite 2 and the jammer, are calculated in the fixed earth coordinate system:

$$R_{SS} = \sqrt{({}^3x_{S2} - {}^3x_{S1})^2 + ({}^3y_{S2} - {}^3y_{S1})^2 + ({}^3z_{S2} - {}^3z_{S1})^2} \quad (6-48)$$

$$R_{JS} = \sqrt{({}^3x_J - {}^3x_{S1})^2 + ({}^3y_J - {}^3y_{S1})^2 + ({}^3z_J - {}^3z_{S1})^2} \quad (6-49)$$

6.3.3.3 Line of Sight Calculation

A line of sight must exist between two satellites before they can communicate using crosslinks, and the sun must be visible to a satellite before it uses its laser (or it will need excessive battery storage). For these reasons the line of sight condition illustrated in Figure 6-10 must be examined. The shaded area is not visible from satellite 1, represented by position vector \vec{R}_1 . For another satellite or the sun, with position vector \vec{R}_2 to be outside of this area,

$$|\vec{R}_1 - \vec{R}_2| < \sqrt{R_1^2 - R_e^2} \quad (6-50a)$$

or

$$\cos \theta > \frac{R_e}{R_1} \quad (6-50b)$$

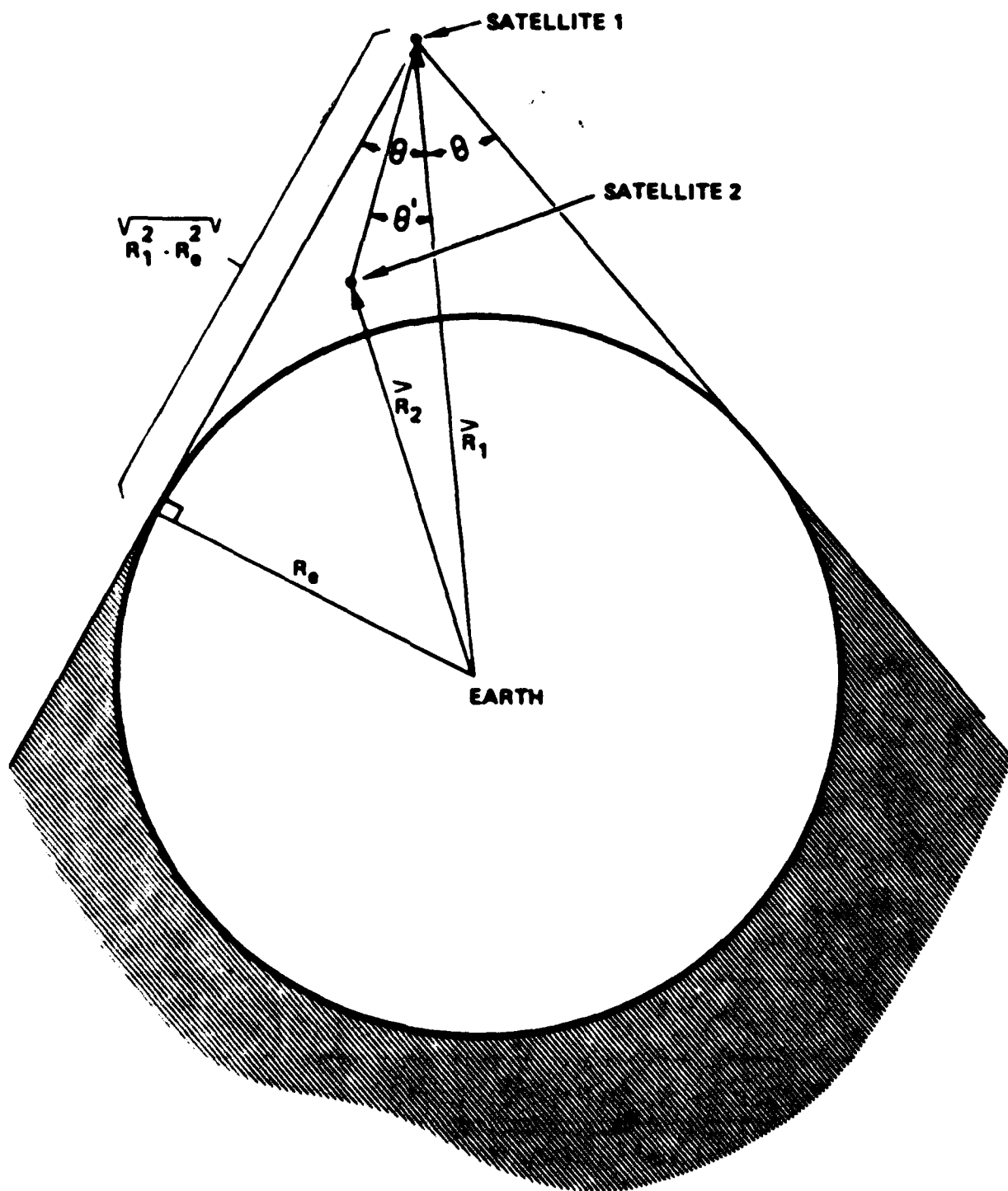


Figure 6-10. Line of Sight Geometry

6.3.3.3 (Continued)

i.e., satellite 2 is visible if it is within $\sqrt{R_1^2 - R_e^2}$ of satellite 1, or if it is outside the cone formed by the satellite and its tangents to the earth. θ^1 is the angle between vector \vec{R}_1 and vector $\vec{R}_1 - \vec{R}_2$ and can be calculated using the vector dot product:

$$\theta^1 = \cos^{-1} \left[\frac{(\vec{R}_1 - \vec{R}_2) \cdot \vec{R}_1}{|\vec{R}_1 - \vec{R}_2| |\vec{R}_1|} \right] \quad (6-51)$$

From Figure 6-10

$$\theta = \sin^{-1} \left(\frac{R_e}{|\vec{R}_1|} \right) = \cos^{-1} \left(\frac{\sqrt{R_1^2 - R_e^2}}{|\vec{R}_1|} \right) \quad (6-52)$$

The second condition then becomes:

$$\frac{(\vec{R}_1 - \vec{R}_2) \cdot \vec{R}_1}{|\vec{R}_1 - \vec{R}_2|} < \sqrt{R_1^2 - R_e^2} \quad (6-50b)$$

Expressed in the rectangular fixed earth coordinates derived in Section 6.3.3.1 the two conditions become:

$$(\bar{x}_1 - \bar{x}_2)^2 + (\bar{y}_1 - \bar{y}_2)^2 + (\bar{z}_1 - \bar{z}_2)^2 < \bar{x}_1^2 + \bar{y}_1^2 + \bar{z}_1^2 - R_e^2 \quad (6-53a)$$

$$\frac{(\bar{x}_1 - \bar{x}_2)\bar{x}_1 + (\bar{y}_1 - \bar{y}_2)\bar{y}_1 + (\bar{z}_1 - \bar{z}_2)\bar{z}_1}{\sqrt{(\bar{x}_1 - \bar{x}_2)^2 + (\bar{y}_1 - \bar{y}_2)^2 + (\bar{z}_1 - \bar{z}_2)^2}} < \sqrt{\bar{x}_1^2 + \bar{y}_1^2 + \bar{z}_1^2 - R_e^2} \quad (6-53b)$$

6.3.3.3 (Continued)

These can be immediately applied if the satellite position vectors are expressed in any rectangular coordinate system. The sun position is defined in the full system model in terms of the latitude, longitude spherical coordinate system and must be converted using equations (6-20) of 6.3.3.1 before the test. For the sun, the first test is useless. Since the sun is very far away and is in reality an extended light source, the vector difference $\hat{R}_1 - \hat{R}_2$ is approximated by the sun position vector. The second condition then becomes:

$$-\hat{R}_2 \cdot \hat{R}_1 < \sqrt{\hat{R}_1^2 - R_e^2} \quad (6-54)$$

where \hat{R}_2 is the unit vector in sun's direction. Therefore using equations (6-20) of Section 6.3.3.1, the line of sight condition to the sun becomes:

$$^3X \cos \alpha_{su} \cos \theta_{su} + ^3Y \cos \alpha_{su} \sin \theta_{su} + ^3Z \sin \alpha_{su} > -\sqrt{^3X^2 + ^3Y^2 + ^3Z^2 - R_e^2} \quad (6-55)$$

This will be required for every satellite at the time it is using its laser, and equations (6-53a) and (6-53b) above will be required for every 2 satellites which are using a crosslink.

6.3.3.4 RF Communication Link Analysis

There are three potential RF communication links: an uplink from the ground station to a satellite, a crosslink between satellites, and a link from the satellite back to the ground station (which will be called a backlink). The uplink and backlink share the same frequency band, but the difference in the transmitter powers, data rates, and noise sources requires separate analysis.

Three signal margins (M_u, M_c, M_b), which determine the success of the links, will be derived using the following inputs:

- B_u, B_c, B_g : Number of bits for each link to transfer.
- t_u, t_c, t_g : Time allowed for each link to transfer data.
- λ_{RF} : Wavelength corresponding to RF center frequency.
- P_s, P_g : Satellite and ground station transmitter powers.

6.3.3.4 (Continued)

- D_S, D_G : Satellite and ground station antenna diameters,
 P_{JG} : Effective radiated power for a jammer,
 η_S, η_G : Satellite and ground station antenna efficiencies,
 R_{GS} : The range from the ground site to the satellite,
 R_{JS} : The range from the jammer site to the satellite,
 R_{GJ} : The range from the jammer site to the ground site,
 R_{SS} : The range from one satellite to another,
 θ_S : The zenith angle to the satellite as measured at the ground site,
 A_{JL} : The required availability for the uplink (and backlink) atmospheric channel,
 θ_{SLEW} : The angle between a jammer at latitude α_J and longitude β_J and a satellite as viewed from another satellite,
 T_{RAIN}, T_{RADOME} : Signal attenuation factors,
 $T_{SUN}, T_{EARTH}, T_{RECEIVER}, T_{RAIN}$: Noise temperatures,
 W : Spread spectrum bandwidth for signal.

The uplink/backlink model is illustrated in Figure 6-11a where the narrow beam of the satellite antenna's gain profile allows a flat earth approximation for the link's footprint. Both satellite and ground station antennas are used for both transmission and reception of all traffic, including satellite telemetry and control as well as the primary communications. The backlink is needed to carry measurements of critical satellite parameters, remote sensor information, message verification and retransmission requests. Figure 6-11b shows the cross-link model in which satellite 1 is receiving from satellite 2 and from a jammer on the earth's surface.

The signal modulation method for the links will not be specified except to note Figure 6-12, which indicates that there are several methods for obtaining a bit error rate of less than 10^{-4} with an energy per bit over noise power per hertz (E_{RF}/N_0) of 12 dB. It will be assumed that with error correction or error

$$d \sin \theta > \text{VS. } 1.146 \lambda \frac{\lambda}{D} R_s$$

FOR $\theta_{\text{min}} = 30^\circ$, $d = 2000 \text{ km}$, $R = 70000 \text{ km}$, $D_{\text{min}} = 0.40 \text{ m}$

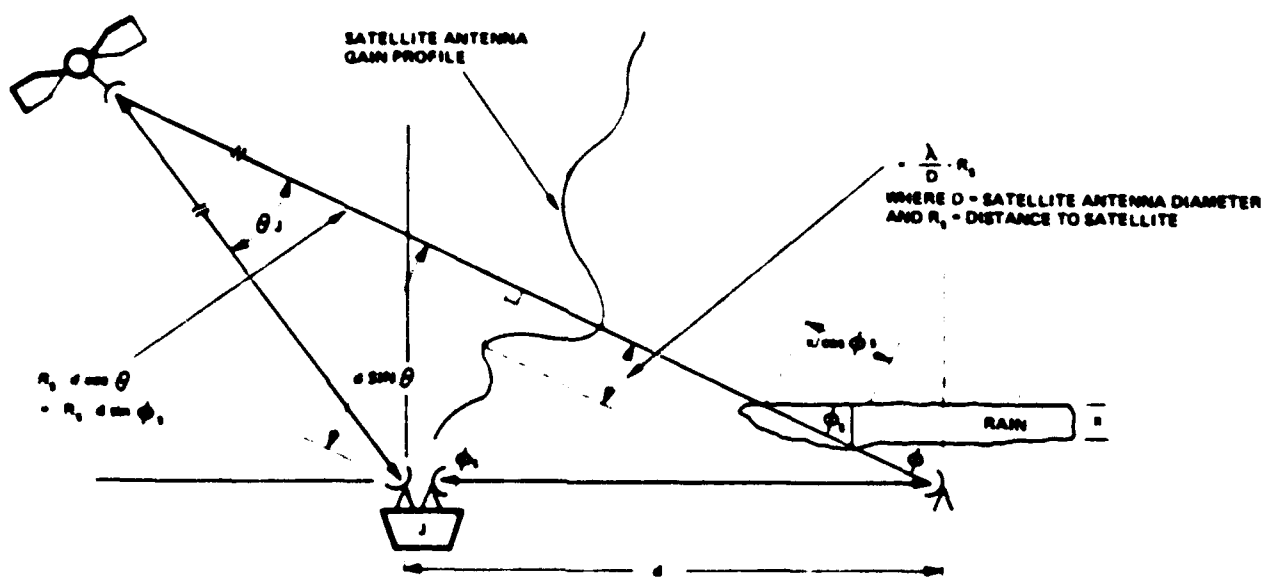


Figure 6-11a. Uplink/Backlink Configuration

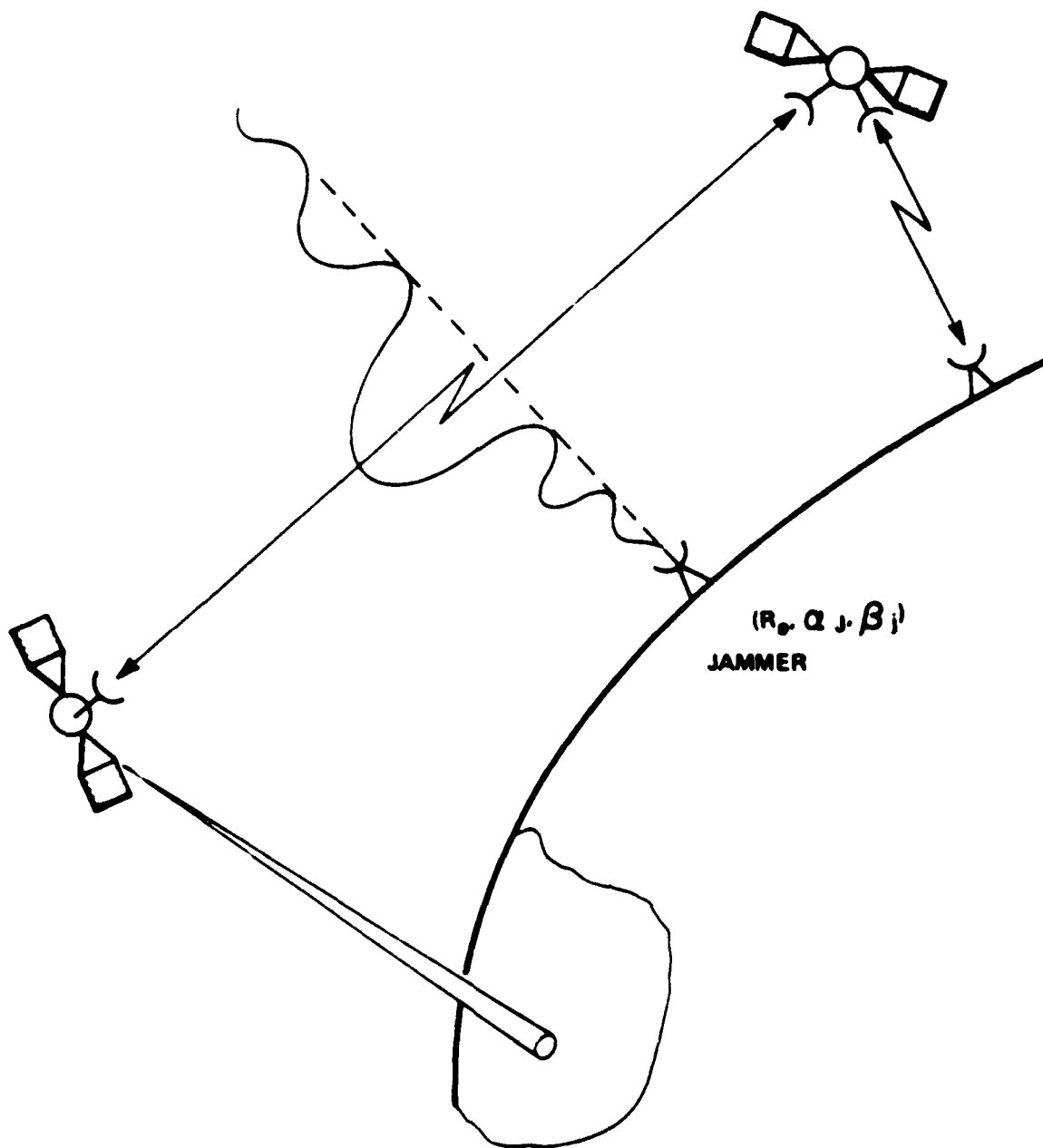


Figure 6-11b. Crosslink Configuration

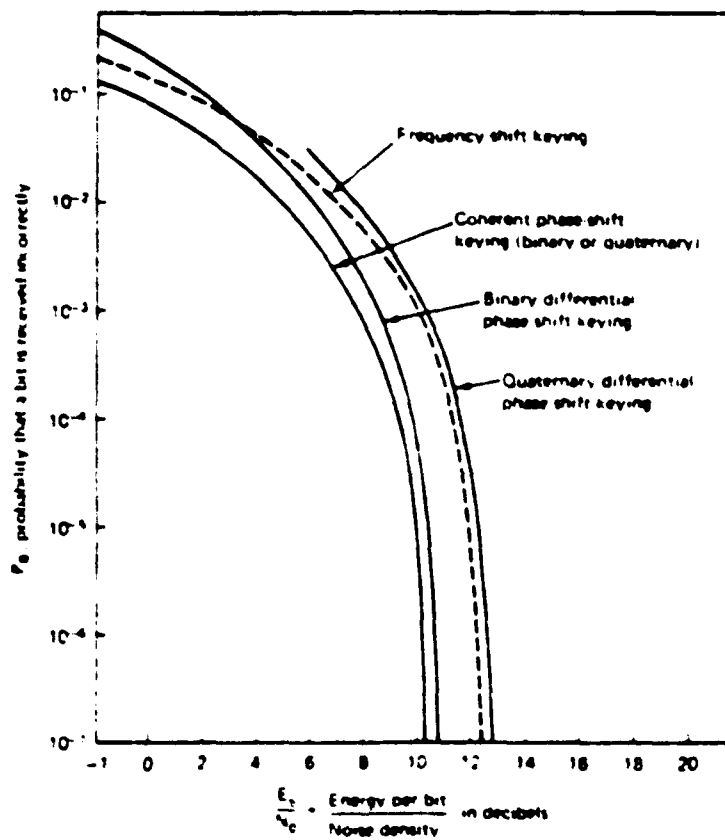


Figure 6-12. Variation in bit error probability with E_b/N_0 .

6.3.3.4 (Continued)

detection followed by possible retransmission, this bit error rate is sufficient. For instance, if 10^6 bits were transmitted with single bit error correction for 31 bit blocks, the probability of an uncorrected error would be only 15%. If 10^4 bit blocks were then used for error detection and retransmission, the probability of uncorrected errors after 1 retransmission would only be .0003. Therefore, 12 dB will be used as the critical $(E/N_0)_C$ for successful communication.

$$\left(\frac{E_{RF}}{N_0}\right)_C = 12 \text{ dB} \quad (6-56)$$

$$\text{and} \quad \left(\frac{S_{RF}}{N_0}\right)_C = \left(\frac{E_{RF}}{N_0}\right)_C \left(\frac{B_{RF}}{t_{RF}}\right) \quad (6-57)$$

where E_{RF} is the energy per message bit,

S_{RF} is the signal power at the receiver,

N_0 is the noise power per hertz density at the receiver,

B_{RF} is the number of bits in the message,

t_{RF} is the message time interval.

In order to overcome intentional jamming, the signal bandwidth, W , is assumed to be increased by spectrum spreading techniques (pseudo-noise, frequency hopping, time hopping, etc). The form of the margin calculations is as follows:

$$M = \frac{\left(\frac{S_{RF}}{N_0}\right)}{\left(\frac{S_{RF}}{N_0}\right)_C} = \frac{S_{RF}}{N_0} \frac{t_{RF}}{B_{RF} \left(E_{RF}/N_0\right)_C} \quad (6-58)$$

The signal power at the receiver is given by:

$$S_{RF} = P_T^{RF} G_T G_R \left(\frac{\lambda_{RF}}{4\pi R_T}\right)^2 T_{P\&In} T_{Radome} T_{Air} \quad (6-59)$$

6.3.3.4 (Continued)

where P_T^{RF} is the transmitter power,

G_T, G_R are the gains of the transmitting and receiving antennas,

λ_{RF} is the RF wavelength,

R_T is the range to the receiver,

and the τ are transmission terms accounting for losses.

This equation assumes there are no antenna pointing errors. Both bore-sight gains are given by:

$$G = \left(\frac{\pi D_{RF}}{\lambda_{RF}} \right)^2 \eta_{RF} \quad (6-60)$$

where D is the antenna diameter and η is the antenna efficiency, generally about 50%.

The signal expression is valid for both uplink and backlink when the appropriate transmitter power value, P_T^{RF} , is used. It is also valid for the crosslink if the atmospheric attenuation factors are dropped. The term, "RAIN", is extracted from the rain attenuation statistics for the ground sight for a given availability. Figure 6-13 shows the zenith path attenuation vs. availability for various frequencies for Rosman, North Carolina.

As shown in Figure 6-14, these statistics are typical for East coast stations, and conservative for most West coast stations. They will be used for all ground station models. The large rain attenuation factors are caused by small convection cells, which are several kilometers in diameter, and pass-by in minutes. The probability of encountering one of these cells is assumed to be proportional to the path length through the atmosphere. Therefore, the availability for a non-zenith path is decreased from the zenith path availability used in Figure 6-13, by:

$$A_{UL} = \left(A_{UL,z} \right)^{\sec \theta_{RF}} \quad (6-61)$$

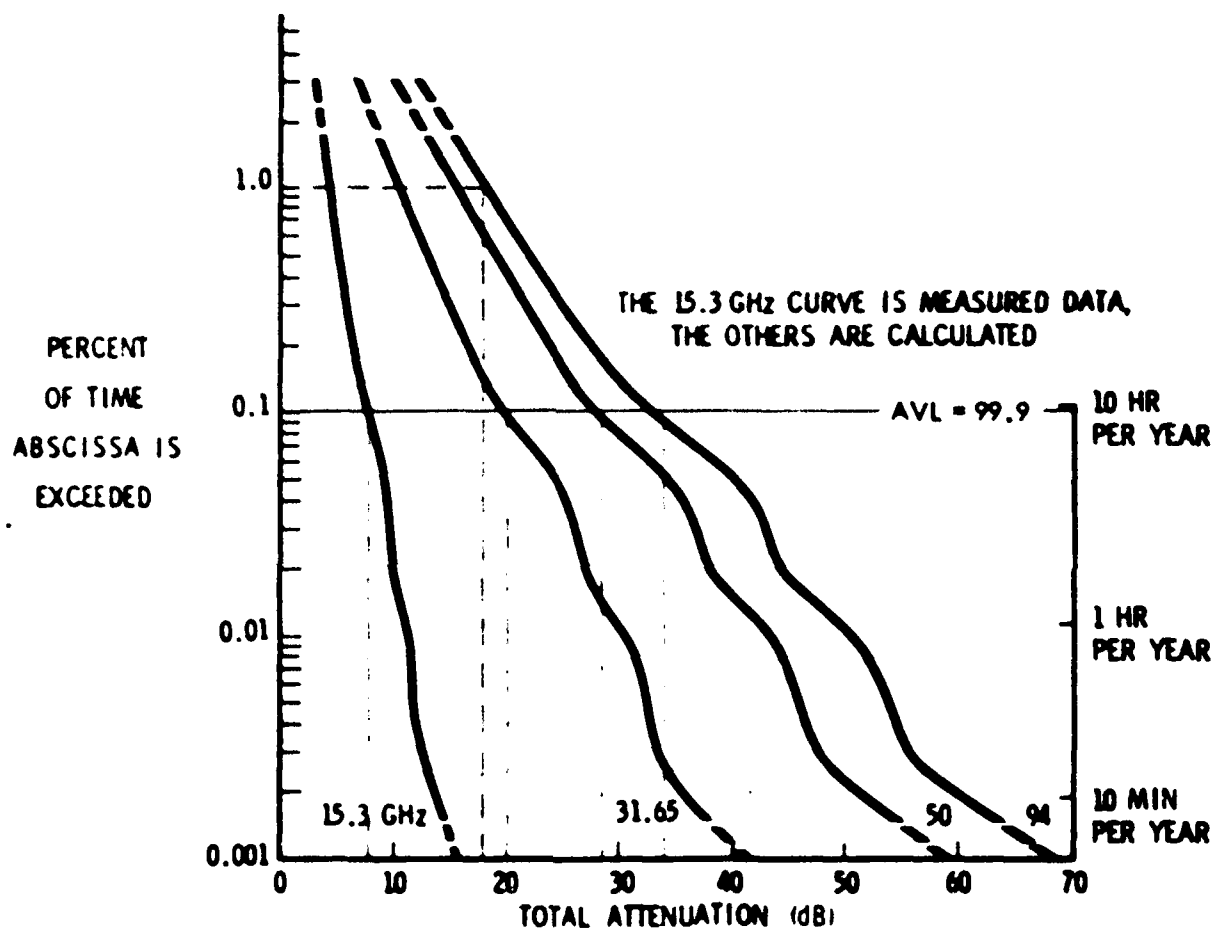


Figure b-13. Attenuation Distributions for Calendar Year 1970 at Roseman, North Carolina

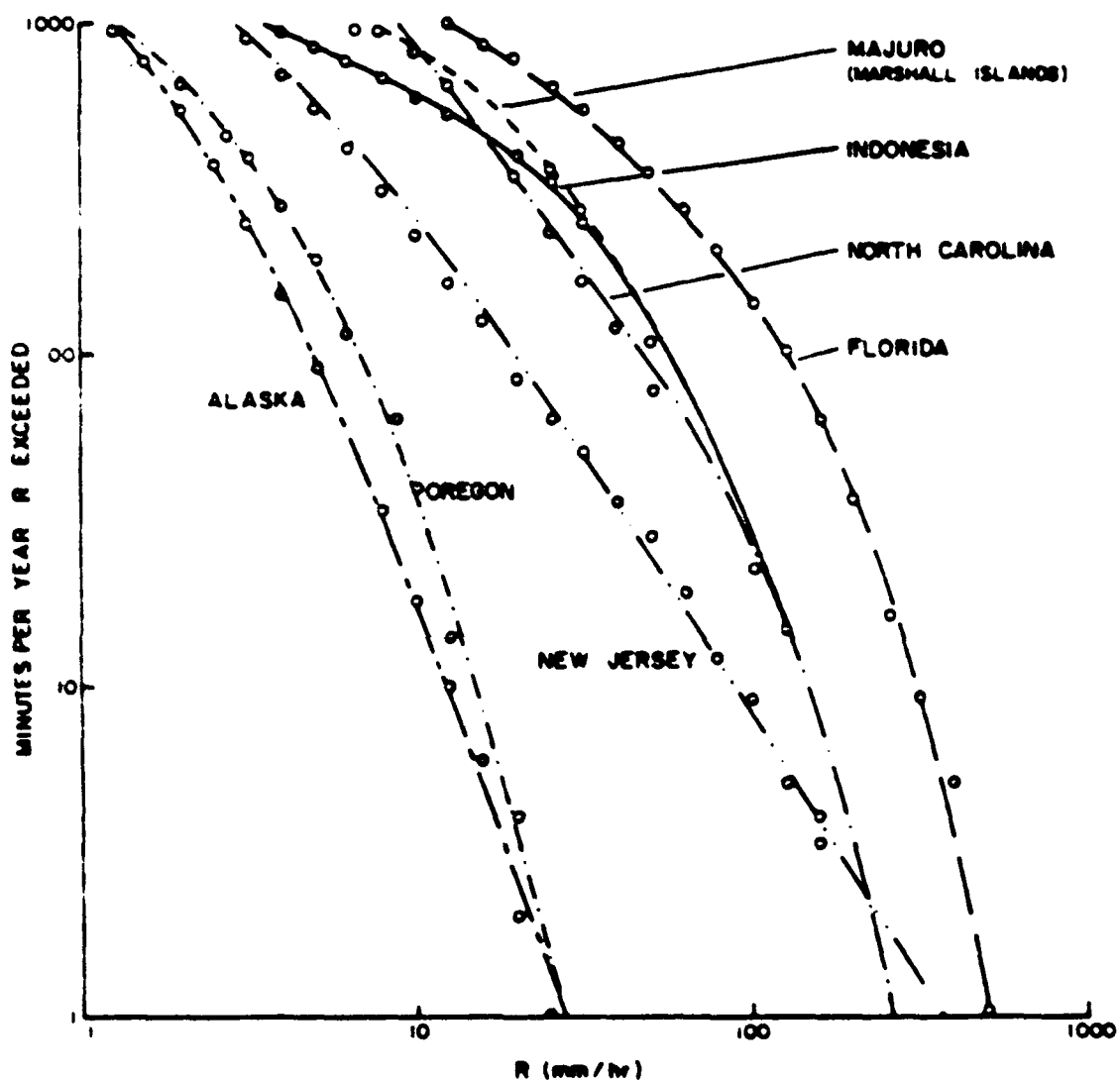


Figure 6-14. Rainfall Intensity Occurrences for Different Geographic Locations

6.3.3.4 (Continued)

where $\sec \theta_s^{RF}$ is the path length factor. If more than one site can communicate with a particular satellite, then the total link availability is increased. The resulting availability from both of these factors is:

$$A_{UL} = 1 - \frac{1}{n_{RF}} \left[1 - (A_{UL,Z})^{\sec \theta_{s1}^{RF}} \right] \quad (6-62)$$

where n_{RF} is the number of ground sites, which are assumed to be separated enough to have uncorrelated heavy rain statistics.

To use Figure 6-13's statistics for 2 ground stations with different zenith angles to the satellite requires a trial and error approach, which minimizes the maximum attenuation of either site, for a given desired total link availability. If, however, the sites are close enough that the zenith angles are roughly equal, but their rain statistics uncorrelated, then the availability to be used in Figure 6-13 can be calculated:

$$A_{UL,Z} = \left(1 - (1 - A_{UL})^{1/n_{RF}} \right) \cos \theta_s^{RF} \quad (6-63)$$

For example, a desired total uplink availability (due to rain) of 99.9% at a zenith angle of 80° is equivalent to a zenith availability of 99.982%, which corresponds to a rain attenuation at 32 GHz of 28 dB (which must be overcome by the transmitter). If two such stations are available, the required zenith availability at each site is only 99.44%, or an attenuation of only 12 dB at 32 GHz.

RADOME, the attenuation factor from the ground antenna's radome, if one is used, can be estimated from Figure 6-15 which given a maximum value of 4.2 dB loss for heavy rain onto a dirty radome at 30 GHz.

CURVE	WATER FILM THICKNESS mm	FILMING CONDITIONS (1)				NON FILMING CONDITIONS (2)			
		100	1000	10000	100000	100	1000	10000	100000
		RAIN RATE mm/hr				RAIN RATE mm/hr			
A	0.0100	1.0	1.4	2.0	3.0	2.0	3.0	4.0	10.2
B	0.0200	1.0	2.0	3.0	6.3	6.0	7.0	12.0	24.0
C	0.0320	2.0	3.0	4.0	9.0	11.0	16.0	24.0	40.2
D	0.0407	3.3	4.0	6.4	13.1	23.0	32.0	40.0	100.0
E	0.0463	4.0	6.4	8.3	16.7	26.0	40.0	72.0	
F	0.0504	6.3	8.0	12.3	26.0	70.2	100.0	100.0	
G	0.0500	10.0	13.0	20.0	42.0	100.0			

Z DRY RADOME ESECOLAM MEMBRANE THICKNESS - 0.0120 mm (0.0005 in.)
NOTES (1) SEI FORMULA THEORETICAL TURBULENT FLOW (2) SEI FORMULA EXPERIMENTAL
(3) WATER FILM TEMPERATURE - 10°C

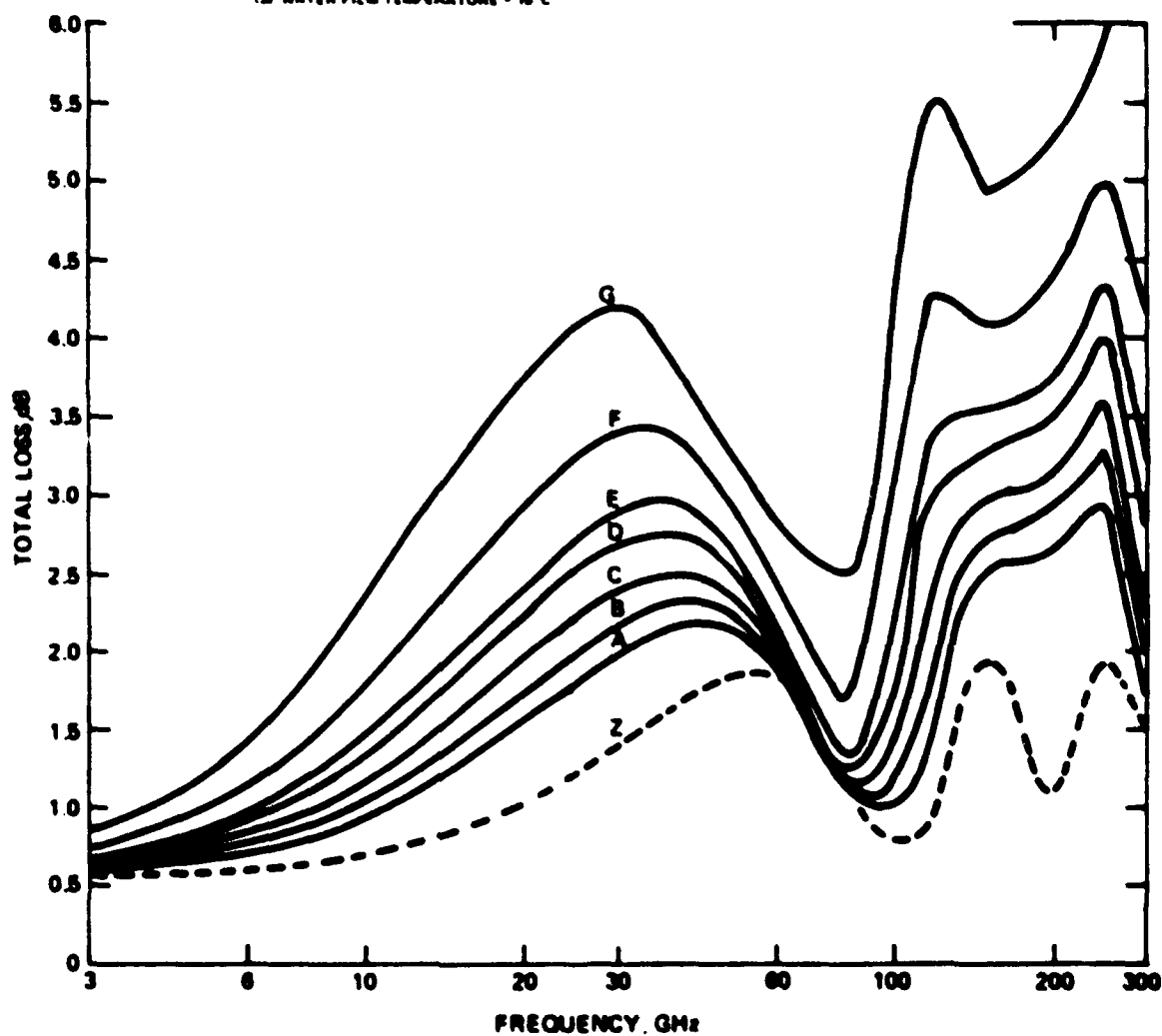


Figure 6-15. Attenuation Factor

6.3.3.4 (Continued)

The clear air attenuation, τ_{AIR} , is very small up to 60 GHz as can be seen from Figure 6-16. Therefore, it will be ignored.

The noise density, N_0 , in equation (6-58) is given by:

$$N_0 = \left[(k T_{SUN})^2 + (k T_{EARTH})^2 + (k T_{RECEIVER})^2 + (k T_{RAIN})^2 + \left(\frac{J}{W}\right)^2 \right]^{1/2} \quad (6-64)$$

T_{SUN} and T_{EARTH} are the noise temperatures for sun and earth when they fill the view of the receiving antenna. $T_{RECEIVER}$ and T_{RAIN} are the receiver noise temperature and the noise temperature due to heavy rain near the receiving antenna. k is Boltzman's constant. T_{EARTH} is zero for the backlink and T_{RAIN} is zero for both uplink and crosslink. A typical value for $T_{RECEIVER}$ is $1000^{\circ}K$ for today's satellite technology, T_{EARTH} is $254^{\circ}K$, and T_{SUN} is between 10^4 and $10^{70}K$ depending on the RF frequency and the sun's activity level. The noise caused by rain is shown in Figure 6-17, where it is evident that $10^{40}K$ is a very liberal estimate for the noise temperature. Obviously if the sun fills the field-of-view of the antenna, it dominates the natural noise sources.

The last term, $\frac{J}{W}$, in equation (6-64) is caused by a broadband noise generating jammer which is assumed to exist at a distance R_{GJ} from the ground station, for the uplink/backlink case, or at latitude λ_j and longitude ϕ_j for the crosslink case.

The jammer noise power is spread evenly over the apparent bandwidth, W , of the signal. J is the noise power at the receiver due to the jammer, and is determined by an equation similar to signal equation (6-59).

$$J = P_J G_J G_R(\phi_J) \left(\frac{1}{4 - R_J} \right)^2 \quad (6-65)$$

where P_J is the jammer transmitter power,

G_J is the jammer antenna boresight gain,

$G_R(\phi_J)$ is the satellite antenna gain in the direction of the jammer,

and R_J is the distance from the jammer, to the receiving antenna.

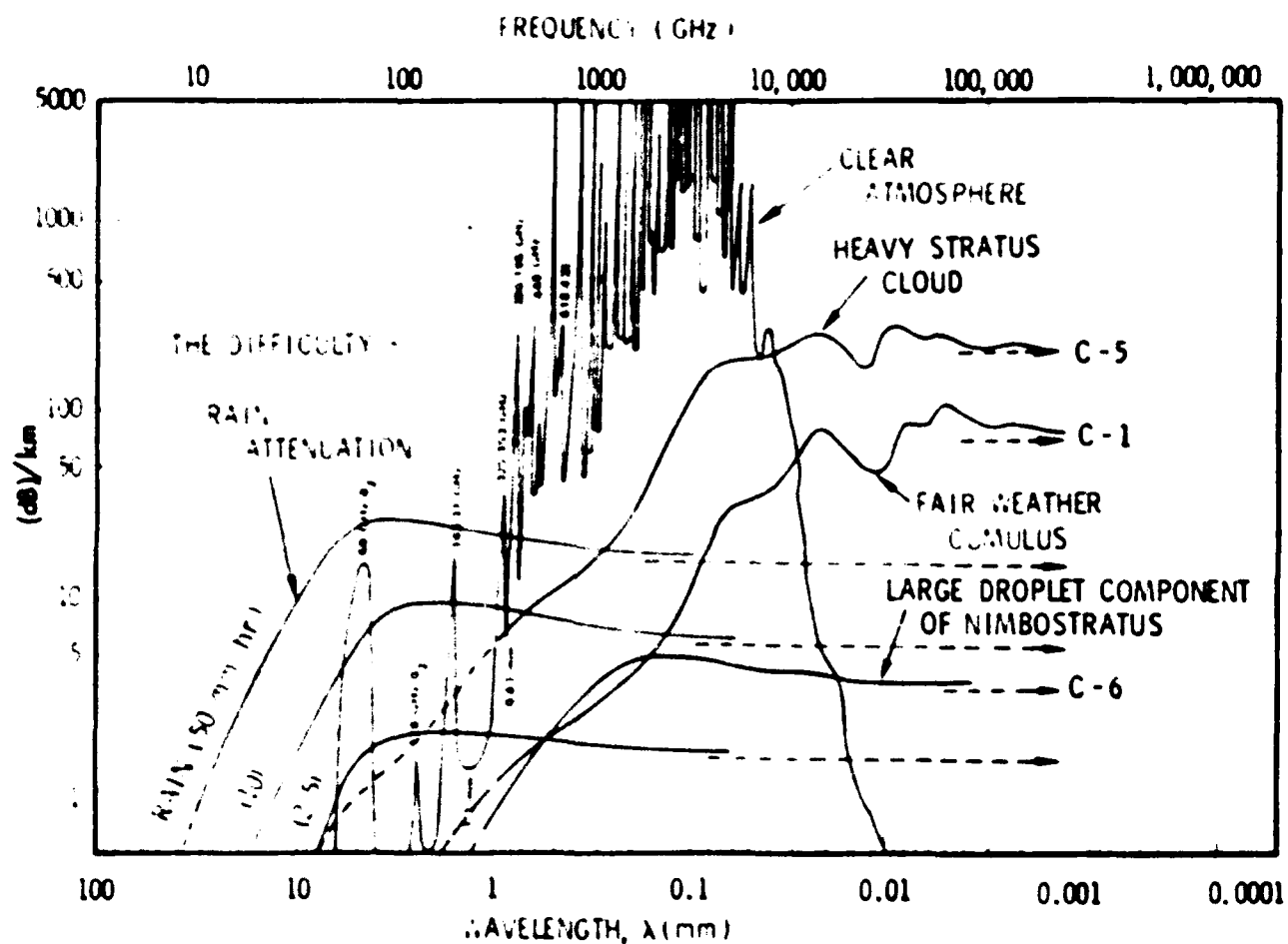


Figure 6-16. Summary of sea-level atmospheric attenuation

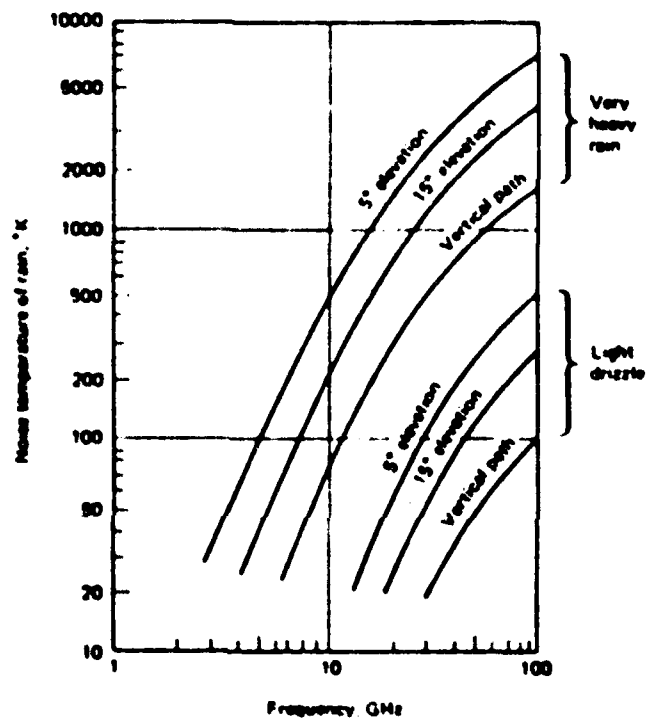


Figure 6-17. Noise caused by heavy cloud, fog, and rain

6.3.3.4 (Continued)

The rain related attenuation factors have not been included because the jammer's heavy rain statistics are assumed not to be well correlated with those of the ground site.

The gain profiles for both the ground station antenna and the satellite antenna are assumed to be that of a parabolic reflector, with tapering to lower the sidelobes to 25 dB below the main beam:

$$G_R(\phi_J) = \left(\frac{\pi D_{RF}}{\lambda_{RF}} \right)^2 \eta_{RF} \left[\frac{2 J_1(x)}{x} \right]^2 \quad \text{if } x < 3.6 \quad (6-66)$$

$$= \left(\frac{\pi D_{RF}}{\lambda_{RF}} \right)^2 \eta_{R-25 \text{ dB}} = \left(\frac{\pi D_{RF}}{\lambda_{RF}} \right)^2 \eta_{RF} \left(\frac{1}{316} \right) \quad \text{if } x > 3.6$$

$$\text{where } x = \frac{\pi D_{RF} \sin \phi_J}{\lambda_{RF}}$$

D_{RF} is the receiving antenna diameter.

η_{RF} is the receiving antenna efficiency.

ϕ_J is the angle between the jammer and the antenna's boresight

and J_1 is the first order Bessel function of the first kind. The gain is maintained at $G_R(0) - 25$ dB beyond the main lobe because it is assumed that jammer will be moved off the satellite antenna profile's nulls.

For the uplink:

$$\phi_J = \sin^{-1} \left(\frac{R_{GJ} \cos \phi_S^{RF}}{R_{GS} - R_{GJ} \sin \phi_S^{RF}} \right) \quad (6-67)$$

For the backlink:

$$\phi_J = \pi/2 - \phi_S^{RF} \quad (6-68)$$

6.3.3.4 (Continued)

For the crosslink:

$$\phi_J = \gamma_{SLEW}$$

Inserting the terms into equation (6-58), the margins become:

$$M_U = \left[\frac{t_u}{B_u (E_{RF}/N_0)_c} \right] \left[\frac{P_G \left(\frac{\pi^2 D_G^2}{\lambda^2} \right) \eta_G \left(\frac{\pi^2 D_S^2}{\lambda^2} \right) \eta_S \left(\frac{\lambda_{RF}}{4\pi R_{GS}} \right)^2 T_{RAIN} T_{RADOME}}{k^2 (T_{SUN}^2 + T_{EARTH}^2 + T_{RECEIVER}^2) + \left(\frac{P_{JGJ}}{W} G_S(\phi) \left(\frac{\lambda_{RF}}{4\pi R_{JS}} \right)^2 \right)^2} \right]^{1/2}$$

where $G_S(\phi) = \left(\frac{\pi D_S}{\lambda_{RF}} \right)^2 \eta_S \left[\frac{2 J_1(\chi)}{\chi} \right]^2$ if $\chi < 3.6$

$$\left(\frac{\pi D_S}{\lambda_{RF}} \right)^2 \eta_S \left(\frac{1}{316} \right) \text{ if } \chi > 3.6$$

and $\chi = \frac{\pi D_S}{\lambda_{RF}} \frac{R_{GJ} \cos \phi_S^{RF}}{R_{GS} - R_{GJ} \sin \phi_S^{RF}}$ (6-69)

6.3.3.4 (Continued)

$$M_B = \left[\frac{t_B}{B (E_{RF}/N_0) c} \right] \frac{P_S \left(\frac{\pi D_S}{\lambda_{RF}} \right)^2 \eta_S \left(\frac{\pi D_G}{\lambda_{RF}} \right)^2 \left(\frac{\lambda_{RF}}{4\pi R_{GS}} \right) \tau_{RAIN} \tau_{RADOME}}{\left[k^2 \left(\tau_{SUN}^2 + \tau_{RECEIVER}^2 + \tau_{RAIN}^2 \right) + \left(\frac{P_J G_J}{W} G_G(\gamma) \left(\frac{\lambda_{RF}}{4\pi R_{GJ}} \right)^2 \right)^2 \right]^{1/2}}$$

where $G_G(\gamma) = \left(\frac{-D_G}{\lambda_{RF}} \right)^2 \tau_G \left[\frac{2 J_1(\gamma)}{\gamma} \right]^2$ if $\gamma < 3.6$

$\left(\frac{-D_G}{\lambda_{RF}} \right)^2 \tau_G \left(\frac{1}{316} \right)$ if $\gamma > 3.6$

$\gamma = \frac{-D_G \cos \theta_S^{RF}}{\lambda_{RF}}$

(6-70)

and τ_{RAIN} is a function of A_{UL} .

6.3.3.4 (Continued)

$$M_C = \left[\frac{t_c}{B_C (E_{RF}/N_0)_C} \right] \left[\frac{P_S \left(\frac{\pi D_S}{\lambda_{RF}} \right)^4 \gamma_S^2 \left(\frac{\lambda_{RF}}{4\pi R_{SS}} \right)^2}{k^2 (T_{SUN}^2 + T_{EARTH}^2 + T_{RECEIVER}^2) + \left(\frac{P_{JJ} G_J}{W} G_S(\psi) \left(\frac{\lambda_{RF}}{4\pi R_{JS}} \right)^2 \right)^2} \right]^{1/2}$$

where $G_S(\psi) = \left(\frac{\pi D_S}{\lambda_{RF}} \right)^2 \gamma_S \left[\frac{2 J_1(x)}{x} \right]^2$ if $x < 3.6$

$\left(\frac{\pi D_S}{\lambda_{RF}} \right)^2 \gamma_S \left(\frac{1}{316} \right)$ if $x > 3.6$

and $x = \frac{\pi D_S}{\lambda_{RF}} \sin \psi_{SLEW}$ (6-71)

Successful communication implies that these margins exceed unity and the line of sight conditions are met for crosslinks.

6.3.3.5 Area Allocation

Environmental resolution elements should be allocated to the satellites in such a manner as to minimize the time required to scan the coverage area. The Full OSCAR System Model calculates the figure of merit (FOM_{ij}) to every environmental resolution element for each satellite in the constellation. Because the time required to cover a resolution element is inversely proportional to the figure of merit, a more appropriate number to use in allocation considerations is the reciprocal of the figure of merit, called the G figure.

The initial allocation is accomplished by giving responsibility for each environmental resolution element to the satellite which can cover it using the lowest G figure. For each satellite, a summation of the G figures for those resolution elements for which it is responsible is calculated. To meet the time requirement, the sum for each satellite must be less than S_T , where

6.3.3.5 (Continued)

$$S_T = \frac{(T_A)(A_{SQ})}{(A_{RE})(M_D)} \quad (6-72)$$

If this condition is met, the allocation procedure is terminated and this initial satellite allocation is used.

When the time requirement is not satisfied, re-allocation is performed. For the satellite with the largest summation of G figures, the responsibility for one or more environmental resolution elements must be transferred until that satellite meets the temporal requirement. These environmental resolution elements must also be reassigned in such a manner as to provide a minimum amount of loading on the other satellites. To accomplish this, for each resolution element assigned to this satellite, the difference between G values for this satellite and the satellite with the next smallest G value is calculated and stored in a table named delta. The delta table is next sorted in increasing order while keeping careful account of the environmental resolution elements associated with each value in the delta table. In this manner, a sorted environmental resolution element table is created. Since the smaller the value in the delta table, the less the impact of area reassignment is upon the other satellites, resolution elements are reassigned to the satellites with the next lowest G figures, in the order that they appear in the sorted table. Elements are reallocated until the G figure summation becomes less than S_T . The remaining environmental resolution elements will comprise the final area allocation to this satellite.

A summation of the G figures for the remaining satellites must now be computed. The summations are again checked to see whether or not they meet the temporal requirement. If the requirement is satisfied for all the satellites, the allocations are completed. Should the requirement not be met, the procedure of forming the delta table and performing environmental resolution element reassignments for that satellite with the largest G figure summation must be repeated. This procedure continues until all satellites satisfy the time requirement, or until all satellites have received their final allocations via the process described above.

6.3.3.6 Remote Sensor Performance

Information derived from a "remote sensor" is desirable at both the submarine terminal and the satellite. This section discusses the information desired and the method(s) of obtaining it.

6.3.3.6.1 Submarine Remote Sensor

In order to optimize the performance of the Submarine Terminal, we can vary:

1. Receiver Field-of-View;
 2. Receiver pointing angle relative to zenith and local longitude;
 3. Detection Bandwidth;
 4. Post Detection Filtering;
 5. Post Detection Processing;
- and, depending on the optical filter type,
6. Filter center wavelength (λ) and the bandpass ($\Delta\lambda$).

In our previous development of the SPDPM, we have assumed that:

- a. The receiver field-of-view is fixed;
- b. it is optimum to point the receiver at the signal ($\theta = 0$);
- c. The received pulse shape is known, and that using

$$B = \frac{0.4}{\Delta f_{1/2}}$$

results in optimum and lossless detection, filtering and processing.

if we further assume that there is a "set" aboard the submarine whose purpose it is to derive enough information so that those six parameters will be optimally selected, we note that in operation the information available to this remote sensor set will include:

1. Satellite locations;
2. Sun/Moon location;
3. Receiver location and depth;

6.3.3.6.1 (Continued)

4. Submarine Speed;
5. Time-of-Day;
6. Time-of-Year;
7. Average Water Data Base there and then;
8. Average Cloud Data Base there and then;
9. Average background level in the operating passband;
10. Verified Propagation Path Models.

The key inputs are the last two, since one may be able to derive the characteristics of the propagation path from passive measurements of the existing background. However, the following information could also be made available:

11. Long range cloud forecasts;
12. Thermocline locations and strength;
13. Relative spectral strength of background;
14. Previous pulse characteristics;
15. Background short term fluctuation properties;
16. Background long term time dependence;
17. Short term weather pattern update (night before).

On another contract we are developing techniques for using all or part of these 17 data inputs to provide the required information on the submarine, and are proposing that experimental verification of these techniques be performed under the development tests defined in Section 9, Volume 4 of the final report.

In the meantime, we take as a submarine remote sensor model:

- a. The receiver field-of-view is fixed at a single value, independent of the propagation path;
- b. The receiver optical axis is pointed exactly back at the axis of the incoming signal;
- c. The received pulse shape and width is exactly known, and lossless detection electrical filtering and processing occurs for the detection bandwidth, B , equal to 40% of the reciprocal of the half power pulse width, $\Delta t_{1/2}$.

6.3.3.6.1 (Continued)

Further analytic and experimental work will certainly modify one, or all three, portion(s) of this model.

6.3.3.6.2 Satellite Remote Sensor

The remote sensing "set" of the satellite terminal could provide information to optimize the following satellite transmitter characteristics (assuming a single "black box" laser operating at a single value of E_p and PRF is available):

1. Transmitter beamwidth;
2. Number of revisits to a given location;
3. Message type (Selective call vis-a-vis General Broadcast, for example);

and if a tunable laser and filter are available:

4. Wavelength (λ).

In our present development of the SPDPM and DCM, we have assumed that:

- a. The satellite transmitter beamwidth is perfectly matched (for the fully adaptive scan) to the propagation path losses in a given environmental resolution element (ERE), so that the required signal-to-noise ratio is exactly matched with the actual signal-to-noise ratio;
- b. No revisits to a given location occur;
- c. The message type is pre-selected before a DCM run, and is not of prime importance since the system is designed to meet the EAM requirements.

The "set" responsible for determining the scan pattern, revisits, and message type will have the following available information:

1. Outputs from all available remote sensors on other satellites;
2. Real Time weather updates from the ground/ships ("ground truth");
3. Coverage Area Location;
4. Data from the previous time interval;

6.3.3.6.2 (Continued)

5. Average Cloud Data Base for that time and place;
6. Average Water Data Base for that time and place;
7. Time of Day;
8. Time of Year;
9. Verified Propagation Path Models.

On another contract we are developing techniques for using all or part of these nine data inputs to provide the information required by the satellite remote sensor set. A significant portion of the other program is devoted to determining the state-of-the art of available and planned remote sensors, and in determining their accuracy in estimating the key cloud, air-water interface, and water properties.

We are proposing that experimental verification of the resulting techniques be performed under the Development Tests, defined in Section 9, Volume 4 of the final report.

In the meantime, we take as a satellite remote sensor model:

- A. A perfectly adaptive scan controls the satellite transmitter beamwidth;
 - B. No revisits to a given location occur; if the $FOM_{ij} < 1$, then the ij 'th ERE is not illuminated at all;
 - C. The system is designed to deliver an EAM; the system knows enough to send a Selective Call message (to maintain connectivity) where a General Broadcast message would require too much time, and so lower the system effectiveness.

6.4 MODEL IMPLEMENTATION

The architecture for the Full OSCAR System Model has been developed in the previous sections. It is not within the scope of this contract to implement a computer program for this FOSM, but it is part of this contract to perform sample calculations using all elements of the FOSM to show example results.

These sample calculations are performed in Section 3 of Volume 4 of this final report. They occur after:

1. A configuration trade-off has been performed in Section 2 of Volume 4. This trade-off results in optimum satellite configurations (orbits and number of satellites) for three types of orbits: geostationary, 12-hour period highly elliptical, and 24-hour period highly elliptical;
2. The SPDPM is evaluated for a range of signal, sun, and moon zenith angles, and cloud and water types;
3. The DCM is evaluated in Section 3.4 of Volume 4 for satellites in the best configurations, fully adaptive scan, time of peak demodulation, data bases for clouds and water provided by NOSC, a single time interval during which the sun is at + 23.5° latitude over the center of the satellite's area coverage responsibility, for the EAM, and typical system design parameters. The downlink availability is scaled to meet the minimum system requirement by deriving a required technology figure of merit:

$$\boxed{\text{TECH}_{\text{FOM}} F_L P_L' \left(\frac{\gamma_R}{B_{\text{OPT}}} \right)^{1/2}} \quad (6-73)$$

for F_L = wall plug laser efficiency;

P_L' = prime power available on the satellite to pump the laser;

γ_R = receiver (primarily optical filter) transmission;

B_{OPT} = optical filter bandpass.

6.4 (Continued)

Then the best of the satellite configurations is chosen as that one requiring the fewest satellites and the smallest value of $TECH_{FOM}$.

Based on these results, we perform the following sample calculations in Volume 4 for the FOSM:

Environmental Inputs: Half the runs with Worst Case NOSC models for clouds and water, Half with the Best Case;
 No ice blockage;
 Sun/moon location in Table 6-4

Requirement Inputs: Full area coverage and full depth EAM
 Full System Effectiveness.

System Design Inputs: $TECH_{FOM}$ and satellite network from DCM.
 Other system design inputs from DCM.
 No crosslink.
 Uplink assumed not to be a driver, but specified.
 No MTBF's or MTTR's for any portion of this link.
 For each of the 12 runs, place one satellite at apogee over an ocean, and allocate the other coverage as appropriate. Alternate the ocean over which the satellite is at apogee in every other run.

6.4 (Continued)

TABLE 6-4. SUN/MOON LOCATIONS FOR SAMPLE FOSM RUNS

SUN		MOON	
LONGITUDE	LATITUDE	LONGITUDE	LATITUDE
0	0	180°	+5.1°
0	+23.5°	180°	+28.6°
0	-23.5°	180°	-18.4°
90°	0	270°	+5.1°
90°	+23.5°	270°	+28.6°
90°	-23.5°	270°	-18.4°
180°	0	0	+5.1°
180°	+23.5°	0	+28.6°
180°	-23.5°	0	-18.4°
270°	0	90°	+5.1°
270°	+23.5	90°	+28.6°
270°	-23.5°	90°	-18.4°

For each of the 12 runs, we calculate a downlink availability. Then the average downlink over the year is taken as the average of these results (weighting the 0° solar latitude results twice).

Given this downlink availability, then, reasonable values will be assigned to the other four portions of the link to arrive at a system-effectiveness which meets the OSCAR requirement.

6.5 DISCUSSION OF ANALYSES

The analyses developed in Section 6.3 differ markedly in their status.

6.5.1 Environmental Models

The sub-models for the predictable data bases presented in Section 6.3.1.1 are not uncertain. Although they are only approximations, the results are adequate for predicting OSCAR performance.

6.6 "Parameter Value" Uncertainties

The parameter value uncertainties for the FOSM include those of the SPDPM and DCM, but also extend to others.

6.6.1 Environmental Parameters

The parameter values for the fixed data bases are well known, and the only uncertainty in the predictable data bases is the exact values for IC_{ij} , fractional ice coverage, to use for a particular ij 'th environmental resolution element during a particular month. This only affects a percent of the total coverage area, so the uncertainty is not of prime importance.

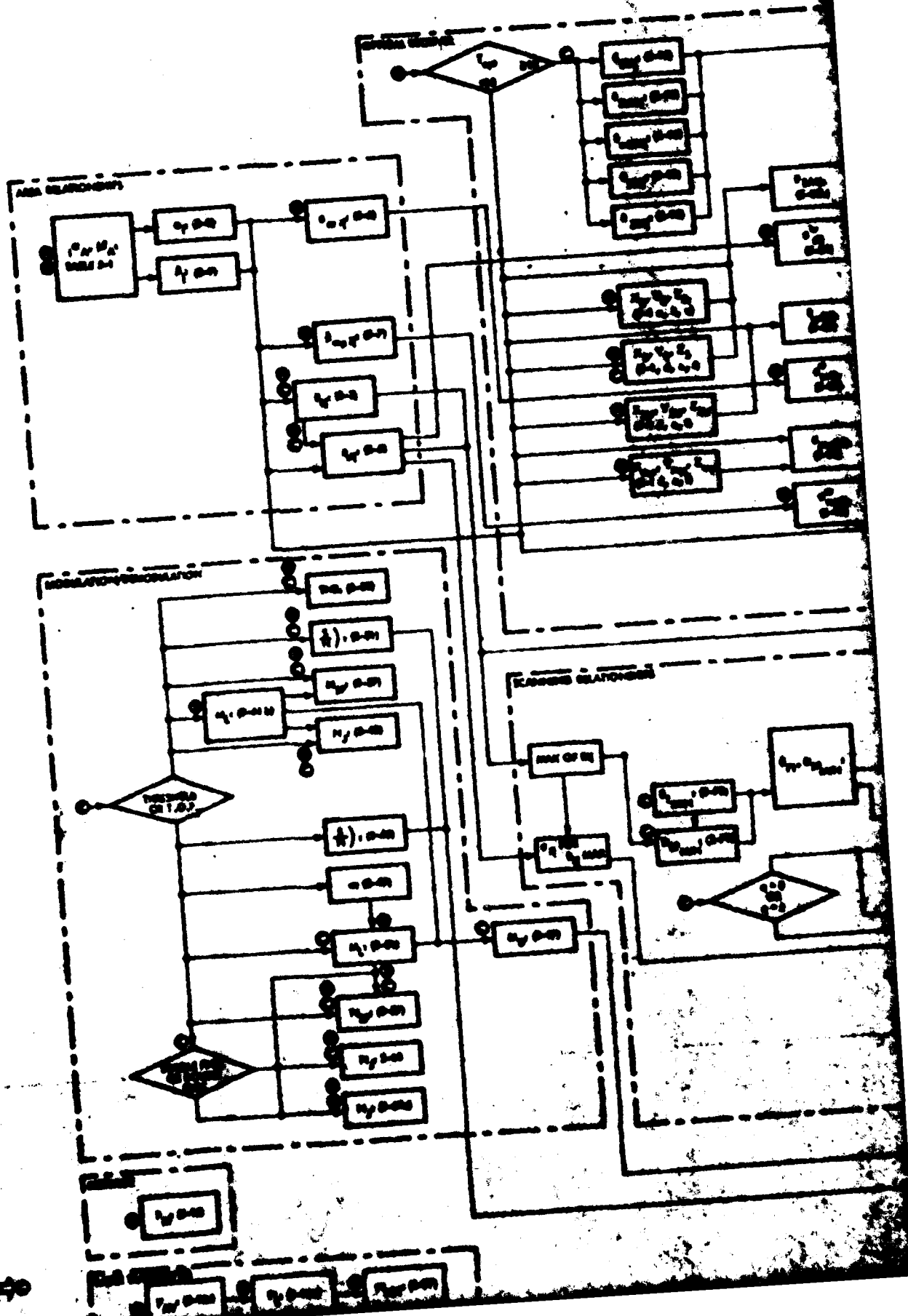
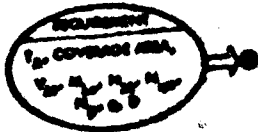
The unpredictable data bases of cloud properties, air-water interface properties and water properties are largely uncertain. In addition to those problems pointed out in the SPDPM and DCM sections; the global, seasonal and diurnal properties now become of importance. In particular, the mean time between outages and mean time to clear are not known at this time, along with real distributions and evolutions of cloud thickness and average extinction coefficient, depth of the thermocline and diffuse attenuation coefficient above and below this thermocline, and the strength and characteristics of bioluminescence.

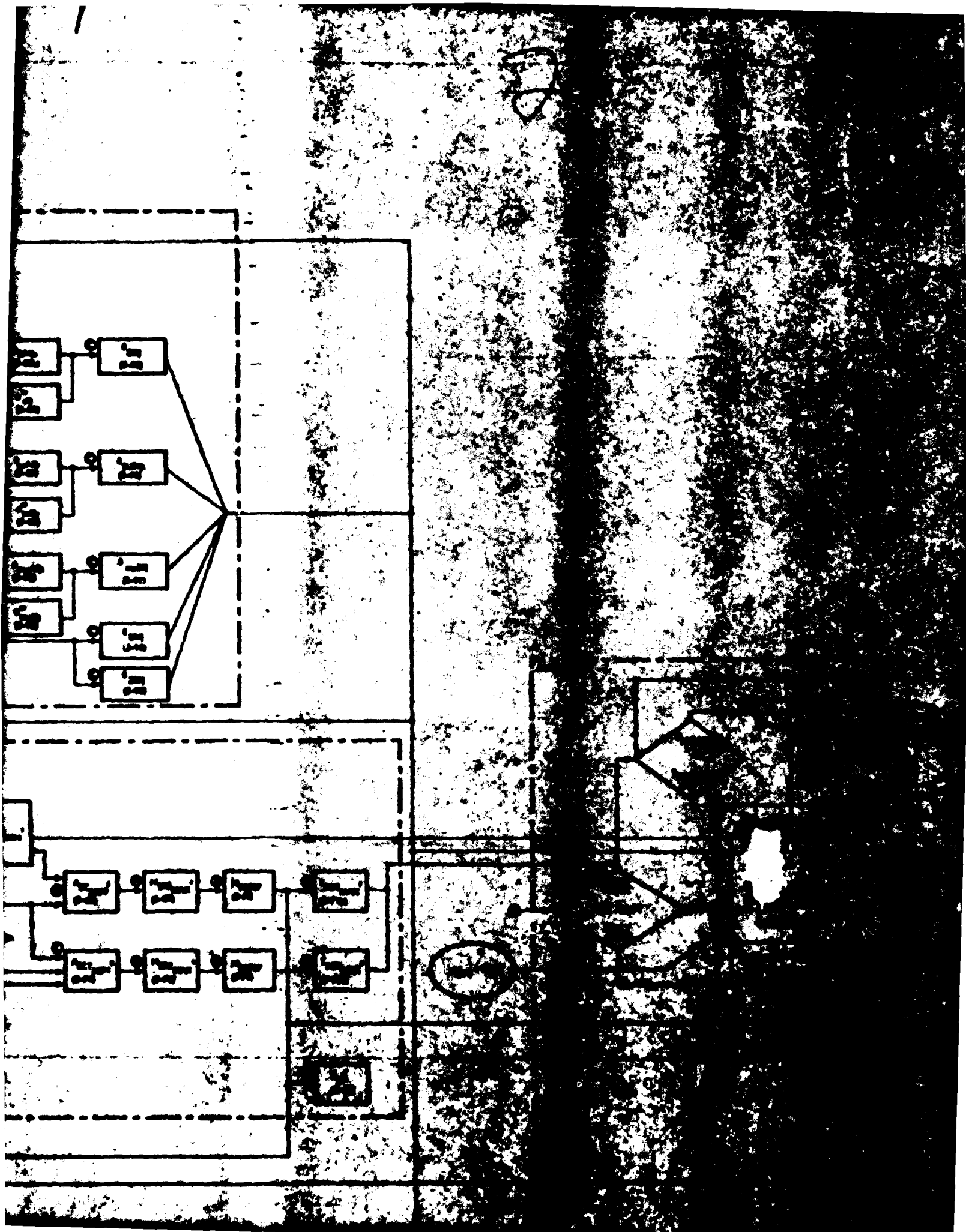
Table 6-5 summarizes only those FOSM input parameters which are uncertain.

Table 6-5. Uncertain Parameters for the FOSM

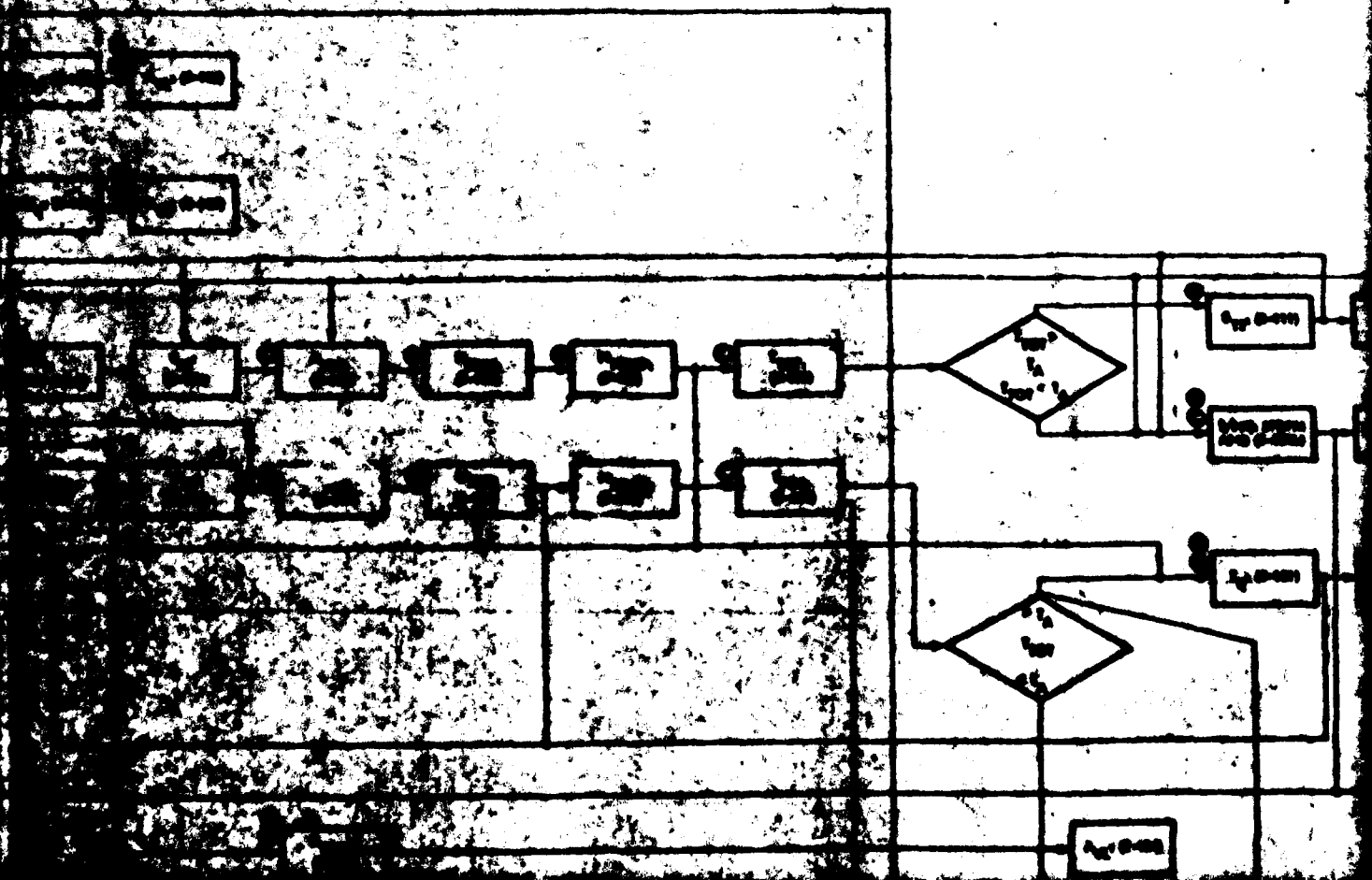
PARAMETER	COMMENTS
<u>ENVIRONMENT</u>	
ICE COVERAGE	A SMALL EFFECT
CLOUD DISTRIBUTION PARAMETERS	NEEDS TO BE RESOLVED
AIR-WATER INTERFACE PARAMETERS	A RELATIVELY SMALL EFFECT
WATER DISTRIBUTION PARAMETERS	NEEDS TO BE RESOLVED

1





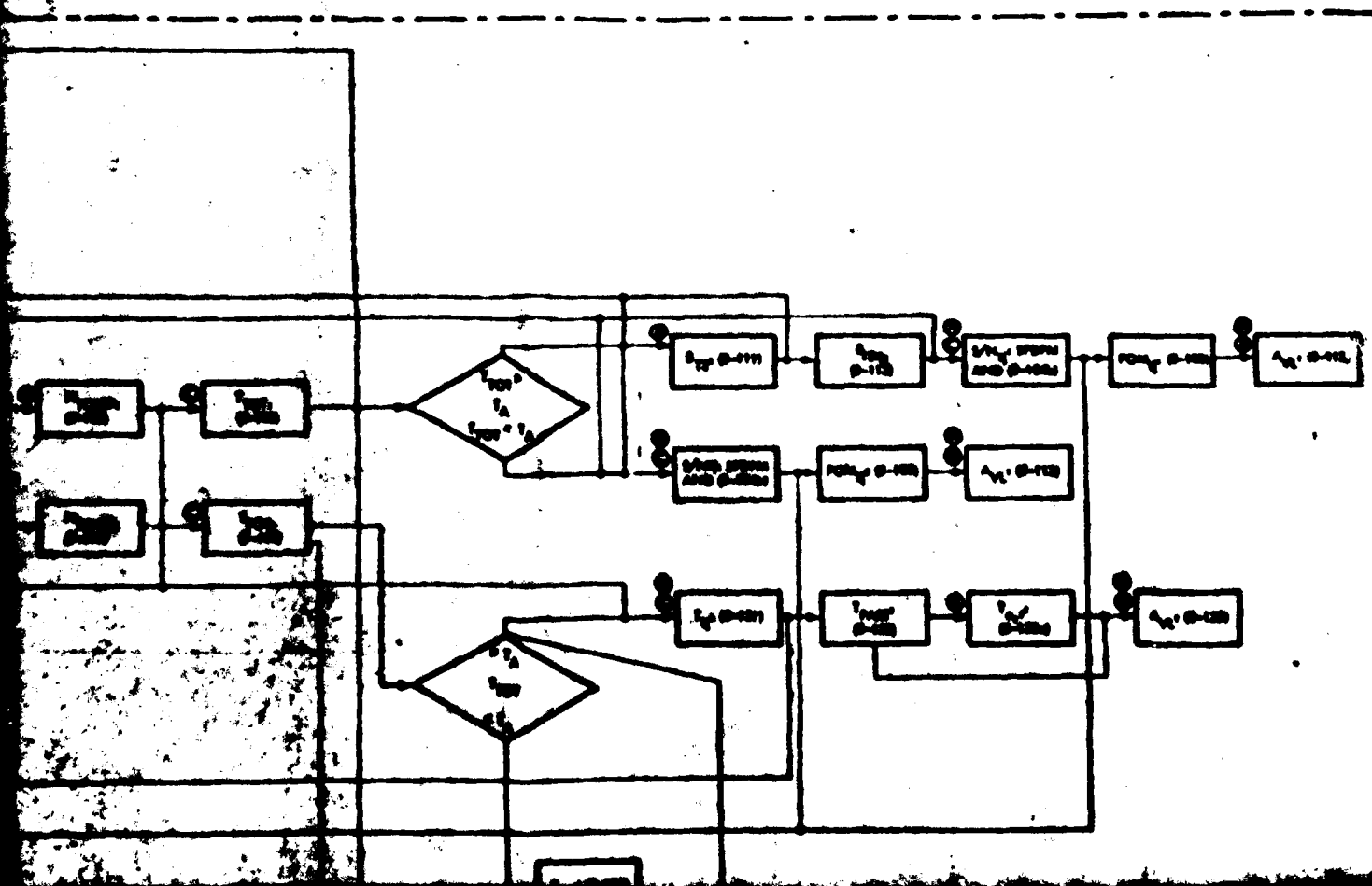
3



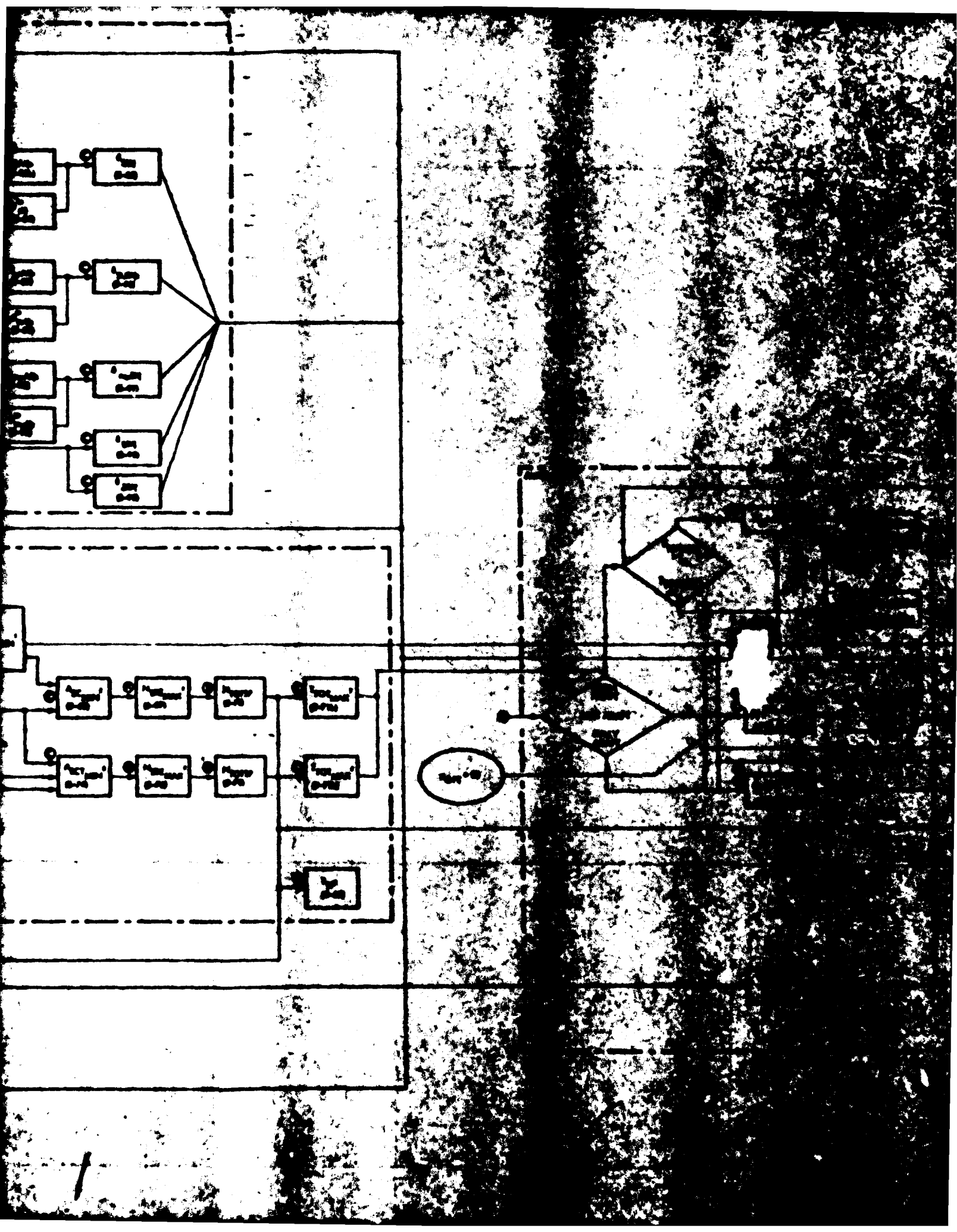
3

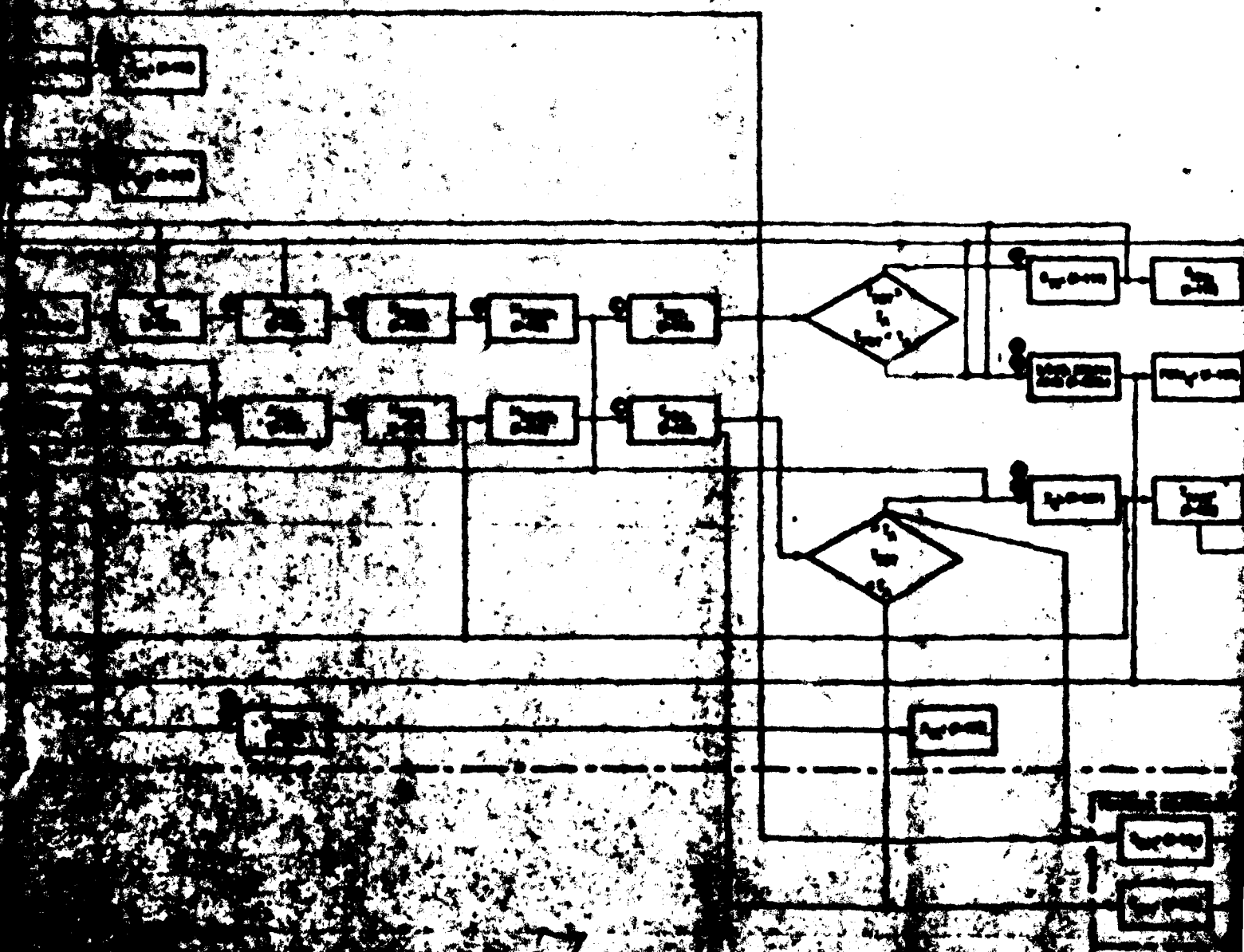
1

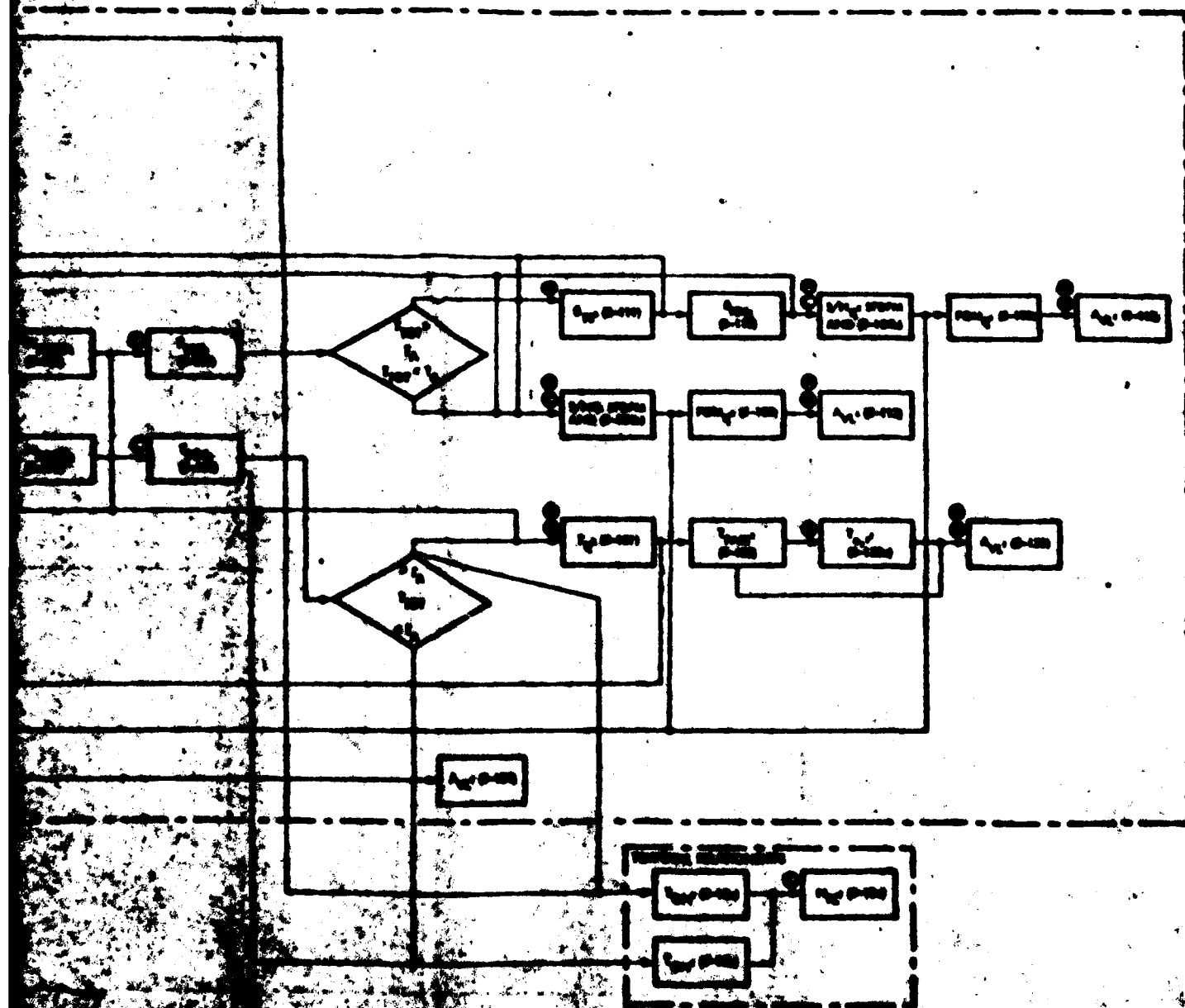
4











1 8